



Ebooko.ir

فروشگاه کتاب های الکترونیکی

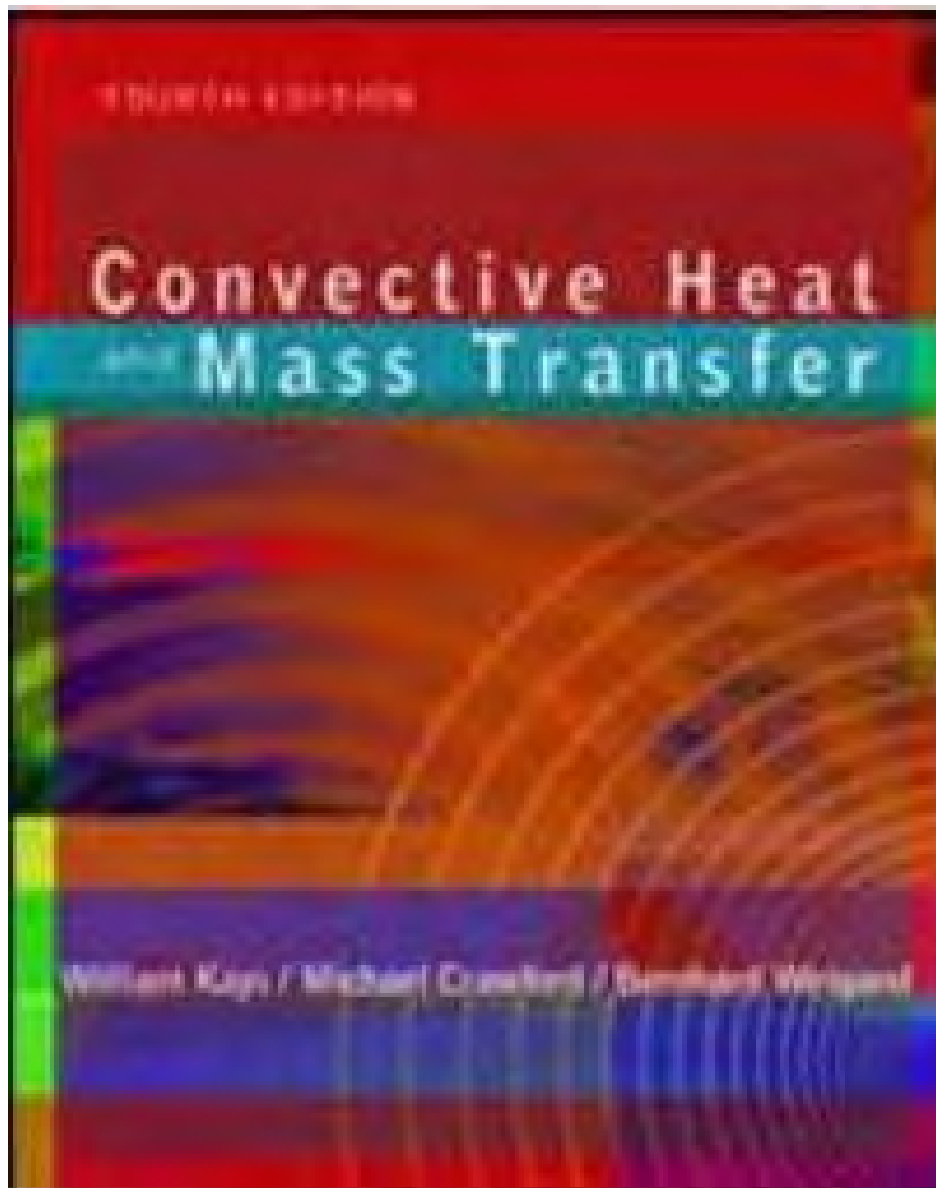
فروشگاه کتاب های الکترونیکی ایبوکو، با هدف فراهم کردن دسترسی آسان و دائمی به کتاب های الکترونیکی در خدمت شماست. در صورت نیاز به کتابی خاص که در وبسایت ایبوکو موجود نمی باشد، می توانید درخواست خود را به آدرس پست الکترونیکی search@ebooko.ir ارسال کنید تا در صورت امکان، در سریعترین زمان به سایت اضافه شود. علاوه بر این، در صورتی که تمایل دارید تا نسخه پرینت و صحافی شده یکی از کتاب های ایبوکو را از طریق پست دریافت کنید، می توانید درخواست خود را به آدرس print@ebooko.ir ارسال کنید.

Solutions Manual

CONVECTIVE HEAT & MASS TRANSFER

4TH EDITION

William M. Kays, Michael E. Crawford & Bernhard Weigand



Solutions Manual to accompany

CONVECTIVE HEAT AND MASS TRANSFER

Fourth Edition

William Kays

Emeritus Professor of Mechanical Engineering
Stanford University

Michael Crawford

Professor of Mechanical Engineering
The University of Texas at Austin

Bernhard Weigand

Professor and Head, Institute of Aerospace Thermodynamics
University of Stuttgart

An Introductory Note

Some of the problems in the text are brief exercises leading to single numerical or algebraic results, but the great majority are much more extensive investigations, some approaching the magnitude of term projects. In the latter cases, there is usually no simple answer. Student initiative is encouraged and this leads to results that may differ numerically or may involve results not asked for in the problem statement. In any case, the authors place more value on a written discussion at the end of the student's papers, and on the development of the analysis, than on numerical results.

It is not practicable to provide a "solutions manual" containing examples of complete papers for assignments of this kind. The authors have chosen rather to provide, in a somewhat abbreviated form, some of the key results for these problems. In some cases rather than give numerical results, a brief discussion of how to attack the problem is provided. Only a small fraction of the problems can be used in any one course, and it is hoped that instructors will find a sufficient number of problems to satisfy a variety of needs, including differing tastes and interests, and differing teaching styles.

4-1

Consider steady flow of a constant-property fluid in a long duct formed by two parallel planes. Consider a point sufficiently far removed from the duct entrance that the y component of velocity is zero and the flow is entirely in the x direction. Write the Navier–Stokes equations for both the x and y directions. What can you deduce about the pressure gradients?

Let $x_1 = x$, $x_2 = y$, $u_1 = u$, and $u_2 = v$ in Eq. (4-17), and the x -direction equation becomes

$$\frac{\partial P}{\partial x} = \frac{\partial^2 u}{\partial x^2}$$

Similarly, the y - direction equation becomes

$$\frac{\partial P}{\partial y} = 0$$

Thus, $P = P(x)$ and $\frac{\partial P}{\partial x} = \frac{dP}{dx}$. The final form of the x -direction equation becomes

$$\frac{dP}{dx} = \mu \frac{d^2 u}{dy^2}$$

4-2

Consider flow in the eccentric annulus of a journal bearing in which there is no axial flow. Deduce the applicable laminar boundary-layer equations (continuity, momentum, energy) for a constant-density fluid, with uniform composition, in an appropriate coordinate system.

Consider the continuity equation (4-5) in cylindrical coordinates with $\nabla \cdot \mathbf{V}$ defined in Appendix D,

$$\nabla \cdot \mathbf{V} = \frac{1}{r} \frac{\partial}{\partial r} (r V_r) + \frac{1}{r} \frac{\partial V_\phi}{\partial \phi} + \frac{\partial V_x}{\partial x} = 0$$

where $V_r = v_r$; $V_\phi = v_\phi$; and $V_x = u$. Let $r = R + y$ and $x = R\phi$, where R is the radius of the inner surface. Note that $\partial/\partial x = 0$ (no axial flow). Thus

$$R \frac{\partial v_r}{\partial y} + y \frac{\partial v_r}{\partial y} + v_r + R \frac{\partial v_\phi}{\partial x} = 0$$

For v_r small and $y \ll R$, the middle two terms in the equation are negligible compared to the first and last terms. Thus the equation becomes identical to (4-7) in Cartesian coordinates. (Actually these are curvilinear coordinates with $y \ll R$). Using similar arguments, the applicable momentum equation is (4-11), with the convective acceleration terms neglected. The applicable energy equation is (4-38).

4-3

Deduce a set of boundary-layer differential equations (continuity, momentum, energy) for steady flow of a constant-property fluid without body forces, and with negligible viscous dissipation, in a coordinate system suitable for analysis of the boundary layer on the surface of a rotating disk.

The appropriate set of coordinates is the fixed, non-rotating cylindrical system with r , the radial direction; ϕ , the circumferential direction; and x , the axial direction above the disk. In the governing equations, all three velocity components will appear, but derivatives with respect to ϕ will be zero due to rotational symmetry.

The flow over a rotating disk is boundary layer in character, but the complete Navier-Stokes equations can be solved in exact form (see Schlichting, ref. 2, page 93). The applicable energy equation is (4-35) with the conduction gradient in the r -direction neglected. (See Schlichting, page 296, for references to heat transfer solutions.)

4-4

Starting with the general viscous energy equation, show by a succession of steps how and why it reduces to the classic heat-conduction equation for a solid, and finally to the Laplace equation.

The applicable energy equation is (4-31). Assume no mass diffusion. Use the definition of enthalpy, $i = e + P/\rho$, and let ρ be constant, yielding

$$\rho \frac{De}{Dt} - \nabla \cdot k \nabla T = S$$

For no fluid motion, the substantial derivative reduces to

$$\rho \frac{\partial e}{\partial t} - \nabla \cdot k \nabla T = S$$

This is the classic heat conduction equation for a solid where the thermal equation of state is $de = cdT$. For steady conduction and constant properties, the Poisson form of the conduction equation is obtained, and when S is equal to zero, the Laplace equation is obtained.

$$\nabla^2 T = \frac{S}{k}$$

4-5

Derive Eq. (4-18) using Eq. (4-1) and the definitions from the Fick's law section of Chap. 3.

Eq. (4-1) can be considered a continuity equation for the j - component of a mixture, but the creation term must be added, resulting in

$$\frac{\partial G_{tot,j,x}}{\partial x} + \frac{\partial G_{tot,j,y}}{\partial y} = \dot{m}_j'''$$

Now substitute $G_{tot,j} = G_{diff,j} + G_{conv,j}$, where $G_{conv,j} = m_j G$ and $G_{diff,j} = -\gamma_j \nabla m_j$. (Recall that G is the total mass flux vector.) Ignore $G_{diff,j,x}$ as a boundary layer approximation and substitute into the continuity equation.

$$m_j \left[\cancel{\frac{\partial G_x}{\partial x}} + \frac{\partial G_y}{\partial y} \right] + G_x \frac{\partial m_j}{\partial x} + G_y \frac{\partial m_j}{\partial y} - \frac{\partial}{\partial y} \left(\gamma_j \frac{\partial m_j}{\partial y} \right) = \dot{m}_j'''$$

4-6

Derive the conservation laws for axisymmetric flow in a pipe using control volume principles similar to that developed in the text for Cartesian coordinate flow. Assume steady flow, steady state, and constant properties. For the momentum equation neglect body forces. For the energy equation neglect body force work and the energy source. Also, for the energy equation use the thermal equation of state for ideal gases or incompressible liquids, and assume the Mach number is small for the case of the ideal gas, but do not neglect viscous dissipation. Assume boundary-layer flow, but do not neglect axial conduction.

For conservation of mass, the terms for mass flow rates (inflow on the radial face and the axial face) are

$$\begin{aligned}\dot{m}_r &= G_r A_r & G_r &= \rho v_r; & A_r &= r d\phi dx \\ \dot{m}_x &= G_x A_x & G_x &= \rho u; & A_x &= r d\phi dr\end{aligned}$$

Application of the procedure leading up to equation (4-2), assuming steady flow, yields

$$\frac{\partial(u\rho)}{\partial x} + \frac{1}{r} \frac{\partial}{\partial r}(r\rho v_r) = 0$$

Note the appearance of r comes from dividing through the equation by the differential volume, $(r d\phi dx)$. For constant properties, Eq. (4-9) is found.

$$\frac{\partial u}{\partial x} + \frac{1}{r} \frac{\partial}{\partial r}(r v_r) = 0$$

For x -momentum, the x -momentum flow rates, inflow on the radial face and the axial face, and the x -forces are

$$\begin{aligned}\dot{M}_r &= u \dot{m}_r = u(G_r A_r) \\ \dot{M}_x &= u \dot{m}_x = u(G_x A_x)\end{aligned}$$

and

$$F_x = -\sigma_x A_x - \tau_{rx} A_r \quad \sigma_x \approx -P \quad \tau_{rx} = \mu \frac{\partial u}{\partial y}$$

Application of the procedure leading up to Eqs. (4-10) and (4-11), assuming steady flow and constant properties yields

$$\rho u \frac{\partial u}{\partial x} + \rho v_r \frac{\partial u}{\partial r} = -\frac{dP}{dx} + \mu \frac{1}{r} \frac{\partial}{\partial r} \left(r \frac{\partial u}{\partial r} \right)$$

For energy, the energy flow rates, inflow on the radial face and on the axial face, and the corresponding heat and work rates are

$$\begin{aligned}\dot{E}_r &= \left(i + \frac{1}{2} u^2 \right) \dot{m}_r = \left(i + \frac{1}{2} u^2 \right) G_r A_r \\ \dot{E}_x &= \left(i + \frac{1}{2} u^2 \right) \dot{m}_x = \left(i + \frac{1}{2} u^2 \right) G_x A_x\end{aligned}$$

and

$$\dot{q}_r = -kA_r \frac{\partial T}{\partial r} \quad \dot{q}_x = -kA_x \frac{\partial T}{\partial x} \quad \dot{W}_{shear,r} = u\tau_{rx}A_r$$

Application of the procedure leading up to Eqs. (4-27) and (4-28), assuming steady flow, no mass diffusion, and constant properties yields

$$\rho u \frac{\partial i}{\partial x} + \rho v_r \frac{\partial i}{\partial r} - \frac{1}{r} \frac{\partial}{\partial r} \left(kr \frac{\partial T}{\partial r} \right) - \mu \left(\frac{\partial u}{\partial r} \right)^2 - u \frac{dP}{dx} = 0$$

and for ideal gases and incompressible liquids, using the approximations similar to the development leading to Eq. (4-38), but retaining the pressure gradient term the enthalpy equation reduces to

$$u \frac{\partial T}{\partial x} + v_r \frac{\partial T}{\partial y} - \alpha \frac{1}{r} \left[\frac{\partial}{\partial r} \left(r \frac{\partial T}{\partial r} \right) \right] - \frac{\text{Pr}}{c} \left(\frac{\partial u}{\partial r} \right)^2 - \frac{1}{\rho c} \frac{dP}{dx} = 0$$

4-7

Derive the constant-property energy equation (4-39) starting with Eq. (4-26). Be sure to state all assumptions made.

These steps are basically the redevelopment of the formulation leading up to Eq. (4-39).

5-1

Develop a momentum integral equation for steady flow without blowing or suction for use in the entry region of a circular tube. Note that Eq. (5-4) is not applicable for this case because it has been assumed that the boundary-layer thickness is small relative to the body radius R ; in the present case the boundary layer ultimately grows to the centerline of the tube.

Let $r = R$ be the wall and $r = y$ be the edge of the control volume where the velocity becomes the inviscid core velocity of the developing flow. Typical terms would be

$$M_x = 2\pi \int_{R-y}^R \rho u^2 r dr \quad \text{and} \quad M_y = (R-y) 2\pi \delta x v_y \rho_y u_y$$

$$\text{Normal stress} = P \int_{R-y}^R 2\pi r dr$$

$$\text{Shear stress :} \quad \tau_s 2\pi R \delta x; \quad \tau_y 2\pi (R-y) \delta x$$

Now follow the procedure on pages 42-43,

$$-\tau_s = \frac{1}{R} \frac{d}{dx} \left[\int_{R-y}^R \rho u^2 r dr \right] - \frac{u_{core}}{R} \frac{d}{dx} \left[\int_{R-y}^R \rho u r dr \right] - (\rho u)_{core} y \left(1 - \frac{y}{2R} \right) \frac{du_{core}}{dx}$$

5-2

Develop the corresponding energy integral equation for Prob. 5-1.

Let $r = R$ be the wall and $r = y$ be the edge of the control volume where the enthalpy is the core enthalpy. Neglect the kinetic energy term, and note that there is no wall transpiration. Typical terms would be

$$\dot{E}_{conv,x} = 2\pi \int_{R-y}^R \rho u (i - i_{core}) r dr$$

$$\dot{q}_s = 2\pi R \delta x \dot{q}_s''$$

Now follow the procedure on pages 47-48,

$$-\dot{q}_s'' = \frac{1}{R} \frac{d}{dx} \int_{R-y}^R (i - i_{core}) r dr$$

5-3

Develop a boundary-layer integral equation for the diffusion of component j in a multicomponent mixture.

Assume: Fick's Law holds; steady flow; concentration boundary layer \geq momentum boundary layer thickness; y -direction gradients \gg x -direction gradients; G at $y = 0$ is in y -direction. Let $m_{j,s}$ be the mass concentration of j at the wall. For the j -component, typical terms are

$$\text{Inflow of } j = \int_0^y G_x m_j dy + G_{y,s} m_{j,s} \delta x - \gamma_j \left(\frac{dm_j}{dy} \right)_s \delta x$$

$$\text{Rate of creation of } j = \int_0^y \dot{m}_j''' \delta x dy$$

The conservation principle that Outflow - Inflow + Increase in Storage = Rate of Creation for specie j is used to obtain the integral equation. Continuity Eq. (5-1) is used and $m_{j,y} = m_{j,\infty}$. Then,

$$-\gamma_j \left(\frac{\partial m_j}{\partial y} \right)_s = \frac{d}{dx} \left[\int_0^y \rho u (m_j - m_{j,\infty}) dy \right] - \rho_s v_s (m_{j,s} - m_{j,\infty}) - \int_0^y \dot{m}_j''' dy$$

5-4

Derive the momentum integral equation (5-8) and the energy integral equation (5-21).

These steps are essentially a repeat of the formulation leading up to Eq. (5-8) and Eq. (5-21).

6-1

Using appropriate assumptions, reduce Eq. (6-9) to compare it with Eq. (4-17).

Note that Eqs. (6-9) and (4-17) are both unsteady forms of the Navier-Stokes equations written in index notation, although (6-9) is for compressible flow with variable viscosity, whereas (4-17) is for constant density flow with constant viscosity. Their forms differ in the convection term and in the stress (or diffusion) term. The form of the convective term in (6-9) is called the conservative form. Chain-rule differentiate the convective term of (6-9) and subtract from it (6-8) to modify the convection term, then assume constant density for the time term. This recovers the left hand side of (4-17). Now, substitute the stress tensor, (6-6) into (6-9) and substitute (6-3) for the strain-rate tensor. Assume constant viscosity and constant density. For constant density flow, the second coefficient of viscosity (the dilatation term) is eliminated. The second term in the strain rate tensor also disappears from the conservation of mass (assuming constant density), and the result is the right hand side of (4-17).

6-2

Convert Eq. (6-11) to Eq. (4-32) using the definition of the substantial (or total) derivative.

Note that Eq. (6-11) is a stagnation enthalpy equation, whereas (4-32) is a static enthalpy equation. Multiply Eq. (6-10) by u and subtract it from (6-11). Note that you will first have to chain-rule the viscous work term in (6-11) to obtain the unsteady static enthalpy equation. Now, substitute (6-6) along with the strain-rate tensor (6-3) into the static enthalpy equation. The result is (4-32).

6-3

Carry out the necessary algebra to show that Eqs. (6-16) represent the appropriate decompositions for the stagnation enthalpy.

We combine the definition of stagnation enthalpy following Eq. (6-11),

$$i^* = e + \frac{P}{\rho} + \frac{1}{2} u_i u_i = i + \frac{1}{2} u_i u_i$$

and the two Reynolds decompositions given by Eq. (6-15)

$$i^* = \overline{i^*} + i^{*'}, \quad i = \bar{i} + i'$$

Combining these, along with the Reynolds decomposition for u_i yields

$$i^* = i + \frac{1}{2} u_i u_i = \bar{i} + i' + \frac{1}{2} (\bar{u}_i + u'_i)(\bar{u}_i + u'_i)$$

Now, expand the velocity term

$$i^* = \bar{i} + i' + \frac{1}{2} (\bar{u} \bar{u}) + (\bar{u}_i u'_i) + \frac{1}{2} (u' u'_i)$$

and collect the time-averaged terms and the fluctuating terms. The result is (6-16), similar to what is found in Ref. 1.

6-4

Using the averaging rules, develop the conservation-of-mass equation (6-21), including all the intermediate steps.

These steps are essentially a repeat of the formulation leading up to Eq. (6-21).

6-5

Reduce Eq. (6-26) to the boundary-layer equation (6-28) using appropriate assumptions.

The first step is to chain-rule the conservative form of the convective term that appears in Eq. (6-26) and apply the conservation of mass equation (6-22). Then apply the index notation rule that repeated subscripts sum, $j = 1, 2$. Note there will not be third term ($j = 3$) because of the two-dimensional boundary layer assumption ($w = 0$). The pressure gradient becomes an ordinary derivative. The diffusion operator changes under the boundary layer assumptions to

$$\frac{\partial(\quad)}{\partial x_j} \rightarrow \frac{\partial(\quad)}{\partial y}$$

In the viscous stress tensor, τ_{ji} , only one term will be present, due to the boundary layer approximation and the constant density assumption. This also applies to the Reynolds stress term. The result is:

$$(\tau_{ji} - \rho \overline{u'_j u'_i}) \rightarrow (\tau_{yx} - \rho \overline{v' u'})$$

This stress is $\tau (= \tau_{yx})$ in Eq. (6-27). Now divide through by the density, and the constant density assumption allows the density to be moved into the diffusion term; μ becomes ν , and the density is removed from the Reynolds stress. Note Eq. (6-28) remains valid for variable viscosity, but not for variable density.

6-6

Derive the stagnation enthalpy equation (6-31), and reduce it to its low-velocity, constant-property boundary-layer form given by Eq. (6-34).

These steps are essentially a repeat of the formulation leading up to Eq. (6-31), followed by the formulation leading to Eq. (6-34). Eq. (6-34) is valid for either an ideal gas or an incompressible liquid (both obeying $de = c \, dT$), and it is valid for variable thermal conductivity, but not for variable density.

6-7

Carry out the derivation of the turbulence kinetic energy equation (6-38).

These steps are essentially a repeat of the formulation leading up to Eq. (6-38).

6-8

The construction of the boundary-layer equations for momentum and energy can be considered using the formulation of Eq. (6-39). Recast the laminar boundary-layer equations for momentum, Eq. (4-10), and energy Eq. (4-39), and their turbulent counterparts, Eqs. (6-28) and (6-34), into the form given by Eq. (6-39) to identify the convection, diffusion, and source terms for each equation.

The structure of the equations follow the format of Eq. (6-39)

$$\text{convection } (\phi) = \text{diffusion } (\phi) \pm \text{source } (\phi)$$

where ϕ is the dependent variable. Rewriting momentum equation (4-10) in this form yields

$$\rho u \frac{\partial u}{\partial x} + \rho v \frac{\partial u}{\partial y} = \frac{\partial}{\partial y} \left(\mu \frac{\partial u}{\partial y} \right) - \frac{dP}{dx}$$

The energy equation (4-39) needs to first be rewritten in variable-property form similar to Eq. (4-37), and then formulated like the momentum equation.

$$u \frac{\partial T}{\partial x} + v \frac{\partial T}{\partial y} = \frac{\partial}{\partial y} \left(\alpha \frac{\partial T}{\partial y} \right)$$

Then, a form similar to Eq. (6-28) results by including the Reynolds stress term,

$$\bar{u} \frac{\partial \bar{u}}{\partial x} + \bar{v} \frac{\partial \bar{u}}{\partial y} = \frac{\partial}{\partial y} \left(\nu \frac{\partial \bar{u}}{\partial y} - \overline{u'v'} \right) - \frac{1}{\rho} \frac{d\bar{P}}{dx}$$

A similar form to Eq. (6-34) results by including the Reynolds heat flux term.

$$\bar{u} \frac{\partial \bar{T}}{\partial x} + \bar{v} \frac{\partial \bar{T}}{\partial y} = \frac{\partial}{\partial y} \left(\alpha \frac{\partial \bar{T}}{\partial y} - \overline{v'T'} \right)$$

Note that both the momentum equation and energy equations have a convective term and a diffusive term, but only the momentum equation has a source term. An equivalent energy source term would be a viscous dissipation term, which could be added.

7-1

Consider steady, laminar, constant-property flow in a duct formed by two parallel planes. Let the velocity be uniform at the duct entrance. Calculate the development of the velocity profile in the entry length, using the momentum integral equation (6-4), and an assumption that the velocity profile may be approximated by a constant-velocity segment across the center portion of the duct and by simple parabolas in the growing boundary layer adjacent to the surfaces. Note that the mean velocity, Eq. (7-3), must be a constant, and thus Eq. (7-4) must be satisfied. [Some help in this problem may be obtained from an examination of the development of the momentum integral equation, Eq. (5-8).] Evaluate the hydrodynamic entry length and compare with Eq. 7-23).

Let the plate spacing of the channel be a and measure y from the plate surface. Reformulate the integral equation (5-4) for a non-axisymmetric geometry (eliminate R) and no transpiration into the boundary layer at the surface ($v_s = 0$),

$$-\tau_s = \frac{d}{dx} \left(\int_0^y \rho u^2 dy \right) - u_{core} \frac{d}{dx} \left(\int_0^y \rho u dy \right) + \int_0^y \left(-\rho u_{core} \frac{du_{core}}{dx} \right) dy$$

where “core” symbol replaces the “ ∞ ” symbol. For a velocity profile, consider first the parabola, $\frac{u}{u_{core}} = a + b \left(\frac{y}{\delta} \right) + c \left(\frac{y}{\delta} \right)^2$. Three boundary conditions are needed to determine a, b, c . The first will be the boundary condition of no-slip, $u(y=0) = 0$. The other two come by applying boundary conditions at the edge of the developing boundary layer within the channel, i.e. the flow between the surface ($y=0$) and the core flow ($y=\delta$). Thus, $u(y=\delta) = u_{core}$ and du/dy at ($y=\delta$) = 0. The resulting profile is

$$\frac{u}{u_{core}} = 2 \left(\frac{y}{\delta} \right) - \left(\frac{y}{\delta} \right)^2$$

The velocity profile is substituted into the integrals of the integral equation. The wall shear stress must also be evaluated, following the idea of Eq. (7-9), and using Eq. (3-1). The resulting momentum integral equation becomes

$$2\nu \left(\frac{u_{core}}{\delta} \right) = \frac{3}{5} \left(\delta u_{core} \frac{du_{core}}{dx} \right) + \frac{2}{15} \left(u_{core}^2 \frac{d\delta}{dx} \right)$$

Now, conservation of mass (continuity) must be applied to the channel, assuming constant density,

$$Va = \left(\frac{\dot{m}}{\rho A_c} \right) a = \text{constant} = 2 \int_0^\delta u dy + 2u_{core}(x) \left(\frac{a}{2} - \delta \right)$$

and, by substituting the parabolic profile into the integral,

$$u_{core} = \frac{V}{\left(1 - \frac{2}{3} \frac{\delta}{a} \right)} \quad \text{and} \quad \frac{du_{core}}{dx} = \frac{V}{\frac{3}{2} a \left(1 - \frac{2}{3} \frac{\delta}{a} \right)^2} \frac{d\delta}{dx}$$

This provides the relationship between the mass-averaged velocity of the channel, V , and the local core velocity. Note that this equation shows how the effect of the no-slip condition (leading to the velocity profile) causes the core velocity to increase, eventually becoming centerline velocity $u_{core} = u(y=a/2) = 1.5V$ for laminar, constant-density flow in a parallel-planes channel.

Now comes lots of algebra and plenty of chances to make mistakes. Substituting for the core velocity (and its derivative into the momentum integral equation leads to

$$30\nu = \left(\frac{3}{2}aV\right) \left[\frac{3a\delta + 7\delta^2}{\left(\frac{3}{2}a - \delta\right)^2} \right] \frac{d\delta}{dx}$$

Note, here one can separate variables and integrate. Hint: the integrand can be split into two integrals of the form

$$I_1 = \int_0^\eta \frac{\eta}{(\alpha + \beta\eta)^2} d\eta = \frac{1}{\beta^2} \left[\ln(\alpha + \beta\eta) + \frac{\alpha}{\alpha + \beta\eta} \right]_0^\eta$$

$$I_2 = \int_0^\eta \frac{\eta^2}{(\alpha + \beta\eta)^2} d\eta = \frac{1}{\beta^3} \left[(\alpha + \beta\eta) - 2\alpha \ln(\alpha + \beta\eta) - \frac{\alpha^2}{\alpha + \beta\eta} \right]_0^\eta$$

The lower limit of integration will be $\delta(x=0) = 0$ and the upper limit will be $\delta(x = x_{fd}) = a/2$, and the result is

$$\frac{2\nu x_{fd}}{aV} = 0.10376748(a/2)$$

Now reformulate the expression in terms of the hydraulic diameter Reynolds number (Eq. 7-17), where $D_h = 2 \times \text{plate spacing} = 2a$, leading to

$$\frac{x_{fd}}{D_h} = 16(0.10376748) \text{Re}_{D_h} = \frac{\text{Re}_{D_h}}{154}$$

This result, $(x/D_h)/\text{Re}_{D_h} = 0.0065$, is quite small compared to the published solution for a circular pipe, Eq. (7-23), $(x/D_h)/\text{Re}_{D_h} = 0.05$

Note, had we assumed a sinusoidal shape for the velocity profile (often considered in viscous fluid mechanics texts, along with the parabolic-profile boundary conditions,

$$\frac{u}{u_{core}} = \sin\left(\frac{\pi}{2} \frac{y}{\delta}\right)$$

and the result would be similar (within 5%).

7-2

Starting with the momentum theorem, develop Eq. (7-19) for the pressure drop in steady flow of a constant-property fluid in a tube of constant cross-sectional shape as a function of the friction coefficient, mean velocity, and tube length. Start with a control volume that is of infinitesimal dimension in the flow direction but that extends across the entire flow section. Then reconsider the problem when fluid density varies in some known manner along the tube but can be considered as effectively constant over the flow cross section. Discuss the implications of the latter assumption.

This problem can be solved two ways. The first method involves partially integrating the differential momentum equation over the flow cross-section. Reformulate Eq. (4-11) into its conservative form by combining it with the continuity equation (4-8), and by recasting the shear stress term back into its stress form

$$\frac{\partial(\rho uu)}{\partial x} + \frac{\partial(\rho v_r u)}{\partial r} = -\frac{dP}{dx} + \frac{1}{r} \frac{\partial}{\partial r}(r \tau_{rx})$$

Then, integrate the momentum equation in a manner similar to how we formulate an integral equation in Chapter 5, namely differential in the flow direction (x) and integrally in the cross-flow direction, from the surface to the centerline of the channel (or over the flow cross-section).

$$\int \left(\frac{\partial(\rho uu)}{\partial x} \right) dA_c dx + \int \left(\frac{\partial(\rho v_r u)}{\partial r} \right) dA_c dx = \int \left(-\frac{dP}{dx} \right) dA_c dx + \frac{1}{r} \int \left(\frac{\partial}{\partial r}(r \tau_{rx}) \right) dA_c dx$$

where dA_c would be $(2\pi r dr)$ for a circular pipe. Now recognize that the cross-stream convective term is zero at the surface and at the channel (or pipe) centerline, reducing the equation to

$$\int_{x_1}^{x_2} (\rho uu) dA_c = [P(x_2) - P(x_1)] A_c + \int_{x_1}^{x_2} \tau_{rx} dx$$

The second method is the control volume formulation, similar to that used in Chapter 5 for the momentum integral equation (pp 41-43),

$$M_{x+\delta x} - M_x = -(\tau_s dA_s) + (PA_c)_x - (PA_c)_{x+\delta x}$$

or

$$dM_x = d\left(\int u dm\right) = d\left(\int \rho u^2 dA_c\right) = -\tau_s dA_s - d(PA_c)$$

where for a circular pipe $dA_s = \pi D dx$ and A_c is the flow cross-sectional area. Note the similarity to Eq. (7-10) when the flow is assumed to be fully-developed flow, and $dM_x=0$.

Now redefine τ_s in terms of the definition of c_f from Eq. (7-13) and integrate between two flow locations "1" and "2" representing the flow distance from $x_1=0$ (the entry location) to some arbitrary x -location, x_2 ,

$$\begin{aligned} \int_1^2 \rho u^2 dA_c &= -\int_1^2 \tau_s \pi D dx - [(PA_c)_2 - (PA_c)_1] \\ \int \rho u^2 dA_c - \rho V^2 A_c &= -\int_1^2 c_f \left(\frac{1}{2} \rho V^2 \right) \pi D dx - [(PA_c)_2 - (PA_c)_1] \end{aligned}$$

where the wall shear stress has been replaced by the local friction coefficient from Eq. (7-13). Rearranging, assuming constant density, and dividing through by the dynamic pressure term yields Eq. (7-19),

$$\frac{(P_2 - P_1)}{\frac{1}{2}\rho V^2} = \frac{\Delta P}{\frac{1}{2}\rho V^2} = c_{f,m} \frac{x}{(D_h/4)} + \frac{2}{A_c} \int \left(\frac{u}{V}\right)^2 dA_c - 2$$

where D_h is the hydraulic diameter ($D_h=D$ for a circular pipe). Note the introduction of the mean friction coefficient from Eq. (7-20).

For the case where x_1 and x_2 are both beyond the fully-developed location, the momentum equation can be written as

$$\int_1^2 d(\dot{m}V) = -\int_1^2 \tau_s dA_s - \int_1^2 d(PA_c)$$

Integration, use of the continuity equation (7-3) and rearranging leads to

$$\dot{m}^2 \left[\frac{1}{\rho_2 A_c} - \frac{1}{\rho_1 A_c} \right] = - \left[c_{f,m} \frac{1}{2} \frac{\dot{m}^2}{\bar{\rho}} \frac{A_s}{A_c^2} \right] - [(P_2 - P_1) A_c]$$

where $\bar{\rho} = \frac{1}{A_s} \int \rho dA_s$ is the average density over the flow distance from x_1 to x_2 . Further rearrangement leads to

$$(P_2 - P_1) = \Delta P = \frac{\dot{m}^2}{2A_c^2} \left[c_{f,m} \frac{1}{\bar{\rho}} \frac{A_s}{A_c} + 2 \left(\frac{1}{\rho_2} - \frac{1}{\rho_1} \right) \right]$$

Here one can see the effect of density variation on the flow, while neglecting the extra pressure drop in the entry region due to acceleration. Note that a change in density will lead to a change in Reynolds number.

7-3

Consider fully developed laminar flow of a constant-property fluid in a circular tube. At a particular flow cross section, calculate the total axial momentum flux by integration over the entire cross section. Compare this with the momentum flux evaluated by multiplying the mass flow rate times the mean velocity. Explain the difference, then discuss the implications for the last part of Prob. 7-2.

For fully-developed flow in a circular tube, the velocity profile is given by Eq. (7-8), where the mean velocity is given by Eq. (7-7). The momentum flow through a flow area is defined by the product of the mass flow rate through the cross-sectional area and the velocity component normal to that area,

$$M_x = \int u dm = \int_0^{r_s} \rho u^2 2\pi r dr = \int_0^{r_s} \rho \left[2V \left(1 - \frac{r^2}{r_s^2} \right) \right]^2 2\pi r dr = \rho V^2 \pi \frac{4}{3} r_s^2$$

and the mass flow rate is given by

$$\dot{m} = \int dm = \int_0^{r_s} \rho u 2\pi r dr = \int_0^{r_s} \rho \left[2V \left(1 - \frac{r^2}{r_s^2} \right) \right] 2\pi r dr = \rho V \pi r_s^2$$

When we talk about 1-dimensional flow, such as in the subjects of thermodynamics or compressible flow, we assume there is a characteristic velocity that represents the flow cross-sectional area, defined from the continuity equation,

$$V = \frac{\dot{m}}{\rho A_c}$$

where the density is assumed constant over the cross-section. If the velocity is uniform over the cross-sectional area, $u(r) = V$, then

$$M_x = \int u dm = V \dot{m} = V \rho V \pi r_s^2 = \rho V^2 \pi r_s^2$$

Comparing these two results, we find that the actual momentum flow rate differs from the one-dimensional flow rate by a factor of 4/3. Or, when $u(r)$ exists, then at a given x -location

$$M_x = \int u dm = \int \rho u^2 dA_c \neq V \dot{m}$$

Therefore, if we assumed a 1-dimensional flow approach we could not obtain the last term of Eq. (7-19), which represents the contribution to the pressure drop due to flow acceleration (kinetic energy change) as the profile changes shape from x_1 to x_2 .

7-4

Two air tanks are connected by two parallel circular tubes, one having an inside diameter of 1 cm and the other an inside diameter of 0.5 cm. The tubes are 2 m long. One of the tanks has a higher pressure than the other, and air flows through the two tubes at a combined rate of 0.00013 kg/s. The air is initially at 1 atm pressure and 16°C. Assuming that fluid properties remain constant and that the entrance and exit pressure losses are negligible, calculate the pressure differences between the two tanks.

For the 2 tubes in parallel between the two tanks, the theory will be

$$\begin{aligned}\dot{m}_1 + \dot{m}_2 &= 0.00013 \text{ kg / s} \\ \Delta P_1 = \Delta P_2 &= \left(\frac{1}{2} \rho V^2 \right) \bar{c}_{f,app} \frac{4x}{D} = \left(\frac{\dot{m}^2}{2 \rho A_c^2} \right) \bar{c}_{f,app} \frac{4x}{D} \\ \text{Re}_D &= \frac{\rho V D}{\mu} = \frac{\left(\dot{m} / A_c \right) D}{\mu} = \frac{4 \dot{m}}{\pi \mu D}\end{aligned}$$

The procedural steps will be:

- (a) arbitrarily select a mass flow rate for the larger tube
- (b) compute the Re for each tube
- (c) compute the parameter $x^+ = (x/D)/\text{Re}$ for each tube
- (d) using Figure 7-7, find the value of $c_{f,app}$ for each tube
- (e) compute the pressure drop for each tube
- (f) iterate the mass flow of the larger tube until the pressure drops balance

Answers:

- (a) mass flow rate for the larger tube is about 89% of the total mass flow
- (b) Re for the larger and smaller tubes will be about 820 and 200 respectively
- (c) pressure drop is about 15.2 Pa (for each tube)

note: for both flows $\text{Re}/(x/D) < 6$ or $x^+ > 0.17$ so the flow is fully-developed

therefore, Figure 7-7 is not needed, and $c_{f,app} \cdot \text{Re} = 17.5$ is ok to use

7-5

A particular heat exchanger is built of parallel plates, which serve to separate the two fluids, and parallel continuous fins, which extend between the plates so as to form rectangular flow passages. For one of the fluids the plate separation is 1 cm and the nominal fin separation is 2 mm. However, manufacturing tolerance uncertainties lead to the possibility of a 10 percent variation in the fin separation. Consider the extreme case where a 10 percent oversize passage is adjacent to a 10 percent undersize passage. Let the flow be laminar and the passages sufficiently long that an assumption of fully developed flow throughout is reasonable. For a fixed pressure drop, how does the flow rate differ for these two passages and how does it compare to what it would be if the tolerance were zero?

Note, this problem requires D to be replaced by D_h , the hydraulic diameter. Note also, we can use Eq. (7-21) for the pressure drop. For this problem, the assumption of fully-developed flow is made, and Figure 7-4 can be used to determine $(c_f \text{Re})$ for these rectangular heat exchanger passages.

$$\alpha^* = \frac{b}{a} = \frac{1 \text{ cm}}{0.2 \text{ cm}} = 5 \quad \frac{1}{\alpha^*} = 0.2 \quad (c_f \text{Re})_\infty = 19.1$$

$$D_h = \frac{4A_c}{\text{perimeter}} = \frac{4(ab)}{2a+2b} = \frac{4a}{2\frac{a}{b}+2} = 1.67a$$

$$\text{Re}_{D_h} = \frac{\rho V D_h}{\mu} = \frac{\left(\frac{\dot{m}}{A_c}\right) D_h}{\mu} = \frac{\dot{m}(1.67a)}{(a \cdot b)\mu} = \frac{1.67\dot{m}}{\mu b}$$

The pressure-drop for a passage becomes

$$\Delta P = \left(\frac{1}{2}\rho V^2\right) \bar{c}_{f,app} \frac{4x}{D} = \left(\frac{\dot{m}^2}{2\rho A_c^2}\right) \bar{c}_{f,app} \frac{4x}{D}$$

$$= \left(\frac{\dot{m}^2}{2\rho A_c^2}\right) \left[\frac{(c_f \text{Re}_{D_h})_\infty}{\text{Re}_{D_h}}\right] \frac{4x}{D_h} = \frac{\dot{m}^2 (c_f \text{Re}_{D_h})_\infty (0.717)x}{\rho a^3 b}$$

Thus, for two parallel passages having the same pressure drop,

$$\Delta P = \frac{\dot{m}_1^2}{a_1^3} \left[\frac{(c_f \text{Re}_{D_h})_\infty (0.717)x}{\rho b}\right] = \frac{\dot{m}_2^2}{a_2^3} \left[\frac{(c_f \text{Re}_{D_h})_\infty (0.717)x}{\rho b}\right]$$

or

$$\frac{\dot{m}_2}{\dot{m}_1} = \left(\frac{a_2}{a_1}\right)^{3/2} = \left(\frac{1.1a}{0.9a}\right)^{3/2} = 1.35$$

A 10 percent oversize of one partition and a 10 percent undersize of an adjacent partition results in a 35 percent difference in the mass flow rates, the higher flow rate in the larger passage.

7-6

Develop the analysis that leads to the linear shear stress distribution described by Eq. (7-12).

These steps are essentially a repeat of the formulation leading up to Eq. (7-12). Define a control volume, such as in Fig. 7-2, assuming fully-developed flow. Identify all of the forces on the control volume surface (pressure and axial shear stress, τ_{rx}). Note that there will be no momentum flux difference into and out of the control volume because of the fully-developed assumption. Applying the momentum theorem Eq. (2-4) leads to the Eq. (7-10). Applying this for $r=r_s$ gives Eq. (7-11). Forming the ratio of Eq. (7-10) to Eq. (7-11) gives Eq. (7-12). This is a very important result for internal flows, because it applies to both laminar and turbulent pipe flow. An alternative solution is to derive the velocity profile for pipe flow, Eq. (7-8) and then form the shear stress for an arbitrary r location and at $r=r_s$, Eq. (7-9). Then forming the ratio of these shear stresses yields Eq. (7-12).

7-7

Using the methodology developed in the text for a circular pipe, develop the fully developed mean velocity profile and fully developed friction coefficient for the flow between parallel planes. Compare your friction result with Fig. 7-4 and Fig. 7-5.

For the parallel-planes geometry y is measured from the centerline and the channel is of width a . Assume fully-developed laminar flow with constant properties. The appropriate boundary layer equation is (4-10),

$$\rho u \frac{\partial u}{\partial x} + \rho v \frac{\partial u}{\partial y} = -\frac{dP}{dx} + \frac{\partial}{\partial y} \left(\mu \frac{\partial u}{\partial y} \right)$$

and for fully-developed flow, $\partial u / \partial x = 0$ and $v=0$, reducing the momentum equation to an ordinary differential equation and boundary conditions

$$\frac{dP}{dx} = \frac{d}{dy} \left(\mu \frac{du}{dy} \right)$$

with boundary conditions of velocity profile symmetry at the channel centerline, and no-slip at the channel surfaces.

$$\left. \frac{du}{dy} \right|_{y=0} = 0 \quad \text{and} \quad u|_{y=\pm a/2} = 0$$

Because the pressure gradient is a constant in the axial flow direction, we can separate variables and integrate, and apply the boundary conditions, leading to the parallel-planes channel velocity profile,

$$u = \frac{h^2}{2\mu} \left(1 - 4 \frac{y^2}{a^2} \right) \left(-\frac{dP}{dx} \right)$$

Note the similarity to Eq. (7-2) for the circular pipe, namely a parabolic profile shape. Next, we create the mean velocity, following Eq. (7-5) for constant density,

$$V = \frac{1}{A_c} \int_{A_c} u \, dA_c = \frac{1}{(a \cdot 1)} \int_{-a/2}^{+a/2} u \, dy = \frac{a^2}{12\mu} \left(-\frac{dP}{dx} \right)$$

where the cross-sectional area is per unit depth. Again, note the similarity to Eq. (7-7) for the circular pipe. Creating the ratio of the velocity profile to the mean velocity yields

$$\frac{u}{V} = \frac{3}{2} \left(1 - 4 \frac{y^2}{a^2} \right)$$

Now evaluate the surface friction, following Eq. (7-9),

$$\tau|_{y=h} = \tau_s = \frac{-6\mu V}{a}$$

Compare this result to Eq. (7-9) for the circular pipe. Now follow the procedure of Eq. (7-13) to form the friction coefficient, considering the absolute value of the shear stress to preserve the fact that the surface shear is in the direction opposite of the flow.

$$|\tau_s| = \frac{6\mu V}{a} = c_f \frac{\rho V^2}{2} \quad \text{or} \quad c_f = \frac{12\mu}{\rho Va} = \frac{24}{\text{Re}_{D_h}}$$

where the hydraulic diameter in the Reynolds number is twice the plate spacing. Comparing the result to Fig. 7-4 for $\alpha^* = b/a \rightarrow \infty$ (the parallel plate case where $b \gg a$, shows $(c_f \text{Re})_\infty = 24$. Note that the “infinity” symbol in Fig. 7-4 implies hydrodynamically fully developed flow. In Fig. 7-5, the radius ratio $r^* \rightarrow 1$ is the limiting geometry of the annulus when the inner and outer radii are almost the same, creating a parallel-planes geometry. Note this is the geometry of journal bearings.

7-8

Repeat Prob. 7-7 for an annulus with radius ratio r^* . Compare your velocity-profile result with Eq. (8-26) and your friction result with Fig. 7-5 and Shah and London.³

For the annulus geometry r is measured from the centerline of the inner pipe, r_i is the radius of the inner pipe, r_o is the radius of the outer pipe, and r^* is the radius ratio, $r^* = r_i/r_o$. Assume fully-developed laminar flow with constant properties. The appropriate boundary layer equation is (4-11),

$$\rho u \frac{\partial u}{\partial x} + \rho v_r \frac{\partial u}{\partial r} = -\frac{dP}{dx} + \frac{1}{r} \frac{\partial}{\partial r} \left(r \mu \frac{\partial u}{\partial r} \right)$$

and for fully-developed flow, $\partial u / \partial x = 0$ and $v_r = 0$, reducing the momentum equation to an ordinary differential equation and boundary conditions

$$\frac{dP}{dx} = \frac{1}{r} \frac{d}{dr} \left(\mu r \frac{du}{dr} \right)$$

with boundary conditions of no-slip at the channel surfaces.

$$u|_{r=r_i} = 0 \quad \text{and} \quad u|_{r=r_o} = 0$$

Because the pressure gradient is a constant in the axial flow direction, we can separate variables and integrate, and apply the boundary conditions, leading to the annular channel velocity profile,

$$u = \frac{r_o^2}{4\mu} \left[1 - \left(\frac{r}{r_o} \right)^2 + B \ln \left(\frac{r}{r_o} \right) \right] \left(-\frac{dP}{dx} \right)$$

where

$$B = \frac{(r^{*2} - 1)}{\ln(r^*)}$$

Note the approximate similarity to Eq. (7-2) for the circular pipe. However, it is somewhat parabolic but it has an extra logarithmic term. For flow in the annular space between two concentric pipes, there will be a peak in the velocity profile, and it is located at r_m (compared to the centerline for the pipe and parallel-planes channel). Next, we create the mean velocity, following Eq. (7-5) for constant density,

$$V = \frac{1}{A_c} \int_{A_c} u \, dA_c = \frac{1}{\pi(r_o^2 - r_i^2)} \int_{r_i}^{r_o} u 2\pi r \, dr = \frac{r_o^2}{8\mu} M \left(-\frac{dP}{dx} \right)$$

where $M = (1 + r^{*2} - B)$. Again, note the approximate similarity to Eq. (7-7) for the circular pipe.

Creating the ratio of the velocity profile to the mean velocity yields an equation similar in form to Eq. (8-26),

$$\frac{u}{V} = \frac{2}{M} \left[1 - \left(\frac{r}{r_o} \right)^2 + B \ln \left(\frac{r}{r_o} \right) \right]$$

We can also derive the maximum velocity for the profile by setting

$$\left. \frac{\partial u}{\partial r} \right|_{r=r_m} = 0$$

where

$$r_m^* = \frac{r_m}{r_o} = \left[\frac{1 - r^{*2}}{2 \ln(1/r^*)} \right]^{1/2}$$

leading to

$$\frac{u_{\max}}{V} = \frac{2 \left(1 - r_m^{*2} + 2 r_m^{*2} \ln(r_m^*) \right)}{\left(1 + r^{*2} - 2 r_m^{*2} \right)}$$

Now evaluate the surface friction for each surface, following Eq. (7-9), but with sign convention that reflects the profile behavior for annular flow.

$$\begin{aligned} \tau_i &= -\mu \left. \frac{\partial u}{\partial r} \right|_{r=r_i} = \frac{-2\mu V}{M} \left(\frac{-2r^*}{r_o} + \frac{B}{r_i} \right) \\ \tau_o &= +\mu \left. \frac{\partial u}{\partial r} \right|_{r=r_o} = \frac{2\mu V}{M} \left(\frac{-2}{r_o} + \frac{B}{r_o} \right) \end{aligned}$$

and formulate an area-weighted average of the friction coefficient, based on the inner surface, A_i , and the outer surface, A_o , described on p. 71

$$c_f = \frac{\tau_i A_i + \tau_o A_o}{\rho V^2 / 2} = \frac{(r_i \tau_i + r_o \tau_o)}{(r_i + r_o) \rho V^2 / 2} = \frac{4\mu V}{M} \frac{(2r^{*2} - B - 2 + B)}{(r_i + r_o) \rho V^2}$$

Define the hydraulic diameter for the annulus, following Eq. (7-17), $D_h = 2(r_o - r_i)$, and transform the friction coefficient,

$$c_f = \frac{12\mu}{\rho V h} = \frac{\frac{16}{M} (1 - r^*)^2}{\text{Re}_{D_h}}$$

The result can be directly compared to Fig. 7-5.

7-9

TEXSTAN analysis of laminar entry flow in a circular pipe: Let the Reynolds number be 1000, and pick fluid properties that are appropriate to the Prandtl number of air or water. You can choose how to set up the TEXSTAN problem in terms of values for the geometrical dimensions and mean velocity for the pipe to provide the required Reynolds number and a pipe length equivalent to $(x/D)/\text{Re} = 0.3$. Note that $(x/D)/\text{Re}$ is the inverse of the Langhaar variable, used in Fig. 7-7. Use constant fluid properties, and note that the energy equation does not have to be solved. For initial conditions let the velocity profile be flat at a value equal to the mean velocity. Use Eq. (7-20) to obtain the mean friction coefficient and use Eq. (7-21) along with the pressure drop data to obtain the apparent friction coefficient, then plot the local, mean, and apparent friction coefficient versus $(x/D_h)/\text{Re}_{D_h}$ to show how the data approach the hydrodynamic fully developed values that are shown on Fig. 7-7 and in Shaw and London.³ Confirm the hydrodynamic entrance length, and compare to Eq. (7-23). Plot the nondimensional velocity profiles at various $(x/D_h)/\text{Re}_{D_h}$ locations and compare to Fig. 7-6 to demonstrate the concept of how the profiles evolve from a flat profile into hydrodynamically fully developed profile. Plot the absolute value of the pressure gradient versus $(x/D_h)/\text{Re}_{D_h}$ to show how the gradient becomes constant beyond the hydrodynamic entrance region. Evaluate the ratio of centerline velocity to mean velocity and plot it versus $(x/D_h)/\text{Re}_{D_h}$ to show how the ratio becomes a constant (2.0) beyond the hydrodynamic entrance region.

Note a small correction to the problem write-up. The variable x^+ has been replaced by $(x/D_h)/\text{Re}_{D_h}$ to avoid confusion with the use of $x^+ = 2(x/D_h)/(\text{Re}_{D_h} \text{Pr})$ as a heat transfer variable in Chapter 8. The $(x/D_h)/\text{Re}_{D_h}$ variable is the reciprocal of the Langhaar variable. Also, change the pipe length to $(x/D_h)/\text{Re}_{D_h} = 0.1$.

The data file for this problem is *7.9.dat.txt*. The data set construction is based on the *s30.dat.txt* file for combined entry length flow in a pipe with a specified surface temperature (initial profiles: flat velocity and flat temperature). Only the momentum results will be discussed. Note that *kout* has been changed to =4.

Here is an abbreviated listing of the output file (it will be called *out.txt* when you execute TEXSTAN using *7.9.dat.txt*):

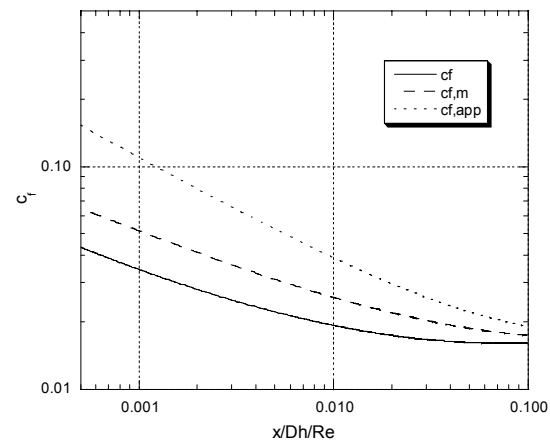
intg	x/dh	cfapp	cf2(I)	cf2(E)	nu(I)	nu(E)
5	2.500E-02	7.323E-01	0.000E+00	6.898E-02	0.000E+00	5.815E+01
50	2.500E-01	2.170E-01	0.000E+00	2.790E-02	0.000E+00	2.035E+01
100	5.000E-01	1.533E-01	0.000E+00	2.171E-02	0.000E+00	1.491E+01
150	9.229E-01	1.140E-01	0.000E+00	1.767E-02	0.000E+00	1.142E+01
200	2.061E+00	7.797E-02	0.000E+00	1.388E-02	0.000E+00	8.195E+00
250	5.096E+00	5.180E-02	0.000E+00	1.105E-02	0.000E+00	5.840E+00
300	1.240E+01	3.570E-02	0.000E+00	9.314E-03	0.000E+00	4.454E+00
350	2.392E+01	2.797E-02	0.000E+00	8.530E-03	0.000E+00	3.903E+00
400	4.137E+01	2.353E-02	0.000E+00	8.163E-03	0.000E+00	3.709E+00
450	6.550E+01	2.090E-02	0.000E+00	8.034E-03	0.000E+00	3.665E+00
500	9.050E+01	1.956E-02	0.000E+00	8.006E-03	0.000E+00	3.659E+00
519	1.000E+02	1.923E-02	0.000E+00	8.003E-03	0.000E+00	3.658E+00

You can also run the data set with *kout* changed from =4 to =8 to see more of the nondimensional variable behavior. Here is an abbreviated listing of the output file (it will be called *out.txt* when you execute TEXSTAN using *7.9b.dat.txt*):

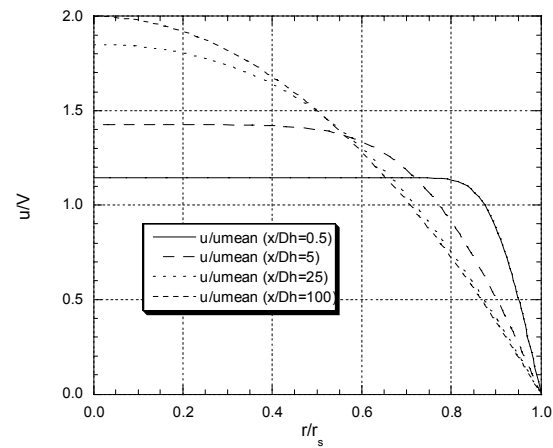
intg	x/dh/re	cf*re	uclr	xplus	nu	th,cl	tm/ts	ts	qflux
5	.00003	137.95	1.037	.00007	58.149	1.018	.968	3.100E+02	2.137E+02
50	.00025	55.81	1.104	.00070	20.347	1.057	.969	3.100E+02	7.203E+01
100	.00050	43.41	1.144	.00141	14.911	1.083	.970	3.100E+02	5.153E+01
150	.00092	35.35	1.192	.00260	11.424	1.117	.971	3.100E+02	3.828E+01
200	.00206	27.77	1.280	.00580	8.195	1.186	.973	3.100E+02	2.585E+01
250	.00510	22.11	1.429	.01433	5.840	1.331	.976	3.100E+02	1.642E+01
300	.01240	18.63	1.652	.03488	4.454	1.580	.980	3.100E+02	1.021E+01
350	.02392	17.06	1.839	.06729	3.903	1.742	.985	3.100E+02	6.857E+00
400	.04137	16.33	1.947	.11636	3.709	1.793	.990	3.100E+02	4.503E+00
450	.06550	16.07	1.986	.18425	3.665	1.799	.994	3.100E+02	2.706E+00
500	.09050	16.01	1.995	.25457	3.659	1.799	.996	3.100E+02	1.619E+00
519	.10000	16.01	1.996	.28129	3.658	1.798	.997	3.100E+02	1.332E+00

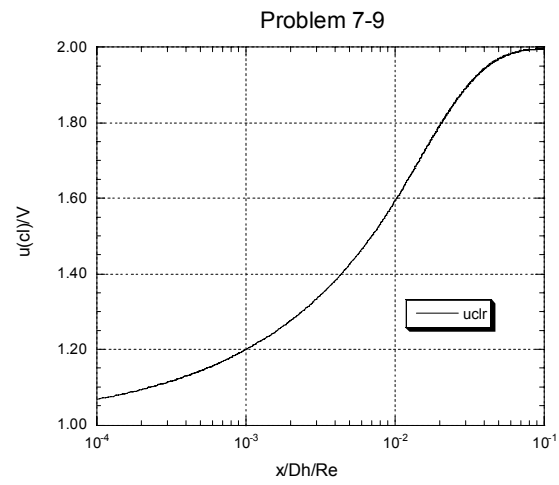
To compare the three friction factors in the entry region you will need to first calculate $c_{f_m}(x)$ by integration of the local friction factor data with respect to x following Eq. (7-20). The file *fm85.txt* contains the friction and pressure drop information to construct $c_{f_m}(x)$ and $c_{f_{app}}(x)$. For a more accurate integration of the local friction coefficient to obtain its mean value, you will want to increase the number of data points in *fm85.txt* by decreasing the *k5* variable in the input data set. If you work with the friction coefficient rather than the wall shear stress, be careful, because *cf2* is the friction coefficient divided by two. The accepted standard formulation for nondimensional friction in laminar internal flow is c_f (hydraulic engineers are usually the only people that use the Moody friction factor) and for turbulent internal flow it is $c_f/2$. TEXSTAN mostly uses the *cf2* formulation. The following graph is the reduced data for the 3 friction coefficients, plotted versus $(x/D_h)/Re_{D_h}$ rather than using the Langhaar variable. Because you have the pressure drop data versus x you can easily construct the pressure gradient variation with x and plot its absolute value logarithmically versus $(x/D_h)/Re_{D_h}$ (a ln-ln plot) to see where the gradient becomes constant. This is a measure of the entry region. To obtain the developing velocity profiles in the hydrodynamic entry region set *k11*=10 in *7.9.dat.txt*. The output profile will then contain velocity profiles at each $x(m)$ station. The profiles will have a set of shapes matching Fig. 7-6. Plotting the ratio u_{cl}/V shows a continual acceleration of the centerline velocity as the velocity profile changes shape over the limits $1 \leq u_{cl}/V \leq 2$. This ratio is also a measure of fully-developed flow.

Problem 7.9



Problem 7-9





7-10

TEXSTAN analysis of laminar entry flow between parallel planes: Follow the instructions for Prob. 7-9 to set up TEXSTAN, but use the geometry option that permits the centerline of the parallel planes channel to be a symmetry line. Use Eq. (7-20) to obtain the mean friction coefficient and use Eq. (7-21) along with the pressure drop data to obtain the apparent friction coefficient, then plot the local, mean, and apparent friction coefficient versus $(x/D_h)/\text{Re}_{D_h}$ to show how the data approach the hydrodynamic fully developed values that are given in Shaw and London.³ Confirm the hydrodynamic entrance length using data in Shaw and London.³ Plot the nondimensional velocity profiles at various $(x/D_h)/\text{Re}_{D_h}$ locations using the ideas in Fig. 7-6 to demonstrate the concept of how the profiles evolve from a flat profile into hydrodynamically fully developed profile, and compare the fully developed profile with that given in Shaw and London.³ Plot the absolute value of the pressure gradient versus $(x/D_h)/\text{Re}_{D_h}$ to show how the gradient becomes constant beyond the hydrodynamic entrance region. Evaluate the centerline velocity to mean velocity ratio and plot it versus $(x/D_h)/\text{Re}_{D_h}$ to show how the ratio becomes a constant (=1.5) beyond the hydrodynamic entrance region.

Note a small correction to the problem write-up. The variable x^+ has been replaced by $(x/D_h)/\text{Re}_{D_h}$ to avoid confusion with the use of $x^+ = 2(x/D_h)/(\text{Re}_{D_h} \text{Pr})$ as a heat transfer variable in Chapter 8. The $(x/D_h)/\text{Re}_{D_h}$ variable is the reciprocal of the Langhaar variable.

The data file for this problem is *7.10.dat.txt*. The data set construction is based on the *s50.dat.txt* file for combined entry length flow between parallel planes with a specified surface temperature and thermal symmetry (initial profiles: flat velocity and flat temperature). Note, for the parallel-planes geometry the variable $rw(m)$ is the half-width of the channel. Only the momentum results will be discussed. Note that *kout* has been changed to =4.

Here is an abbreviated listing of the output file (it will be called *out.txt* when you execute TEXSTAN using *7.10.dat.txt*):

intg	x/dh	cfapp	cf2(I)	cf2(E)	nu(I)	nu(E)
5	1.250E-02	1.037E+00	0.000E+00	9.607E-02	0.000E+00	8.279E+01
100	2.500E-01	2.171E-01	0.000E+00	2.953E-02	0.000E+00	2.182E+01
200	5.000E-01	1.541E-01	0.000E+00	2.334E-02	0.000E+00	1.641E+01
300	1.018E+00	1.097E-01	0.000E+00	1.884E-02	0.000E+00	1.255E+01
400	2.964E+00	6.706E-02	0.000E+00	1.456E-02	0.000E+00	9.004E+00
500	9.012E+00	4.213E-02	0.000E+00	1.237E-02	0.000E+00	7.609E+00
600	1.881E+01	3.308E-02	0.000E+00	1.202E-02	0.000E+00	7.537E+00
700	3.367E+01	2.912E-02	0.000E+00	1.200E-02	0.000E+00	7.538E+00
800	5.575E+01	2.712E-02	0.000E+00	1.200E-02	0.000E+00	7.538E+00
900	8.075E+01	2.615E-02	0.000E+00	1.200E-02	0.000E+00	7.538E+00
977	1.000E+02	2.574E-02	0.000E+00	1.200E-02	0.000E+00	7.538E+00

You can also run the data set with *kout* changed from =4 to =8 to see more of the nondimensional variable behavior. Here is an abbreviated listing of the output file (it will be called *out.txt* when you execute TEXSTAN using *7.10b.dat.txt*):

intg	x/dh/re	cf*re	uclr	xplus	nu	th,cl	tm/ts	ts	qflux
5	.00001	192.13	1.026	.00004	82.792	1.013	.968	3.100E+02	3.059E+02
100	.00025	59.05	1.104	.00070	21.822	1.059	.970	3.100E+02	7.711E+01
200	.00050	46.68	1.144	.00141	16.414	1.087	.970	3.100E+02	5.650E+01
300	.00102	37.69	1.202	.00286	12.547	1.133	.972	3.100E+02	4.145E+01
400	.00296	29.12	1.335	.00834	9.004	1.249	.975	3.100E+02	2.658E+01
500	.00901	24.75	1.473	.02535	7.609	1.321	.981	3.100E+02	1.712E+01
600	.01881	24.03	1.498	.05292	7.537	1.319	.987	3.100E+02	1.119E+01
700	.03367	23.99	1.499	.09471	7.538	1.319	.993	3.100E+02	5.973E+00
800	.05575	23.99	1.500	.15682	7.538	1.319	.997	3.100E+02	2.352E+00
900	.08075	23.99	1.500	.22715	7.538	1.319	.999	3.100E+02	8.193E-01
977	.10000	23.99	1.500	.28129	7.538	1.319	1.000	3.100E+02	3.637E-01

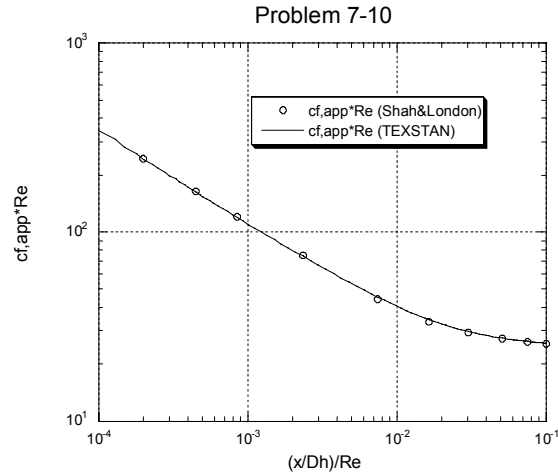
To compare the three friction factors in the entry region you will need to first calculate $c_{f_m}(x)$ by integration of the local friction factor data with respect to x following Eq. (7-20). The file *ftn85.txt* contains the friction and pressure drop information to construct $c_{f_m}(x)$ and $c_{f_{app}}(x)$. For a more accurate integration of the local friction coefficient to obtain its mean value, you will want to increase the number of data points in *ftn85.txt* by decreasing the *k5* variable in the input data set. If you work with the friction coefficient rather than the wall shear stress, be careful, because *cf2* is the friction coefficient divided by two. The accepted standard formulation for nondimensional friction in laminar internal flow is c_f (hydraulic engineers are usually the only people that use the Moody friction factor) and for turbulent internal flow it is $c_f/2$. TEXSTAN mostly uses the *cf2* formulation. The following graph is the reduced data for the 3 friction coefficients, plotted versus $(x/D_h)/Re_{D_h}$ rather than using the Langhaar variable.

The *cf* value is local nondimensional wall shear stress, and it approaches its asymptotic value for the smallest value of $(x/D_h)/Re_{D_h}$ (largest value of the abscissa variable in Fig. 7-7). The *cfapp* value requires nearly four times more length for its asymptotic state to be reached. This difference can be seen in the references by Shah and London³ and Shah.⁹ For example, here are equations for parallel planes from the Shah and London reference,

$$C_{f,app} \cdot Re_{D_h} = \frac{3.44}{\sqrt{(x/D)/Re}} + \frac{24 + 0.674/[4(x/D)/Re] - 3.44/\sqrt{(x/D)/Re}}{1 + 0.000029[(x/D)/Re]^2}$$

$$\frac{L_{hy}}{D_h} = \frac{0.315}{0.0175 Re_{D_h} + 1} + 0.011 Re_{D_h}$$

For $Re_{D_h} = 1000$, $L_{hy}/D_h = 11$. To obtain the same result based on $cf_{app} \cdot Re = 24$ (within 5%), $(x/D_h)/Re_{D_h}$ needs to be between 0.05 and 0.10. For example, a value of 0.05 (similar to what is used for circular pipe estimates) gives $L_{hy}/D_h = 50$, almost a factor of five longer entry length. This is reflective of the viscous transport mechanism in laminar flows where the core flow adjustment is not in sync with the wall shear flow region. This can be tested in TEXSTAN by using *kout=4* to produce output that includes the pressure drop, and convert this to *cfapp* using Eq. (7-21) to confirm the Shah and London equation for $cfapp \cdot Re$. The result shows $(x/D_h)/Re_{D_h} \approx 0.06$. At the same time, *cf* becomes within 5% of its asymptotic value at $(x/D_h)/Re_{D_h} \approx 0.008$.



Because you have the pressure drop data versus x you can easily construct the pressure gradient variation with x and plot its absolute value logarithmically versus $(x/D_h)/Re_{D_h}$ (a ln-ln plot) to see where the gradient becomes constant. This is a measure of the entry region. To obtain the developing velocity profiles in the hydrodynamic entry region set $k10=11$ in *7.10.dat.txt*. The output profile will then contain velocity profiles at each $x(m)$ station. The profiles will have a set of shapes similar to that for a pipe in Fig. 7-6. Plotting the ratio $u_C l/V$ shows a continual acceleration of the centerline velocity as the velocity profile changes shape over the limits $1 \leq u_C l/V \leq 1.5$. This ratio is also a measure of fully-developed flow.

7-11

TEXSTAN analysis of laminar entry flow in a circular-tube annulus with $r^* = 0.5$: Follow the instructions for Prob. 7-9 to set up TEXSTAN, but use the geometry option that permits the annulus. Use Eq. (7-20) to obtain the mean friction coefficient and use Eq. (7-21) along with the pressure drop data to obtain the apparent friction coefficient, then plot the local, mean, and apparent friction coefficient versus $(x/D_h)/\text{Re}_{D_h}$ to show how the data approach the hydrodynamic fully-developed values that are given in Shaw and London.³ Confirm the hydrodynamic entrance length using data in Shaw and London.³ Plot the nondimensional velocity profiles at various $(x/D_h)/\text{Re}_{D_h}$ locations using the ideas in Fig. 7-6 to demonstrate the concept of how the profiles evolve from a flat profile into hydrodynamically fully developed profile, and compare the fully developed profile with that given in Eq. (8-26). Plot the absolute value of the pressure gradient versus $(x/D_h)/\text{Re}_{D_h}$ to show how the gradient becomes constant beyond the hydrodynamic entrance region. Evaluate the ratio of centerline velocity to mean velocity and plot it versus $(x/D_h)/\text{Re}_{D_h}$ to show how the ratio becomes a constant beyond the hydrodynamic entrance region.

Note several small corrections to the problem write-up. The variable x^+ has been replaced by $(x/D_h)/\text{Re}_{D_h}$ to avoid confusion with the use of $x^+ = 2(x/D_h)/(\text{Re}_{D_h} \text{Pr})$ as a heat transfer variable in Chapter 8. The $(x/D_h)/\text{Re}_{D_h}$ variable is the reciprocal of the Langhaar variable. Plot the entry-region distributions of the local friction coefficients for inner and outer radius, the area-weighted average friction coefficient, and the apparent friction coefficients. The idea of evaluating the centerline velocity is not meaningful for an annulus. Instead, examine the maximum velocity and the location of the maximum. The analysis leading to these formulations is given as a part of problem 7-8 and it can be found in Shah and London.³

The data file for this problem is *8.21.dat.txt*. The data set construction is based on the *s60.dat.txt* file for combined entry length flow in a $r^*=0.5$ annulus with a specified surface temperature on each surface (initial profiles: flat velocity and flat temperature). Note, for the annulus geometry the variable $rw(m)$ is the inner radius and $aux2(m)$ is the annular separation (the outer radius will be the sum of $rw(m)$ and $aux2(m)$, leading to $r^* = r_o/r_i = (0.035 + 0.035)/0.035 = 0.5$). Only the momentum results will be discussed. Note that $kout$ has been changed to =4.

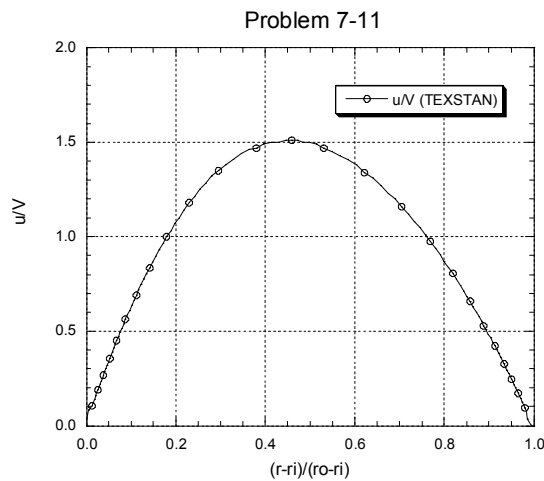
Here is an abbreviated listing of the output file (it will be called *out.txt* when you execute TEXSTAN using *7.11.dat.txt*):

intg	x/dh	cfapp	cf2(I)	cf2(E)	nu(I)	nu(E)
5	1.250E-02	1.037E+00	9.753E-02	9.533E-02	8.417E+01	8.210E+01
100	2.500E-01	2.172E-01	3.093E-02	2.880E-02	2.313E+01	2.114E+01
200	5.000E-01	1.541E-01	2.476E-02	2.260E-02	1.773E+01	1.572E+01
300	1.018E+00	1.097E-01	2.030E-02	1.808E-02	1.389E+01	1.183E+01
400	2.964E+00	6.712E-02	1.612E-02	1.373E-02	1.044E+01	8.213E+00
500	9.012E+00	4.216E-02	1.413E-02	1.141E-02	9.328E+00	6.606E+00
600	1.881E+01	3.305E-02	1.386E-02	1.096E-02	9.412E+00	6.416E+00
700	3.367E+01	2.903E-02	1.385E-02	1.093E-02	9.436E+00	6.400E+00
800	5.575E+01	2.699E-02	1.385E-02	1.093E-02	9.437E+00	6.399E+00
900	8.075E+01	2.600E-02	1.385E-02	1.093E-02	9.437E+00	6.399E+00
977	1.000E+02	2.558E-02	1.385E-02	1.093E-02	9.437E+00	6.399E+00

The friction factors for comparison include the local $c_f(x)$ for the inner and outer radii, $c_{f_{app}}(x)$ for pressure-drop calculations, and the area-averaged local friction coefficient for $(x/D)/\text{Re} \rightarrow \infty$, relating to Fig. 7-5. The $c_{f_m}(x)$ value is not generally used for the annulus. The file *fm85.txt* contains the friction and pressure drop information to construct and $c_{f_{app}}(x)$. For a more accurate pressure gradient, you will want to increase the number of data points in *fm85.txt* by decreasing the *k5* variable in the input data set. Note also that *cf2* is the friction coefficient divided by two. The accepted standard formulation for nondimensional friction in laminar internal flow is c_f (hydraulic engineers are usually the only people that use the Moody friction factor) and for turbulent internal flow it is $c_f/2$. TEXSTAN mostly uses the *cf2* formulation. Because you have the pressure drop data versus x you can easily construct the pressure gradient variation with x and plot its absolute value logarithmically versus $(x/D_h)/\text{Re}_{D_h}$ (a ln-ln plot) to see where the gradient becomes constant. This is a measure of the entry region. To obtain the developing velocity profiles in the hydrodynamic entry region set *k10*=11 in *7.11.dat.txt*. The output profile will then contain velocity profiles at each $x(m)$ station. As noted in the correction to this problem statement, the request to plot the ratio u_C/V is not very meaningful for an annular geometry. The student can find the maximum velocity within the annulus and plot this ratio as a measure of fully-developed flow. See the solution to problem 7-8 for the theoretical value for this maximum velocity and its location

$$\frac{u_{\max}}{V} = \frac{2(1 - r_m^{*2} + 2r_m^{*2} \ln(r_m^*))}{(1 + r^{*2} - 2r_m^{*2})} \quad \text{at} \quad r_m^* = \frac{r_m}{r_o} = \left[\frac{1 - r^{*2}}{2 \ln(1/r^*)} \right]^{1/2}$$

For this problem, $r_m^* = 0.7355$ and $u_{\max}/V = 1.5078$ which is confirmed by TEXSTAN. The plot below shows this profile at the last x -location, $x/D_h=100$, which is hydrodynamically fully-developed. The maximum-velocity location is $(r_m - r_i)/(r_o - r_i) = 0.4711$, which shows a slight bias towards the inner radius for this $r^*=0.5$ annulus. However, for this radius ratio the profile shape and maximum is very similar to that for the parallel planes.



8-1

Starting from the appropriate momentum and energy differential equations, evaluate the Nusselt number for both surfaces of a parallel-plane channel in which there is fully developed laminar flow (both velocity and temperature developed) and in which there is heating from both surfaces but the heat flux from one surface is twice the flux from the other surface, and again when the heat flux from one surface is 5 times the flux from the other surface. The heat-transfer rate per unit of duct length is constant. Compare your results with those given in the text (Table 8-1). TEXSTAN can be used to confirm the results of this problem.

Let the plate spacing be a . This solution is derived based on the origin $y = 0$ located on the channel centerline. Let the heat flux into the lower surface (1) be \dot{q}_1'' and its corresponding surface temperature be $T_{s,1}$, and let the heat flux into the upper surface (2) be \dot{q}_2'' and its corresponding surface temperature be $T_{s,2}$. Note that we have implied a sign convention such that a positive heat flux is in the $+y$ direction (into the fluid from surface 1 or out of the fluid from surface 2) and a negative heat flux is in the $-y$ direction (out of the fluid from surface 1 or into the fluid from surface 2).

Assume steady laminar flow with constant properties. For this coordinate system, the velocity profile has been derived in problem 7-7. The appropriate boundary layer equation is (4-10),

$$\rho u \frac{\partial u}{\partial x} + \rho v \frac{\partial u}{\partial y} = -\frac{dP}{dx} + \frac{\partial}{\partial y} \left(\mu \frac{\partial u}{\partial y} \right)$$

and for fully-developed flow, $\partial u / \partial x = 0$ and $v=0$, reducing the momentum equation to an ordinary differential equation and boundary conditions

$$\frac{dP}{dx} = \frac{d}{dy} \left(\mu \frac{du}{dy} \right)$$

with boundary conditions of velocity profile symmetry at the channel centerline, and no-slip at the channel surfaces.

$$\left. \frac{du}{dy} \right|_{y=0} = 0 \quad \text{and} \quad u|_{y=\pm a/2} = 0$$

Because the pressure gradient is a constant in the axial flow direction, we can separate variables and integrate, and apply the boundary conditions, leading to the parallel-planes channel velocity profile,

$$u = \frac{h^2}{2\mu} \left(1 - 4 \frac{y^2}{a^2} \right) \left(-\frac{dP}{dx} \right)$$

Note the similarity to Eq. (7-2) for the circular pipe, namely a parabolic profile shape. Next, we create the mean velocity, following Eq. (7-5) for constant density,

$$V = \frac{1}{A_c} \int_{A_c} u \, dA_c = \frac{1}{(a \cdot 1)} \int_{-a/2}^{+a/2} u \, dy = \frac{a^2}{12\mu} \left(-\frac{dP}{dx} \right)$$

where the cross-sectional area is per unit depth. Again, note the similarity to Eq. (7-7) for the circular pipe.

Creating the ratio of the velocity profile to the mean velocity yields

$$\frac{u}{V} = \frac{3}{2} \left(1 - 4 \frac{y^2}{a^2} \right)$$

Now consider the energy equation, neglecting viscous dissipation, and assuming constant properties for an ideal gas and steady state. Equation (4-39) is

$$u \frac{\partial T}{\partial x} + v \frac{\partial T}{\partial y} = \alpha \frac{\partial^2 T}{\partial y^2}$$

For thermally fully-developed flow, $v=0$ and from Eq. (8-7) $\partial T / \partial x = dT_m / dx$ and the energy equation becomes

$$\frac{\partial^2 T}{\partial y^2} = \frac{u}{\alpha} \frac{dT_m}{dx} = \frac{3V}{2\alpha} \frac{dT_m}{dx} \left(1 - 4 \frac{y^2}{a^2} \right)$$

which integrates to yield

$$T(y) = \frac{3V}{2\alpha} \frac{dT_m}{dx} \left(\frac{y^2}{2} - \frac{y^4}{3a^2} \right) + C_1 y + C_2$$

Now, carry out an energy balance on a control volume for an element of the flow, similar to that depicted in Fig. 8-3 for a curricular pipe,

$$\left(\frac{dT_m}{dx} \right) = \frac{\dot{q}_1'' + \dot{q}_2''}{a \rho V c}$$

To obtain a solution for the Nusselt numbers on each surface, the solution, the most straightforward approach is to apply a superposition idea because the two boundary conditions are both Neumann or Type 2 from a differential equation point of view. That is, only C_1 can be resolved. Split the solution into the linear sum of two problems,

$$T = t_1 + t_2 \quad \text{and} \quad T_m = t_{m,1} + t_{m,2}$$

where

$$\begin{aligned} \left. \frac{dt_1}{dx} \right|_{y=+a/2} &= 0 \quad \text{and} \quad t_1|_{y=-a/2} = t_{s,1} \\ \left. \frac{dt_2}{dx} \right|_{y=-a/2} &= 0 \quad \text{and} \quad t_2|_{y=+a/2} = t_{s,2} \end{aligned}$$

Now solve for t_1 and t_2 ,

$$\begin{aligned} t_1 &= t_{1,s} + \frac{3V}{2\alpha} \frac{dt_{m,1}}{dx} \left(\frac{y^2}{2} - \frac{y^4}{3a^2} - \frac{1}{3}ay - \frac{13}{48}a^2 \right) \\ t_2 &= t_{2,s} + \frac{3V}{2\alpha} \frac{dt_{m,2}}{dx} \left(\frac{y^2}{2} - \frac{y^4}{3a^2} + \frac{1}{3}ay - \frac{13}{48}a^2 \right) \end{aligned}$$

Now compute the mass-averaged fluid temperatures for these two solutions following Eq. (8-5),

$$\begin{aligned}
 t_{m,1} &= \frac{1}{V(a \cdot 1)} \int_{-a/2}^{+a/2} \frac{3}{2} V \left(1 - 4 \frac{y^2}{a^2} \right) \left[t_{1,s} + \frac{3V}{2\alpha} \frac{dt_{m,1}}{dx} \left(\frac{y^2}{2} - \frac{y^4}{3a^2} - \frac{1}{3} ay - \frac{13}{48} a^2 \right) \right] (dy \cdot 1) \\
 &= t_{1,s} - \frac{52}{140} \frac{V}{\alpha} \frac{dt_{m,1}}{dx} a^2
 \end{aligned}$$

Now, carry out an energy balance on a control volume for an element of the flow, with heating only on surface 1,

$$\left(\frac{dt_{m,1}}{dx} \right) = \frac{\dot{q}_1''}{a\rho Vc}$$

Substitution of this into the formulation for $t_{m,1}$ yields

$$t_{m,1} = t_{1,s} - \frac{26}{70} \frac{\dot{q}_1'' a}{k}$$

Carrying out the same procedure for $t_{m,2}$ yields

$$t_{m,2} = t_{2,s} - \frac{26}{70} \frac{\dot{q}_2'' a}{k}$$

and thus the superposition formulations become

$$\begin{aligned}
 T &= t_{1,s} + t_{2,s} + \frac{3}{2ka} \left[(\dot{q}_1'' + \dot{q}_2'') \left(\frac{y^2}{2} - \frac{y^4}{3a^2} - \frac{13}{48} a^2 \right) - (\dot{q}_1'' - \dot{q}_2'') \frac{1}{3} ay \right] \\
 T_m &= t_{1,s} + t_{2,s} - \frac{26}{70} \frac{a}{k} (\dot{q}_1'' + \dot{q}_2'')
 \end{aligned}$$

Now evaluate the surface temperatures in terms of the superposition temperatures,

$$\begin{aligned}
 T_{s,1} &= T|_{y=-a/2} = t_{s,1} + t_{s,2} - \frac{a}{2k} \dot{q}_2'' \\
 T_{s,2} &= T|_{y=+a/2} = t_{s,1} + t_{s,2} - \frac{a}{2k} \dot{q}_1''
 \end{aligned}$$

Finally, we formulate the Nusselt numbers for each surface. For surface 1,

$$\begin{aligned}
 \text{Nu}_1 &= \frac{h_1 D_h}{k} = \frac{\dot{q}_1''}{(T_{s,1} - T_m)} \frac{2a}{k} = \frac{4\dot{q}_1''}{\frac{26}{35} \dot{q}_1'' - \frac{9}{35} \dot{q}_2''} = \frac{1}{\frac{13}{70} - \frac{9}{140} \frac{\dot{q}_2''}{\dot{q}_1''}} \\
 &= \frac{5.385}{1 - 0.346 \frac{\dot{q}_2''}{\dot{q}_1''}}
 \end{aligned}$$

and for surface 2, following the same idea

$$\text{Nu}_2 = \frac{h_2 D_h}{k} = \frac{5.385}{1 - 0.346 \frac{\dot{q}_1''}{\dot{q}_2''}}$$

For this problem, where the heating on surface 2 is two times (2x) the heating on surface 1,

$$\text{Nu}_1 = 17.5 \quad \text{and} \quad \text{Nu}_2 = 6.51$$

and for the case where the heating on surface 2 is five times (5x) the heating on surface 1,

$$\text{Nu}_1 = -7.37 \quad \text{and} \quad \text{Nu}_2 = 5.79$$

Compare this analysis to the development on page 94, and Table 8-1. For parallel planes, $r^* = 1$ and both influence coefficients are 0.346. When the heat flux ratio $\dot{q}_2''/\dot{q}_1'' = 26/9 \approx 2.9$, Nu_1 becomes infinite, indicating that $(T_{s,1} - T_m)$ has become zero, and for larger heat flux ratios the mean temperature exceeds the surface-1 temperature. Note that a flux-flux boundary condition problem does not have a unique temperature level, but rather it is set by a thermal boundary condition on the “other side of one of the surfaces”. Note, the solution for this problem can also be carried out without strictly considering linear superposition.

To verify the analysis the TEXSTAN data file for this problem choose the data set *8.1.dat.txt*. The data set construction is based on the *s556.dat.txt* file for thermal entry length flow between parallel planes with a specified surface heat flux on each surface (initial profiles: hydrodynamically fully-developed velocity and flat temperature). Note this is not the correct thermal initial condition for this problem but the solution will converge to a thermally fully-developed solution.

For this problem set we arbitrarily chose $+20 \text{ W/m}^2$ for the heat flux at the inner surface (I-surface). For 2x heating, the outer surface (E-surface) will be $+40 \text{ W/m}^2$. Note a slight change in the problem statement. the channel length should be 100 hydraulic diameters.

Here is an abbreviated listing of the *8.1-two.out.txt* output file:

intg	x/dh	cfapp	cf2(I)	cf2(E)	nu(I)	nu(E)
750	4.376E+01	2.410E-02	1.199E-02	1.199E-02	1.662E+01	6.572E+00
800	5.575E+01	2.408E-02	1.199E-02	1.199E-02	1.712E+01	6.534E+00
850	6.825E+01	2.406E-02	1.199E-02	1.199E-02	1.733E+01	6.519E+00
900	8.075E+01	2.405E-02	1.199E-02	1.199E-02	1.741E+01	6.513E+00
950	9.325E+01	2.404E-02	1.199E-02	1.199E-02	1.745E+01	6.511E+00
977	1.000E+02	2.404E-02	1.199E-02	1.199E-02	1.745E+01	6.510E+00

Because the initial conditions were for a thermal entry length calculation, only the thermal boundary layer develops on the channel surfaces, and the flow becomes thermally fully developed within about 95% at about $x/D, h \approx 44$, which converts to $x^+ = (2x/D_h)/(\text{Re Pr}) = 0.12$. Table 8-13 shows a similar x^+ range for thermally fully-developed flow to be in the range 0.1 to 0.2. For this problem $\text{Nu} = 17.47$ in *8.1-two.out.txt* agrees with our derived solution for the I surface (17.5) and $\dot{q}_{E\text{-surface}}'' = 2 \times \dot{q}_{I\text{-surface}}''$, and $\text{Nu} = 6.511$ agrees with our derived solution for the E-surface(6.51).

The files *fin83.txt* and *fn83.txt* and can be used to confirm h , T_s , T_m , for the I-surface and E-surface. For the I-surface we found that the Nusselt number is positive, so we will expect $T_s > T_m$. For the E-surface we found that the Nusselt number is also positive, so we will expect $T_s > T_m$. Here is an abbreviated output from *fn83.txt* (for the I-surface),

intg	x/dh	htc	qflux	tm	ts
750	4.3761544E+01	6.2177E+00	2.0000E+01	3.1974E+02	3.2295E+02
800	5.5750000E+01	6.4041E+00	2.0000E+01	3.2514E+02	3.2826E+02
850	6.8249961E+01	6.4841E+00	2.0000E+01	3.3078E+02	3.3386E+02

900	8.0749945E+01	6.5156E+00	2.0000E+01	3.3642E+02	3.3949E+02
950	9.3250004E+01	6.5279E+00	2.0000E+01	3.4205E+02	3.4512E+02
977	9.9999920E+01	6.5310E+00	2.0000E+01	3.4510E+02	3.4816E+02

and here is an abbreviated output from *fm84.txt* (for the E-surface),

intg	x/dh	htc	qflux	tm	ts
750	4.3761544E+01	2.4591E+00	4.0000E+01	3.1974E+02	3.3600E+02
800	5.5750000E+01	2.4450E+00	4.0000E+01	3.2514E+02	3.4150E+02
850	6.8249961E+01	2.4392E+00	4.0000E+01	3.3078E+02	3.4718E+02
900	8.0749945E+01	2.4370E+00	4.0000E+01	3.3642E+02	3.5283E+02
950	9.3250004E+01	2.4362E+00	4.0000E+01	3.4205E+02	3.5847E+02
977	9.9999920E+01	2.4359E+00	4.0000E+01	3.4510E+02	3.6152E+02

For the I-surface, from the *fm83.txt* output we see $T_s > T_m$ and with the positive heat flux we expect a positive Nu. For the E-surface, from the *fm84.txt* output we also see $T_s > T_m$, and with the positive heat flux we again expect a positive Nu.

Here is an abbreviated listing of the *8.1-five.out.txt* output file:

intg	x/dh	cfapp	cf2(I)	cf2(E)	nu(I)	nu(E)
750	4.376E+01	2.410E-02	1.199E-02	1.199E-02	-8.078E+00	5.863E+00
800	5.575E+01	2.408E-02	1.199E-02	1.199E-02	-7.646E+00	5.815E+00
850	6.825E+01	2.406E-02	1.199E-02	1.199E-02	-7.481E+00	5.796E+00
900	8.075E+01	2.405E-02	1.199E-02	1.199E-02	-7.419E+00	5.788E+00
950	9.325E+01	2.404E-02	1.199E-02	1.199E-02	-7.395E+00	5.785E+00
977	1.000E+02	2.404E-02	1.199E-02	1.199E-02	-7.389E+00	5.785E+00

For $\dot{q}_{E-surface}'' = 5 \times \dot{q}_{I-surface}''$ the Nu = -7.383 in *8.1-five.out.txt* agrees with our derived solution for the I surface (-7.37) and , and Nu = +5.786 agrees with our derived solution for the E-surface(5.79).

The files *fm83.txt* and *fm84.txt* and can be used to explain the Nusselt number behavior. For the I-surface we find that the Nusselt number is negative, so we will expect $T_m > T_s$, even though the heat flux is positive. For the E-surface we find that the Nusselt number is positive, so we will expect $T_s > T_m$. Here is an abbreviated output from *fm83.txt* (for the I-surface),

intg	x/dh	htc	qflux	tmean	twall
750	4.3761544E+01	-3.0228E+00	2.0000E+01	3.3947E+02	3.3285E+02
800	5.5750000E+01	-2.8608E+00	2.0000E+01	3.5028E+02	3.4329E+02
850	6.8249961E+01	-2.7991E+00	2.0000E+01	3.6156E+02	3.5441E+02
900	8.0749945E+01	-2.7759E+00	2.0000E+01	3.7283E+02	3.6563E+02
950	9.3250004E+01	-2.7670E+00	2.0000E+01	3.8411E+02	3.7688E+02
977	9.9999920E+01	-2.7648E+00	2.0000E+01	3.9019E+02	3.8296E+02

and here is an abbreviated output from *fm84.txt* (for the E-surface),

intg	x/dh	htc	qflux	tmean	twall
------	------	-----	-------	-------	-------

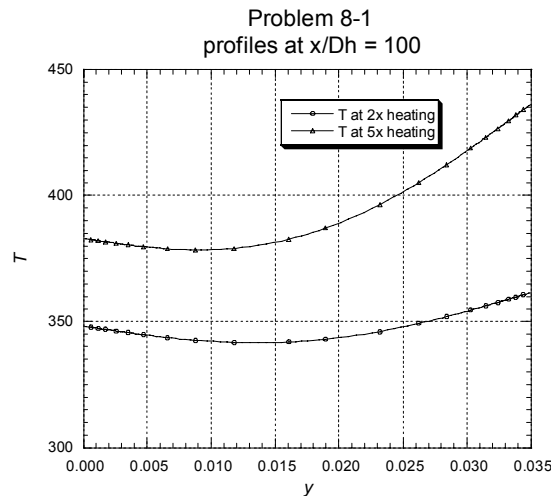
750	4.3761544E+01	2.1938E+00	1.0000E+02	3.3947E+02	3.8505E+02
800	5.5750000E+01	2.1759E+00	1.0000E+02	3.5028E+02	3.9624E+02
850	6.8249961E+01	2.1687E+00	1.0000E+02	3.6156E+02	4.0767E+02
900	8.0749945E+01	2.1659E+00	1.0000E+02	3.7283E+02	4.1900E+02
950	9.3250004E+01	2.1648E+00	1.0000E+02	3.8411E+02	4.3030E+02
977	9.9999920E+01	2.1645E+00	1.0000E+02	3.9019E+02	4.3639E+02

For the I-surface, from the *fm83.txt* output we see $T_m > T_s$ and with the positive heat flux we verify why the Nusselt number is negative. For the E-surface, from the *fm84.txt* output we see $T_s > T_m$ and with the positive heat flux we again expect a positive Nu.

To better understand any negative Nusselt number, the temperature profiles need to be examined. By resetting *k10* =11 in *five.dat.txt* the output file will also contain profiles of $T(y)$ at each of the 5 $x(m)$ locations. The following plot compares the profiles for both heating ratios.

We can see both heat fluxes are into the fluid, but for the higher heating level, the mean temperature becomes greater than the wall temperature, creating a discrepancy between the local wall temperature gradient and $(T_s - T_m)$ for that wall.

In summary, it is important to emphasize that the heat transfer coefficient and its non-dimensional equivalent, Nu, reflect the definition based on $(T_s - T_m)$ in Newton's law of cooling, whereas the heat flux at the surface is governed by the local temperature gradient and how Fourier's law is defined. We saw that Fourier's law for the E-surface has had a sign change to make it agree with the thermodynamic-like sign convention in TEXSTAN (heat transfer into the fluid is positive). Of equal importance is the examination of the temperature profiles.



8-2

With a low-Prandtl-number fluid, the temperature profile in a tube develops more rapidly than the velocity profile. Thus, as the Prandtl number approaches zero, the temperature profile can approach a fully developed form before the velocity profile has even started to develop (although this is a situation of purely academic interest). Convection solutions based on a uniform velocity over the cross section, as described, are called *slug-flow* solutions. Develop an expression for the slug-flow, fully developed temperature-profile Nusselt number for constant heat rate per unit of tube length for a concentric circular-tube annulus with a radius ratio of 0.60 for the case where the inner tube is heated and the outer tube is insulated. Compare with the results in Table 8-1 and discuss.

For the annulus geometry r is measured from the centerline of the inner pipe, r_i is the radius of the inner pipe, r_o is the radius of the outer pipe, and r^* is the radius ratio, $r^* = r_i/r_o$. Now consider the energy equation (8-1). This equation assumes no viscous dissipation, and it assumes constant properties for an ideal gas and steady state. Let the temperature profile vary with x and r only. The equation becomes

$$\rho c u \frac{\partial T}{\partial x} + \rho c v_r \frac{\partial T}{\partial r} = \frac{k}{r} \frac{\partial}{\partial r} \left(r \frac{\partial T}{\partial r} \right)$$

With the assumption of a slug flow, $u=V$ and $v_r=0$, and with the assumption of a thermally fully-developed temperature profile with constant heat rate, Eq. (8-8), the energy equation becomes

$$\frac{1}{r} \frac{\partial}{\partial r} \left(r \frac{\partial T}{\partial r} \right) = \frac{V}{\alpha} \left(\frac{dT_m}{dx} \right)$$

The boundary conditions for the annulus are a constant heat rate at r_i and an adiabatic surface at r_o . These two boundary conditions are very much similar to those for a circular pipe (zero heat flux at the pipe centerline and a uniform heat flux at the surface). Thus the boundary conditions are to that following Eq. (8-10)

$$\left. \frac{\partial T}{\partial r} \right|_{r=r_o} = 0 \quad \text{and} \quad T|_{r=r_i} = T_{s,r_i}$$

Note that any time we have a Neumann-Neumann boundary (adiabatic surface and heat-flux surface for this problem or a pipe with a heat-flux surface), we can not find the two constants of integration when we separate variables and integrate. So, we substitute for one of the Neumann conditions with it's Dirichlet counterpart (in this case the surface temperature) and we bring in the heat flux through the energy balance when we determine dT_m/dx .

Separate variables and integrate the 2nd-order ordinary differential equation, and apply the boundary conditions,

$$T = T_{s,r_i} - \frac{V r_o^2}{4\alpha} \frac{dT_m}{dx} \left[\frac{r^2}{r_o^2} - r^{*2} - 2 \ln \left(\frac{r}{r_i} \right) \right]$$

where $r^* = r_i/r_o$. Now compute the mean temperature using Eq. (8-5)

$$T_m = \frac{1}{V\pi(r_o^2 - r_i^2)} \int_{r_i}^{r_o} V \left[T_{s,r_i} - \frac{Vr_o^2}{4\alpha} \frac{dT_m}{dx} \left[\frac{r^2}{r_o^2} - r^{*2} - 2 \ln \left(\frac{r}{r_i} \right) \right] \right] (2\pi r dr)$$

$$= T_{s,r_i} + \frac{Vr_o^2}{\alpha} \frac{dT_m}{dx} \left[\frac{3}{8} - \frac{1}{8} r^{*2} + \frac{\ln(r^*)}{2(1-r^{*2})} \right]$$

Now formulate the convective rate equation for the r_i surface,

$$\dot{q}_i'' = h_i (T_{s,r_i} - T_m) = -h \frac{Vr_o^2}{\alpha} \frac{dT_m}{dx} \left[\frac{3}{8} - \frac{1}{8} r^{*2} + \frac{\ln(r^*)}{2(1-r^{*2})} \right]$$

The next step can be carried out one of two ways. The first way is form an energy balance similar to Eq. (8-15), and then equate the surface heat flux to the convective rate equation and form a Nusselt number. The second approach is to independently formulate the surface heat flux using Fourier's law, equate the two forms of heat flux and form a Nusselt number. Using the first approach

$$\dot{q}_i'' = \frac{(r_o^2 - r_i^2)}{2r_i} (\rho c V) \frac{dT_m}{dx}$$

and form a Nusselt number and evaluate it at $r^*=0.6$,

$$Nu_i = \left(\frac{h_i D_h}{k} \right) = \frac{\frac{(r_o - r_i)}{r_i} (r_i^2 - r_o^2)}{\frac{3r_o^2 - r_i^2}{8} + \frac{r_o^4 \ln(r_i/r_o)}{2(r_o^2 - r_i^2)}} = \frac{\left(\frac{1}{r^*} - 1 \right) (1 - r^{*2})}{\left(\frac{r^{*2} - 3}{8} - \frac{\ln(r^*)}{2(1 - r^{*2})} \right)}$$

$$Nu_i \Big|_{r^*=0.6} = 6.176$$

Note, compare this solution with Table 8-1 for the Nusselt number solution for the inner wall heated and the outer wall adiabatic, $Nu_{ii}(r^*)$, and you will find a very close agreement for small r^* between the plug-flow solution and the solution with hydrodynamically fully-developed profiles. The profile shapes are not that dissimilar.

Compare this solution with Table 8-1 for the Nusselt number solution for the inner wall heated and the outer wall adiabatic, $Nu_{ii}(r^*)$. For $r^*=0.6$ $Nu_{ii} = 5.912$, showing the slug-flow analysis (relating to x -convection) leads to an error of about 4.5%.

8-3

Consider a 0.6 cm inside-diameter circular tube that is of sufficient length that the flow is hydrodynamically fully developed. At some point beyond the fully developed location, a 1.2-m length of the tube is wound by an electric resistance heating element to heat the fluid, an organic fuel, from its entrance temperature of 10°C to a final value of 65°C. Let the mass flow rate of the fuel be 1.26×10^{-3} kg/s. The following average properties may be treated as constant:

$$\begin{aligned} \text{Pr} &= 10 \\ \rho &= 753 \text{ kg/m}^3 \\ c &= 2.092 \text{ kJ/(kg} \cdot \text{K)} \\ k &= 0.137 \text{ W/(m} \cdot \text{K)} \\ \mu &= 0.00065 \text{ Pa} \cdot \text{s} \end{aligned}$$

Note, there is a small correction to the problem statement. If you fix the values of Pr, μ , and c, the thermal conductivity calculates to be 0.136 W/m-K. Calculate and plot both tube surface temperature and fluid mean temperature as functions of tube length. What is the highest temperature experienced by any of the fluid?. TEXSTAN can be used to confirm the results of this problem.

To begin this problem, first compute the thermal entry length for laminar heat transfer as suggested by Table 8-6 for a uniform heat flux boundary condition, $x^+ = 0.10$, or $x = 2.47$ m, showing the entire heat transfer occurs in the developing region, which violates the assumption of constant h (or constant Nu).

The solution for the variation of mean temperature with x is a straightforward application of an energy balance for a uniform heat flux boundary condition,

$$\begin{aligned} \dot{q}_s'' A_s &= \dot{m} c [T_m(x) - T_m(x=0)] \\ T_m(x) &= T_m(x=0) + \frac{\dot{q}_s'' \pi D}{\dot{m} c} \end{aligned}$$

and for this problem, the uniform heat flux is computed to be

$$\dot{q}_s'' = \frac{\dot{m} c [T_m(x=L) - T_m(x=0)]}{A} = 6409.3 \text{ W/m}^2$$

To obtain the surface temperature, apply the local convective rate equation,

$$\begin{aligned} \dot{q}_s''(x) &= h_x [T_s(x) - T_m(x)] \\ T_s(x) &= T_m(x) + \frac{\dot{q}_s''(x)}{h_x} \end{aligned}$$

To evaluate h_x , we need to use the Nu_x solution for an unheated starting length and a uniform heat flux, Eq. (8-42),

$$\text{Nu}_x = \left[\frac{1}{\text{Nu}_\infty} - \frac{1}{2} \sum_{m=1}^{\infty} \frac{\exp(-\gamma_m^2 x^+)}{A_m \gamma_m^4} \right]^{-1}$$

For the infinite series, let $m=5$, as this can reproduce Table 8-6 to within about 1%. The solution to this problem requires calculation of the infinite series to obtain Nu_x , then calculating h_x , and then calculating and plotting the mean and surface temperature $0 \leq x \leq L$.

To verify the analysis the TEXSTAN data file for this problem choose the data set *8.3.dat.txt*. The data set construction is based on the *s35.dat.txt* file for thermal entry length flow in a pipe with a specified surface heat flux (initial profiles: hydrodynamically fully-developed velocity and flat temperature). Note that *kout* has been changed to =4.

To set up the input data file, the hydraulic diameter Reynolds number needs to be computed, $Re_D = (4\dot{m})/(\pi\mu D) = 411$, because it is an input file variable. The variables that were changed in *s35.dat.txt* to create *8.3.dat.txt* include *rhoc*, *visc*, *gam/cp*, *prc(1)*, the set of six *x(m)* and *aux1(m)* values, the six *ff(E,1,m)* values, *xend*, *reyn*, *tref* and *twall*. Note: feel free to adjust the selected *x(m)* values. The *x(m)* values in the data set are intended to create more integration points in the initial part of the developing thermal boundary layer region based on the logarithmic behavior of the x^+ variable.

Here is an abbreviated listing of the *8.3.out.txt* output file:

intg	x/dh	cfapp	cf2(I)	cf2(E)	nu(I)	nu(E)
5	2.500E-02	3.889E-02	0.000E+00	1.945E-02	0.000E+00	7.194E+01
100	5.000E-01	3.888E-02	0.000E+00	1.944E-02	0.000E+00	2.554E+01
200	1.000E+00	3.888E-02	0.000E+00	1.944E-02	0.000E+00	2.017E+01
300	1.500E+00	3.888E-02	0.000E+00	1.945E-02	0.000E+00	1.758E+01
400	2.000E+00	3.888E-02	0.000E+00	1.945E-02	0.000E+00	1.596E+01
500	2.500E+00	3.888E-02	0.000E+00	1.944E-02	0.000E+00	1.480E+01
600	3.000E+00	3.888E-02	0.000E+00	1.945E-02	0.000E+00	1.392E+01
700	3.500E+00	3.888E-02	0.000E+00	1.945E-02	0.000E+00	1.322E+01
800	4.000E+00	3.888E-02	0.000E+00	1.945E-02	0.000E+00	1.265E+01
900	4.840E+00	3.899E-02	0.000E+00	1.945E-02	0.000E+00	1.187E+01
1000	1.061E+01	3.936E-02	0.000E+00	1.945E-02	0.000E+00	9.202E+00
1100	4.556E+01	3.932E-02	0.000E+00	1.945E-02	0.000E+00	5.987E+00
1200	9.556E+01	3.910E-02	0.000E+00	1.945E-02	0.000E+00	5.044E+00
1300	1.456E+02	3.903E-02	0.000E+00	1.945E-02	0.000E+00	4.698E+00
1400	1.953E+02	3.900E-02	0.000E+00	1.945E-02	0.000E+00	4.537E+00
1410	2.000E+02	3.900E-02	0.000E+00	1.945E-02	0.000E+00	4.527E+00

To confirm the fact that h will significantly vary through the tube, we examine output from *fn84.txt* (for the E-surface),

intg	x/dh	htc	qflux	tm	ts
5	2.4999999E-02	1.6304E+03	6.4093E+03	1.0007E+01	1.3938E+01
100	5.0000003E-01	5.7874E+02	6.4093E+03	1.0138E+01	2.1212E+01
200	9.9999969E-01	4.5721E+02	6.4093E+03	1.0275E+01	2.4293E+01
300	1.5000006E+00	3.9851E+02	6.4093E+03	1.0413E+01	2.6496E+01
400	2.0000000E+00	3.6161E+02	6.4093E+03	1.0550E+01	2.8275E+01
500	2.4999997E+00	3.3545E+02	6.4093E+03	1.0688E+01	2.9795E+01
600	3.0000008E+00	3.1555E+02	6.4093E+03	1.0825E+01	3.1137E+01
700	3.4999986E+00	2.9970E+02	6.4093E+03	1.0963E+01	3.2349E+01

800	4.0000000E+00	2.8666E+02	6.4093E+03	1.1100E+01	3.3459E+01
900	4.8404098E+00	2.6910E+02	6.4093E+03	1.1332E+01	3.5149E+01
1000	1.0610173E+01	2.0855E+02	6.4093E+03	1.2919E+01	4.3652E+01
1100	4.5564888E+01	1.3569E+02	6.4093E+03	2.2535E+01	6.9770E+01
1200	9.5564843E+01	1.1432E+02	6.4093E+03	3.6290E+01	9.2355E+01
1300	1.4556492E+02	1.0647E+02	6.4093E+03	5.0045E+01	1.1024E+02
1400	1.9533328E+02	1.0283E+02	6.4093E+03	6.3736E+01	1.2607E+02
1410	1.9999993E+02	1.0260E+02	6.4093E+03	6.5020E+01	1.2749E+02

Here is the results from evaluating the infinite series and from the TEXSTAN calculations.

x^+	0.00098	0.0025	0.01484	0.03916	0.06348	0.09728
x/D_h	2.00	5.12	30.5	80.5	131	200
N_{ux}	14.01	11.34	6.67	5.22	4.77	4.52
TEXSTAN	15.96	11.65	6.68	5.23	4.78	4.53

8-4

Consider fully developed, constant-property laminar flow between parallel planes with constant heat rate per unit of length and a fully developed temperature profile. Suppose heat is transferred to the fluid on one side and out of the fluid on the other at the *same rate*. What is the Nusselt number on each side of the passage? Sketch the temperature profile. Suppose the fluid is an oil for which the viscosity varies greatly with temperature, but all the other properties are relatively unaffected by temperature. Is the velocity profile affected? Is the temperature profile affected? Is the Nusselt number affected? Explain. TEXSTAN can be used to confirm the Nusselt number result of this problem.

Note that the Nusselt number functions for this problem have been derived as a part of problem 8-1. Let the plate spacing be a . Let the heat flux into the lower surface (1) be \dot{q}_1'' and its corresponding surface temperature be $T_{s,1}$, and let the heat flux into the upper surface (2) be \dot{q}_2'' and its corresponding surface temperature be $T_{s,2}$. The sign convention is such that a positive heat flux is in the $+y$ direction (into the fluid from surface 1 or out of the fluid from surface 2) and a negative heat flux is in the $-y$ direction (out of the fluid from surface 1 or into the fluid from surface 2).

The Nusselt number for the lower surface is Eq. (8-28) and for the upper surface Eq. (8-29), along with Table 8-1, and $r^*=1.00$ (parallel planes)

$$\text{Nu}_1 = \frac{h_1 D_h}{k} = \frac{\dot{q}_1''}{(T_{s,1} - T_m)} \frac{2a}{k} = \frac{5.385}{1 - 0.346 \frac{\dot{q}_2''}{\dot{q}_1''}}$$

$$\text{Nu}_2 = \frac{h_2 D_h}{k} = \frac{\dot{q}_2''}{(T_{s,2} - T_m)} \frac{2a}{k} = \frac{5.385}{1 - 0.346 \frac{\dot{q}_1''}{\dot{q}_2''}}$$

For this problem statement, $\dot{q}_1'' = -\dot{q}_2''$, and this leads to $\text{Nu}_1 = 4.00$ and $\text{Nu}_2 = 4.00$. To show that the temperature profile is linear we start with Eq. (8-7) for thermally fully-developed flow,

$$\frac{\partial^2 T}{\partial y^2} = \frac{u}{\alpha} \frac{dT_m}{dx}$$

We then do an energy balance on a control volume similar to Fig. 8-3, which yields $dT_m/dx = 0$, and the energy equation becomes $d^2T/dy^2 = 0$, leading to a linear temperature profile, regardless of the shape of the velocity profile. Let the origin $y = 0$ located on the channel centerline (same as used in problem 8-1), and the solution becomes

$$T(y) = \frac{T_{s,1} + T_{s,2}}{2} + \left(\frac{T_{s,2} - T_{s,1}}{2a} \right) y$$

If viscosity is a function of temperature the velocity profile will be affected, but it may or may not have an influence on temperature profile (and) Nusselt number. It will not have an affect if the $\mu(T)$ does not alter the assumption of hydrodynamically fully-developed. If the flow continues to accelerate, then the full energy equation (4-38) with or without viscous dissipation has to be solved because $v \neq 0$.

To verify the analysis the TEXSTAN data file for this problem choose the data set *8.1.dat.txt*. The data set construction is based on the *s556.dat.txt* file for thermal entry length flow between parallel planes with a specified surface heat flux on each surface (initial profiles: hydrodynamically fully-developed velocity and flat temperature). Note this is not the correct thermal initial condition but it will converge to a thermally fully-developed solution.

To verify the analysis the TEXSTAN data file for this problem is *8.4.dat.txt*. The data set construction is based on the *s536.dat.txt* file. This data set is for thermally fully-developed flow between parallel planes with a constant heat flux surface. For this problem make the channel length about 100 hydraulic diameters (the problem statement says 20-40).

Here is an abbreviated listing of the *8.4.out.txt* output file:

intg	x/dh	cfapp	cf2(I)	cf2(E)	nu(I)	nu(E)
5	1.250E-02	2.403E-02	1.199E-02	1.199E-02	8.234E+00	-1.149E+01
50	7.500E-01	2.793E-02	1.199E-02	1.199E-02	7.957E+00	7.692E+01
100	7.000E+00	2.440E-02	1.199E-02	1.199E-02	6.216E+00	6.926E+00
150	1.325E+01	2.420E-02	1.199E-02	1.199E-02	5.220E+00	5.303E+00
200	1.950E+01	2.413E-02	1.199E-02	1.199E-02	4.690E+00	4.702E+00
250	2.575E+01	2.409E-02	1.199E-02	1.199E-02	4.403E+00	4.405E+00
300	3.200E+01	2.407E-02	1.199E-02	1.199E-02	4.240E+00	4.241E+00
350	3.825E+01	2.406E-02	1.199E-02	1.199E-02	4.145E+00	4.145E+00
400	4.450E+01	2.404E-02	1.199E-02	1.199E-02	4.089E+00	4.089E+00
450	5.075E+01	2.404E-02	1.199E-02	1.199E-02	4.054E+00	4.054E+00
500	5.700E+01	2.403E-02	1.199E-02	1.199E-02	4.033E+00	4.033E+00
550	6.325E+01	2.402E-02	1.199E-02	1.199E-02	4.021E+00	4.021E+00
600	6.950E+01	2.402E-02	1.199E-02	1.199E-02	4.013E+00	4.013E+00
650	7.575E+01	2.402E-02	1.199E-02	1.199E-02	4.008E+00	4.008E+00
700	8.200E+01	2.401E-02	1.199E-02	1.199E-02	4.005E+00	4.005E+00
730	8.571E+01	2.401E-02	1.199E-02	1.199E-02	4.004E+00	4.004E+00

In the output we see the confirmation of $Nu(I)=Nu(E)$ for $\dot{q}_1'' = -\dot{q}_2''$. However, we see it takes quite a long time to reach this thermally fully-developed flow. This is because TEXSTAN does not have a correct thermally fully-developed temperature profile for a flux-flux thermal boundary condition, and the incorrect initial profile takes time to damp out (in the output you will see it will take about 30-40 hydraulic diameters for the solution to converge towards a thermally fully-developed solution, whereas the velocity solution is correct from the *xstart* location).

8-5

Consider a concentric circular-tube annulus, with outer diameter 2.5 cm and inner diameter 1.25 cm, in which air is flowing under fully developed, constant-heat-rate conditions. Heat is supplied to the inner tube, and the outer tube is externally insulated. The radiation emissivity of both tube surfaces is 0.8. The mixed mean temperature of the air at a particular point in question is 260°C. The inner-tube surface temperature at this point is 300°C. What is *total* heat flux from the inner-tube surface at this point? What is the outer-tube surface temperature at this point? What percentage of the heat supplied to the inner tube is transferred directly to the air, and what percentage indirectly from the outer surface? Assume that the Reynolds number is sufficiently low that the flow is laminar. Assume that the air is transparent to the thermal radiation. Make use of any of the material in the text as needed.

First formulate the thermal radiation exchange using a radiative thermal circuit for exchange between two diffuse-gray surfaces with a non-participating medium between the surfaces. This formulation can be found in most undergraduate heat transfer texts.

$$\dot{q}_{rad,net,i} = \frac{E_{b,i} - E_{b,o}}{\frac{1-\varepsilon_i}{A_i\varepsilon_i} + \frac{1}{A_iF_{io}} + \frac{1-\varepsilon_o}{A_o\varepsilon_o}} = \frac{\sigma(T_i^4 - T_o^4)}{\frac{1-\varepsilon_i}{A_i\varepsilon_i} + \frac{1}{A_iF_{io}} + \frac{1-\varepsilon_o}{A_i(r_o/r_i)\varepsilon_o}} = \frac{A_i\sigma(T_i^4 - T_o^4)}{\left[\frac{1-\varepsilon_i}{\varepsilon_i} + \frac{1}{F_{io}} + \frac{1-\varepsilon_o}{(r_o/r_i)\varepsilon_o} \right]} = -\dot{q}_{rad,net,o}$$

where the radiation view factor $F_{io}=1$ for concentric circular cylinders. This problem will be analyzed on a flux basis, so convert the radiative heat transfer rate to a flux,

$$\dot{q}_{rad,net,i}'' = \frac{\dot{q}_{rad,net,i}}{A_i} = \frac{\sigma(T_i^4 - T_o^4)}{\left[\frac{1-\varepsilon_i}{\varepsilon_i} + \frac{1}{F_{io}} + \frac{1-\varepsilon_o}{(r_o/r_i)\varepsilon_o} \right]}$$

and

$$\dot{q}_{rad,net,o}'' = \frac{\dot{q}_{rad,net,o}}{A_o} = \frac{-\dot{q}_{rad,net,i}}{A_o} = -\left(\frac{A_i}{A_o} \right) \dot{q}_{rad,net,i}'' = -r^* \dot{q}_{rad,net,i}''$$

where $(A_i/A_o) = r_i/r_o = r^*$.

Now we consider the convective heat transfer for the two surfaces. The overall energy balance for the adiabatic outer surface is

$$\dot{q}_o'' = 0 = \dot{q}_{conv,o}'' + \dot{q}_{rad,net,o}'' = h_o(T_o - T_m) + \dot{q}_{rad,net,o}''$$

and h_o comes from the Nusselt number equation (8-29) for the outer surface of an annulus with fully-developed velocity and temperature profiles.

$$Nu_o = \frac{Nu_{oo}}{1 - (\dot{q}_{conv,i}'' / \dot{q}_{conv,o}'') \theta_o^*} = \frac{h_o D_h}{k} = \frac{\dot{q}_{conv,o}'' D_h}{k(T_o - T_m)}$$

where the hydraulic diameter for the annulus is $D_h=2(r_o-r_i)$. For the inner surface the overall energy balance is

$$\dot{q}_i'' = \dot{q}_{conv,i}'' + \dot{q}_{rad,net,i}'' = h_i(T_i - T_m) + \dot{q}_{rad,net,i}''$$

and h_i comes from the Nusselt number equation (8-28) for the inner surface of an annulus with fully-developed velocity and temperature profiles.

$$\text{Nu}_i = \frac{\text{Nu}_{ii}}{1 - (\dot{q}_{\text{conv},o}'' / \dot{q}_{\text{conv},i}'') \theta_i^*} = \frac{h_i D_h}{k} = \frac{\dot{q}_{\text{conv},i}'' D_h}{k (T_i - T_m)}$$

At this point, the two Nusselt number equations can be combined to eliminate $\dot{q}_{\text{conv},i}''$

$$\frac{k (T_o - T_m)}{D_h \dot{q}_{\text{conv},o}''} = \frac{1}{\text{Nu}_{oo}} - \frac{\left(\frac{\theta_o^*}{\text{Nu}_{oo}} \right) \left(\frac{1}{\text{Nu}_{ii}} \right) \dot{q}_{\text{conv},o}''}{\frac{k (T_i - T_m)}{D_h} + \left(\frac{\theta_i^*}{\text{Nu}_{ii}} \right) \dot{q}_{\text{conv},o}''}$$

Now, eliminate $\dot{q}_{\text{conv},o}''$ using the energy balance for the outer surface,

$$0 = \frac{1}{\text{Nu}_{oo}} - \frac{k (T_o - T_m)}{D_h r^* \dot{q}_{\text{rad},\text{net},i}''} - \frac{\left(\frac{\theta_o^*}{\text{Nu}_{oo}} \right) \left(\frac{1}{\text{Nu}_{ii}} \right) r^* \dot{q}_{\text{rad},\text{net},i}''}{\frac{k (T_i - T_m)}{D_h} + \left(\frac{\theta_i^*}{\text{Nu}_{ii}} \right) r^* \dot{q}_{\text{rad},\text{net},i}''}$$

For the problem statement all terms in this equation are known except T_o .

Iteration on this equation gives $T_o = 551\text{K} = 278^\circ\text{C}$. Note, this value can vary depending on how closely you converge the solution and on the property of air (which was selected at 550K). With this T_o value, the net radiative heat flux from the inner surface can be computed, $\dot{q}_{\text{rad},\text{net},i}'' = 644 \text{ W/m}^2$, and thus the outer-surface convective heat flux is computed to be $\dot{q}_{\text{conv},o}'' = 322 \text{ W/m}^2$. With the outer-surface temperature and heat flux now known, the inner surface total heat flux can be computed by rearranging the Nusselt number equation for the inner surface,

$$\dot{q}_{\text{conv},i}'' = \frac{k (T_i - T_m)}{D_h \left(\frac{1}{\text{Nu}_{ii}} \right)} + \theta_i^* \dot{q}_{\text{conv},o}'' = 1024 \text{ W/m}^2$$

and thus the total heat flux for the inner surface becomes

$$\dot{q}_{\text{total},i}'' = \dot{q}_{\text{conv},i}'' + \dot{q}_{\text{rad},\text{net},i}'' = 1669 \text{ W/m}^2$$

Based on these numbers, 61 percent of the total heat flux to the inner surface is transferred directly into the fluid by convection and the remainder is transferred to the outer surface via thermal radiation through the non-participating air medium and then into the fluid from the outer surface by convection because the outer surface is overall adiabatic.

8-6

The heat flux along a flat cooling tube in a typical nuclear power reactor may often be approximated by

$$\dot{q}_s'' = a + b \sin \frac{\pi x}{L}$$

where L is the length of the flat tube and x is the distance along the flat tube. A particular air-cooled reactor is to be constructed of a stack of fuel plates with a 3-mm air space between them. The length of the flow passage will be 1.22 m, and the heat flux at the plate surfaces will vary according to the above equation with $a = 900 \text{ W/m}^2$ and $b = 2500 \text{ W/m}^2$. The air mass velocity is to be $7.5 \text{ kg/(s}\cdot\text{m}^2)$. The air enters the reactor at 700 kPa and 100°C . The properties of air at 250°C may be used in the analysis and treated as constant. Prepare a scale plot of heat flux, air mean temperature, and plate surface temperature as a function of distance along the flow passage. Although the heat flux is not constant along the passage, the passage length-to-gap ratio is sufficiently large that the constant-heat-rate heat-transfer solution for the conductance h is not a bad approximation. Therefore assume h is a constant. We are most interested here in the peak surface temperature; if this occurs in a region where the heat flux is varying only slowly, the approximation is still better. This is a point for discussion. TEXSTAN can be used to help understand the results of this problem.

The solution begins by performing an energy balance on a control volume for an element of the parallel-planes channel, similar to that depicted in Fig. 8-3 for a curricular pipe. Let H be the channel height and L be the channel length.

$$\left(\frac{dT_m}{dx} \right) = \frac{2\dot{q}_s''}{H\rho Vc} = \frac{4\dot{q}_s''}{D_h\dot{m}''c}$$

Substitute the heat flux function and integrate from the channel entrance where the inlet temperature is $T_{m,x=0}$

$$T_m(x) = T_{m,x=0} + \frac{4}{D_h\dot{m}''c} \left[ax + \frac{bL}{\pi} \left(1 - \cos \left(\frac{\pi x}{L} \right) \right) \right]$$

To obtain the surface temperature, apply the local convective rate equation,

$$\begin{aligned} \dot{q}_s''(x) &= h_x [T_s(x) - T_m(x)] \\ T_s(x) &= T_m(x) + \frac{\dot{q}_s''(x)}{h_x} \end{aligned}$$

For this problem statement thermally fully-developed flow is assumed, and h is obtained from Table 8-2 for flow between parallel plates with a constant heat on both surfaces, $\text{Nu}=8.235$. The computing equation for the surface temperature becomes

$$T_s(x) = T_{m,x=0} + \frac{4}{D_h\dot{m}''c} \left[ax + \frac{bL}{\pi} \left(1 - \cos \left(\frac{\pi x}{L} \right) \right) \right] + \frac{1}{\text{Nu}} \frac{D_h}{k} \left[a + b \sin \left(\frac{\pi x}{L} \right) \right]$$

Evaluation of these two temperature equations at selected x -locations are shown in the table below

x	x/D_h	$\dot{q}_s''(x)$	$T_s(x)$	$T_m(x)$
-----	---------	------------------	----------	----------

(m)		(W/m ²)	(deg C)	(deg C)
0	0.0	900.0	116.0	100.0
0.01	1.7	964.4	117.9	100.8
0.02	3.3	1028.7	119.9	101.7
0.05	8.3	1221.0	126.2	104.6
0.1	16.7	1536.7	137.8	110.5
0.2	33.3	2131.4	164.1	126.3
0.3	50.0	2644.9	193.8	146.9
0.4	66.7	3043.3	225.5	171.4
0.5	83.3	3300.4	257.4	198.8
0.6	100.0	3399.2	288.1	227.7
0.7	116.7	3333.2	315.9	256.8
0.8	133.3	3106.7	339.7	284.6
0.9	150.0	2734.7	358.3	309.8
1	166.7	2241.7	371.0	331.3
1.1	183.3	1660.3	377.5	348.1
1.22	203.3	900.0	377.3	361.3

Note there are several small x -values, which will be required as a part of the TEXSTAN data set construction.

To verify the analysis the TEXSTAN data file for this problem choose the data set *8.6.dat.txt*. The data set construction is based on the *s51.dat.txt* file for combined entry length flow between parallel planes with a specified surface heat flux and thermal symmetry (initial profiles: flat velocity and flat temperature). Note that k_{out} has been changed to =4. A slight correction to the problem statement - do not use the specified $Re=1000$, but calculate the actual value.

$$Re_D = \dot{m}'' D_h / \mu = 1624$$

$$(x_{fd,hydro} / D_h) / Re = 0.05 \rightarrow x_{fd,hydro} = 0.05 D_h Re = 0.49 \text{ m}$$

$$(x_{fd,thermal} / D_h) / (Re Pr) = 0.05 \rightarrow x_{fd,thermal} = 0.05 D_h Re Pr = 0.34 \text{ m}$$

Note, the choice of 0.05 is a very simple estimate for parallel-planes channel. We see that the approximation of a thermally fully-developed entry region may not be a good assumption, but it can be verified by TEXSTAN. Use properties of air at $250^\circ \sim 525K$, and be careful to modify the density for the much higher pressure. You must construct the boundary condition table in the input data set to reflect the sine-function surface heat flux distribution. You can use the table entries given above, but you need to add 3 more data points near $x=0$ because you are using $kstart=1$. For internal flows, the numerical mesh is required to extend from surface to centerline (or surface to surface). For entry flows, the developing shear layer (boundary layer) is a very small part of this mesh, and therefore TEXSTAN must take very small flow-direction integration steps. Making the stepsize proportional to the boundary layer thickness is not

convenient. Therefore, internal entry flows require a different stepsize mechanism. Instead of using *deltax*, we set the flag *kdx*=1, and input “*deltax*” using the array *aux1(m)*. The definition of both *deltax* and *aux1* is $\Delta x/rw$. For this problem I suggest adding three points at $x=0.01$, 0.02 , and $0.05m$. Note the integration stepsize control starts extremely small and then increases, as reflected in *aux1(m)* starting at 0.01 and finally becoming 1.00.

###	x(m)	rw(m)	aux1(m)	aux2(m)	aux3(m)
	0.0000000	0.0015	0.0100	0.0000	0.0000
	0.0100000	0.0015	0.0100	0.0000	0.0000
	0.0200000	0.0015	0.2500	0.0000	0.0000
	0.0500000	0.0015	1.0000	0.0000	0.0000
	0.1000000	0.0015	1.0000	0.0000	0.0000
	0.2000000	0.0015	1.0000	0.0000	0.0000
	0.3000000	0.0015	1.0000	0.0000	0.0000
	0.4000000	0.0015	1.0000	0.0000	0.0000
	0.5000000	0.0015	1.0000	0.0000	0.0000
	0.6000000	0.0015	1.0000	0.0000	0.0000
	0.7000000	0.0015	1.0000	0.0000	0.0000
	0.8000000	0.0015	1.0000	0.0000	0.0000
	0.9000000	0.0015	1.0000	0.0000	0.0000
	1.0000000	0.0015	1.0000	0.0000	0.0000
	1.1000000	0.0015	1.0000	0.0000	0.0000
	1.2200000	0.0015	1.0000	0.0000	0.0000

The variables that were changed in *s51.dat.txt* to create *8.6.dat.txt* include *po*, *rhoc*, *viscoc*, *gam/cp*, *prc*(1), the two *nxbc* variables (16 total), the set of *x(m)*, *rw(m)*, and *aux1(m)* values, the set of *fj*(E,1,*m*) values, *xend*, *reyn*, *tref* and *twall*. Note: feel free to adjust the selected *x(m)* values.

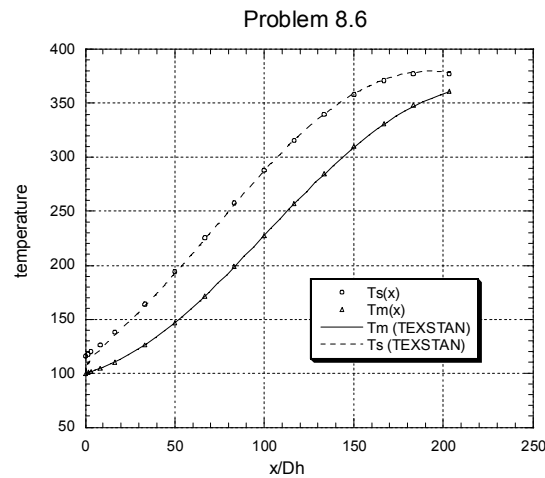
Here is an abbreviated listing of the *8.6.out.txt* output file:

integ	x/dh	cfapp	cf2(I)	cf2(E)	nu(I)	nu(E)
5	1.250E-02	8.156E-01	0.000E+00	7.414E-02	0.000E+00	1.547E+02
100	2.500E-01	1.703E-01	0.000E+00	2.176E-02	0.000E+00	3.635E+01
200	5.000E-01	1.205E-01	0.000E+00	1.692E-02	0.000E+00	2.676E+01
300	7.500E-01	9.864E-02	0.000E+00	1.476E-02	0.000E+00	2.253E+01
400	1.000E+00	8.570E-02	0.000E+00	1.346E-02	0.000E+00	2.003E+01
500	1.250E+00	7.691E-02	0.000E+00	1.258E-02	0.000E+00	1.833E+01
600	1.500E+00	7.045E-02	0.000E+00	1.193E-02	0.000E+00	1.709E+01
700	1.782E+00	6.493E-02	0.000E+00	1.137E-02	0.000E+00	1.602E+01
800	3.282E+00	4.903E-02	0.000E+00	9.739E-03	0.000E+00	1.297E+01
900	1.412E+01	2.645E-02	0.000E+00	7.643E-03	0.000E+00	9.246E+00
1000	3.908E+01	1.918E-02	0.000E+00	7.389E-03	0.000E+00	8.596E+00

1100	6.400E+01	1.747E-02	0.000E+00	7.387E-03	0.000E+00	8.440E+00
1200	8.883E+01	1.672E-02	0.000E+00	7.387E-03	0.000E+00	8.303E+00
1300	1.138E+02	1.629E-02	0.000E+00	7.387E-03	0.000E+00	8.210E+00
1400	1.386E+02	1.602E-02	0.000E+00	7.387E-03	0.000E+00	8.081E+00
1500	1.635E+02	1.583E-02	0.000E+00	7.387E-03	0.000E+00	7.940E+00
1600	1.883E+02	1.569E-02	0.000E+00	7.387E-03	0.000E+00	7.663E+00
1660	2.033E+02	1.562E-02	0.000E+00	7.387E-03	0.000E+00	7.315E+00

In the output we see the local friction coefficient $cf_2(E)$ approaching a constant value when x/D_h is about 15. If we were using cf_{app} as a measure of hydrodynamically fully developed flow, this number would be about four times larger. We also see $nu(E)$ becomes nearly constant for x/D_h of about 15.

The figure below is a comparison of the calculated values for $T_s(x)$ and $T_m(x)$ with TEXSTAN to further verify the assumption of $Nu = \text{constant}$.



8-7

A lubricating oil flows through a long 0.6-cm (inner-diameter) tube at a mean velocity of 6 m/s. If the tube is effectively insulated, calculate and plot the temperature distribution, resulting from *frictional* heating, in terms of the pertinent parameters. Let the fluid properties be those of a typical engine oil at 100°C. Start with Eq. (4-28).

For this problem we will assume the properties are constant. This may not be a good assumption, depending on the heat rise due to the viscous dissipation. The Reynolds number for this flow is 1758. We will assume the flow is hydrodynamically fully developed, because the difference between hydrodynamically and thermally fully developed flow is proportional to the Pr and for oil at 100°C the Pr=280. Neglect mass transfer and pressure work in Eq. (4-28) and it reduces to

$$\rho u \frac{\partial i}{\partial x} = -\frac{1}{r} \frac{\partial}{\partial r} \left(r k \frac{\partial T}{\partial r} \right) + \mu \left(\frac{\partial u}{\partial r} \right)^2$$

For oil, $di=cdT$, and the equation reduces to

$$\rho u c \frac{\partial T}{\partial x} = -\frac{1}{r} \frac{\partial}{\partial r} \left(r k \frac{\partial T}{\partial r} \right) + \mu \left(\frac{\partial u}{\partial r} \right)^2$$

The boundary conditions on this problem are a zero temperature gradient at the pipe centerline and a specified temperature gradient (in this case zero, adiabatic) at the pipe surface. This is a special case of the constant heat rate problem, and from Eq. (8-9) $\partial T / \partial x = dT_m / dx$, and the differential equation for constant properties reduces to

$$\frac{u}{\alpha} \frac{dT_m}{dx} = -\frac{1}{r} \frac{\partial}{\partial r} \left(r \frac{\partial T}{\partial r} \right) + \frac{\text{Pr}}{c} \left(\frac{\partial u}{\partial r} \right)^2$$

The boundary conditions for the adiabatic pipe are a constant (zero) heat rate at r_s and symmetry at the centerline, leading to a Neumann-Neumann boundary problem (specified temperature gradients at both the centerline and at the surface). Therefore, we can not find the two constants of integration when we separate variables and integrate. So, we substitute for one of the Neumann conditions with it's Dirichlet counterpart (in this case the surface temperature) and we bring in the surface heat flux (in this case there is no surface heat flux, but rather the fluid heating comes from the viscous dissipation) through the energy balance when we determine dT_m / dx . Thus the boundary conditions are the same as those following Eq. (8-10)

$$\left. \frac{\partial T}{\partial r} \right|_{r=0} = 0 \quad \text{and} \quad T|_{r=r_s} = T_s$$

For the circular pipe with the hydrodynamically fully developed velocity profile is Eq. (7-8). Substitute this into the differential equation (including the viscous dissipation term), separate variables, integrate, and apply the boundary conditions to obtain the temperature profile

$$T(r, x) = T_s(x) - \frac{2V}{\alpha} \left(\frac{dT_m}{dx} \right) \left(\frac{3r_s^2}{16} + \frac{r^4}{16r_s^2} - \frac{r^2}{4} \right) + \frac{\text{Pr} V^2}{c} \left(1 - \left(\frac{r}{r_s} \right)^4 \right)$$

Now solve for T_m using Eq. (8-12),

$$T_m(x) = T_s(x) - \frac{11}{96} \frac{2V}{\alpha} \left(\frac{dT_m}{dx} \right) r_s^2 + \frac{5}{6} \frac{\text{Pr} V^2}{c}$$

Compare this temperature profile to Eq. (8-13) for the circular pipe with constant heat rate, but without viscous dissipation. Now develop an equation for the mean temperature gradient by performing an energy balance similar to Fig. 8-3. There will be no surface heat transfer, but rather a volumetric heating due to the viscous dissipation

$$S = \int_V \left[\mu \left(\frac{\partial u}{\partial r} \right)^2 \right] 2\pi r dr dx$$

and the mean temperature gradient becomes

$$\frac{dT_m}{dx} = \frac{8\mu V}{\rho c r_s^2} = \frac{8\alpha V \text{Pr}}{c r_s^2}$$

or

$$T_m(x) = T_m|_{x=0} + \frac{8\mu V}{\rho c r_s^2} x$$

And from the mean temperature equation

$$(T_s - T_m) = \frac{\text{Pr} V^2}{c}$$

For the temperature profile

$$\theta = \left(\frac{T_s - T}{T_s - T_m} \right) = 2 \left[1 - 2 \left(\frac{r}{r_s} \right)^2 + \left(\frac{r}{r_s} \right)^4 \right]$$

The profile is a fourth-order inflecting curve with zero gradients at $r=0$ and $r=r_s$, and the magnitude grows with x because $T_s=T_s(x)$. The wall will be hotter than the core. As the viscous heating increases the overall temperature field, the strong variation of the thermal properties will affect the solution.

8-8

Consider a journal bearing using the oil of Prob. 8-7. Let the journal diameter be 7.6 cm, the clearance be 0.025 cm, and the rpm be 3600. Neglecting end effects, and assuming no flow of oil into or out of the system, calculate the temperature distribution in the oil film on the assumption that there is no heat transfer into the journal (the inner surface) but that the bearing (the outer surface) is maintained at 80°C. Calculate the rate of heat transfer per square meter of bearing surface. Assume no eccentricity, that is, no load on the bearing. How much power is needed to rotate the journal if the bearing is 10 cm long?

This analysis can be carried out in either axisymmetric coordinates or in Cartesian coordinates, and the answers will be the same, because the journal clearance is such that radial effects on mass flow rate are negligible. For simplicity we choose the Cartesian analysis. The journal forms the inner surface, and it is modeled as an adiabatic surface that rotates at an angular velocity ω such that its velocity is $V = \omega r_i$. The bearing forms the outer surface, and it has a constant surface temperature. Define the coordinate y to originate from the inner journal surface, and the clearance distance is H . This problem reduces to a couette-flow problem, and for constant properties, the velocity profile will be linear. The governing equation is Eq. (4-10)

$$\rho u \frac{\partial u}{\partial x} + \rho v \frac{\partial u}{\partial y} = -\frac{dP}{dx} + \frac{\partial}{\partial y} \left(\mu \frac{\partial u}{\partial y} \right)$$

Based on the couette-flow model (no x -convection, no radial velocity component, and no pressure gradient) the governing equation and boundary conditions are

$$\mu \frac{d^2 u}{dy^2} = 0 \quad \text{and} \quad u|_{y=0} = V \quad \text{and} \quad u|_{y=H} = 0$$

which integrates to give a velocity profile which is linear

$$u = V \frac{y}{H}$$

where $V = \omega r_i = 14.326$ m/s. The governing energy equation for constant properties is Eq. (4-38)

$$u \frac{\partial T}{\partial x} + v \frac{\partial T}{\partial y} - \alpha \left[\frac{\partial^2 T}{\partial y^2} + \frac{\text{Pr}}{c} \left(\frac{\partial u}{\partial y} \right)^2 \right] = 0$$

Based on the couette-flow model the governing equation and boundary conditions are

$$k \frac{d^2 T}{dy^2} = -\mu \left(\frac{du}{dy} \right)^2 \quad \text{and} \quad \frac{dT}{dy} \Big|_{y=0} = 0 \quad \text{and} \quad T|_{y=H} = T_s$$

Solving the energy equation gives the fluid temperature profile

$$T(y) = \frac{\mu V^2}{2k} \left[1 - \left(\frac{y}{H} \right)^2 \right] + T_s$$

From this profile the film temperature can be determined

$$T_f = \frac{T_{y=0} + T_{y=H}}{2} = T_s + \frac{\mu V^2}{4k}$$

To evaluate the properties at the film temperature, there needs to be an interpolation of the properties and it is iterative. Hint: the lowest temperature will be on the bearing surface, specified as 80°C, and the journal surface (which is adiabatic) will be hotter. So linearly interpolate the entries in Table A-14 for oil between 75°C and 100°C and the film temperature converges to be 89.8°C (363K). Now compute the heat flux at the bearing surface using Fourier's law,

$$\dot{q}''|_{y=H} = -k \frac{dT}{dy} \Big|_{y=H} = \frac{\mu V^2}{2} = 21,554 \text{ W/m}^2$$

Now, carry out a First-Law energy balance on the control volume of the fluid in the clearance. The shaft work does work on the fluid, which causes viscous dissipation to overcome friction, which in turn generates heat, and that heat must be removed at the outer surface to maintain steady state couette flow (no heat rise in the x -direction, where x is the direction of rotation).

$$\begin{aligned} \dot{w}_{shaft} &= \dot{q}_{s,out} \\ &= (2\pi r_o L) \dot{q}''|_{y=H} = 518 \text{ W} \end{aligned}$$

Note, as a check, the power input to the fluid can also be computed as

$$\begin{aligned} \dot{w}_{shaft} &= \left(\tau \Big|_{y=0} \right) A_{s,y=0} \times V \\ &= \left[\mu \frac{du}{dy} \Big|_{y=0} \right] (2\pi r_i L) V = \mu \frac{V^2}{H} (2\pi r_i L) = 515 \text{ W} \end{aligned}$$

8-9

Consider uniform-temperature laminar flow in a circular tube with a fully developed velocity profile. At some point $x^+ = 0$ the surface temperature is raised above the fluid temperature by an amount a . It remains constant at this value until a point $x^+ = x_1^+$ is reached, where the surface temperature is again raised an amount b , remaining constant thereafter. Develop a general expression for the surface heat flux, and for the mean fluid temperature θ_m , in the part of the tube following the second step in surface temperature. Use variable-surface-temperature theory.

This problem concerns the section in the chapter about the effect of axial variation of the surface temperature with hydrodynamically fully developed flow using linear superposition theory. The surface heat flux is given by Eq. (8-44)

$$\dot{q}_s''(x^+) = -\frac{k}{r_s} \left[\int_0^{x^+} \theta_{r^+}(x^+ - \xi, 1) \frac{dT_s}{d\xi} d\xi + \sum_{i=1}^k \theta_{r^+}(x^+ - \xi_i, 1) \Delta T_{s,i} \right]$$

where the theta function is Eq. (8-45)

$$\theta_{r^+}(x^+ - \xi, 1) = -2 \sum_{n=0}^{\infty} G_n \exp[-\lambda_n^2 (x^+ - \xi)]$$

Because this problem only has the two steps, which are the discontinuities, Eq. (8-44) reduces to

$$\begin{aligned} \dot{q}_s''(x^+) &= \frac{2k}{r_s} \left\{ \sum_{n=0}^{\infty} G_n \exp[-\lambda_n^2 x^+] \Delta T_{s,1} + \sum_{n=0}^{\infty} G_n \exp[-\lambda_n^2 (x^+ - x_1^+)] \Delta T_{s,1} \right\} \\ &= \frac{2k}{r_s} \left\{ a \sum_{n=0}^{\infty} G_n \exp[-\lambda_n^2 x^+] + b \sum_{n=0}^{\infty} G_n \exp[-\lambda_n^2 (x^+ - x_1^+)] \right\} \quad x^+ > x_1^+ \end{aligned}$$

To find the mixed mean temperature carry out an energy balance on a control volume similar to that described following Eq. (8-46)

$$\dot{q} = \frac{4\pi r_s^3 V \rho c}{k} \int_0^{x^+} \dot{q}_s'' dx^+ = \pi r_s^2 V \rho c (T_m - T_e)$$

Now, insert the heat flux equation and integrate,

$$T_m(x^+) - T_e = -8a \sum_{n=0}^{\infty} \frac{G_n}{\lambda_n^2} \exp(-\lambda_n^2 x^+) + 8a \sum_{n=0}^{\infty} \frac{G_n}{\lambda_n^2} - 8b \sum_{n=0}^{\infty} \frac{G_n}{\lambda_n^2} \exp[-\lambda_n^2 (x^+ - x_1^+)] + 8b \sum_{n=0}^{\infty} \frac{G_n}{\lambda_n^2}$$

We now focus on the second and fourth terms of this equation. For a step temperature change, the nondimensional temperature profile for the mean temperature is given by Eq. (8-38),

$$\theta_m = \frac{T_s - T_m}{T_s - T_e} = 8 \sum_{n=0}^{\infty} \frac{G_n}{\lambda_n^2} \exp(-\lambda_n^2 x^+)$$

and from this equation,

$$\theta_m|_{x^+=0} = 1 = 8 \sum_{n=0}^{\infty} \frac{G_n}{\lambda_n^2}$$

We use this relationship to reduce the second and fourth terms, and the equation for the mean temperature reduces to

$$T_m(x^+) - T_e = a - 8a \sum_{n=0}^{\infty} \frac{G_n}{\lambda_n^2} \exp(-\lambda_n^2 x^+) + b - 8b \sum_{n=0}^{\infty} \frac{G_n}{\lambda_n^2} \exp[-\lambda_n^2 (x^+ - x_1^+)] \quad x^+ > x_1^+$$

Finally, formulate the nondimensional temperature profile

$$\begin{aligned} \theta_m(x^+) &= \frac{T_s - T_m}{T_s - T_e} = \frac{(T_s - T_e) - (T_m - T_e)}{T_s - T_e} = 1 - \frac{T_m - T_e}{T_s - T_e} \\ &= 1 - \frac{T_m - T_e}{(a + b)} \end{aligned}$$

and

$$\theta_m(x^+) = \frac{8}{(a + b)} \left\{ a \sum_{n=0}^{\infty} \frac{G_n}{\lambda_n^2} \exp(-\lambda_n^2 x^+) + b \sum_{n=0}^{\infty} \frac{G_n}{\lambda_n^4} \exp[-\lambda_n^2 (x^+ - x_1^+)] \right\}$$

We also note that the Nusselt number can be easily formed from its definition.

$$\text{Nu}_x = \frac{hD_h}{k} = \frac{-D_h \dot{q}_s''(x^+)}{k(T_s - T_e)\theta_m(x^+)}$$

8-10

Consider laminar flow in a circular tube with a fully developed velocity profile. Let heat be added at a constant rate along the tube from $x^+ = 0$ to $x^+ = 0.10$. Thereafter let the tube surface be adiabatic. Calculate and plot the tube surface temperature as a function of x^+ . TEXSTAN can be used to confirm this analysis.

This problem concerns the section in the chapter about the effect of axial variation of the surface heat flux with hydrodynamically fully developed flow using linear superposition theory. The surface temperature is given by Eq. (8-50) along with Eq. (8-51) and Table 8-5 for the infinite-series coefficients.

For $0 \leq x^+ \leq 0.1$ the equation for the surface temperature becomes

$$\begin{aligned} T_s(x^+) - T_e &= \frac{r_s}{k} \int_0^{x^+} g(x^+ - \xi) \dot{q}_s''(\xi) d\xi \\ &= \frac{r_s}{k} \int_0^{x^+} \left[4 + \sum_m \frac{\exp(-\gamma_m^2(x^+ - \xi))}{\gamma_m^2 A_m} \right] \dot{q}_s''(\xi) d\xi \\ &= \frac{r_s \dot{q}_s''}{k} \int_0^{x^+} 4 d\xi + \frac{r_s \dot{q}_s''}{k} \int_0^{x^+} \left[\sum_m \frac{\exp(-\gamma_m^2(x^+ - \xi))}{\gamma_m^2 A_m} \right] d\xi \end{aligned}$$

To carry out the integration, use the transformation $u = (x^+ - \xi)$ and $du = -d\xi$, along with limit transformations $\xi = x^+ \rightarrow u = 0$ and $\xi = 0 \rightarrow u = x^+$,

$$\begin{aligned} T_s(x^+) - T_e &= \frac{r_s}{k} \int_0^{x^+} \left[4 + \sum_m \frac{\exp(-\gamma_m^2(x^+ - \xi))}{\gamma_m^2 A_m} \right] \dot{q}_s''(\xi) d\xi \\ &= \frac{r_s \dot{q}_s''}{k} \int_0^{x^+} 4 d\xi - \frac{r_s \dot{q}_s''}{k} \sum_m \int_{x^+}^0 \frac{\exp(-\gamma_m^2 u)}{\gamma_m^2 A_m} du \\ &= \frac{r_s \dot{q}_s''}{k} \int_0^{x^+} 4 d\xi + \frac{r_s \dot{q}_s''}{k} \sum_m \left[\frac{\exp(-\gamma_m^2 u)}{\gamma_m^4 A_m} \right]_{x^+}^0 \\ &= \frac{r_s \dot{q}_s''}{k} \left[4x^+ + \sum_m \frac{[1 - \exp(-\gamma_m^2 x^+)]}{\gamma_m^4 A_m} \right] \quad 0 \leq x^+ \leq 0.1 \end{aligned}$$

For $x^+ > 0.1$, $\dot{q}_s'' = 0$ and the equation for the surface temperature becomes

$$\begin{aligned} T_s(x^+) - T_e &= \frac{r_s}{k} \left[\int_0^{0.1} 4 \dot{q}_s'' d\xi + \int_{0.1}^{x^+} 4 \cancel{\dot{q}_s''} d\xi \right] \\ &\quad + \frac{r_s}{k} \left\{ \int_0^{0.1} \left[\sum_m \frac{\exp(-\gamma_m^2(x^+ - \xi))}{\gamma_m^2 A_m} \right] \dot{q}_s'' d\xi + \int_{0.1}^{x^+} \left[\sum_m \frac{\exp(-\gamma_m^2(x^+ - \xi))}{\gamma_m^2 A_m} \right] \cancel{\dot{q}_s''} d\xi \right\} \\ &= \frac{r_s \dot{q}_s''}{k} \left[0.4 + \sum_m \frac{\exp(-\gamma_m^2(x^+ - 0.1)) - \exp(-\gamma_m^2 x^+)}{\gamma_m^4 A_m} \right] \quad x^+ > 0.1 \end{aligned}$$

To obtain the mean temperature along the tube, use Eq. (8-52),

$$\begin{aligned} T_m(x^+) - T_e &= \frac{4r_s}{k} \int_0^{x^+} \dot{q}_s''(\xi) d\xi \\ &= \frac{4r_s}{k} \dot{q}_s'' x^+ \quad 0 \leq x^+ \leq 0.1 \end{aligned}$$

and

$$\begin{aligned} T_m(x^+) - T_e &= \frac{4r_s}{k} \int_0^{x^+} \dot{q}_s''(\xi) d\xi = \frac{4r_s}{k} \int_0^{0.1} \dot{q}_s''(\xi) d\xi + \frac{4r_s}{k} \int_{0.1}^{x^+} \dot{q}_s'''(\xi) d\xi \\ &= \frac{0.4r_s}{k} \dot{q}_s'' \quad x^+ > 0.1 \end{aligned}$$

Note the mean temperature is fixed for $x^+ > 0.1$. To evaluate the series you must use at least 20 terms. Table 8-5 contains the first 5 terms, so use the algorithm at the bottom of the table to generate the 6th through the 20th terms. The reason for the large number of terms is the series is simulating a step heat flux (similar to a square wave), rather than a slowly-changing heat flux.

To verify the analysis the TEXSTAN data file for this problem choose the data set *8.10.dat.txt*. The data set construction is based on the *s35.dat.txt* file for thermal entry length flow in a pipe with a specified surface heat flux (initial profiles: hydrodynamically fully-developed velocity and flat temperature). Note that *kout* has been changed to =4.

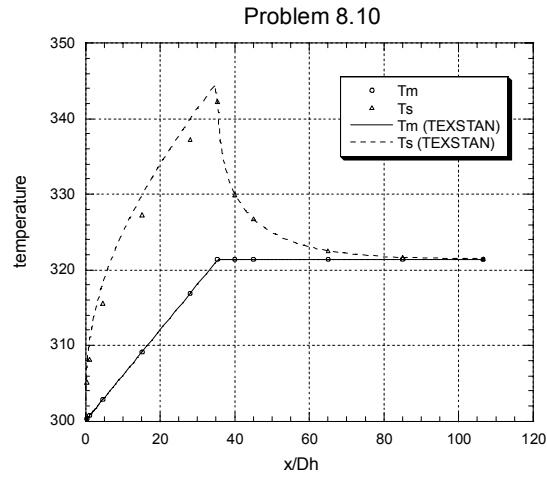
To set up the input data file, you will need to compute the region of heating $0 \leq x^+ \leq 0.1$ followed by the adiabatic region of the tube, $x^+ = 0.3$. The variables that were changed in *s35.dat.txt* to create *8.10.dat.txt* include *rhoc*, *viscoc*, *gam/cp*, *prc(1)*, the set of six *x(m)* and *aux1(m)* values, the six *fj(E,1,m)* values, *xend*, *reyn*, *tref* and *twall*. Note: feel free to adjust the selected *x(m)* values. The *x(m)* values in the data set are intended to create more integration points in the initial part of the developing thermal boundary layer region based on the logarithmic behavior of the parameter $(x/D_h)/\text{Re}$.

Here is an abbreviated listing of the *8.10.fnm84.txt* output file using *k5=20* print spacing

intg	x/dh	htc	qflux	tm	ts
5	2.5000001E-02	1.4875E+01	4.0000E+01	3.0002E+02	3.0270E+02
20	1.0000002E-01	9.1371E+00	4.0000E+01	3.0006E+02	3.0444E+02
40	2.0000005E-01	7.2029E+00	4.0000E+01	3.0012E+02	3.0567E+02
60	3.0000006E-01	6.2744E+00	4.0000E+01	3.0018E+02	3.0656E+02
80	3.9999983E-01	5.6923E+00	4.0000E+01	3.0024E+02	3.0727E+02
100	5.0000000E-01	5.2801E+00	4.0000E+01	3.0030E+02	3.0788E+02
120	6.2148713E-01	4.9091E+00	4.0000E+01	3.0037E+02	3.0852E+02
140	8.0200949E-01	4.5099E+00	4.0000E+01	3.0048E+02	3.0935E+02
160	1.0702576E+00	4.1010E+00	4.0000E+01	3.0064E+02	3.1040E+02
180	1.4688589E+00	3.6996E+00	4.0000E+01	3.0088E+02	3.1169E+02
200	2.0611587E+00	3.3201E+00	4.0000E+01	3.0124E+02	3.1329E+02
220	2.9412879E+00	2.9721E+00	4.0000E+01	3.0177E+02	3.1523E+02
240	4.2491096E+00	2.6613E+00	4.0000E+01	3.0255E+02	3.1758E+02
260	6.1631569E+00	2.3937E+00	4.0000E+01	3.0370E+02	3.2042E+02

280	9.0503060E+00	2.1628E+00	4.0000E+01	3.0544E+02	3.2393E+02
300	1.2982654E+01	1.9859E+00	4.0000E+01	3.0780E+02	3.2795E+02
320	1.8000862E+01	1.8581E+00	4.0000E+01	3.1082E+02	3.3235E+02
340	2.4404760E+01	1.7668E+00	4.0000E+01	3.1467E+02	3.3731E+02
360	3.2577007E+01	1.7049E+00	4.0000E+01	3.1958E+02	3.4304E+02
380	3.5781336E+01	0.0000E+00	0.0000E+00	3.2138E+02	3.3964E+02
400	3.5935409E+01	0.0000E+00	0.0000E+00	3.2138E+02	3.3835E+02
420	3.6164353E+01	0.0000E+00	0.0000E+00	3.2138E+02	3.3711E+02
440	3.6504570E+01	0.0000E+00	0.0000E+00	3.2138E+02	3.3580E+02
460	3.7010076E+01	0.0000E+00	0.0000E+00	3.2138E+02	3.3440E+02
480	3.7766605E+01	0.0000E+00	0.0000E+00	3.2138E+02	3.3289E+02
500	3.8882826E+01	0.0000E+00	0.0000E+00	3.2138E+02	3.3127E+02
520	4.0541463E+01	0.0000E+00	0.0000E+00	3.2138E+02	3.2957E+02
540	4.3006092E+01	0.0000E+00	0.0000E+00	3.2138E+02	3.2781E+02
560	4.6291759E+01	0.0000E+00	0.0000E+00	3.2138E+02	3.2622E+02
580	4.9962469E+01	0.0000E+00	0.0000E+00	3.2138E+02	3.2498E+02
600	5.4049830E+01	0.0000E+00	0.0000E+00	3.2138E+02	3.2402E+02
620	5.8601126E+01	0.0000E+00	0.0000E+00	3.2138E+02	3.2327E+02
640	6.3669020E+01	0.0000E+00	0.0000E+00	3.2138E+02	3.2269E+02
660	6.9312113E+01	0.0000E+00	0.0000E+00	3.2138E+02	3.2225E+02
680	7.5595761E+01	0.0000E+00	0.0000E+00	3.2138E+02	3.2194E+02
700	8.2592630E+01	0.0000E+00	0.0000E+00	3.2138E+02	3.2172E+02
720	9.0383681E+01	0.0000E+00	0.0000E+00	3.2138E+02	3.2158E+02
740	9.9059068E+01	0.0000E+00	0.0000E+00	3.2138E+02	3.2149E+02
756	1.0671433E+02	0.0000E+00	0.0000E+00	3.2138E+02	3.2144E+02

The figure below is a comparison of the calculated values for $T_s(x)$ and $T_m(x)$ with TEXSTAN to further verify the assumption of $Nu=\text{constant}$.



In the figure we see the slight underprediction of the surface temperature with the analytical method using 20 terms in the series. Note that with 5 terms it is quite underpredicted, and perhaps with more terms it would come closer to the TEXSTAN calculations. We expect complete agreement between TEXSTAN and analysis for the mean temperature because this both procedures incorporate the First Law energy balance into their respective formulations.

8-11

Consider laminar flow in a circular tube with a fully developed velocity profile. Let the tube surface be alternately heated at a constant rate per unit of length and adiabatic, with each change taking place after intervals of x^+ of 0.020. How large must x^+ be for the effects of the original entry length to damp out? How does the Nusselt number vary along the heated segments after the effects of the original entry length have damped out? TEXSTAN can be used to confirm this analysis.

The analytic solution to this problem involves the same procedure as 8-10 except that the procedure is repeated at x^+ intervals of 0.02. For the mean temperature, the equation for 3 intervals, $x^+ > \xi_2$, will be

$$\begin{aligned} T_m(x^+) - T_e &= \frac{4r_s}{k} \int_0^{x^+} \dot{q}_s''(\xi) d\xi = \frac{4r_s}{k} \left[\int_0^{\xi_1} \dot{q}_s''(\xi) d\xi + \int_{\xi_1}^{\xi_2} \dot{q}_s'(\xi) d\xi + \int_{\xi_2}^{x^+} \dot{q}_s''(\xi) d\xi \right] \\ &= \frac{r_s}{k} \dot{q}_s'' \left[(\xi_1 - 0) + 0 + (x^+ - \xi_2) \right] \\ &= \frac{r_s}{k} \dot{q}_s'' \left[\xi_1 + (x^+ - \xi_2) \right] \end{aligned}$$

and the surface temperature for the same 3 intervals, $x^+ > \xi_2$,

$$\begin{aligned} T_s(x^+) &= T_e + \frac{r_s}{k} \left[\int_0^{\xi_1} 4\dot{q}_s'' d\xi + \int_{\xi_1}^{\xi_2} 4\dot{q}_s' d\xi + \int_{\xi_2}^{x^+} 4\dot{q}_s'' d\xi \right] + \frac{r_s}{k} \left\{ \int_0^{\xi_1} \left[\sum_m \frac{\exp(-\gamma_m^2(x^+ - \xi))}{\gamma_m^2 A_m} \right] \dot{q}_s'' d\xi \right\} \\ &\quad + \frac{r_s}{k} \left\{ \int_{\xi_1}^{\xi_2} \left[\sum_m \frac{\exp(-\gamma_m^2(x^+ - \xi))}{\gamma_m^2 A_m} \right] \dot{q}_s' d\xi \right\} + \frac{r_s}{k} \left\{ \int_{\xi_2}^{x^+} \left[\sum_m \frac{\exp(-\gamma_m^2(x^+ - \xi))}{\gamma_m^2 A_m} \right] \dot{q}_s'' d\xi \right\} \\ &= T_m(x^+) + \frac{r_s}{k} \left\{ \int_0^{\xi_1} \left[\sum_m \frac{\exp(-\gamma_m^2(x^+ - \xi))}{\gamma_m^2 A_m} \right] \dot{q}_s'' d\xi \right\} \\ &\quad + \frac{r_s}{k} \left\{ \int_{\xi_1}^{\xi_2} \left[\sum_m \frac{\exp(-\gamma_m^2(x^+ - \xi))}{\gamma_m^2 A_m} \right] \dot{q}_s' d\xi \right\} + \frac{r_s}{k} \left\{ \int_{\xi_2}^{x^+} \left[\sum_m \frac{\exp(-\gamma_m^2(x^+ - \xi))}{\gamma_m^2 A_m} \right] \dot{q}_s'' d\xi \right\} \end{aligned}$$

Carrying out the integrations yields

$$\begin{aligned} T_s(x^+) - T_m(x^+) &= \frac{r_s \dot{q}_s''}{k} \left\{ \sum_m \frac{\exp(-\gamma_m^2(x^+ - \xi_1)) - \exp(-\gamma_m^2 x^+)}{\gamma_m^4 A_m} \right\} \\ &\quad + \frac{r_s \dot{q}_s''}{k} \left\{ \sum_m \frac{1 - \exp(-\gamma_m^2(x^+ - \xi_2))}{\gamma_m^4 A_m} \right\} \end{aligned}$$

Derivation of the terms for the additional heating intervals is straightforward, and the extra terms look similar to those for the 3-term (heating-adiabatic-heating) interval. A local Nusselt number is readily evaluated from its definition

$$\text{Nu}(x^+) = \frac{(2r_s \dot{q}_s''/k)}{T_s(x^+) - T_m(x^+)}$$

To verify the analysis the TEXSTAN data file for this problem choose the data set *8.11.dat.txt*. The data set construction is based on the *s35.dat.txt* file for thermal entry length flow in a pipe with a specified surface heat flux (initial profiles: hydrodynamically fully-developed velocity and flat temperature). Note that *kout* has been changed to =4.

Note a slight change to the input instructions. Let the Reynolds number be 100, and choose the fluid to be water at an inlet temperature of 20 °C and a heat flux of 2000 W/m² (recall this is water which can take a high heat flux). For the geometry, choose a tube radius of 1 cm. The tube heating is periodic, beginning at $x=0$ for a distance $\Delta x^+ = 0.02$, followed by an adiabatic wall for the next $\Delta x^+ = 0.02$, and then heating, and so forth. The distance $\Delta x^+ = 0.02$ translates into a heating length of $\Delta x = 0.14$ m. The problem statement suggests the tube be a length equal to $x^+ = 0.3$, providing 15 segments, with 8 of these segments heating, and an overall tube length of 2.1 m.

Setting up the boundary conditions for a variable heat flux problem is described in the user's manual for all internal laminar flows, *s30.man*, which should be helpful to the new user. Because of the variable heating, it is easiest to set all *aux1(m)* values to a uniform integration stepsize of 0.05, which makes TEXSTAN integrate in the flow direction at intervals of 5% of the tube radius. For a tube radius of 1 cm, this will cause TEXSTAN to have about 280 integration steps over each $\Delta x^+ = 0.02$. Here is a partial listing of how the variable heat flux boundary condition has been set up in the *8.11.dat.txt* data set.

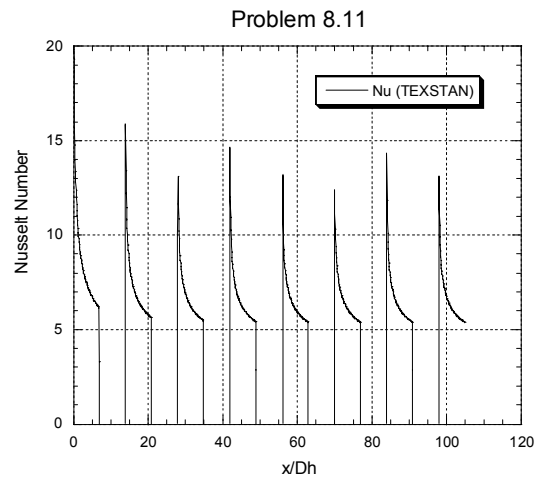
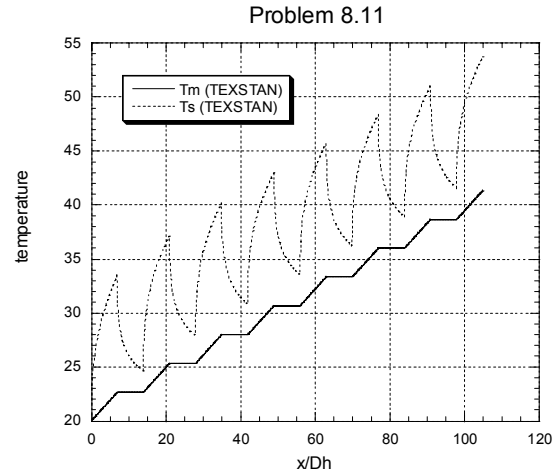
###	x(m)	rw(m)	aux1(m)	aux2(m)	aux3(m)
	0.0000000	0.0100	0.0500	0.0000	0.0000
	0.1400000	0.0100	0.0500	0.0000	0.0000
	0.1410000	0.0100	0.0500	0.0000	0.0000
	0.2800000	0.0100	0.0500	0.0000	0.0000
	0.2810000	0.0100	0.0500	0.0000	0.0000

and the listing of the boundary condition table that go with these *x(m)* locations is

###	ubI(m)	am(I,m)	fj(I,1,m)	fj(I,2,m)	fj(I,3,m)	fj(I,4,m)	fj(I,5,m)
###	ubE(m)	am(E,m)	fj(E,1,m)	fj(E,2,m)	fj(E,3,m)	fj(E,4,m)	fj(E,5,m)
	0.00	0.0	0.000				
	0.00	0.000	2000.0				
	0.00	0.0	0.000				
	0.00	0.000	2000.0				
	0.00	0.0	0.000				
	0.00	0.000	0.0				
	0.00	0.0	0.000				
	0.00	0.000	0.0				
	0.00	0.0	0.000				
	0.00	0.000	2000.0				

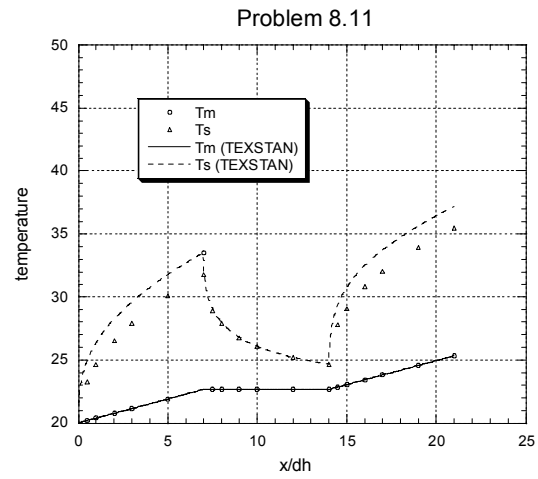
From these listings you can see the heat flux (2000 W/m²) is applied over the interval $0 \leq x \leq 0.14$ m, and at $x=0.141$ m the heat flux is reduced to zero over the interval $0.141 \leq x \leq 0.28$ m, and the periodic heating is resumed at $x=0.281$ m. Supplying TEXSTAN with a variable boundary condition is quite easy.

The figures below show the TEXSTAN-calculated values for $T_s(x)$, $T_m(x)$ and $Nu(x)$ for this periodic heating condition.



We see from the $Nu(x)$ graph that the periodic heating seems to become “steady-periodic” by about the 3rd or 4th heating segment. A value of $x/D_h=50$ translates into an $x^+ = 0.14$, and the heat transfer designer could take an average Nu number for this interval, about 7, compared to 4.36 for a continuously heated tube. Periodic heating can be a very effective means of achieving a high heat transfer coefficient. However, the overall temperature rise is still governed by the energy balance.

The graph shown below compares the mean and surface temperatures predicted by TEXSTAN with the analysis for 3 intervals using 20 terms in the series (note more terms will considerably improve the comparison).



8-12

Evaluate and plot both local and mean Nusselt numbers for fully developed laminar flow in a square tube. At what value of x^+ does the local Nusselt number come within two percent of the asymptotic value?

Note the problem statement should include the requirement of a constant surface temperature boundary condition. The analysis uses Eq. (8-39) for Nu_x and Eq. (8-40) for Nu_m along with Table 8-8.

x^+	Nu_x	Nu_m
0.01	4.55	9.00
0.02	4.10	6.66
0.05	3.42	4.88
0.1	3.08	4.05
0.2	2.99	3.53
5	2.98	3.00

Nu_x comes within 2% of its asymptotic value at about $x^+ = 0.12$.

8-13

Consider the problem posed by Eq. (8-53). Let $\beta = 6$ and let the tube be circular. Evaluate and plot the local Nusselt number as a function of x/L . Explain physically the reasons for the behavior noted.

Equation (8-53) describes the sinusoidal axial variation in surface heat flux over a tube of length L ,

$$\frac{\dot{q}_s''}{\dot{q}_{s,\max}''} = \sin \frac{\pi x}{L}$$

Eq. (8-54) is the equation for the mean temperature,

$$T_m - T_e = \frac{4\dot{q}_{s,\max}'' r_s}{k\beta} (1 - \cos \beta x^+)$$

Combining this equation with Eq. (8-55) for the surface temperature gives

$$\begin{aligned} T_s(x^+) - T_m(x^+) = & \frac{\dot{q}_{s,\max}'' r_s}{k} \left\{ \sin(\beta x^+) \left[\sum_m \frac{1}{A_m(\gamma_m^4 + \beta^2)} \right] \right\} \\ & - \frac{\dot{q}_{s,\max}'' r_s}{k} \left\{ \beta \cos \beta x^+ \left[\sum_m \frac{1}{\gamma_m^2 A_m(\gamma_m^4 + \beta^2)} \right] \right\} \\ & + \frac{\dot{q}_{s,\max}'' r_s}{k} \left\{ \beta \cos \beta x^+ \left[\frac{\exp(-\gamma_m^2 x^+)}{\gamma_m^2 A_m(\gamma_m^4 + \beta^2)} \right] \right\} \end{aligned}$$

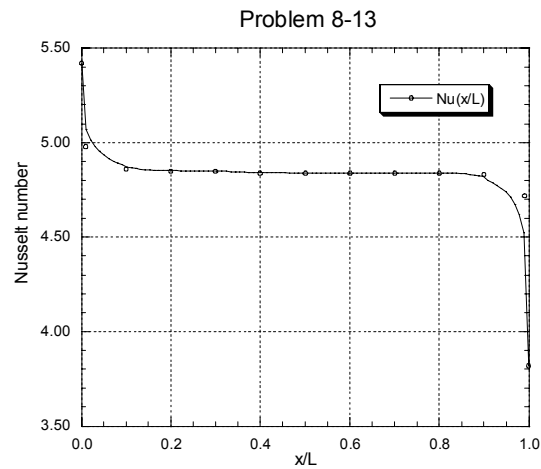
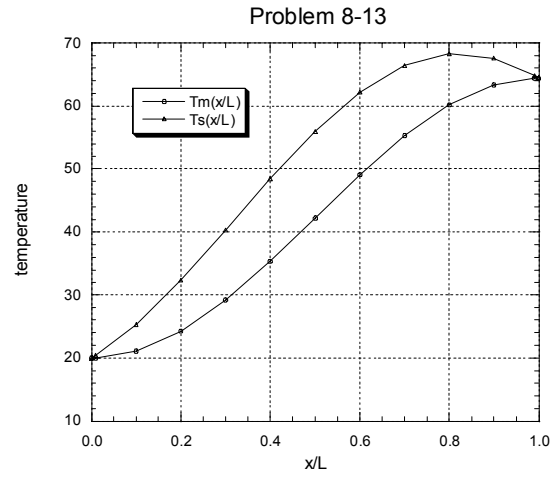
where

$$\begin{aligned} \beta &= r_s \text{Re Pr } \pi / L \\ \beta x^+ &= [r_s \text{Re Pr } \pi / L][2(x/D)/\text{Re Pr}] = \pi x / L \\ x^+ &= 2(x/D)/(\text{Re Pr}) = (\pi x)/(\beta L) \end{aligned}$$

The variation of Nu_x is given by formulating its definition,

$$\text{Nu}(x^+) = \frac{2r_s \dot{q}_s'' / k}{T_s(x^+) - T_m(x^+)} = \frac{(2r_s/k) \dot{q}_{s,\max}'' \sin \beta x^+}{T_s(x^+) - T_m(x^+)}$$

To plot the profiles for this analysis choose some physical variables. Let the Reynolds number be 100, and choose the fluid to be water at an inlet temperature of 20 °C with a maximum heat flux of 2000 W/m². For the geometry, choose a tube radius of 1 cm. The tube heating is sinusoidal as described in the problem statement, beginning at $x=0$, with an overall tube length of 2.1 m. Beta is 6. The temperature and Nusselt number plots are



In the plot of Nu we see a mostly constant value, suggesting $Nu=4.36$ would be ok for most of the tube, but it would significantly underestimate the surface temperature at the end of the tube.

8-14

Consider fully developed laminar flow in a circular tube in which the heat flux varies axially according to the relation

$$\dot{q}_s'' = a + b \sin \frac{\pi x}{L}$$

where L is the total length of the tube, and a and b are constants (this is an approximation for a nuclear reactor cooling tube). Derive a general expression for the mean fluid temperature T_m as a function of x^+ and the tube surface temperature T_s as a function of x , using variable-heat-flux theory [that is, an expression corresponding to Eq. (8-55) for the simple sinusoidal variation of heat flux].

For this problem the surface temperature is given by Eq. (8-50) along with Eq. (8-51)

$$\begin{aligned} T_s(x^+) - T_e &= \frac{r_s}{k} \int_0^{x^+} g(x^+ - \xi) \dot{q}_s''(\xi) d\xi \\ &= \frac{r_s}{k} \int_0^{x^+} \left[4 + \sum_m \frac{\exp(-\gamma_m^2(x^+ - \xi))}{\gamma_m^2 A_m} \right] (a + b \sin \beta \xi) d\xi \\ &= \frac{r_s}{k} \int_0^{x^+} 4(a + b \sin \beta \xi) d\xi + \frac{r_s}{k} \int_0^{x^+} \left[\sum_m \frac{\exp(-\gamma_m^2(x^+ - \xi))}{\gamma_m^2 A_m} \right] (a + b \sin \beta \xi) d\xi \end{aligned}$$

where

$$\begin{aligned} \beta &= r_s \text{Re Pr } \pi / L \\ \beta x^+ &= [r_s \text{Re Pr } \pi / L] [2(x/D) / \text{Re Pr}] = \pi x / L \\ x^+ &= 2(x/D) / (\text{Re Pr}) = (\pi x) / (\beta L) \end{aligned}$$

The equation can be broken into four terms

$$\begin{aligned} T_s(x^+) - T_e(x^+) &= \underbrace{\frac{4r_s}{k} \int_0^{x^+} (a + b \sin \beta \xi) d\xi}_1 \\ &\quad + \underbrace{\frac{r_s a}{k} \sum_m \int_0^{x^+} \frac{\exp(-\gamma_m^2(x^+ - \xi))}{\gamma_m^2 A_m} d\xi}_2 \\ &\quad + \underbrace{\frac{r_s b}{k} \sum_m \int_0^{x^+} \sin \beta \xi \frac{\exp(-\gamma_m^2(x^+ - \xi))}{\gamma_m^2 A_m} d\xi}_3 \end{aligned}$$

Before we evaluate this equation, consider the equation for the mean temperature,

$$\begin{aligned} T_m(x^+) - T_e &= \frac{4r_s}{k} \int_0^{x^+} [a + b \sin \beta x^+] d\xi \\ &= \frac{4r_s}{k} \left(ax^+ + \frac{b}{\beta} (1 - \cos \beta x^+) \right) \end{aligned}$$

So the first integral of the surface temperature equation is related to the mean temperature, and it can be substituted directly. For the second integral you can use the transformation $u = (x^+ - \xi)$ and $du = -d\xi$, along with limit transformations $\xi = x^+ \rightarrow u = 0$ and $\xi = 0 \rightarrow u = x^+$,

$$\begin{aligned} I_2 &= \int_0^{x^+} \frac{\exp(-\gamma_m^2(x^+ - \xi))}{\gamma_m^2 A_m} d\xi = - \int_{x^+}^0 \frac{\exp(-\gamma_m^2 u)}{\gamma_m^2 A_m} du = \left[\frac{\exp(-\gamma_m^2 u)}{\gamma_m^4 A_m} \right]_{x^+}^0 \\ &= \frac{[1 - \exp(-\gamma_m^2 x^+)]}{\gamma_m^4 A_m} \end{aligned}$$

The third integral reduces to

$$\begin{aligned} I_3 &= \int_0^{x^+} \sin \beta \xi \frac{\exp(-\gamma_m^2(x^+ - \xi))}{\gamma_m^2 A_m} d\xi \\ &= \frac{1}{\gamma_m^2 A_m} \exp(-\gamma_m^2 x^+) \int_0^{x^+} \exp(+\gamma_m^2 \xi) \sin \beta \xi d\xi \\ &= \frac{1}{\gamma_m^2 A_m} \frac{\exp(-\gamma_m^2 x^+)}{\beta} \underbrace{\int_0^{x^+} \exp\left(+\frac{\gamma_m^2}{\beta}(\beta \xi)\right) \sin(\beta \xi) d(\beta \xi)}_4 \end{aligned}$$

Integral 4 can be found in standard integration tables: $\int \exp(cx) \sin x dx = \frac{\exp(cx)}{c^2 + 1} (c \sin x - \cos x)$.

Evaluation of integral 4 gives

$$I_4 = \left[\frac{\exp\left(+\frac{\gamma_m^2}{\beta}(\beta x^+)\right)}{\left(\frac{\gamma_m^2}{\beta}\right)^2 + 1} \left(\frac{\gamma_m^2}{\beta} \sin(\beta x^+) - \cos(\beta x^+) \right) \right]_0^{x^+}$$

Evaluation of I_4 and substitution into I_3 gives

$$I_3 = \frac{1}{\gamma_m^2 A_m} \left(\frac{1}{\gamma_m^4 + \beta^2} \right) \left[\gamma_m^2 \sin(\beta x^+) - \beta \cos(\beta x^+) + \beta \exp(-\gamma_m^2 x^+) \right]$$

Finally, the surface temperature expression becomes

$$\begin{aligned} T_s(x^+) - T_m(x^+) &= \frac{r_s a}{k} \sum_m \frac{1}{\gamma_m^4 A_m} [1 - \exp(-\gamma_m^2 x^+)] \\ &\quad + \frac{r_s b}{k} \sum_m \frac{1}{\gamma_m^2 A_m} \left(\frac{1}{\gamma_m^4 + \beta^2} \right) \left[\gamma_m^2 \sin(\beta x^+) - \beta \cos(\beta x^+) + \beta \exp(-\gamma_m^2 x^+) \right] \end{aligned}$$

This equation compares with Eq. (8-55) in the textbook when $a=0$ and when the T_m expression is replaced using the mean temperature equation.

8-15

Consider fully developed laminar flow in a circular-tube annulus with $r^* = 0.50$. Let there be heat transfer from the inner tube only (outer tube insulated), and let the heat flux on the inner tube vary as in Prob. 8-14. Describe in detail a computing procedure for evaluating both the inner- and outer-tube surface temperatures as functions of length along the tube.

The heat flux distribution is based on the sine-function variation of problem 8-14,

$$\dot{q}_s'' = a + b \sin \frac{\pi x}{L}$$

where

$$\begin{aligned}\beta &= r_s \text{Re Pr } \pi / L \\ \beta x^+ &= [r_s \text{Re Pr } \pi / L] [2(x/D)/\text{Re Pr}] = \pi x / L \\ x^+ &= 2(x/D)/(\text{Re Pr}) = (\pi x)/(\beta L)\end{aligned}$$

For this problem the inner-surface heat flux becomes

$$\dot{q}_i''(x^+) = a + b \sin \beta x^+$$

Eqs.(8-56) and (8-57) provide the basis for the procedure, and $\dot{q}_o'' = 0$ in both equations.

$$\begin{aligned}T_i(x^+) - T_m &= \frac{D_h}{k} \left[\int_0^{x^+} \frac{1}{\text{Nu}_{ii}(x^+ - \xi)} d\dot{q}_i''(\xi) \right] \\ T_o(x^+) - T_m &= \frac{D_h}{k} \left[-\int_0^{x^+} \frac{\theta_o^*(x^+ - \xi)}{\text{Nu}_{oo}(x^+ - \xi)} d\dot{q}_i''(\xi) \right]\end{aligned}$$

and for the mean temperature, use an energy balance,

$$T_m(x) - T_e = \frac{1}{\rho A V c} \int_0^x (\dot{q}_i'' + \dot{q}_o'') dA_s$$

and convert x to $x^+ = 2(x/D_h)/(\text{Re}_{D_h} \text{Pr}) = (2xk)/(\rho V D_h^2 c)$, which gives (for $\dot{q}_o'' = 0$)

$$T_m(x^+) - T_e = \frac{4r_i(r_o - r_i)}{(r_o + r_i)k} \int_0^{x^+} \dot{q}_i''(\xi) d\xi$$

The integrations must be carried out numerically, using the basic data from Table 8-11. Note that at each station x^+ , integration must be carried out from $\xi = 0$ to $\xi = x^+$. Note that, for example, if you are evaluating the surface temperatures at $x^+ = 1.0$ and in the numerical integration scheme $\xi = 0.8$, then $\text{Nu}_{ii}(x^+ - \xi) = \text{Nu}_{ii}(0.2) = 6.19$ for $r^* = 0.5$ at that value of ξ .

8-16

Helium flows through a thin-walled 1.25-cm-diameter circular tube at a mean velocity of 6 m/s under the following conditions at a particular point along the tube:

$$P = 345 \text{ kPa}, \quad T_m = 200^\circ\text{C}$$

The tube is exposed on one side to an infinite *plane* that emits black-body radiation at 1100°C , while the remainder of the surrounding space is effectively nonradiating. Assuming that (1) the tube wall is sufficiently thin that peripheral conduction in the wall is negligible and (2) the outer surface is a black body, and evaluating radiation *from* the tube as if the entire tube were at a uniform temperature of 300°C (re-radiation will be relatively small and an exact solution would require iteration), calculate the net heat flux to the tube and estimate the temperature distribution in the wall around the tube. Assume that the heat-transfer resistance of the wall is negligible in the radial direction and that fluid properties are constant.

This problem is designed as an application of Eq. (8-23) and Fig. 8-5 when tube-surface heating has a cosine variation of the form

$$\dot{q}_s''(\phi) = \dot{q}_a''(1 + b \cos \phi)$$

where \dot{q}_a'' is the average heating value and b represents the maximum variation. To show that plane radiation incident on a circular tube is a cosine function, compute the radiation view factor (or shape factor or configuration factor) between the plane and the cylinder, and you will show it contains a cosine.

For reference, <http://www.me.utexas.edu/~howell/tablecon.html>.

The Nusselt number variation is given by Eq. (8-23)

$$\text{Nu}(\phi) = \frac{1 + b \cos \phi}{\frac{11}{48} + \frac{1}{2} b \cos \phi}$$

The source of plane radiation will produce a heat flux into the tube that varies around the periphery. The re-radiation will produce a heat flux from the tube that subtracts slightly from the inflow on one side, and results in net radiation from the tube on the other. The tube-wall temperature is evaluated from

$$T_s(\phi) = T_m + \frac{2\dot{q}_s''(\phi)r_s/k}{\text{Nu}(\phi)}$$

8-17

Consider steady flow in a tube with a fully developed velocity profile at the tube entrance. Let the fluid temperature at the tube entrance be uniform at T_e . Then let the tube surface temperature vary axially according to the relation

$$T_s - T_e = \frac{a}{b} [\exp(bx^+) - 1]$$

where a and b are arbitrary constants. Derive an expression for the local Nusselt number as a function of x^+ . Show that all members of this family of solutions lead to Nusselt numbers that are independent of x^+ at sufficiently large values of x^+ . What are the implications of this result? Discuss how the constant b affects the asymptotic Nusselt number.

This problem is solved by substituting the proposed expression for T_s into Eq.(8-44) and carrying out the indicated integration (the summation term in (8-44) is not used because there are no step-temperature changes). The $\theta_{r^+}(x^+ - \xi)$ is given by Eq. (8-45).

$$\dot{q}_s''(x^+) = \frac{2ak}{r_s} \sum_n \frac{G_n}{(\lambda_n^2 + b)} [\exp(bx^+) - \exp(-\lambda_n^2 x^+)]$$

Equation (8-52) is the energy balance for the mean temperature, and substitution of the heat flux expression gives

$$\begin{aligned} T_m(x^+) - T_e &= \frac{4r_s}{k} \int_0^{x^+} \dot{q}_s''(\xi) d\xi \\ &= 8a \sum_n \frac{G_n}{(\lambda_n^2 + b)} \left[\frac{1}{b} [\exp(bx^+) - 1] - \frac{1}{\lambda_n^2} [\exp(-\lambda_n^2 x^+) - 1] \right] \end{aligned}$$

Now formulate the Nusselt number

$$\text{Nu}(x^+) = \frac{2r_s \dot{q}_s''/k}{T_s(x^+) - T_m(x^+)}$$

and substitute for the surface heat flux, T_s and T_m to give

$$\text{Nu}_x = \frac{4 \sum_n \frac{G_n}{(\lambda_n^2 + b)} [\exp(bx^+) - \exp(-\lambda_n^2 x^+)]}{\frac{1}{b} [\exp(bx^+) - 1] - 8 \sum_n \frac{G_n}{(\lambda_n^2 + b)} \left[\frac{1}{b} [\exp(bx^+) - 1] - \frac{1}{\lambda_n^2} [\exp(-\lambda_n^2 x^+) - 1] \right]}$$

As $x^+ \rightarrow \infty$, the Nusselt number expression reduces to

$$\text{Nu}_x \approx \frac{4 \sum_n \frac{G_n}{(\lambda_n^2 + b)}}{\frac{1}{b} \left[1 - 8 \sum_n \frac{G_n}{(\lambda_n^2 + b)} \right]} \approx \frac{4b \sum_n \frac{G_n}{(\lambda_n^2 + b)}}{1 - 8 \sum_n \frac{G_n}{(\lambda_n^2 + b)}}$$

A value of $(bx^+) > 5$ removes the x^+ dependency. Let $b \ll \lambda_n^2$ for all n , then

$$\text{Nu}_x \approx \frac{4b \sum_n \frac{G_n}{(\lambda_n^2 + b)}}{1 - 8 \sum_n \frac{G_n}{(\lambda_n^2 + b)}} \approx \frac{4b \sum_n \frac{G_n}{\lambda_n^2} \left[1 - \frac{b}{\lambda_n^2} + \left(\frac{b}{\lambda_n^2} \right)^2 \right]}{1 - 8 \sum_n \frac{G_n}{\lambda_n^2} \left[1 - \frac{b}{\lambda_n^2} + \left(\frac{b}{\lambda_n^2} \right)^2 \right]} \approx \frac{4b \sum_n \frac{G_n}{\lambda_n^2} \left[1 - \frac{b}{\lambda_n^2} + \left(\frac{b}{\lambda_n^2} \right)^2 \right]}{8 \sum_n \frac{G_n}{\lambda_n^2} \left[\frac{b}{\lambda_n^2} + \left(\frac{b}{\lambda_n^2} \right)^2 \right]}$$

since $\sum (G_n / \lambda_n^2) = 1/8$, and the final approximation for small b is

$$\text{Nu}_x \approx \frac{\sum_n \frac{G_n}{\lambda_n^2}}{2 \sum_n \frac{G_n}{\lambda_n^4}} \approx \frac{1/8}{2(0.01433)} = 4.364$$

8-18

Consider fully developed laminar flow with constant properties in a circular tube. Let there be heat transfer to or from the fluid at a constant rate per unit of tube length. Determine the Nusselt number if the effect of frictional heating (viscous mechanical energy dissipation) is included in the analysis. How does frictional heating affect the Nusselt number? What are the significant new parameters? Consider some numerical examples and discuss the results.

For the tube geometry r is measured from the centerline of the inner pipe and r_s is the radius of the tube. Now consider the energy equation (8-1). This equation assumes no viscous dissipation, and it assumes constant properties for an ideal gas and steady state. Add in a viscous dissipation term similar to Eq. (4-32). Let the temperature profile vary with x and r only. The equation becomes

$$\rho c u \frac{\partial T}{\partial x} + \rho c v_r \frac{\partial T}{\partial r} = \frac{k}{r} \frac{\partial}{\partial r} \left(r \frac{\partial T}{\partial r} \right) + \mu \phi$$

With the assumption of a hydrodynamically fully-developed flow, $v_r=0$ and Eq. (7-8) is the velocity profile

$$u = 2V \left(1 - \frac{r^2}{r_s^2} \right)$$

and with the assumption of a thermally fully-developed temperature profile with constant heat rate, Eq. (8-8), the energy equation becomes

$$\frac{1}{r} \frac{\partial}{\partial r} \left(r \frac{\partial T}{\partial r} \right) = \frac{V}{\alpha} \left(\frac{dT_m}{dx} \right) - \frac{\text{Pr}}{c} \left(\frac{\partial u}{\partial r} \right)^2$$

The boundary conditions for the pipe are a constant heat rate at r_s and thermal profile symmetry (zero temperature gradient) at the pipe centerline. Thus the boundary conditions are to that following Eq. (8-10)

$$\left. \frac{\partial T}{\partial r} \right|_{r=0} = 0 \quad \text{and} \quad T|_{r=r_s} = T_s$$

Note that any time we have a Neumann-Neumann boundary (temperature gradients specified at both boundaries), we can not find the two constants of integration when we separate variables and integrate. So, we substitute for one of the Neumann conditions with it's Dirichlet counterpart (in this case the surface temperature) and we bring in the heat flux through the energy balance when we determine dT_m/dx .

Separate variables and integrate the 2nd-order ordinary differential equation, and apply the boundary conditions,

$$T = T_s - \frac{2V}{\alpha} \frac{dT_m}{dx} \left[\frac{3r_s^2}{16} + \frac{r^4}{16r_s^2} - \frac{r^2}{4} \right] - \frac{\text{Pr}}{c} \frac{V^2}{r_s^4} (r^4 - r_s^4)$$

Formulate the mean temperature using Eq. (8-5)

$$\begin{aligned} T_m &= \frac{1}{V\pi r_s^2} \int_0^{r_s} \left[2V \left(1 - \frac{r^2}{r_s^2} \right) \right] \left[T_s - \frac{2V}{\alpha} \frac{dT_m}{dx} \left[\frac{3r_s^2}{16} + \frac{r^4}{16r_s^2} - \frac{r^2}{4} \right] - \frac{\text{Pr}}{c} \frac{V^2}{r_s^4} (r^4 - r_s^4) \right] (2\pi r dr) \\ &= T_s - \frac{11}{96} \left(\frac{2V}{\alpha} \right) \left(\frac{dT_m}{dx} \right) r_s^2 + \frac{5}{6} \frac{\text{Pr}}{c} V^2 \end{aligned}$$

Now, evaluate the mean temperature gradient by carrying out an energy balance similar to what is depicted in Fig. 8-3, including the volumetric heating term,

$$\frac{dT_m}{dx} = \frac{2\dot{q}_s''r_s + 8\mu V^2}{\rho c V r_s^2}$$

and the mean temperature equation becomes

$$T_s - T_m = \frac{11}{48} \frac{\dot{q}_s'' D}{k} + \frac{\text{Pr}}{c} V^2$$

Inserting this into the Nusselt number formulation gives

$$\text{Nu}_x = \frac{\dot{q}_s'' D}{(T_s - T_m) k} = \frac{48}{11} \left[\frac{1}{1 + \frac{48}{11} \frac{\mu V^2}{\dot{q}_s'' D}} \right] = \frac{192}{(44 + 3\lambda)}$$

which compares with Eq. (8-25). The variable $\lambda = 64Br'$, where $Br' = (\mu V^2)/(\dot{q}_s'' D)$, the Brinkman number, a nondimensional parameter for viscous dissipation in surface heat flux problems.

8-19

Consider fully developed laminar flow with constant properties in a circular tube. Let there be heat transfer to or from the fluid at a constant rate per unit of tube length. Additionally, let there be heat generation within the fluid (perhaps by nuclear reaction) at a rate S , W/m³, that is everywhere the same. Determine an expression for the Nusselt number as a function of the pertinent parameters. (What are they?) Evaluate the convection conductance in the usual manner, on the basis of heat flux through the surface, surface temperature, and fluid mixed mean temperature.

For the tube geometry r is measured from the centerline of the inner pipe and r_s is the radius of the tube. Now consider the energy equation (8-1). This equation assumes no viscous dissipation, and it assumes constant properties for an ideal gas and steady state. Add in a volumetric source term similar to Eq. (4-32). Let the temperature profile vary with x and r only. The equation becomes

$$\rho c u \frac{\partial T}{\partial x} + \rho c v_r \frac{\partial T}{\partial r} = \frac{k}{r} \frac{\partial}{\partial r} \left(r \frac{\partial T}{\partial r} \right) + S$$

With the assumption of a hydrodynamically fully-developed flow, $v_r=0$ and Eq. (7-8) is the velocity profile

$$u = 2V \left(1 - \frac{r^2}{r_s^2} \right)$$

and with the assumption of a thermally fully-developed temperature profile with constant heat rate, Eq. (8-8), the energy equation becomes

$$\frac{1}{r} \frac{\partial}{\partial r} \left(r \frac{\partial T}{\partial r} \right) = \frac{V}{\alpha} \left(\frac{dT_m}{dx} \right) - \frac{S}{k}$$

The boundary conditions for the pipe are a constant heat rate at r_s and thermal profile symmetry (zero temperature gradient) at the pipe centerline. Thus the boundary conditions are to that following Eq. (8-10)

$$\left. \frac{\partial T}{\partial r} \right|_{r=0} = 0 \quad \text{and} \quad T|_{r=r_s} = T_s$$

Note that any time we have a Neumann-Neumann boundary (temperature gradients specified at both boundaries), we can not find the two constants of integration when we separate variables and integrate. So, we substitute for one of the Neumann conditions with it's Dirichlet counterpart (in this case the surface temperature) and we bring in the heat flux through the energy balance when we determine dT_m/dx .

Separate variables and integrate the 2nd-order ordinary differential equation, and apply the boundary conditions,

$$T = T_s - \frac{2V}{\alpha} \frac{dT_m}{dx} \left[\frac{3r_s^2}{16} + \frac{r^4}{16r_s^2} - \frac{r^2}{4} \right] - \frac{S}{4k} (r^2 - r_s^2)$$

Formulate the mean temperature using Eq. (8-5)

$$\begin{aligned} T_m &= \frac{1}{V\pi r_s^2} \int_0^{r_s} \left[2V \left(1 - \frac{r^2}{r_s^2} \right) \right] \left[T_s - \frac{2V}{\alpha} \frac{dT_m}{dx} \left[\frac{3r_s^2}{16} + \frac{r^4}{16r_s^2} - \frac{r^2}{4} \right] - \frac{S}{4k} (r^2 - r_s^2) \right] (2\pi r dr) \\ &= T_s - \frac{11}{96} \left(\frac{2V}{\alpha} \right) \frac{dT_m}{dx} r_s^2 + \frac{S r_s^2}{6k} \end{aligned}$$

Now, evaluate the mean temperature gradient by carrying out an energy balance similar to what is depicted in Fig. 8-3, including the volumetric heating term,

$$\frac{dT_m}{dx} = \frac{2\dot{q}_s'' + r_s S}{\rho c V r_s}$$

and the mean temperature equation becomes

$$T_s - T_m = \frac{11}{48} \frac{\dot{q}_s'' D}{k} + \frac{3}{48} \frac{S r_o^2}{k}$$

Inserting this into the Nusselt number formulation gives

$$\text{Nu}_x = \frac{\dot{q}_s'' D}{(T_s - T_m) k} = \frac{48}{11} \left[\frac{1}{1 + \frac{3}{44} \frac{SD}{\dot{q}_s''}} \right] = \frac{192}{(44 + 3\lambda)}$$

which compares with Eq. (8-25).

8-20

Consider fully developed laminar flow with constant properties in a circular tube. Let the surface be insulated, but let there be heat generation within the fluid at a rate S , W/m³, that is everywhere the same. From an examination of the applicable energy differential equation alone, deduce the approximate shape of the temperature profile within the fluid, and determine whether the highest temperature of the fluid at any axial position occurs at the tube surface or at the tube centerline. Explain the reasons for the result.

This solution is a variation on problem 8-19. From that solution

$$T = T_s - \frac{2V}{\alpha} \frac{dT_m}{dx} \left[\frac{3r_s^2}{16} + \frac{r^4}{16r_s^2} - \frac{r^2}{4} \right] - \frac{S}{4k} (r^2 - r_s^2)$$

and

$$\frac{dT_m}{dx} = \frac{S}{\rho c V}$$

So,

$$\begin{aligned} T &= T_s - \frac{2S}{k} \left[\frac{3r_s^2}{16} + \frac{r^4}{16r_s^2} - \frac{r^2}{4} \right] - \frac{S}{4k} (r^2 - r_s^2) \\ &= T_s + \frac{S}{k} \left[\frac{r^2}{4} - \frac{r^4}{8r_s^2} - \frac{r_s^2}{8} \right] \end{aligned}$$

We can see several trends. The mean temperature continues to increase with x . The lowest temperature is at the centerline, and the maximum is at the wall.

8-21

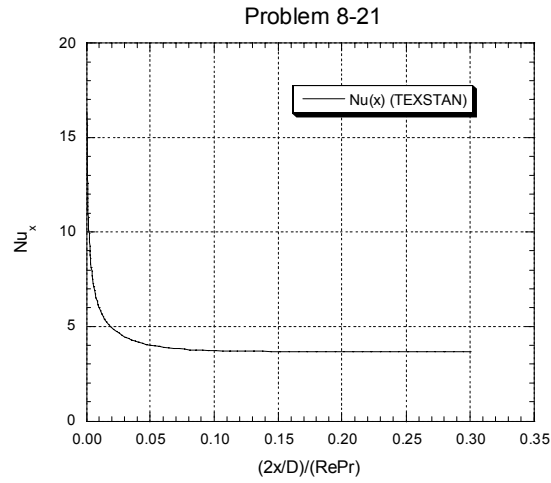
TEXSTAN analysis of laminar thermal entry flow in a circular pipe with constant surface temperature: Calculate the flow and construct a plot similar to Fig. 8-10 to show development of the Nusselt number with $x^+ = 2(x/D_h)/\text{Re Pr}$ over the range $x^+ = 0-0.3$. Let the Prandtl number be 0.7. Compare the results with Table 8-4. Feel free to evaluate the non-dimensional temperature profiles at various x^+ locations to demonstrate the concept of how the profiles evolve from a flat profile into thermally fully developed profile, and to investigate any other attribute of the entry region or thermally fully developed region of the flow. Let the Reynolds number be 1000, and pick fluid properties that are appropriate to the chosen Prandtl number. You can choose how to set up the TEXSTAN problem in terms of values for the thermal boundary and initial conditions, and for geometrical dimensions and mass flow rate for the pipe to provide the required Reynolds number and a pipe length equivalent to $x^+ = 0.3$. Use constant fluid properties and do not consider viscous dissipation. For initial conditions let the velocity profile be hydrodynamically fully developed and the temperature profile be flat at some value T_e .

The data file for this problem is *8.21.dat.txt*. The data set construction is based on the *s34.dat.txt* file for thermal entry length flow in a pipe with a specified surface temperature (initial profiles: hydrodynamically fully-developed velocity and flat temperature).

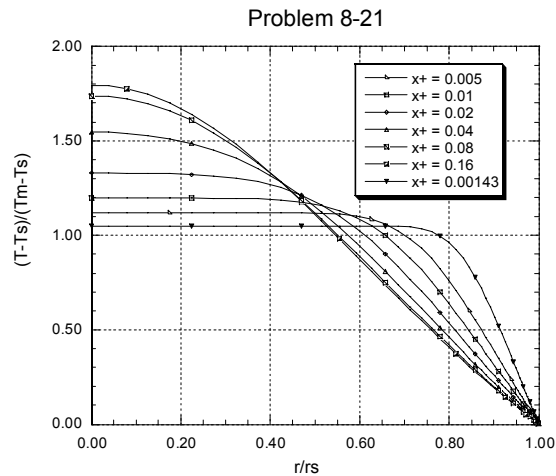
Here is an abbreviated listing of the output file (it will be called *out.txt* when you execute TEXSTAN using *8.21.dat.txt*):

intg	x/dh/re	cf*re	uclr	xplus	nu	th,cl	tm/ts	ts	qflux
5	.00002	15.99	1.997	.00007	33.266	1.007	.968	3.100E+02	1.256E+02
50	.00025	15.99	1.997	.00071	14.454	1.032	.969	3.100E+02	5.325E+01
100	.00050	15.99	1.997	.00143	11.379	1.050	.969	3.100E+02	4.117E+01
150	.00092	15.99	1.996	.00264	9.244	1.076	.970	3.100E+02	3.264E+01
200	.00206	15.99	1.996	.00589	7.098	1.134	.972	3.100E+02	2.380E+01
250	.00509	15.99	1.995	.01455	5.381	1.258	.974	3.100E+02	1.625E+01
300	.01239	15.99	1.995	.03541	4.288	1.502	.979	3.100E+02	1.065E+01
350	.02391	15.99	1.995	.06831	3.838	1.701	.984	3.100E+02	7.325E+00
400	.04135	16.00	1.994	.11813	3.688	1.779	.989	3.100E+02	4.857E+00
450	.06547	16.00	1.994	.18705	3.662	1.794	.993	3.100E+02	2.915E+00
500	.09045	16.00	1.994	.25844	3.659	1.795	.996	3.100E+02	1.732E+00
529	.10495	16.00	1.994	.29985	3.659	1.795	.997	3.100E+02	1.281E+00

To compare to Fig. 8-10, plot the Nu_x data from output file *ftn82.dat.txt*.



To examine the temperature profiles, modify *8.21.dat.txt* to print profiles by changing *kout*=4 and add *x*(m) locations corresponding to $x^+=0.00143, 0.005, 0.01, 0.02, 0.04, 0.08$, and 0.16 . The file *out.txt* contains the profiles for plotting.



8-22

TEXSTAN analysis of the effects of Prandtl number on laminar thermal entry flow in a circular pipe with constant surface temperature: This is a variation of Prob. 8-21 to show the independence of Pr as the thermally fully developed flow condition is met. For this problem, choose Pr values of 0.01, 1.0, and 10, and compare the results to Table 8-2. Follow the TEXSTAN setup described in Prob. 8-21, but adjust the pipe length such that a thermally fully developed Nusselt number is achieved for the selected Pr.

There are three data files for this, one for each Prandtl number. Each data set is labeled 8.22.dat.txt and “a” is for Pr=0.01, “b” is for Pr=1, and “c” is for Pr=10. The data set construction is based on the s34.dat.txt file for thermal entry length flow in a pipe with a specified surface temperature (initial profiles: hydrodynamically fully-developed velocity and flat temperature).

The $x(m)$ array has to be adjusted for each Pr value. The thermal entry region correlates logarithmically with $2(x/D_h)/(Re_{D_h} Pr)$, so this becomes an easy way of estimating how to create a distribution of x -locations for varying $aux1$. Choose the set of points to be $2(x/D_h)/(Re_{D_h} Pr) = 0, 0.0005, 0.005, 0.05$ and start $aux1(m)$ at a very low value ($=0.01$) and in the region 0-0.0005-0.005 increase the nondimensional stepsize $aux1$ to 0.25 and then further increase it to a larger value ($=1.0$) in the region 0.005-0.05, and then $aux1$ can remain constant out to $x^+=0.3$.

With the Pr set =1, the $x(m)$ array becomes

###	x(m)	rw(m)	aux1(m)	aux2(m)	aux3(m)
	0.0000000	0.0350	0.0100	0.0000	0.0000
	0.0175000	0.0350	0.0100	0.0000	0.0000
	0.1750000	0.0350	0.2500	0.0000	0.0000
	1.7500000	0.0350	1.0000	0.0000	0.0000
	10.5000000	0.0350	1.0000	0.0000	0.0000

and an abbreviated listing of the output file (it will be called *out.txt* when you execute TEXSTAN using 8.22b.dat.txt) for Pr=1 is

intg	x/dh/re	cf*re	uclr	xplus	nu	th,cl	tm/ts	ts	qflux
5	.00002	15.99	1.997	.00005	37.568	1.005	.968	3.100E+02	9.942E+01
50	.00025	15.99	1.997	.00050	16.335	1.025	.969	3.100E+02	4.240E+01
100	.00067	15.99	1.997	.00135	11.615	1.048	.969	3.100E+02	2.947E+01
150	.00181	15.99	1.996	.00362	8.322	1.095	.971	3.100E+02	2.022E+01
200	.00484	15.99	1.996	.00967	6.076	1.191	.973	3.100E+02	1.357E+01
250	.01308	15.99	1.995	.02616	4.600	1.404	.977	3.100E+02	8.676E+00
300	.03348	15.99	1.994	.06697	3.849	1.696	.984	3.100E+02	5.198E+00
350	.05847	16.00	1.994	.11694	3.690	1.778	.989	3.100E+02	3.432E+00
400	.08346	16.00	1.994	.16692	3.664	1.792	.992	3.100E+02	2.364E+00
450	.10845	16.00	1.994	.21689	3.660	1.794	.995	3.100E+02	1.640E+00
500	.13343	16.00	1.994	.26687	3.659	1.795	.996	3.100E+02	1.139E+00
533	.14993	16.00	1.994	.29985	3.659	1.795	.997	3.100E+02	8.953E-01

We obtain the expected $Nu=3.66$ and the thermally-fully developed x^+ value is within 5% at about $x^+=0.07$.

With the Pr set =0.01, the $x(m)$ array becomes

###	x(m)	rw(m)	aux1(m)	aux2(m)	aux3(m)
	0.0000000	0.0350	0.0100	0.0000	0.0000
	0.0001750	0.0350	0.0100	0.0000	0.0000
	0.0017500	0.0350	0.2500	0.0000	0.0000
	0.0175000	0.0350	1.0000	0.0000	0.0000
	0.1050000	0.0350	1.0000	0.0000	0.0000

and an abbreviated listing of the output file (it will be called *out.txt* when you execute TEXSTAN using *8.22a.dat.txt*) for $Pr=0.01$ (note the *kspace* interval significantly reduced from the $Pr=1$ case) is

intg	x/dh/re	cf*re	uclr	xplus	nu	th,cl	tm/ts	ts	qflux
5	.00002	15.99	1.997	.00450	8.166	1.108	.971	3.100E+02	1.962E+03
10	.00004	15.99	1.997	.00900	6.369	1.178	.973	3.100E+02	1.438E+03
20	.00009	15.99	1.997	.01899	5.051	1.314	.975	3.100E+02	1.022E+03
30	.00014	15.99	1.997	.02899	4.515	1.432	.978	3.100E+02	8.315E+02
40	.00019	15.99	1.997	.03898	4.221	1.529	.980	3.100E+02	7.129E+02
50	.00025	15.99	1.997	.04998	4.025	1.611	.981	3.100E+02	6.214E+02
60	.00032	15.99	1.997	.06332	3.882	1.679	.983	3.100E+02	5.398E+02
70	.00040	15.99	1.997	.07958	3.783	1.729	.985	3.100E+02	4.649E+02
80	.00050	15.99	1.997	.09940	3.720	1.762	.987	3.100E+02	3.945E+02
90	.00062	15.99	1.997	.12357	3.685	1.781	.989	3.100E+02	3.273E+02
100	.00077	15.99	1.997	.15303	3.668	1.790	.991	3.100E+02	2.630E+02
110	.00094	15.99	1.996	.18893	3.661	1.793	.993	3.100E+02	2.025E+02
120	.00116	15.99	1.996	.23271	3.659	1.795	.995	3.100E+02	1.476E+02
130	.00143	15.99	1.996	.28606	3.659	1.795	.997	3.100E+02	1.007E+02
133	.00150	15.99	1.996	.29985	3.658	1.795	.997	3.100E+02	9.117E+01

We again obtain the expected $Nu=3.66$ and the thermally-fully developed x^+ value is within 5% at about $x^+=0.07$.

With the Pr set =10, the $x(m)$ array becomes

###	x(m)	rw(m)	aux1(m)	aux2(m)	aux3(m)
	0.0000000	0.0350	0.0100	0.0000	0.0000
	0.1750000	0.0350	0.0100	0.0000	0.0000
	1.7500000	0.0350	0.2500	0.0000	0.0000
	17.5000000	0.0350	1.0000	0.0000	0.0000
	105.0000000	0.0350	1.0000	0.0000	0.0000

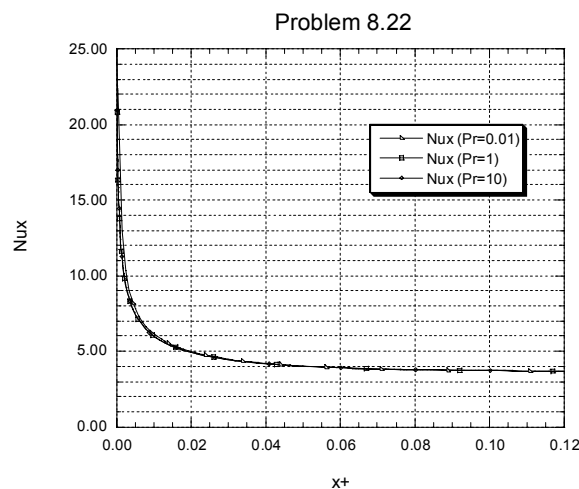
and an abbreviated listing of the output file (it will be called *out.txt* when you execute TEXSTAN using *8.22c.dat.txt*) for $Pr=10$ (note the *kpace* interval significantly increased from the $Pr=1$ case) is

intg	x/dh/re	cf*re	uclr	xplus	nu	th,cl	tm/ts	ts	qflux
5	.00002	15.99	1.997	.00000	82.001	1.001	.968	3.100E+02	2.179E+01
400	.00200	15.99	1.996	.00040	17.563	1.022	.968	3.100E+02	4.574E+00
800	.00618	15.99	1.995	.00124	11.926	1.046	.969	3.100E+02	3.034E+00
1200	.03784	16.00	1.994	.00757	6.544	1.160	.972	3.100E+02	1.501E+00
1600	.12096	16.00	1.994	.02419	4.680	1.382	.977	3.100E+02	8.985E-01
2000	.28086	16.00	1.994	.05617	3.934	1.653	.982	3.100E+02	5.769E-01
2400	.48076	16.00	1.994	.09615	3.721	1.762	.987	3.100E+02	4.027E-01
2800	.68066	16.00	1.994	.13613	3.673	1.787	.990	3.100E+02	2.960E-01
3200	.88056	16.00	1.994	.17611	3.662	1.793	.993	3.100E+02	2.201E-01
3600	1.08046	16.00	1.994	.21609	3.660	1.794	.995	3.100E+02	1.642E-01
4000	1.28036	16.00	1.994	.25607	3.659	1.795	.996	3.100E+02	1.225E-01
4400	1.48026	16.00	1.994	.29605	.000	1.795	.997	3.100E+02	9.145E-02
4438	1.49925	16.00	1.994	.29985	.000	1.795	.997	3.100E+02	8.894E-02

We again obtain the expected $Nu=3.66$ and the thermally-fully developed x^+ value is within 5% at about $x^+=0.07$. Note the Nu values are not calculated as the heat transfer approaches zero. The fluid temperature has reached the surface temperature, equivalent to a 100% effectiveness heat exchanger.

The three results are plotted to show how x^+ correlates the thermal entry length, independent of Pr , for the same Re_{Dh} . Note only the data to $x^+=0.12$ has been plotted to show thermally-fully developed x^+ value is within 5% at about $x^+=0.07$, and within 2% at about $x^+=0.10$ matching the discussion in the textbook on p. 103,

$$x^+ = 0.1 = \frac{2(x/D_h)}{(Re Pr)} \rightarrow (x/D_h)_{fully-dev} \approx 0.05 Re Pr$$



8-23

TEXSTAN analysis of laminar thermal entry flow in a circular pipe with constant surface heat flux, heating case: Calculate the flow and construct a plot to show development of the Nusselt number with $x^+ = 2(x/Dh)/Re Pr$ over the range $x^+ = 0-0.3$. Let the Prandtl number be 0.7. Compare the results with Table 8-6. Follow the TEXSTAN setup described in Prob. 8-21.

The data file for this problem is *8.23.dat.txt*. The data set construction is based on the *s35.dat.txt* file for thermal entry length flow in a pipe with a specified surface heat flux (initial profiles: hydrodynamically fully-developed velocity and flat temperature).

Here is an abbreviated listing of the output file (it will be called *out.txt* when you execute TEXSTAN using *8.23.dat.txt*):

intg	x/dh/re	cf*re	uclr	xplus	nu	th,cl	tm/ts	ts	qflux
5	.00002	15.99	1.997	.00007	39.544	1.006	.998	3.007E+02	1.000E+01
50	.00025	15.99	1.997	.00071	17.747	1.025	.995	3.015E+02	1.000E+01
100	.00050	15.99	1.997	.00143	14.038	1.040	.994	3.019E+02	1.000E+01
150	.00092	15.99	1.996	.00264	11.448	1.060	.992	3.024E+02	1.000E+01
200	.00206	15.99	1.996	.00589	8.830	1.104	.990	3.033E+02	1.000E+01
250	.00509	15.99	1.995	.01455	6.718	1.195	.987	3.047E+02	1.000E+01
300	.01239	15.99	1.995	.03541	5.343	1.366	.984	3.068E+02	1.000E+01
350	.02391	15.99	1.995	.06831	4.724	1.520	.982	3.092E+02	1.000E+01
400	.04135	16.00	1.994	.11813	4.460	1.601	.981	3.121E+02	1.000E+01
450	.06547	16.00	1.994	.18705	4.381	1.626	.981	3.158E+02	1.000E+01
500	.09045	16.00	1.994	.25844	4.368	1.630	.981	3.196E+02	1.000E+01
529	.10495	16.00	1.994	.29985	4.366	1.631	.981	3.218E+02	1.000E+01

Here is the comparison with Table 8-6, using Nu_x data from output file *out.txt* with $k_{space}=1$ to obtain enough entries to avoid interpolation.

x^+	Nu_x (Table 8-6)	Nu_x (TEXSTAN)
0	∞	
0.002	12.00	12.52
0.004	9.93	10.0
0.010	7.49	7.50
0.020	6.14	6.14
0.040	5.19	5.20
0.100	4.51	4.52
∞	4.36	4.37

8-24

TEXSTAN analysis of laminar thermal entry flow in a parallel planes channel with constant surface temperature for both planes: Calculate the flow and construct a plot to show development of the Nusselt number with $x^+ = 2(x/D_h)/\text{Re Pr}$ over the range $x^+ = 0-0.3$. Let the Prandtl number be 0.7. Compare the results with the entries for $b/a = \infty$ in Table 8-9. Feel free to evaluate the nondimensional temperature profiles at various x^+ locations to demonstrate the concept of how the profiles evolve from a flat profile into a thermally fully developed profile, and to investigate any other attribute of the entry region or thermally fully developed region of the flow. Let the Reynolds number be 1000, and pick fluid properties that are appropriate to the chosen Prandtl number. You can choose how to set up the TEXSTAN problem in terms of values for the thermal boundary and initial conditions, and for geometrical dimensions and mass flow rate for the channel to provide the required Reynolds number and a channel length equivalent to $x^+ = 0.3$. Use constant fluid properties and do not consider viscous dissipation. For initial conditions let the velocity profile be hydrodynamically fully developed and the temperature profile be flat at some value T_e . Because this problem has symmetrical thermal boundary conditions, choose the option in TEXSTAN that permits the centerline of the parallel planes channel to be a symmetry line.

The data file for this problem is *8.24.dat.txt*. The data set construction is based on the *s54.dat.txt* file for thermal entry length flow between parallel planes with a specified surface temperature and thermal symmetry (initial profiles: hydrodynamically fully-developed velocity and flat temperature).

Here is an abbreviated listing of the output file (it will be called *out.txt* when you execute TEXSTAN using *8.24.dat.txt*):

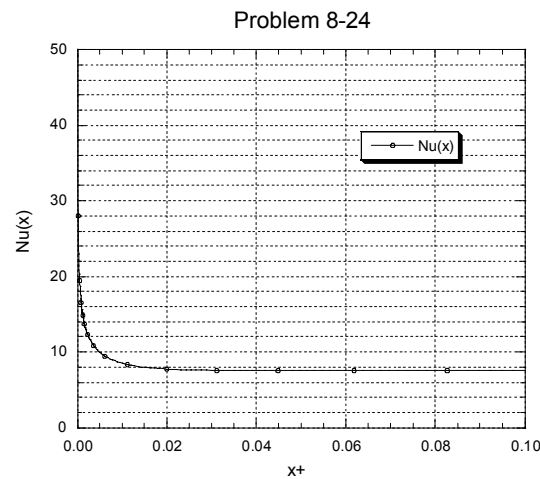
intg	x/dh/re	cf*re	uclr	xplus	nu	th,cl	tm/ts	ts	qflux
5	.00001	24.00	1.499	.00004	49.495	1.005	.968	3.100E+02	1.843E+02
50	.00012	23.99	1.499	.00035	22.180	1.023	.968	3.100E+02	8.110E+01
100	.00025	23.99	1.499	.00070	17.713	1.038	.969	3.100E+02	6.388E+01
150	.00037	23.99	1.499	.00105	15.584	1.050	.969	3.100E+02	5.555E+01
200	.00050	23.99	1.499	.00141	14.258	1.061	.970	3.100E+02	5.030E+01
250	.00068	23.99	1.499	.00190	13.018	1.075	.970	3.100E+02	4.531E+01
300	.00102	23.99	1.499	.00286	11.563	1.101	.971	3.100E+02	3.931E+01
350	.00168	23.99	1.499	.00472	10.099	1.145	.972	3.100E+02	3.299E+01
400	.00296	23.98	1.499	.00834	8.837	1.212	.974	3.100E+02	2.698E+01
450	.00544	23.98	1.499	.01531	7.962	1.280	.977	3.100E+02	2.166E+01
500	.00901	23.98	1.499	.02534	7.627	1.310	.980	3.100E+02	1.776E+01
550	.01340	23.98	1.499	.03770	7.550	1.317	.983	3.100E+02	1.458E+01
600	.01881	23.98	1.499	.05291	7.537	1.318	.987	3.100E+02	1.158E+01
650	.02547	23.98	1.499	.07164	7.536	1.318	.990	3.100E+02	8.738E+00
700	.03366	23.98	1.499	.09469	7.536	1.318	.993	3.100E+02	6.180E+00
750	.04375	23.98	1.499	.12308	7.536	1.318	.995	3.100E+02	4.037E+00
800	.05574	23.98	1.499	.15679	7.536	1.318	.997	3.100E+02	2.435E+00
850	.06824	23.98	1.499	.19195	7.536	1.318	.998	3.100E+02	1.437E+00
900	.08073	23.98	1.499	.22710	7.536	1.318	.999	3.100E+02	8.486E-01
950	.09323	23.98	1.499	.26226	7.536	1.318	.999	3.100E+02	5.010E-01

977	.09998	23.98	1.499	.28124	7.536	1.318	1.000	3.100E+02	3.769E-01
-----	--------	-------	-------	--------	-------	-------	-------	-----------	-----------

Here is the comparison with the $b/a = \infty$ table entry (parallel planes) in Table 8-9, using Nu_x data from output file *out.txt* with *kpace*=1 to obtain enough entries to avoid interpolation..

x^+	Nu_x (Table 8-9)	Nu_x (TEXSTAN)
0	∞	
0.01	8.52	8.51
0.02	7.75	7.74
0.05	7.55	7.54
0.1	7.55	7.54
0.2	7.55	7.54
∞	7.55	7.54

The results are plotted to show how x^+ correlates the thermal entry length, Note only the data to $x^+=0.05$ has been plotted to show thermally-fully developed x^+ value is within 5% at about $x^+=0.017$, and within 2% at about $x^+=0.03$ matching the discussion in the textbook on p. 103, This value is about one-third of what it is for the pipe. This matches the conclusion in problem 7-10 for the hydrodynamic entry region. As with the hydrodynamic problem, it is important to remember that there are two contributions to the total pressure drop, surface friction and flow acceleration. The combined effect leads to a longer entry length than is measured by the wall friction.



8-25

TEXSTAN analysis of laminar thermal entry flow in a parallel planes channel with constant surface heat flux, heating case, for both planes: Calculate the flow and construct a plot to show development of the Nusselt number with $x^+ = 2(x/D_h)/Re Pr$ over the range $x^+ = 0-0.3$. Let the Prandtl number be 0.7. Compare the results with the entries for $b/a = \infty$ in Tables 8-10. Feel free to evaluate the nondimensional temperature profiles at various x^+ locations to demonstrate the concept of how the profiles evolve from a flat profile into thermally fully developed profile, and to investigate any other attribute of the entry region or thermally fully developed region of the flow. Follow the TEXSTAN setup described in Prob. 8-24.

The data file for this problem is *8.25.dat.txt*. The data set construction is based on the *s55.dat.txt* file for thermal entry length flow between parallel planes with a specified surface heat flux and thermal symmetry (initial profiles: hydrodynamically fully-developed velocity and flat temperature).

Here is an abbreviated listing of the output file (it will be called *out.txt* when you execute TEXSTAN using *8.25.dat.txt*):

intg	x/dh/re	cf*re	uclr	xplus	nu	th,cl	tm/ts	ts	qflux
5	.00001	24.00	1.499	.00004	58.460	1.004	.998	3.005E+02	1.000E+01
50	.00012	23.99	1.499	.00035	26.780	1.019	.997	3.010E+02	1.000E+01
100	.00025	23.99	1.499	.00070	21.385	1.030	.996	3.013E+02	1.000E+01
150	.00037	23.99	1.499	.00105	18.798	1.040	.995	3.015E+02	1.000E+01
200	.00050	23.99	1.499	.00141	17.181	1.048	.995	3.016E+02	1.000E+01
250	.00068	23.99	1.499	.00190	15.662	1.060	.994	3.018E+02	1.000E+01
300	.00102	23.99	1.499	.00286	13.867	1.079	.994	3.021E+02	1.000E+01
350	.00168	23.99	1.499	.00472	12.038	1.113	.993	3.025E+02	1.000E+01
400	.00296	23.98	1.499	.00834	10.413	1.167	.992	3.030E+02	1.000E+01
450	.00544	23.98	1.499	.01531	9.178	1.229	.990	3.037E+02	1.000E+01
500	.00901	23.98	1.499	.02534	8.562	1.266	.990	3.045E+02	1.000E+01
550	.01340	23.98	1.499	.03770	8.327	1.280	.989	3.052E+02	1.000E+01
600	.01881	23.98	1.499	.05291	8.252	1.284	.989	3.061E+02	1.000E+01
650	.02547	23.98	1.499	.07164	8.233	1.285	.989	3.071E+02	1.000E+01
700	.03366	23.98	1.499	.09469	8.230	1.286	.989	3.083E+02	1.000E+01
750	.04375	23.98	1.499	.12308	8.230	1.286	.990	3.098E+02	1.000E+01
800	.05574	23.98	1.499	.15679	8.230	1.286	.990	3.116E+02	1.000E+01
850	.06824	23.98	1.499	.19195	8.230	1.286	.990	3.135E+02	1.000E+01
900	.08073	23.98	1.499	.22710	8.230	1.286	.990	3.154E+02	1.000E+01
950	.09323	23.98	1.499	.26226	8.230	1.286	.990	3.173E+02	1.000E+01
977	.09998	23.98	1.499	.28124	8.230	1.286	.990	3.183E+02	1.000E+01

Here is the comparison with the $r^* = 1$ table entry (parallel planes) in Table 8-10, using Nu_x data from output file *out.txt* with *kpace*=1 to obtain enough entries to avoid interpolation.

x^+	Nu_x (Table 8-10)	Nu_x (TEXSTAN)
0	∞	
0.01		9.99
0.02	8.80	8.80
0.05		8.26
0.1	8.25	8.23
0.2		8.23
∞	8.235	8.23

8-26

TEXSTAN analysis of laminar thermal entry flow in a parallel-plane channel with asymmetrical heat flux in which one plane has a constant surface heat flux, heating case, and the other plane has an adiabatic surface: Calculate the flow and construct a plot to show development of the Nusselt number with $x^+ = 2(x/D_h)/Re Pr$ over the range $x^+ = 0-0.3$. Let the Prandtl number be 0.7. Compare the results with the $Nu_{ii} = Nu_{oo}$ values for $r^* = 1.00$ in Table 8-11 (note the influence coefficients are not used for this problem). Feel free to evaluate the nondimensional temperature profiles at various x^+ locations to demonstrate the concept of how the profiles evolve from a flat profile into thermally fully developed profile, and to investigate any other attribute of the entry region or thermally fully developed region of the flow. Let the Reynolds number be 1000, and pick fluid properties that are appropriate to the chosen Prandtl number. You can choose how to set up the TEXSTAN problem in terms of values for the thermal boundary and initial conditions, and for geometrical dimensions and mass flow rate for the channel to provide the required Reynolds number and a channel length equivalent to $x^+ = 0.3$. Use constant fluid properties and do not consider viscous dissipation. For initial conditions let the velocity profile be hydrodynamically fully developed and the temperature profile be flat at some value T_e . Because this problem has asymmetrical thermal boundary conditions, choose the option in TEXSTAN that permits the calculation from surface to surface of the parallel-plane channel.

The data file for this problem is *8.26.dat.txt*. The data set construction is based on the *s556.dat.txt* file for thermal entry length flow between parallel planes with a specified surface heat flux on each surface (initial profiles: hydrodynamically fully-developed velocity and flat temperature).

Here is an abbreviated listing of the output file (it will be called *out.txt* when you execute TEXSTAN using *8.26.dat.txt*):

intg	x/dh	cfapp	cf2(I)	cf2(E)	nu(I)	nu(E)
5	1.250E-02	2.403E-02	1.199E-02	1.199E-02	5.834E+01	0.000E+00
50	1.250E-01	2.402E-02	1.199E-02	1.199E-02	2.653E+01	0.000E+00
100	2.500E-01	2.402E-02	1.199E-02	1.199E-02	2.107E+01	0.000E+00
150	3.750E-01	2.402E-02	1.199E-02	1.199E-02	1.843E+01	0.000E+00
200	5.000E-01	2.401E-02	1.199E-02	1.199E-02	1.678E+01	0.000E+00
250	6.761E-01	2.409E-02	1.199E-02	1.199E-02	1.521E+01	0.000E+00
300	1.018E+00	2.417E-02	1.199E-02	1.199E-02	1.334E+01	0.000E+00
350	1.680E+00	2.423E-02	1.199E-02	1.199E-02	1.139E+01	0.000E+00
400	2.964E+00	2.426E-02	1.199E-02	1.199E-02	9.581E+00	0.000E+00
450	5.443E+00	2.426E-02	1.199E-02	1.199E-02	8.048E+00	0.000E+00
500	9.012E+00	2.419E-02	1.199E-02	1.199E-02	7.055E+00	0.000E+00
550	1.341E+01	2.415E-02	1.199E-02	1.199E-02	6.438E+00	0.000E+00
600	1.881E+01	2.413E-02	1.199E-02	1.199E-02	6.026E+00	0.000E+00
650	2.547E+01	2.412E-02	1.199E-02	1.199E-02	5.750E+00	0.000E+00
700	3.367E+01	2.411E-02	1.199E-02	1.199E-02	5.573E+00	0.000E+00
750	4.376E+01	2.410E-02	1.199E-02	1.199E-02	5.470E+00	0.000E+00
800	5.575E+01	2.408E-02	1.199E-02	1.199E-02	5.418E+00	0.000E+00
850	6.825E+01	2.406E-02	1.199E-02	1.199E-02	5.397E+00	0.000E+00
900	8.075E+01	2.405E-02	1.199E-02	1.199E-02	5.389E+00	0.000E+00

950	9.325E+01	2.404E-02	1.199E-02	1.199E-02	5.386E+00	0.000E+00
977	1.000E+02	2.404E-02	1.199E-02	1.199E-02	5.385E+00	0.000E+00

Here is the comparison with the $r^*=1$ table entry (parallel planes) in Table 8-11, using Nu_x data from output file *fn81.txt* with *kpace*=1 to obtain enough entries to avoid interpolation. Note you will have to convert x/D_h to x^+ in that output file.

x^+	Nu_{ii} (Table 8-11)	Nu_x (TEXSTAN)
0	∞	
0.0005	23.5	23.5
0.005	11.2	11.2
0.02	7.49	7.50
0.1	5.55	5.55
0.25	5.39	5.39
∞	8.385	5.38

8-27

TEXSTAN analysis of laminar combined entry flow in a circular pipe with constant surface temperature: Calculate the flow and construct a plot similar to Fig. 8-10 to show development of the Nusselt number with $x^+ = 2(x/D_h)/\text{Re Pr}$ over the range $x^+ = 0-0.3$. Let the Prandtl number be 0.7. Compare the results with Table 8-12. Feel free to evaluate the non-dimensional temperature profiles at various x^+ locations to demonstrate the concept of how the profiles evolve from a flat profile into thermally fully developed profile, and to investigate any other attribute of the entry region or thermally fully developed region of the flow. Let the Reynolds number be 1000, and pick fluid properties that are appropriate to the chosen Prandtl number. You can choose how to set up the TEXSTAN problem in terms of values for the thermal boundary and initial conditions, and for geometrical dimensions and mean velocity for the pipe to provide the required Reynolds number and a pipe length equivalent to $x^+ = 0.3$. Use constant fluid properties and do not consider viscous dissipation. For initial conditions let the velocity profile be flat at a value equal to the mean velocity and the temperature profile be flat at some value T_e .

The data file for this problem is *8.27.dat.txt*. The data set construction is based on the *s30.dat.txt* file for combined entry length flow in a pipe with a specified surface temperature (initial profiles: flat velocity and flat temperature).

Here is an abbreviated listing of the output file (it will be called *out.txt* when you execute TEXSTAN using *8.27.dat.txt*) and $\text{Pr}=0.7$:

intg	x/dh/re	cf*re	uclr	xplus	nu	th,cl	tm/ts	ts	qflux
5	.00003	137.95	1.037	.00007	57.858	1.018	.968	3.100E+02	2.160E+02
50	.00025	55.81	1.104	.00071	20.239	1.058	.969	3.100E+02	7.273E+01
100	.00050	43.41	1.144	.00143	14.833	1.084	.970	3.100E+02	5.202E+01
150	.00092	35.35	1.192	.00264	11.365	1.118	.971	3.100E+02	3.864E+01
200	.00206	27.77	1.280	.00589	8.155	1.188	.973	3.100E+02	2.608E+01
250	.00510	22.11	1.429	.01456	5.815	1.335	.976	3.100E+02	1.655E+01
300	.01240	18.63	1.652	.03543	4.441	1.585	.980	3.100E+02	1.028E+01
350	.02392	17.06	1.839	.06835	3.897	1.746	.985	3.100E+02	6.891E+00
400	.04137	16.33	1.947	.11819	3.708	1.794	.990	3.100E+02	4.506E+00
450	.06550	16.07	1.986	.18714	3.665	1.799	.994	3.100E+02	2.688E+00
500	.09050	16.01	1.995	.25857	3.659	1.799	.996	3.100E+02	1.595E+00
519	.10000	16.01	1.996	.28571	3.658	1.798	.997	3.100E+02	1.309E+00

Here is the comparison with the $\text{Pr}=0.7$ entries in Table 8-12, using Nu_x data from output file *out.txt* with *kpace=1* to obtain enough entries to avoid interpolation..

x^+	Nu_x (Table 8-12)	Nu_x (TEXSTAN)
0	∞	
0.001	16.8	17.4
0.002	12.6	12.8
0.004	9.6	9.55

0.006	8.25	8.07
0.01	6.8	6.63
0.02	5.3	5.23
0.05	4.2	4.11
∞	3.66	3.66

8-28

TEXSTAN analysis of laminar combined entry flow in a parallel planes channel with asymmetrical heat flux in which one plane has a constant surface heat flux, heating case, and the other plane has an adiabatic surface: Calculate the flow and construct a plot to show development of the Nusselt number with $x^+ = 2(x/D_h)/Re Pr$ over the range $x^+ = 0-0.3$. Let the Prandtl number be 0.7. Compare the results with the Nu_{11} values for parallel planes in Table 8-13 (note the influence coefficient is not used for this problem). Feel free to evaluate the nondimensional temperature profiles at various x^+ locations to demonstrate the concept of how the profiles evolve from a flat profile into thermally fully developed profile, and to investigate any other attribute of the entry region or thermally fully developed region of the flow. Let the Reynolds number be 1000, and pick fluid properties that are appropriate to the chosen Prandtl number. You can choose how to set up the TEXSTAN problem in terms of values for the thermal boundary and initial conditions, and for geometrical dimensions and mass flow rate for the channel to provide the required Reynolds number and a channel length equivalent to $x^+ = 0.3$. Use constant fluid properties and do not consider viscous dissipation. For initial conditions let the velocity profile be flat at a value equal to the mean velocity and the temperature profile be flat at some value t_c . Because this problem has asymmetrical thermal boundary conditions, choose the option in TEXSTAN that permits the calculation from surface to surface.

The data file for this problem is *8.28.dat.txt*. The data set construction is based on the *s596.dat.txt* file for combined entry length flow between parallel planes with a specified surface heat flux on each surface (initial profiles: flat velocity and flat temperature).

Here is an abbreviated listing of the output file (it will be called *out.txt* when you execute TEXSTAN using *8.28.dat.txt*) and $Pr=0.7$ (note the use of $kout=4$ because $kgeom=6$)

intg	x/dh	cfapp	cf2(I)	cf2(E)	nu(I)	nu(E)
5	1.250E-02	1.037E+00	9.607E-02	9.607E-02	1.212E+02	0.000E+00
50	1.250E-01	3.076E-01	3.816E-02	3.816E-02	3.935E+01	0.000E+00
100	2.500E-01	2.171E-01	2.953E-02	2.953E-02	2.859E+01	0.000E+00
150	3.750E-01	1.775E-01	2.566E-02	2.566E-02	2.383E+01	0.000E+00
200	5.000E-01	1.541E-01	2.334E-02	2.334E-02	2.099E+01	0.000E+00
250	6.761E-01	1.332E-01	2.123E-02	2.123E-02	1.842E+01	0.000E+00
300	1.018E+00	1.097E-01	1.884E-02	1.884E-02	1.550E+01	0.000E+00
350	1.680E+00	8.674E-02	1.653E-02	1.653E-02	1.265E+01	0.000E+00
400	2.964E+00	6.706E-02	1.456E-02	1.456E-02	1.018E+01	0.000E+00
450	5.443E+00	5.159E-02	1.311E-02	1.311E-02	8.252E+00	0.000E+00
500	9.012E+00	4.213E-02	1.237E-02	1.237E-02	7.096E+00	0.000E+00
550	1.341E+01	3.659E-02	1.210E-02	1.210E-02	6.432E+00	0.000E+00
600	1.881E+01	3.308E-02	1.202E-02	1.202E-02	6.012E+00	0.000E+00
650	2.547E+01	3.074E-02	1.200E-02	1.200E-02	5.738E+00	0.000E+00
700	3.367E+01	2.912E-02	1.200E-02	1.200E-02	5.565E+00	0.000E+00
750	4.376E+01	2.796E-02	1.200E-02	1.200E-02	5.466E+00	0.000E+00
800	5.575E+01	2.712E-02	1.200E-02	1.200E-02	5.416E+00	0.000E+00
850	6.825E+01	2.655E-02	1.200E-02	1.200E-02	5.396E+00	0.000E+00
900	8.075E+01	2.615E-02	1.200E-02	1.200E-02	5.389E+00	0.000E+00

950	9.325E+01	2.586E-02	1.200E-02	1.200E-02	5.386E+00	0.000E+00
977	1.000E+02	2.574E-02	1.200E-02	1.200E-02	5.385E+00	0.000E+00

Here is the comparison with the Pr=0.7 parallel planes entries in Table 8-13, using Nu_x data from output file *fn81.txt* with *kpace*=1 to obtain enough entries to avoid interpolation. Note you will have to convert x/D_h to x^+ in that output file.

x^+	Nu_x (Table 8-13)	Nu_x (TEXSTAN)
0	∞	
0.002	18.5	18.1
0.010	9.62	9.59
0.020	7.68	7.63
0.10	5.55	5.55
0.20	5.40	5.39
∞	5.39	5.39

8-29

TEXSTAN analysis of laminar combined entry flow in a circular-tube annulus with $r^* = 0.5$ and asymmetrical surface heat flux in which one surface has a constant heat flux, heating case, and the other surface is adiabatic: Calculate the flow and construct a plot to show development of the Nusselt number with $x^+ = 2(x/D_h)/Re Pr$ over the range $x^+ = 0-0.3$. Let the Prandtl number be 0.7. Test two cases: constant heat flux on the inside surface and the outside surface adiabatic, and then the opposite case. Compare the results with the Nu_{ii} and Nu_{oo} entries for $r^* = 0.5$ in Table 8-13 (note the influence coefficients are not used for this problem). Feel free to evaluate the nondimensional temperature profiles at various x^+ locations to demonstrate the concept of how the profiles evolve from a flat profile into thermally fully developed profile, and to investigate any other attribute of the entry region or thermally fully developed region of the flow. Let the Reynolds number be 1000, and pick fluid properties that are appropriate to the chosen Prandtl number. You can choose how to set up the TEXSTAN problem in terms of values for the thermal boundary and initial conditions, and for geometrical dimensions and mass flow rate for the channel to provide the required Reynolds number, a value of $r^* = 0.5$, and a channel length equivalent to $x^+ = 0.3$. Use constant fluid properties and do not consider viscous dissipation. For initial conditions let the velocity profile be flat at a value equal to the mean velocity and the temperature profile be flat at some value T_c . Because this problem has asymmetrical thermal boundary conditions, choose the option in TEXSTAN that permits the calculation from surface to surface.

The data file for this problem is *8.29.dat.txt*. The data set construction is based on the *s61.dat.txt* file for combined entry length flow in a $r^*=0.5$ annulus with a specified surface heat flux on each surface (initial profiles: flat velocity and flat temperature).

Here is an abbreviated listing of the output file (it will be called *out.txt* when you execute TEXSTAN using *8.29.dat.txt*) and $Pr=0.7$ (note the use of $kout=4$ because $kgeom=7$)

intg	x/dh	cfapp	cf2(I)	cf2(E)	nu(I)	nu(E)
5	1.250E-02	1.037E+00	9.753E-02	9.533E-02	1.223E+02	0.000E+00
50	1.250E-01	3.077E-01	3.956E-02	3.745E-02	4.034E+01	0.000E+00
100	2.500E-01	2.172E-01	3.093E-02	2.880E-02	2.956E+01	0.000E+00
150	3.750E-01	1.776E-01	2.707E-02	2.493E-02	2.478E+01	0.000E+00
200	5.000E-01	1.541E-01	2.476E-02	2.260E-02	2.193E+01	0.000E+00
250	6.761E-01	1.333E-01	2.267E-02	2.049E-02	1.935E+01	0.000E+00
300	1.018E+00	1.097E-01	2.030E-02	1.808E-02	1.642E+01	0.000E+00
350	1.680E+00	8.680E-02	1.802E-02	1.574E-02	1.355E+01	0.000E+00
400	2.964E+00	6.712E-02	1.612E-02	1.373E-02	1.107E+01	0.000E+00
450	5.443E+00	5.165E-02	1.476E-02	1.221E-02	9.119E+00	0.000E+00
500	9.012E+00	4.216E-02	1.413E-02	1.141E-02	7.952E+00	0.000E+00
550	1.341E+01	3.660E-02	1.391E-02	1.108E-02	7.275E+00	0.000E+00
600	1.881E+01	3.305E-02	1.386E-02	1.096E-02	6.841E+00	0.000E+00
650	2.547E+01	3.068E-02	1.385E-02	1.093E-02	6.554E+00	0.000E+00
700	3.367E+01	2.903E-02	1.385E-02	1.093E-02	6.371E+00	0.000E+00
750	4.376E+01	2.785E-02	1.385E-02	1.093E-02	6.266E+00	0.000E+00
800	5.575E+01	2.699E-02	1.385E-02	1.093E-02	6.213E+00	0.000E+00
850	6.825E+01	2.641E-02	1.385E-02	1.093E-02	6.193E+00	0.000E+00

900	8.075E+01	2.600E-02	1.385E-02	1.093E-02	6.185E+00	0.000E+00
950	9.325E+01	2.571E-02	1.385E-02	1.093E-02	6.182E+00	0.000E+00
977	1.000E+02	2.558E-02	1.385E-02	1.093E-02	6.181E+00	0.000E+00

Here is the comparison with the $Pr=0.7$ annulus with $r^*=0.5$ entries in Table 8-13, using Nu_x data from output file *fin81.txt* with *kpace*=1 to obtain enough entries to avoid interpolation. Note you will have to convert x/D_h to x^+ in that output file.

x^+	Nu_x (Table 8-13)	Nu_x (TEXSTAN)
0	∞	
0.002	19.22	19.1
0.010	10.48	10.5
0.020	8.52	8.49
0.10	6.35	6.35
0.20	6.19	6.19
∞	6.18	6.18

8-30

TEXSTAN analysis of laminar thermal-entry flow in a circular pipe with the effect of axial variation of surface temperature, $T_s = f(x)$ from Fig. 8-14 over the distance $0.0 \leq x^+ \leq 0.2$: Let the Reynolds number be 1000, and pick fluid properties that are appropriate to an air Prandtl number of 0.7. You can choose how to set up the TEXSTAN problem in terms of values for the thermal boundary and initial conditions, and for geometrical dimensions and mass flow rate for the pipe to provide the required Reynolds number and a pipe length equivalent to $x^+ = 0.2$. Use constant fluid properties and do not consider viscous dissipation. For initial conditions let the velocity profile be hydrodynamically fully developed and the temperature profile be flat at some value T_c . Calculate the flow and compare the results Fig. 8-14. Discuss the behavior of the various variables in terms of the temperature profiles obtained as a part of the computer analysis.

The data file for this problem is *8.30.dat.txt*. The data set construction is based on the *s34.dat.txt* file for thermal entry length flow in a pipe with a specified surface temperature (initial profiles: hydrodynamically fully-developed velocity and flat temperature).

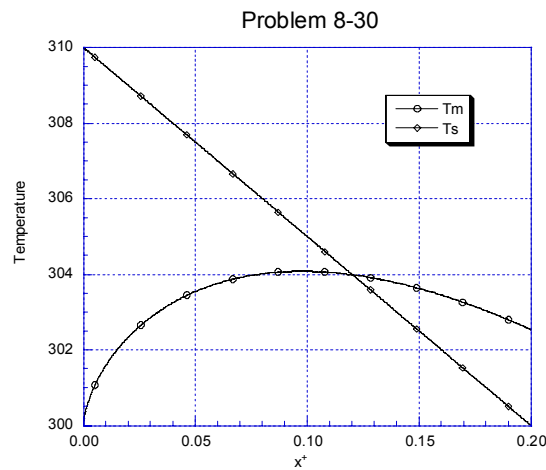
The $T_s(x)$ distribution is linear over the interval $0.0 \leq x^+ \leq 0.2$ as seen in Fig. 8-14, so a set of 21 $x(m)$ points were used at equal intervals of $x^+=0.05$. The *deltax* control was handled similarly to problem 8-11,. Instead of using *deltax* in the *aux1(m)* array, *kdx* was set =0 and *deltax*=0.05. A smaller value would generate more points.

Here is an abbreviated listing of the output file *fn84.txt* that contains physical heat transfer data. This data has been generated using *k5*=200 to reduce the number of data points for printing here. You will want to use a very small number (say *k5*=5) to generate enough data points to resolve the temperature changes.

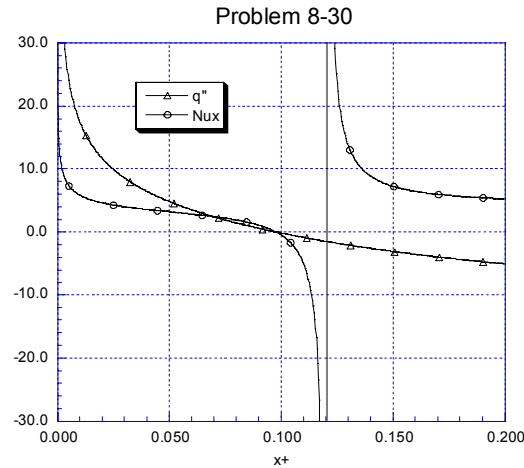
intg	x/dh	htc	qflux	tm	ts
5	2.5000001E-02	1.2641E+01	1.2552E+02	3.0007E+02	3.1000E+02
100	7.7025698E-01	3.7150E+00	3.4406E+01	3.0063E+02	3.0989E+02
200	3.1681002E+00	2.2932E+00	1.8465E+01	3.0150E+02	3.0955E+02
300	5.6500000E+00	1.8854E+00	1.3415E+01	3.0208E+02	3.0919E+02
400	8.1499961E+00	1.6622E+00	1.0494E+01	3.0252E+02	3.0884E+02
500	1.0650005E+01	1.5096E+00	8.4574E+00	3.0288E+02	3.0848E+02
600	1.3149994E+01	1.3905E+00	6.8947E+00	3.0316E+02	3.0812E+02
700	1.5650006E+01	1.2881E+00	5.6252E+00	3.0340E+02	3.0776E+02
800	1.8149993E+01	1.1925E+00	4.5544E+00	3.0359E+02	3.0741E+02
900	2.0650008E+01	1.0960E+00	3.6268E+00	3.0374E+02	3.0705E+02
1000	2.3149992E+01	9.9140E-01	2.8071E+00	3.0386E+02	3.0669E+02
1100	2.5650008E+01	8.6935E-01	2.0717E+00	3.0395E+02	3.0634E+02
1200	2.8149991E+01	7.1593E-01	1.4039E+00	3.0402E+02	3.0598E+02
1300	3.0650009E+01	5.0660E-01	7.9171E-01	3.0406E+02	3.0562E+02
1400	3.3149991E+01	1.9069E-01	2.2631E-01	3.0408E+02	3.0526E+02
1500	3.5650009E+01	-3.5974E-01	-2.9902E-01	3.0408E+02	3.0491E+02
1600	3.8149995E+01	-1.5957E+00	-7.8942E-01	3.0406E+02	3.0455E+02
1700	4.0650005E+01	-7.0946E+00	-1.2489E+00	3.0402E+02	3.0419E+02
1800	4.3149995E+01	1.3348E+01	-1.6807E+00	3.0396E+02	3.0384E+02

1900	4.5650005E+01	5.0650E+00	-2.0874E+00	3.0389E+02	3.0348E+02
2000	4.8149995E+01	3.6153E+00	-2.4710E+00	3.0380E+02	3.0312E+02
2100	5.0650005E+01	3.0117E+00	-2.8335E+00	3.0371E+02	3.0276E+02
2200	5.3150000E+01	2.6805E+00	-3.1763E+00	3.0359E+02	3.0241E+02
2300	5.5650000E+01	2.4714E+00	-3.5009E+00	3.0347E+02	3.0205E+02
2400	5.8150000E+01	2.3273E+00	-3.8082E+00	3.0333E+02	3.0169E+02
2500	6.0650000E+01	2.2222E+00	-4.0995E+00	3.0318E+02	3.0134E+02
2600	6.3150000E+01	2.1421E+00	-4.3755E+00	3.0302E+02	3.0098E+02
2700	6.5650000E+01	2.0791E+00	-4.6373E+00	3.0285E+02	3.0062E+02
2800	6.8150033E+01	2.0284E+00	-4.8856E+00	3.0267E+02	3.0026E+02
2874	6.9999967E+01	1.9968E+00	-5.0610E+00	3.0253E+02	3.0000E+02

In this abbreviated output we can see the trends of Fig. 8-14. A more detailed distribution is shown in the figure below.



We see that $x^+ 0.12$ is the approximate location where $(T_s - T_m) \rightarrow 0$ which will create an infinite Nusselt number. The heat transfer information are plotted in the figure below.



In this figure we again see the shapes match those of Fig. 8-14. We see the $x^+ = 0.12$ is the approximate location where $(T_s - T_m) \rightarrow 0$ which creates the infinite Nusselt number. Recall the definitions of the heat flux and heat transfer coefficient for the pipe surface is

$$\dot{q}_s'' = +k \left. \frac{\partial T}{\partial y} \right|_{\text{E-surface}} = h(T_s - T_m)|_{\text{E-surface}}$$

where $y = (r_s - r)$. At $x^+ = 0.097$ the surface heat flux passes through zero and becomes negative, reflecting the decreasing wall temperature. This is also the location where $dT_m/dx = 0$ in the temperature figure, and for larger x^+ the T_m must decrease because heat is being removed from the fluid. Note it takes an x^+ distance of about $(0.12 - 0.097)$ before the removal of heat from the fluid at the wall will cause the $(T_s - T_m) \rightarrow 0$ and the strange behavior of the Nusselt number. Past $x^+ = 0.12$ the heat flux is negative and $(T_s - T_m) < 0$, and once again the Nusselt number is positive.

To fully understand the variable surface temperature behavior it is important that you plot the temperature profiles. This data is easily generated by rerunning the data set with $k10$ set =10 or =11 (only for pipe flows can you generate nondimensional profiles using $k10=10$).

9-1

Air at 26°C and 1 atm pressure flows normally to a 5 cm diameter circular cylinder at a velocity of 9 m/s. It can be shown from potential flow theory that in the vicinity of the forward stagnation point for flow normal to a cylinder the velocity along the surface, u_∞ (which is the velocity just outside of any boundary layer), is given by

$$u_\infty = \frac{4Vx}{D}$$

where V is the oncoming normal velocity, x is the distance along the surface measured from the stagnation point, and D is the diameter of cylinder. Calculate the displacement thickness of the boundary layer at the stagnation point, and discuss the significance of the result.

The stagnation point flow is part of the family of flows called the Falkner-Skan similarity flows where the local free stream velocity is given by the potential flow solution for inviscid flow over a wedge, $u_\infty = Cx^m$. The m parameter is depicted in Fig. 9-2, where $m = (\beta/\pi)/[2 - (\beta/\pi)]$ and for stagnation point flow, $\beta = \pi$, yielding $m=1$. Inviscid flow over a cylinder of radius R has a potential flow solution $u_\infty/V_{\text{app}} = 2\sin(x/R)$ where V_{app} is the velocity of the flow field approaching the cylinder. The first term of the Taylor-series approximation for the sine function for $(x/R) \ll 1$ is $u_\infty(x) = 2V_{\text{app}}(x/R) = Cx^1$ where $C = (2V_{\text{app}})/R = (4V_{\text{app}})/D$. Thus, the region for $-15^\circ \leq \phi \leq 15^\circ$ is the so-called stagnation point flow, where $\phi = (x/R)$.

For this problem we will assume a constant density, i.e. no density variation through the boundary layer which forms over the wedge. Density variation throughout the boundary layer is caused either by an imposed thermal boundary condition (wall temperature or wall heat flux) which leads to a large wall-to-free stream temperature difference, or when viscous heating associated with viscous work cause local temperature variation in the region near the surface. For gases, we find experimentally that we can ignore variable properties (including density) when $0.95 \leq T_s/T_\infty \leq 1.05$ and when $M \leq 0.4$. For this problem we have no information about the thermal boundary condition. The Mach number for an ideal gas can be computed to be

$$M = \frac{V}{\sqrt{\gamma RT}}$$

where γ is the ratio of specific heats, R is the gas constant ($R=R/\mathcal{M}$ where R is the universal gas constant, and \mathcal{M} is the fluid molecular weight). For this problem, $M \approx 0.03$, and the assumption of constant density is justified in the absence of thermal boundary condition information. Thus, displacement thickness Eq. (5-5) reduces to

$$\delta_1 = \int_0^\infty \left(1 - \frac{u}{u_\infty}\right) dy$$

and this equation transforms using

$$\eta = \frac{y}{\sqrt{\nu x/u_\infty}} = \frac{y}{\sqrt{\nu/C}} \quad \text{and} \quad \zeta'(\eta) = \frac{u}{u_\infty}$$

into

$$\delta_1 = \sqrt{\frac{\nu}{C}} \int_0^\infty (1 - \zeta'(\eta)) d\eta = \sqrt{\frac{\nu}{C}} [\eta - \zeta(\eta)]_0^\infty$$

Note: the function $[\eta - \zeta(\eta)]$ is zero at the lower limit and becomes a constant value at the upper limit. Table 9-1 contains information only for $m=0$, and so another source must be used to obtain $\zeta(\eta)$. One source is tabulated in Schlichting¹.

The other source is to solve Eq. (9-24) with the indicated boundary conditions and $m=1$ using traditional numerical methods such as Runge-Kutta and a “shooting method”. Here

$$\begin{aligned} Y_1 &= \zeta & Y_1' &= Y_2 \\ Y_2 &= \zeta' & Y_2' &= Y_3 \\ Y_3 &= \zeta'' & Y_3' &= mY_2^2 - \frac{(m+1)}{2} Y_1 Y_3 - m \end{aligned}$$

along with $Y_1(0)=0$, $Y_2(0)=0$, and $Y_2(\infty)=1$ (recall for the shooting method we will require $Y_3(0)=\text{guessed value}$). The results are as follows:

η	$\zeta(\eta)$	$\zeta'(\eta)$	$\zeta''(\eta)$
0	0	0	1.233
0.1	0.0060	0.1183	1.1328
0.2	0.0233	0.2266	1.0345
0.3	0.0510	0.3252	0.9386
0.4	0.0881	0.4145	0.8463
0.5	0.1336	0.4946	0.7583
0.6	0.1867	0.5663	0.6752
0.7	0.2466	0.6299	0.5974
0.8	0.3124	0.6859	0.5251
0.9	0.3835	0.7351	0.4587
1.0	0.4592	0.7779	0.3980
1.2	0.6220	0.8467	0.2938
1.4	0.7967	0.8968	0.2110
1.6	0.9798	0.9323	0.1474
1.8	1.1689	0.9568	0.1000
2.0	1.3620	0.9732	0.0658
2.2	1.5578	0.9839	0.0420
2.4	1.7553	0.9906	0.0260
2.6	1.9538	0.9946	0.0156
2.8	2.1530	0.9970	0.0091

3.0	2.3526	0.9984	0.0051
3.5	2.8522	0.9997	0.0010
4.0	3.3521	1.000	0.0002
4.5	3.8521	1.000	0.0000

Evaluation of this table shows $[\eta - \zeta(\eta)] \rightarrow 0.4379$. Note that one can also obtain this value by carrying out the integration of the displacement equation using Simpson's rule. The final answer is $\delta_l = 0.096$ mm.

An alternative solution for this problem is to use Eq. (9-44) with R removed (recall R is the transverse radius of curvature, not the curvature in the flow direction).

$$\delta_2 = \frac{0.664\nu^{0.5}}{u_\infty^{2.84}} \left(\int_0^x u_\infty^{4.68} dx \right)^{0.5}$$

Substituting $u_\infty = \frac{4Vx}{D}$ into the integral and carrying out the integration yields

$$\delta_2 = 0.664\nu^{0.5} \left(\frac{D}{4Vx} \right)^{2.84} \left(\frac{4V}{D} \right)^{\frac{4.68}{2}} \left(\frac{x^{5.68}}{5.68} \right)^{0.5}$$

At this point, one sees that x removes itself from the equation, which is characteristic of the stagnation point flows, namely that δ , δ_l , and δ_2 are all constant values over the stagnation region. Evaluation yields a value of δ_2 of about 0.041 mm. This permits the parameter defined by Eq. (9-39) to be evaluated, $\lambda=0.078$. From Table 9-4, we find the shape factor $H = 2.34$, and from Eq. (9-37) $\delta_l = 0.096$ mm (the same answer obtained from the numerical solution).

9-2

Derive Eq. (9-21) from potential flow theory.

This solution proceeds from the ideas of the velocity potential and the stream function,

$$\frac{\partial \phi}{\partial x} = \frac{\partial \psi}{\partial y} = u \quad \text{and} \quad \frac{\partial \phi}{\partial y} = -\frac{\partial \psi}{\partial x} = v$$

and the fact that both functions satisfy their respective Laplace equation formulations. In complex variable theory, potential flow solutions are greatly simplified if the flow domain can be transformed into a semi-infinite domain. A complex potential is constructed as $F(z) = \phi(x, y) + i\psi(x, y)$ where $F(z)$ is an analytical function such that

$$\frac{dF}{dz} = \frac{\partial \phi}{\partial x} + i \frac{\partial \psi}{\partial x} = u - iv \equiv \bar{w}$$

and where $w = u + iv$. For uniform parallel flow the complex potential function is $F(z) = V_o z$. The domain is now transformed to the upper-half of the w -plane. Then if the transformation $w = w(z)$ is conformal and $z = \infty \Rightarrow w = \infty$, then $F(z) = Aw(z)$ where A is determined such that $u_\infty = V_o$.

Applied for the wedge geometry, the transformation is $w(z) = Az^{\pi/\gamma}$ to map the “wedge” domain of opening γ into the semi-infinite domain. Then, if $F(z) = Aw(z)$,

$$|\bar{w}| = \left| A \frac{dF}{dz} \right| = A \frac{\pi}{\gamma} z^{\frac{\pi}{\gamma}-1}$$

From wedge-flow geometry $\gamma = \pi - \beta/2$, then

$$|\bar{w}| = \left| \frac{A\pi}{\pi - \beta/2} z^{\frac{\beta/2}{\pi - \beta/2}} \right| = |Cz^m|$$

Here, $z = re^{i\phi} = xe^{i\gamma}$. Thus,

$$|\bar{w}| = |u_\infty| = |Cx^m e^{i\gamma m}| = Cx^m$$

9-3

Solve the laminar boundary layer for constant free-stream velocity, using the momentum integral equation and an assumption that the velocity profile may be approximated by

$$\frac{u}{u_\infty} = \sin \frac{\pi y}{2\delta}$$

Evaluate the momentum thickness, displacement thickness, and friction coefficient, and compare with the exact solution.

The applicable momentum integral equation is (5-9), rewritten as Eq. (9-31) by substituting for the surface shear stress,

$$\frac{c_f}{2} = \frac{\tau_s}{\rho_\infty u_\infty^2} = \frac{\nu}{u_\infty^2} \left(\frac{\partial u}{\partial y} \right)_s = \frac{d\delta_2}{dx}$$

This requires evaluation of the momentum thickness for the sine-function velocity profile. From Eq. (5-6), assuming constant properties, substituting for the profile, and integrating from the surface to the edge of the boundary layer (replacing ∞ by δ in the upper limit.

$$\delta_2 = \int_0^\infty \frac{\rho u}{\rho_\infty u_\infty} \left(1 - \frac{u}{u_\infty} \right) dy = \int_0^\infty \frac{u}{u_\infty} \left(1 - \frac{u}{u_\infty} \right) dy = \delta \left(\frac{2}{\pi} - \frac{1}{2} \right)$$

Substitute the velocity profile into the wall-gradient term on the left-hand side (LHS) of the momentum integral equation and the momentum thickness function into the right-hand side (RHS) of the equation, separate variable and integrate, assuming $\delta(x=0)=0$, to obtain

$$\delta = 4.80 \left(\frac{\nu x}{u_\infty} \right)^{1/2} \quad \text{or} \quad \frac{\delta}{x} = 4.80 \text{Re}_x^{-1/2}$$

Substitute the solution for δ into the momentum thickness, and the result is

$$\frac{\delta_2}{x} = 0.655 \text{Re}_x^{-1/2}$$

Following the same procedure for evaluation of the displacement thickness from Eq. (5-5) gives

$$\frac{\delta_1}{x} = 1.74 \text{Re}_x^{-1/2}$$

For the friction coefficient, the definition is combined with the velocity profile and the solution for δ to give

$$c_f = \frac{\tau_s}{\frac{1}{2} \rho_\infty u_\infty^2} = \frac{2\nu}{u_\infty^2} \left(\frac{\partial u}{\partial y} \right)_s = 0.655 \text{Re}_x^{-1/2}$$

Comparing these results with the similarity solution shows errors of +0.6% for δ_1 , -1.4% for δ_2 and for c_f .

9-4

Redevelop Eq. (9-42) for the case where density and dynamic viscosity are functions of x .

From momentum integral equation (5-7),

$$\frac{\tau_s}{\rho_\infty u_\infty^2} + \frac{\rho_s v_s}{\rho_\infty u_\infty} = \frac{d\delta_2}{dx} + \delta_2 \left[\left(2 + \frac{\delta_1}{\delta_2} \right) \frac{1}{u_\infty} \frac{du_\infty}{dx} + \frac{1}{\rho_\infty} \frac{d\rho_\infty}{dx} + \frac{1}{R} \frac{dR}{dx} \right]$$

we can see that the density term is similar in form to the transverse-radius term. Thus, it is easily added to Eq. (9-38),

$$\frac{u_\infty}{\nu} \frac{d\delta_2^2}{dx} + \frac{\delta_2^2 u_\infty}{\nu} \left[\frac{2}{R} \frac{dR}{dx} + \frac{2}{\rho_\infty} \frac{d\rho_\infty}{dx} \right] = 2 \left[T - (2 + H) \frac{\delta_2^2}{\nu} \frac{du_\infty}{dx} \right]$$

Rearranging this equation using the ideas used in Eq. (9-40) and Eq. (9-41),

$$\frac{u_\infty}{\nu} \frac{d\delta_2^2}{dx} + \frac{\delta_2^2 u_\infty}{\nu} \left[\frac{2}{R} \frac{dR}{dx} + \frac{2}{\rho_\infty} \frac{d\rho_\infty}{dx} \right] = (a - b\lambda) = a - b \left(\frac{\delta_2^2}{\nu} \frac{du_\infty}{dx} \right)$$

At this point the development follows that on page 144 of the 4th Edition. We need to use the following derivative ideas,

$$d(u_\infty^b) = b u_\infty^{b-1} du_\infty \quad \text{and} \quad d(R^2) = 2R dR \quad \text{and} \quad d(\rho_\infty^2) = 2\rho_\infty d\rho_\infty$$

Move the b -term to the LHS, multiply and then multiply and divide each of the four LHS terms with the appropriate variables to obtain terms with the same denominator,

$$\frac{u_\infty^b R^2 \rho_\infty^2}{\nu u_\infty^{b-1} R^2 \rho_\infty^2} \frac{d\delta_2^2}{dx} + \frac{\delta_2^2 R^2 \rho_\infty^2}{\nu u_\infty^{b-1} R^2 \rho_\infty^2} \frac{du_\infty^b}{dx} + \frac{u_\infty^b \delta_2^2 \rho_\infty^2}{\nu u_\infty^{b-1} R^2 \rho_\infty^2} \frac{dR^2}{dx} + \frac{u_\infty^b \delta_2^2 R^2}{\nu u_\infty^{b-1} R^2 \rho_\infty^2} \frac{d\rho_\infty^2}{dx} = a$$

Now, recognize this as an exact differential of four terms, and multiply through the denominator and separate variables,

$$d(R^2 \rho_\infty^2 \delta_2^2 u_\infty^b) = a \nu u_\infty^{b-1} R^2 \rho_\infty^2 dx$$

From this point the integration of this equation is exactly like the procedure leading to Eq. (9-42).

9-5

Air emerges from the axisymmetric nozzle shown in Fig. 9-3 at a centerline velocity of 10 m/s at 1 atm pressure and 21°C. Assuming an essentially constant-density and constant-temperature process (and this is ensured by the low velocity), calculate the displacement thickness of the boundary layer at the nozzle throat, assuming that the free-stream velocity along the inner surface of the nozzle varies linearly with distance, starting with $u_\infty = 0$ at the sharp corner. Calculate the air mass flow rate through the nozzle and the overall pressure drop through the nozzle. On the basis of these results, discuss the concept of a nozzle “discharge coefficient.” What would be the discharge coefficient of this nozzle? If you were to define a Reynolds number based on throat diameter and mean velocity, how would the discharge coefficient vary with Reynolds number?

The analysis procedure for this problem is: to calculate δ_2 using Eq. (9-42); formulate λ from Eq. (9-39); use Table 9-4 to find H , and then from its definition, Eq. (9-37), determine δ_1 ; calculate the mass flow rate using Eq. (7-3); calculate a pressure drop using a Bernoulli equation; and finally calculate a discharge coefficient, the ratio of actual to theoretical mass flow through the nozzle. The problem requires assumptions of steady flow and constant properties.

There are several geometric variables to be defined. The nozzle radius of curvature is $r_{noz} = 0.0375$ m. The nozzle transverse radius at the throat, $R_b = 0.0125$ m, and nozzle transverse radius at the start of the nozzle ($x_a = 0$) is $R_a = 0.05$ m. From geometry, $x_b = r_{noz} \pi/2 = 0.058905$ m. Using this geometry, the function for the transverse radius of the nozzle wall becomes

$$R(x) = R_a - r_{noz} \sin(\theta) = R_a - r_{noz} \sin\left(\frac{x}{r_{noz}}\right)$$

and Eq. (9-42) becomes

$$\delta_2(x_b) = \frac{0.664\nu^{1/2}}{R_b u_{\infty,b}^{2.84}} \left[\int_{x_a}^{x_b} [u_\infty(x)]^{4.86} \left(R_a - r_{noz} \sin \frac{x}{r_{noz}} \right)^2 dx \right]^{1/2}$$

The free stream velocity just outside the boundary layer of the nozzle wall really needs to be developed from an inviscid or Euler analysis of the incompressible flow in a converging nozzle.

The first approximation for this axisymmetric nozzle is to assume the free stream velocity at the nozzle wall varies linearly along the nozzle surface from the sharp corner to the throat, $x_a \leq x \leq x_b$, with $u_{\infty,a} = 0$ and $u_{\infty,b} = 10$ m/s

$$u_\infty(x) = \cancel{u_{\infty,a}} + \left(\frac{u_{\infty,b} - u_{\infty,a}}{x_b - x_a} \right) (x - x_a) = 169.8x \text{ m/s}$$

Note that the requirement of $u_{\infty,a} = 0$ is a requirement of the problem statement and is not really needed.

Equation (9-42) can be evaluated using standard methods for the integral. We use a Simpson's rule with 12 intervals and evaluating the properties at 20°C to obtain the momentum thickness. Compute the pressure gradient parameter λ using Eq. (9-39) with the velocity gradient coming from the linear velocity profile. Interpolate Table 9-4 for the shape factor H , and then compute the displacement thickness.

$$\begin{aligned}\delta_2 &= 1.1602\text{E-}04 \text{ m} \\ \lambda &= 0.1515 \\ H &= 2.174 \\ \delta_1 &= 2.5226\text{E-}04 \text{ m}\end{aligned}$$

The actual mass flow rate in the nozzle will be based on the flow cross-sectional area, corrected for the displacement thickness,

$$\dot{m}_{actual} = \rho V_b (A_b - A_{block}) = \rho V_b \pi (r_b - \delta_{1,b})^2 = 5.68 \times 10^{-3} \text{ kg/s}$$

and the discharge coefficient becomes

$$C = \frac{\dot{m}_{actual}}{\dot{m}_{theo}} = \frac{\rho V_b (A_b - A_{block})}{\rho V_b A_b} = 0.96$$

The pressure drop through the nozzle, based on the Bernoulli equation, is

$$\Delta P = (P_b - P_a) = \frac{1}{2} \rho (V_b^2 - V_a^2) = -60.2 \text{ Pa}$$

Based on laminar boundary layer behavior, as Re increases, the displacement thicknesses decreases, as shown in Eq. (9-19), leading to a reduced flow blockage and a nozzle discharge coefficient that approaches unity.

The second approximation for this axisymmetric nozzle is to assume the free stream velocity at the nozzle wall is defined by the 1-D mass flow rate equation along the nozzle surface from the sharp corner to the throat, $x_a \leq x \leq x_b$, with $u_{\infty,a} = 0$ and $u_{\infty,b} = 10 \text{ m/s}$

$$u_{\infty}(x) = \frac{\dot{m}}{\rho A_c} = \frac{\dot{m}}{\rho \pi [R(x)]^2}$$

Equation (9-42) is re-evaluated using standard methods for the integral.

$$\begin{aligned}\delta_2 &= 1.0205\text{E-}04 \text{ m} \\ \lambda &= 0.04276 \\ H &= 2.458 \\ \delta_1 &= 2.5083\text{E-}04 \text{ m}\end{aligned}$$

We note the two approximations for the boundary layer edge velocity give about the same solution.

This problem is appropriate for TEXSTAN. The data file for this problem is *9.5.dat.txt*. The data set construction is based on the *s9010.dat.txt* file for flow inside an axisymmetric nozzle with variable free stream velocity and specified surface temperature (initial profiles: Falkner-Skan $m=1$ velocity and Falkner-Skan $m=1$ temperature). This geometry is *kgeom=3*, which is flow inside a surface of revolution. Because it is axisymmetric flow, the geometry transverse radius variable of the nozzle wall, $R(x)$ in this analysis, is used to create the array $rw(m)$ at $x(m)$ locations. For this data set, the x -locations were the same used in the Simpson's Rule quadrature for integration of the integral, 20 evenly-spaced locations along the nozzle surface from $x=0$ at the start of the nozzle to the x -value at the throat. Note this makes the data input variable $nxbc=21$. Because TEXSTAN linearly interpolates the $rw(m)$ array, this should be sufficient. Note that this same $x(m)$ array is used to generate the velocity distribution for the free stream boundary condition, $u_{\infty}(x)$, which is linear, because of the problem specification. The initial profiles for this axisymmetric nozzle problem (*kstart=6*) are the same profiles that are used with a cylinder in crossflow.

It is very important that the free stream velocity array, $ubl(m)$, which is the $u_{\infty}(x)$ function evaluated at each $x(m)$ location, be such that the array is mathematically very smooth, because it is used to create the pressure gradient for the momentum equation using Bernoulli's equation. TEXSTAN uses cubic spline interpolation of the free stream velocity to help with the smoothness. When in doubt, you can use a special flag in TEXSTAN, $k8=36$, to print files of how TEXSTAN converts the array, $ubl(m)$ into a pressure-gradient distribution. Plotting this pressure-gradient distribution will help the user be sure their free stream velocity array, $ubl(m)$, is differentially smooth.

Here is an abbreviated listing of the file *fm84.dat.txt*, which contains the momentum thickness ($del2$) and shape factor ($h12$) distribution between the start of integration and the nozzle throat. The free stream velocity distribution for this problem is the first approximation (linear free stream velocity profile):

x/s	yl	uinf	del2	h12	del3
2.9807465E-03	7.103E-04	5.060E-01	8.715E-05	2.217E+00	0.000E+00
3.7674002E-03	7.203E-04	6.396E-01	8.816E-05	2.212E+00	0.000E+00
6.9530356E-03	7.349E-04	1.180E+00	8.966E-05	2.206E+00	0.000E+00
1.0626524E-02	7.500E-04	1.804E+00	9.105E-05	2.198E+00	0.000E+00
1.4368821E-02	7.674E-04	2.439E+00	9.268E-05	2.189E+00	0.000E+00
1.8222421E-02	7.888E-04	3.094E+00	9.458E-05	2.180E+00	0.000E+00
2.2233437E-02	8.136E-04	3.774E+00	9.680E-05	2.169E+00	0.000E+00
2.6392100E-02	8.428E-04	4.480E+00	9.941E-05	2.156E+00	0.000E+00
3.0585223E-02	8.758E-04	5.192E+00	1.021E-04	2.144E+00	0.000E+00
3.5011648E-02	9.125E-04	5.944E+00	1.051E-04	2.130E+00	0.000E+00
3.9610990E-02	9.497E-04	6.725E+00	1.078E-04	2.118E+00	0.000E+00
4.4375136E-02	9.828E-04	7.533E+00	1.100E-04	2.108E+00	0.000E+00
4.9312901E-02	9.963E-04	8.372E+00	1.102E-04	2.105E+00	0.000E+00
5.4198382E-02	9.819E-04	9.201E+00	1.079E-04	2.111E+00	0.000E+00
5.8904861E-02	9.375E-04	1.000E+01	1.033E-04	2.127E+00	0.000E+00

From the output we find a predicted value $\delta_2 = 1.033E-04$ m and $H_{12} = 2.127$, which compares to our analysis values of $\delta_2 = 1.16E-04$ m and $H=2.174$. This is reasonable agreement between TEXSTAN and the analysis.

9-6

Derive Eq. (9-24) in a manner similar to that used in the development of Eq. (9-8) for zero pressure gradient.

Start with Eq. (9-23), and transform the dependent variables u and v using Eq. (9-9),

$$\frac{\partial \psi}{\partial y} \frac{\partial}{\partial x} \left(\frac{\partial \psi}{\partial y} \right) - \frac{\partial \psi}{\partial x} \left(\frac{\partial^2 \psi}{\partial y^2} \right) = \frac{u_\infty^2 m}{x} + \nu \frac{\partial^3 \psi}{\partial y^3}$$

Now, transform the independent variables, x and y using the Blasius variable Eq. (9-11) for y , and define the stream function using Eq. (9-10):

$$\begin{aligned}\xi &= x \\ \eta &= y \sqrt{\frac{u_\infty}{\nu x}} = y \sqrt{\frac{C}{\nu}} x^{(m-1)/2} \\ \psi(\xi, \eta) &= G(\xi) \zeta(\eta) = \sqrt{\nu x u_\infty} \zeta(\eta) = \sqrt{\nu C} x^{(m+1)/2} \zeta(\eta)\end{aligned}$$

Transform the various derivatives using the chain rule:

$$\begin{aligned}\frac{\partial(\quad)}{\partial x} &= \frac{\partial(\quad)}{\partial \xi} \frac{\partial \xi}{\partial x} + \frac{\partial(\quad)}{\partial \eta} \frac{\partial \eta}{\partial x} \\ \frac{\partial(\quad)}{\partial y} &= \frac{\partial(\quad)}{\partial \xi} \frac{\partial \xi}{\partial y} + \frac{\partial(\quad)}{\partial \eta} \frac{\partial \eta}{\partial y}\end{aligned}$$

At this point, you can do one of two procedures: the first is to transform the ψ equation differential operators, keeping ψ as the independent variable, and then introduce its definition to obtain an equation in G and ζ . Upon introducing the functional form of G , the equation separates and Eq. (9-24) is obtained. A second procedure is to transform the differential operators and ψ simultaneously. Either works.

9-7

TEXSTAN analysis of the laminar momentum boundary layer over a flat plate with zero pressure gradient: Choose a starting x -Reynolds number of about 1000 and pick fluid properties that are appropriate to air, evaluated at a free stream temperature of 300 K. Use constant fluid properties, and note that the energy equation does not have to be solved. The geometrical dimensions of the plate are 1 m wide (a unit width) by 0.2 m long in the flow direction, corresponding to an ending Re_x of about 2×10^5 . Let the velocity boundary condition at the free stream be 15 m/s. The initial velocity profile appropriate to the starting x -Reynolds number (a Blasius profile) can be supplied by using the $kstart=4$ choice in TEXSTAN. Calculate the boundary layer flow and compare the results with the similarity solution for development in the streamwise direction of such quantities as the boundary-layer thickness (see Table 9-1), displacement thickness (see Eq. 9-17), and momentum thickness (see Eq. 9-18). Evaluate the concept of boundary-layer similarity by comparing non-dimensional velocity profiles at several x -locations to themselves and to Table 9-1. Compare the friction coefficient results based on x -Reynolds number with Eq. (9-13) and momentum-thickness Reynolds number with Eq. (9-16). Calculate the friction coefficient distribution using momentum integral Eq. (5-11) and compare with the TEXSTAN calculations. Feel free to investigate any other attribute of the boundary-layer flow.

The data file for this problem is *9.7.dat.txt*. The data set construction is based on the *s10.dat.txt* file for flow over a flat plate with constant free stream velocity and specified surface temperature (initial profiles: Blasius velocity and Blasius temperature). Note that *kout* has been changed to =2.

Here is an abbreviated listing of the output file (it will be called *out.txt* when you execute TEXSTAN using *9.7.dat.txt*):

intg	x	rem	cf2	h12	reh	st
5	1.049E-03	2.100E+01	1.050E-02	2.590E+00	2.578E+01	1.313E-02
100	2.276E-03	3.094E+01	7.131E-03	2.590E+00	3.822E+01	8.914E-03
200	5.307E-03	4.726E+01	4.667E-03	2.590E+00	5.862E+01	5.831E-03
300	9.605E-03	6.358E+01	3.469E-03	2.590E+00	7.900E+01	4.332E-03
400	1.517E-02	7.990E+01	2.760E-03	2.590E+00	9.937E+01	3.445E-03
500	2.201E-02	9.622E+01	2.292E-03	2.590E+00	1.197E+02	2.860E-03
600	3.011E-02	1.125E+02	1.960E-03	2.590E+00	1.401E+02	2.445E-03
700	3.948E-02	1.289E+02	1.712E-03	2.590E+00	1.605E+02	2.135E-03
800	5.011E-02	1.452E+02	1.519E-03	2.590E+00	1.808E+02	1.895E-03
900	6.202E-02	1.615E+02	1.366E-03	2.590E+00	2.012E+02	1.703E-03
1000	7.519E-02	1.778E+02	1.240E-03	2.590E+00	2.215E+02	1.547E-03
1100	8.964E-02	1.941E+02	1.136E-03	2.590E+00	2.419E+02	1.417E-03
1200	1.053E-01	2.104E+02	1.048E-03	2.590E+00	2.622E+02	1.307E-03
1300	1.223E-01	2.268E+02	9.727E-04	2.590E+00	2.825E+02	1.213E-03
1400	1.405E-01	2.431E+02	9.073E-04	2.590E+00	3.029E+02	1.131E-03
1500	1.599E-01	2.593E+02	8.507E-04	2.590E+00	3.231E+02	1.061E-03
1600	1.807E-01	2.756E+02	8.003E-04	2.590E+00	3.434E+02	9.978E-04
1688	2.000E-01	2.899E+02	7.607E-04	2.590E+00	3.613E+02	9.484E-04

The two *fin* files that contain momentum results are *fin84.txt* and *fin85.txt*. Here are abbreviated listings of these files.

fn84.txt

x/s	yl	uinf	del2	h12	del3
1.0491386E-03	1.631E-04	1.500E+01	2.204E-05	2.590E+00	2.707E-05
1.2356458E-03	1.770E-04	1.500E+01	2.392E-05	2.590E+00	2.942E-05
2.2758737E-03	2.404E-04	1.500E+01	3.249E-05	2.590E+00	4.012E-05
...					
2.0000000E-01	2.253E-03	1.500E+01	3.044E-04	2.590E+00	3.794E-04

fn85.txt

x/s	rex	rem	cf/2	reh	st	htc
1.0491386E-03	9.9925781E+02	2.0995E+01	1.050E-02	2.578E+01	1.313E-02	2.329E+02
1.2356458E-03	1.1768977E+03	2.2785E+01	9.678E-03	2.802E+01	1.210E-02	2.146E+02
2.2758737E-03	2.1676684E+03	3.0941E+01	7.131E-03	3.822E+01	8.914E-03	1.581E+02
...						
2.0000000E-01	1.9049110E+05	2.8995E+02	7.607E-04	3.613E+02	9.484E-04	1.682E+01

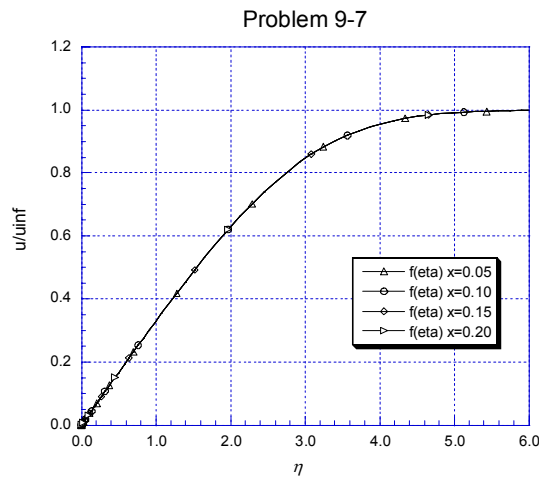
Here is the abbreviated *out.txt* with *kout=8*.

intg	rex	rem	cf2	nu	cfrat	nurat	h12	reh
5	9.993E+02	2.100E+01	1.050E-02	9.3	1.000	.995	2.590	2.578E+01
100	2.168E+03	3.094E+01	7.131E-03	13.7	1.000	.995	2.590	3.822E+01
200	5.054E+03	4.726E+01	4.667E-03	21.0	.999	.994	2.590	5.862E+01
300	9.149E+03	6.358E+01	3.469E-03	28.2	.999	.993	2.590	7.900E+01
400	1.445E+04	7.990E+01	2.760E-03	35.4	.999	.993	2.590	9.937E+01
500	2.096E+04	9.622E+01	2.292E-03	42.6	1.000	.992	2.590	1.197E+02
600	2.868E+04	1.125E+02	1.960E-03	49.9	1.000	.992	2.590	1.401E+02
700	3.761E+04	1.289E+02	1.712E-03	57.1	1.000	.992	2.590	1.605E+02
800	4.773E+04	1.452E+02	1.519E-03	64.3	1.000	.992	2.590	1.808E+02
900	5.907E+04	1.615E+02	1.366E-03	71.5	1.000	.992	2.590	2.012E+02
1000	7.162E+04	1.778E+02	1.240E-03	78.8	1.000	.992	2.590	2.215E+02
1100	8.537E+04	1.941E+02	1.136E-03	86.0	1.000	.992	2.590	2.419E+02
1200	1.003E+05	2.104E+02	1.048E-03	93.2	1.000	.992	2.590	2.622E+02
1300	1.165E+05	2.268E+02	9.727E-04	100.4	1.000	.992	2.590	2.825E+02
1400	1.339E+05	2.431E+02	9.073E-04	107.7	1.000	.992	2.590	3.029E+02
1500	1.523E+05	2.593E+02	8.507E-04	114.9	1.000	.992	2.590	3.231E+02
1600	1.721E+05	2.756E+02	8.003E-04	122.1	1.000	.992	2.590	3.434E+02
1688	1.905E+05	2.899E+02	7.607E-04	128.5	1.000	.992	2.590	3.613E+02

We can see from the various files that there is duplication, and which to choose depends on the plotting data needs. In the benchmark output (*kout=8*) we see the *cfrat* and *nurat*, which present a ratio of

TEXSTAN-calculated values for c_f and Nu to Blasius-solution values at the same x -Reynolds number, Eq. (9-13) form momentum and Eq. (10-13) for heat transfer. We can use these ratios to help determine if a data set construction is correct. At the present time only some of the “s” data sets in Appendix H can be used with $kout=8$.

To plot the developing velocity profiles, choose either $k10=10$ for nondimensional profiles (Blasius variables) or $k10=11$ for dimensional variables. The profiles will be printed as a part of the file *out.txt*. You can choose where to print the profiles by adding x locations to the $x(m)$. Be sure to change the two $nxbc$ variables and add the appropriate sets of two lines of boundary condition information for each new x -location. This is explained in detail in the *s10.man* user manual. The plot shown below confirms the Blasius similarity for the flat-plate laminar boundary layer with $u_\infty = c$.



9-8

TEXSTAN analysis of the laminar momentum boundary layer stagnation flow (the Falkner-Skan $m = 1$ case): Choose a starting x -Reynolds number of about 200 and pick fluid properties that are appropriate to air, evaluated at a free-stream temperature of 300 K. Use constant fluid properties, and note that the energy equation does not have to be solved. The geometrical dimensions of the plate are 1 m wide (a unit width) by 0.12 m long in the flow direction, corresponding to an ending Re_x of about 4×10^5 . The initial velocity profile appropriate to the starting x -Reynolds number (a Falkner-Skan $m = 1$ profile) can be supplied by using the $kstart=5$ choice in TEXSTAN. Note that the profile comes from solving Eq. (9-24). Because this is a variable free-stream-velocity flow, there are two choices within TEXSTAN: either the user provides a table of u_∞ versus x , computed from the function $u_\infty(x) \propto x^m$, or the user lets TEXSTAN supply the distribution for $m = 1$ by using the $k4=4$. With the latter choice, TEXSTAN builds the table using

$$u_\infty(x) \propto x^m = A \left(\frac{x-C}{B-C} \right)^m$$

The user will supply the values for A , B , C (called axx , bxx , and cxx in TEXSTAN), where C is a virtual origin for the flow, which for stagnation flow corresponds to $C = 0$, and A and B are linked to make sure that whatever starting x -value is chosen gives a free-stream velocity such that the starting x -Reynolds number is correct. Typically we can set $B = 1$, and then for a given choice of starting Re_x , the corresponding u_∞ value permits calculation of A .

Calculate the boundary layer flow and compare the friction coefficient results based on x -Reynolds number with the results in the text. Evaluate the concept of boundary-layer similarity by comparing nondimensional velocity profiles at several x -locations with each other. Calculate the friction coefficient distribution using momentum integral Eq. (5-8) and compare with the TEXSTAN calculations. Feel free to investigate any other attribute of the boundary-layer flow and to compare your results with other open-literature solutions.

The data file for this problem is *9.10.dat.txt*. The data set construction is based on the *s15.dat.txt* file for flow over a flat plate with variable free stream velocity and specified surface temperature (initial profiles: Falkner-Skan $m=1$ velocity and temperature). Note that *kout* has been changed to =2.

There needs to be a slight modification to the instructions in the problem statement regarding the calculations of $xstart$ and axx . For the given starting x -Reynolds number =200, there are not unique numbers for $xstart$ and axx , so choose $xstart$ (=0.00195 m) which uniquely determines the value of free stream velocity at that location (=1.615 m/s), and then calculate A (which is the variable axx) to match this velocity, $u_\infty = A \cdot xstart$ for $B=1$, $C=0$ and $m=1$.

Here is an abbreviated listing of the output file (it will be called *out.txt* when you execute TEXSTAN using *9.8.dat.txt*):

intg	x	rem	cf2	h12	reh	st
5	1.966E-03	4.169E+00	8.640E-02	2.216E+00	1.001E+01	4.920E-02
200	7.172E-03	1.523E+01	2.364E-02	2.216E+00	3.648E+01	1.349E-02
400	1.374E-02	2.916E+01	1.235E-02	2.216E+00	6.993E+01	7.040E-03
600	2.030E-02	4.305E+01	8.366E-03	2.216E+00	1.033E+02	4.768E-03
800	2.687E-02	5.698E+01	6.321E-03	2.216E+00	1.367E+02	3.602E-03
1000	3.343E-02	7.090E+01	5.080E-03	2.216E+00	1.701E+02	2.894E-03
1200	4.000E-02	8.482E+01	4.246E-03	2.216E+00	2.036E+02	2.419E-03
1400	4.657E-02	9.874E+01	3.648E-03	2.216E+00	2.370E+02	2.078E-03

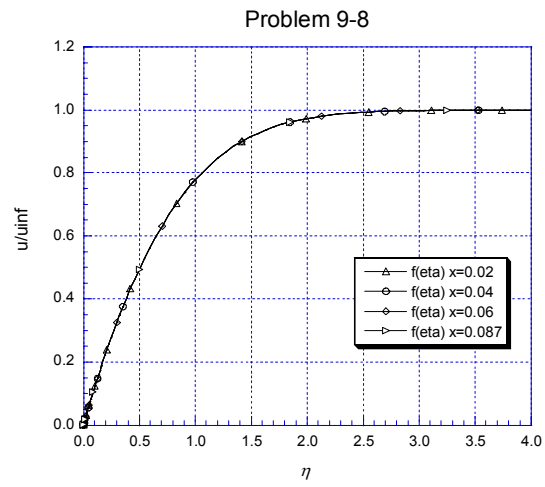
1600	5.314E-02	1.127E+02	3.197E-03	2.216E+00	2.704E+02	1.821E-03
1800	5.970E-02	1.266E+02	2.845E-03	2.216E+00	3.038E+02	1.621E-03
2000	6.627E-02	1.405E+02	2.563E-03	2.216E+00	3.373E+02	1.460E-03
2200	7.284E-02	1.544E+02	2.332E-03	2.216E+00	3.707E+02	1.329E-03
2400	7.941E-02	1.684E+02	2.139E-03	2.216E+00	4.041E+02	1.219E-03
2600	8.597E-02	1.823E+02	1.976E-03	2.216E+00	4.375E+02	1.126E-03
2638	8.721E-02	1.849E+02	1.948E-03	2.216E+00	4.438E+02	1.110E-03

Here is the abbreviated *out.txt* with *kout=8*.

intg	rex	rem	cf2	nu	cfrat	nurat	hl2	reh
5	2.034E+02	4.169E+00	8.640E-02	7.1	.999	.997	2.216	1.001E+01
200	2.705E+03	1.523E+01	2.364E-02	25.9	.997	.997	2.216	3.648E+01
400	9.936E+03	2.916E+01	1.235E-02	49.7	.998	.997	2.216	6.993E+01
600	2.166E+04	4.305E+01	8.366E-03	73.4	.999	.997	2.216	1.033E+02
800	3.796E+04	5.698E+01	6.321E-03	97.2	.999	.997	2.216	1.367E+02
1000	5.879E+04	7.090E+01	5.080E-03	121.0	.999	.997	2.216	1.701E+02
1200	8.415E+04	8.482E+01	4.246E-03	144.7	.999	.997	2.216	2.036E+02
1400	1.141E+05	9.874E+01	3.648E-03	168.5	.999	.997	2.216	2.370E+02
1600	1.485E+05	1.127E+02	3.197E-03	192.3	.999	.997	2.216	2.704E+02
1800	1.875E+05	1.266E+02	2.845E-03	216.0	.999	.997	2.216	3.038E+02
2000	2.310E+05	1.405E+02	2.563E-03	239.8	.999	.997	2.216	3.373E+02
2200	2.790E+05	1.544E+02	2.332E-03	263.6	.999	.997	2.216	3.707E+02
2400	3.316E+05	1.684E+02	2.139E-03	287.3	.999	.997	2.216	4.041E+02
2600	3.888E+05	1.823E+02	1.976E-03	311.1	.999	.997	2.216	4.375E+02
2638	4.000E+05	1.849E+02	1.948E-03	315.6	.999	.997	2.216	4.438E+02

We can see from the various files that there is duplication, and which to choose depends on the plotting data needs. In the benchmark output (*kout=8*) we see the *cfrat* and *nurat*, which present a ratio of TEXSTAN-calculated values for c_f and Nu to Falkner-Skan $m=1$ solution values at the same x -Reynolds number, Eq. (9-25) and Table 9-2 for momentum and Table 10-2 for heat transfer. We can use these ratios to help determine if a data set construction is correct. At the present time only some of the “s” data sets in Appendix H can be used with *kout=8*.

To plot the developing velocity profiles, choose either $k10=10$ for nondimensional profiles (Blasius variables) or $k10=11$ for dimensional variables. The profiles will be printed as a part of the file *out.txt*. You can choose where to print the profiles by adding x locations to the $x(m)$. Be sure to change the two *nxbc* variables and add the appropriate sets of two lines of boundary condition information for each new x -location. This is explained in detail in the *s10.man* user manual. The plot shown below confirms the Falkner-Skan similarity for the flat-plate laminar boundary layer with $u_\infty = Cx^m$. Note the much thinner boundary layer thickness.



10-1

Derive Eqs. (10-11), and (10-12) in the text. (See App. C for tables of error and gamma functions.)

This problem is the Blasius solution to the flat plate boundary layer with constant free stream velocity and constant surface temperature. The governing equation is Eq. (4-39) with T transformed into a nondimensional form,

$$u \frac{\partial \theta}{\partial x} + v \frac{\partial \theta}{\partial y} = \alpha \frac{\partial^2 \theta}{\partial y^2}$$

where the form of θ and its boundary conditions are

$$\begin{aligned}\theta &= \frac{T_s - T}{T_s - T_\infty} \\ \theta &= 0 \quad \text{at } y = 0 \\ \theta &= 1 \quad \text{at } y \rightarrow \infty \\ \theta &= 1 \quad \text{at } x = 0\end{aligned}$$

To develop the Blasius similarity solution, follow the textbook on pp. 150-151 to obtain Eq. (10-4)

$$\theta'' + \frac{\text{Pr}}{2} \zeta \theta' = 0$$

The low-Pr solution follows the development on p. 153 where Eq. (10-4) is differentiated with respect to η , which changes the ζ term into ζ' .

$$\frac{d(\theta/\theta')}{d\eta} + \frac{\text{Pr}}{2} \zeta' = 0$$

For low Pr flows the thermal boundary layer is assumed to develop much faster than the momentum boundary layer, leading to the approximation $\zeta' = u/u_\infty = 1$ and the partial differential equation simplifies. Integrating three times yields and applying boundary conditions $\theta''(0) = 0$ and $\theta(0) = 0$, gives

$$\theta = C_1 \int_0^\eta \exp\left(-\frac{\text{Pr}}{4} \eta^2\right) d\eta$$

Applying the boundary condition $\theta(\infty) = 1$ leads to

$$\theta = \frac{\int_0^\eta \exp\left(-\frac{\text{Pr}}{4} \eta^2\right) d\eta}{\int_0^\infty \exp\left(-\frac{\text{Pr}}{4} \eta^2\right) d\eta}$$

Now formulate the Nusselt number

$$\text{Nu}_x = \frac{hx}{k} = \frac{\dot{q}_s'' x}{(T_s - T_\infty)k} = \frac{-k(T_\infty - T_s) \frac{\partial \theta}{\partial y} \Big|_{y=0} x}{(T_s - T_\infty)k} = \theta'(0) \sqrt{\frac{x u_\infty}{\nu}} = \theta'(0) \text{Re}_x^{1/2}$$

and obtain $\theta'(0)$ from the $\theta(\eta)$ solution

$$\theta'(0) = \frac{1}{\int_0^\infty \exp\left(-\frac{\text{Pr}}{4}\eta^2\right) d\eta}$$

We recognize the integral as being error function, as given in Table C-4 of Appendix C, so we can transform this integral by letting $\alpha = \frac{\sqrt{\text{Pr}}}{2}\eta$, leading to

$$\begin{aligned}\theta'(0) &= \frac{\sqrt{\text{Pr}}}{2} \frac{2}{\sqrt{\pi}} \frac{1}{\text{erf}(\infty)} \\ &= 0.564 \text{Pr}^{1/2}\end{aligned}$$

and the solution becomes

$$\text{Nu}_x = 0.564 \text{Pr}^{1/2} \text{Re}_x^{1/2}$$

The procedure for developing the solution for high Pr follows that on p. 153 for an approximation to $\zeta(\eta)$. This assumption is justified because the thermal boundary layer is so much smaller than the momentum boundary layer, it resides in the region where $\zeta(\eta)$ is linear. Substituting the linear representation into Eq. (10-4) and integrating two times yields and applying boundary condition $\theta(0) = 0$, gives

$$\theta = C_1 \int_0^\eta \exp\left(-\frac{0.3321}{12} \text{Pr} \eta^3\right) d\eta$$

Applying the boundary condition $\theta(\infty) = 1$ leads to

$$\theta = \frac{\int_0^\eta \exp\left(-\frac{0.3321}{12} \text{Pr} \eta^3\right) d\eta}{\int_0^\infty \exp\left(-\frac{0.3321}{12} \text{Pr} \eta^3\right) d\eta}$$

Now formulate the Nusselt number

$$\text{Nu}_x = \frac{hx}{k} = \frac{\dot{q}_s'' x}{(T_s - T_\infty)k} = \frac{-k(T_\infty - T_s) \frac{\partial \theta}{\partial y} \Big|_{y=0} x}{(T_s - T_\infty)k} = \theta'(0) \sqrt{\frac{x u_\infty}{\nu}} = \theta'(0) \text{Re}_x^{1/2}$$

and obtain $\theta'(0)$ from the $\theta(\eta)$ solution

$$\theta'(0) = \frac{1}{\int_0^\infty \exp\left(-\frac{0.3321}{12} \text{Pr} \eta^3\right) d\eta}$$

We recognize the integral as being related to the Gamma function, as given in Table C-1 of Appendix C, so we can transform this integral by letting $C = \frac{0.3321}{4} \text{Pr}$ and $\alpha = \frac{C}{3} \eta^3$, leading to

$$\begin{aligned}\theta'(0) &= \frac{C}{\int_0^\eta \eta^{-2} \exp(-\alpha) d\alpha} = \frac{3^{2/3} \left[\left(\frac{0.3321}{4} \text{Pr} \right) \right]^{1/3}}{\Gamma\left(\frac{1}{3}\right)} = \frac{3^{2/3} \left[\left(\frac{0.3321}{4} \text{Pr} \right) \right]^{1/3}}{3\Gamma\left(\frac{4}{3}\right)} \\ &= \frac{\left[\left(\frac{0.3321}{12} \text{Pr} \right) \right]^{1/3}}{\Gamma\left(\frac{4}{3}\right)} \\ &= 0.339 \text{Pr}^{1/3}\end{aligned}$$

and the solution becomes

$$\text{Nu}_x = 0.339 \text{Pr}^{1/3} \text{Re}_x^{1/2}$$

10-2

For flow along a plate with constant free-stream velocity and constant fluid properties develop a similarity solution for a constant-temperature plate for a fluid with $Pr = 0.01$. Compare with the approximate results of Prob. 10-1. Note that numerical integration is required.

This problem is the Blasius solution to the flat plate boundary layer with constant free stream velocity and constant surface temperature. The governing equation is Eq. (4-39) with T transformed into a nondimensional form,

$$u \frac{\partial \theta}{\partial x} + v \frac{\partial \theta}{\partial y} = \alpha \frac{\partial^2 \theta}{\partial y^2}$$

where the form of θ and its boundary conditions are

$$\begin{aligned}\theta &= \frac{T_s - T}{T_s - T_\infty} \\ \theta &= 0 \quad \text{at } y = 0 \\ \theta &= 1 \quad \text{at } y \rightarrow \infty \\ \theta &= 1 \quad \text{at } x = 0\end{aligned}$$

Transform the various derivatives using the chain rule:

$$\begin{aligned}\frac{\partial(\quad)}{\partial x} &= \frac{\partial(\quad)}{\partial \xi} \frac{\partial \xi}{\partial x} + \frac{\partial(\quad)}{\partial \eta} \frac{\partial \eta}{\partial x} \\ \frac{\partial(\quad)}{\partial y} &= \frac{\partial(\quad)}{\partial \xi} \frac{\partial \xi}{\partial y} + \frac{\partial(\quad)}{\partial \eta} \frac{\partial \eta}{\partial y}\end{aligned}$$

To develop the Blasius similarity solution, follow the textbook on pp. 150-151 to obtain Eq. (10-4)

$$\theta'' + \frac{Pr}{2} \zeta \theta' = 0$$

with boundary condition s

$$\theta(0) = 0 \quad \text{and} \quad \theta(\infty) = 1$$

This equation is similar in form to the Blasius momentum equation

$$\zeta''' + \frac{1}{2} \zeta \zeta'' = 0$$

with boundary condition s

$$\zeta(0) = 0, \quad \zeta'(0) = 0, \quad \text{and} \quad \zeta'(\infty) = 1$$

There are two methods for solving this problem. The first method is to solve this set of coupled equations by traditional numerical methods such as a Runge-Kutta numerical algorithm and a “shooting technique” for the boundary-value problem ($\theta'(0)$ is unknown, just as $\zeta''(0) = 0$ would be unknown if we were solving only the momentum Blasius problem). Here is the formulation necessary for the Runge-Kutta method.

For the Blasius momentum equation

$$\begin{aligned} Y_1 &= \zeta & Y_1' &= Y_2 \\ Y_2 &= \zeta' & Y_2' &= Y_3 \\ Y_3 &= \zeta'' & Y_3' &= -\frac{1}{2}Y_1Y_3 \end{aligned}$$

along with $Y_1(0) = 0$, $Y_2(0) = 0$, and $Y_2(\infty) = 1$ specified. Note this last boundary condition has become an initial condition, which would have to be iteratively determined until $Y_2(\infty) = 1$. We will use $Y_2(0) = \zeta''(0) = 0.332$ from the Blasius momentum solution.

For the Blasius energy equation

$$\begin{aligned} Y_4 &= \theta & Y_4' &= Y_5 \\ Y_5 &= \theta' & Y_5' &= -\frac{1}{2}\text{Pr} Y_1Y_5 \end{aligned}$$

along with $Y_4(0) = 0$ and $Y_5(0) = \text{specified}$. Note this last boundary condition has become an initial condition, iteratively determined using the shooting method until $Y_4(\infty) = 1$.

This solution is a bit difficult because we need to estimate the infinite value for η . For the momentum solution, Table 9-1 shows $\eta_\infty > 5$, and from Eq. (10-27) we have an approximation that the ratio of the thermal boundary layer to momentum boundary layer can be estimated as $r = \Delta/\delta = 1/(1.026\text{Pr}^{1/3}) \approx 4.5$. So our first estimate is η_∞ (momentum) ≈ 6 and η_∞ (energy) ≈ 27 . However, we really need to use much larger infinite-state values to insure the boundary value problem is correct, and nothing is lost by using a much larger number. Using a 4th-order Runge-Kutta numerical method and $\eta_\infty \approx 50$, we find the answer that converges to $\theta'(0) = 0.052$. We formulate the Nusselt number as

$$\text{Nu}_x = \frac{hx}{k} = \frac{\dot{q}_s'' x}{(T_s - T_\infty)k} = \frac{-k(T_\infty - T_s) \frac{\partial \theta}{\partial y} \Big|_{y=0} x}{(T_s - T_\infty)k} = \theta'(0) \sqrt{\frac{x u_\infty}{\nu}} = \theta'(0) \text{Re}_x^{1/2}$$

and obtain $\theta'(0)$ from numerical solution, and the result is

$$\text{Nu}_x = 0.052 \text{Re}_x^{1/2}$$

which compares with Table 10-1 (the coefficient in the table is 0.0516 for $\text{Pr}=0.01$). This can be compared to Eq. (10-11), where $\text{Nu}_x = 0.565 \text{Pr}^{1/2} \text{Re}_x^{1/2}$ evaluated at $\text{Pr}=0.01$ gives a coefficient of 0.0565.

The second method for solution of this problem is to use the similarity analysis on p. 151, and differentiation of Eq. (10-8) leads to the expression for $\theta'(0)$

$$\theta'(0) = \frac{1}{\int_0^\infty \left[\exp\left(-\frac{\text{Pr}}{2} \int_0^\eta \zeta d\eta\right) \right] d\eta}$$

To numerically evaluate this integral, you will need to curve-fit Table 9-1 for $\zeta(\eta)$. An approximate curve fit is $\zeta(\eta) = -0.060252 + 0.16613\eta + 0.10320\eta^2$ for the range $0 \leq \eta \leq 5$. Make use of the recursion relation $\zeta(\eta) = \eta - 1.72$ for higher values of $\zeta(\eta)$. Evaluation of this expression with $\text{Pr}=0.01$ should

compare with the numerical solution $\theta'(0) = 0.052$. As with the Runge-Kutta solution we need to estimate η_∞ .

10-3

Develop an approximate solution of the energy equation for flow at a two-dimensional stagnation point for a fluid with very low Prandtl number, using the assumption that the thermal boundary layer is very much thicker than the momentum boundary layer. From this, develop an equation for heat transfer at the stagnation point of a circular cylinder in cross flow, in terms of the oncoming velocity and the diameter of the tube.

The stagnation point flow is part of the family of flows called the Falkner-Skan similarity flows where the local free stream velocity is given by the potential flow solution for inviscid flow over a wedge, $u_\infty = Cx^m$. The m parameter is depicted in Fig. 9-2, where $m = (\beta/\pi)/[2 - (\beta/\pi)]$ and for stagnation point flow, $\beta = \pi$, yielding $m=1$. Inviscid flow over a cylinder of radius R has a potential flow solution $u_\infty/V_{\text{app}} = 2\sin(x/R)$ where V_{app} is the velocity of the flow field approaching the cylinder. The first term of the Taylor-series approximation for the sine function for $(x/R) \ll 1$ is $u_\infty(x) = 2V_{\text{app}}(x/R) = Cx^1$ where $C = (2V_{\text{app}})/R = (4V_{\text{app}})/D$. Thus, the region for $-15^\circ \leq \phi \leq 15^\circ$ is the so-called stagnation point flow, where $\phi = (x/R)$.

The governing equation for momentum with the Falkner-Skan free-stream velocity distribution is given by Eq. (9-24)

$$\zeta''' + \frac{1}{2}(m+1)\zeta\zeta'' + m(1-\zeta'^2) = 0$$

with boundary conditions given by

$$\zeta(0) = 0, \quad \zeta'(0) = 0, \quad \zeta'(\infty) = 1$$

To develop a similar energy equation, the stream-function transformations Eqs. (9-9) and (9-10) are used, along with the Blasius transformation, Eq. (9-11), and using $u_\infty = Cx^m$ in all the transformations. Equation (10-2) transforms into

$$\theta'' + \frac{\text{Pr}}{2}(m+1)\zeta\theta' = 0$$

with boundary conditions given by

$$\theta(0) = 0, \quad \theta(\infty) = 1$$

Separating variables and integration of the energy equation gives a form similar to Eq. (10-8) with the added term that represents the Falkner-Skan similarity behavior,

$$\theta(\eta) = \frac{\int_0^\eta \left[\exp\left(-\frac{m+1}{2}\text{Pr} \int_0^\eta \zeta d\eta\right) \right] d\eta}{\int_0^\infty \left[\exp\left(-\frac{m+1}{2}\text{Pr} \int_0^\eta \zeta d\eta\right) \right] d\eta}$$

Now, for $\text{Pr} \ll 1$ the $\zeta'(\eta) = u/u_\infty \approx 1$ and the solution reduces to

$$\theta(\eta) = \frac{\int_0^\eta \exp\left(-\frac{m+1}{4}\text{Pr}\eta^2\right) d\eta}{\int_0^\infty \exp\left(-\frac{m+1}{4}\text{Pr}\eta^2\right) d\eta}$$

Now formulate the Nusselt number

$$\text{Nu}_x = \frac{hx}{k} = \frac{\dot{q}_s'' x}{(T_s - T_\infty)k} = \frac{-k(T_\infty - T_s) \frac{\partial \theta}{\partial y} \Big|_{y=0} x}{(T_s - T_\infty)k} = \theta'(0) \sqrt{\frac{x u_\infty}{\nu}} = \theta'(0) \text{Re}_x^{1/2}$$

and differentiate the expression for $\theta(\eta)$ to obtain the expression for $\theta'(0)$

$$\theta'(0) = \frac{1}{\int_0^\infty \exp\left(-\frac{m+1}{4} \text{Pr} \eta^2\right) d\eta}$$

We recognize the integral as being similar to an error function, as given in Table C-4 of Appendix C, so we can transform this integral by letting $\alpha = \frac{\sqrt{(m+1)\text{Pr}}}{2} \eta$, leading to

$$\begin{aligned} \theta'(0) &= \frac{\sqrt{(m+1)\text{Pr}}}{2} \frac{2}{\sqrt{\pi}} \frac{1}{\text{erf}(\infty)} \\ &= \sqrt{\frac{(m+1)}{\pi}} \text{Pr}^{1/2} \end{aligned}$$

and the solution for $m=1$ becomes

$$\begin{aligned} \text{Nu}_x &= \sqrt{\frac{(m+1)}{\pi}} \text{Pr}^{1/2} \text{Re}_x^{1/2} \\ &= 0.798 \text{Pr}^{1/2} \text{Re}_x^{1/2} \end{aligned}$$

We now need to convert the local x -Reynolds number into a cylinder Reynolds number using the approach velocity and the cylinder diameter, where $u_\infty(x) = 2V_{\text{app}}(x/R)$

$$\text{Nu}_D = 1.596 \text{Pr}^{1/2} \text{Re}_D^{1/2}$$

10-4

Repeat Prob. 10-2 for a two-dimensional stagnation point and compare with the results of Prob. 10-3. The following results from the momentum equation solution for the stagnation point are needed:

η	$\zeta(\eta)$
0	0
0.5	0.12
1.0	0.46
1.5	0.87
2.0	1.36
3.0	2.35
$\eta > 3.0$	$\zeta = \eta - 0.65$

To develop a similar energy equation, the stream-function transformations Eqs. (9-9) and (9-10) are used, along with the Blasius transformation, Eq. (9-11), and using $u_\infty = Cx^m$ in all the transformations. Equation (10-2) transforms into

$$\theta'' + \frac{\text{Pr}}{2}(m+1)\zeta\theta' = 0$$

with boundary conditions given by

$$\theta(0) = 0, \quad \theta(\infty) = 1$$

Separating variables and integration of the energy equation gives a form similar to Eq. (10-8) with the added term that represents the Falkner-Skan similarity behavior,

$$\theta(\eta) = \frac{\int_0^\eta \left[\exp\left(-\frac{m+1}{2}\text{Pr} \int_0^\eta \zeta d\eta\right) \right] d\eta}{\int_0^\infty \left[\exp\left(-\frac{m+1}{2}\text{Pr} \int_0^\eta \zeta d\eta\right) \right] d\eta}$$

The Nusselt number is formulated as

$$\text{Nu}_x = \frac{hx}{k} = \frac{\dot{q}_s'' x}{(T_s - T_\infty)k} = \frac{-k(T_\infty - T_s) \frac{\partial \theta}{\partial y} \Big|_{y=0} x}{(T_s - T_\infty)k} = \theta'(0) \sqrt{\frac{xu_\infty}{\nu}} = \theta'(0) \text{Re}_x^{1/2}$$

and differentiate the expression for $\theta(\eta)$ to obtain the expression for $\theta'(0)$

$$\theta'(0) = \frac{1}{\int_0^\infty \left[\exp\left(-\frac{m+1}{2}\text{Pr} \int_0^\eta \zeta d\eta\right) \right] d\eta}$$

To numerically evaluate this integral, we use the $\zeta(\eta)$ table that accompanies the problem statement. An approximate curve fit is $\zeta(\eta) = -0.00045 + 0.40686\eta + 0.13381\eta^2$ for the range $0 \leq \eta \leq 3$. Make use of the recursion relation $\zeta(\eta) = \eta - 0.65$ for higher values of $\zeta(\eta)$. Evaluation of this expression with $\text{Pr}=0.01$ should compare with the numerical solution $\theta'(0) = 0.052$. This solution is a bit difficult because we need to estimate the infinite value for η . For the momentum solution, Table 9-1 is for $m=0$, and it shows $\eta_\infty > 5$, and from Eq. (10-27) we have an approximation that the ratio of the thermal boundary

layer to momentum boundary layer can be estimated as $r = \Delta/\delta = 1/(1.026\text{Pr}^{1/3}) \approx 4.5$. We also know that for $m>0$, infinite value for η decreases for momentum. If we use a conservative estimate for η_∞ (momentum) ≈ 4 then η_∞ (energy) ≈ 20 . Using a 4th-order Runge-Kutta numerical method, we find $\theta'(0) = 0.077$ for $\text{Pr}=0.01$. If we continue to increase η_∞ we get a slightly lower answer that converges to 0.076 when η_∞ (energy) ≈ 30 and the solution for $m=1$ becomes

$$\text{Nu}_x = 0.76\text{Pr}^{1/2} \text{Re}_x^{1/2}$$

We now need to convert the local x -Reynolds number into a cylinder Reynolds number using the approach velocity and the cylinder diameter, where $u_\infty(x) = 2V_{\text{app}}(x/R)$

$$\text{Nu}_D = 1.52\text{Pr}^{1/2} \text{Re}_D^{1/2}$$

Comparison of this stagnation-point similarity solution for $\text{Pr}=0.01$ with the approximate solution in problem 10-3 shows an agreement within 5%.

10-5

Consider constant-property flow along a surface with constant free-stream velocity. Let the temperature difference between the surface and the fluid, $T_s - T_\infty$, vary as x^m , where m is a constant. Show that a similarity solution to the energy equation is obtainable under these conditions. Carry out the necessary calculations to obtain the Nusselt number as a function of Reynolds number for $Pr = 0.7$ and $m = 1$.

This problem is a Blasius type solution to the flat plate boundary layer with constant free stream velocity and variable surface temperature. The governing equation is Eq. (4-39)

$$u \frac{\partial T}{\partial x} + v \frac{\partial T}{\partial y} = \alpha \frac{\partial^2 T}{\partial y^2}$$

with boundary conditions

$$\begin{aligned} T(0, y) &= T_\infty \\ T(x, 0) &= T_s \\ T(x, \infty) &= T_\infty \end{aligned}$$

Introduce this nondimensional temperature

$$\tau = \frac{T - T_\infty}{T_s - T_\infty} = \frac{T - T_\infty}{\phi(x)} = \frac{T - T_\infty}{Cx^m}$$

and the governing equation becomes

$$u \left(\frac{\partial \tau}{\partial x} + \frac{m}{x} \tau \right) + v \frac{\partial \tau}{\partial y} = \alpha \frac{\partial^2 \tau}{\partial y^2}$$

with boundary conditions

$$\begin{aligned} \tau(0, y) &= 0 \\ \tau(x, 0) &= 1 \\ \tau(x, \infty) &= 0 \end{aligned}$$

Now introduce the momentum transformation variables, Eqns. (9-9) and (9-10)

$$u = \frac{\partial \psi}{\partial y} \quad v = -\frac{\partial \psi}{\partial x} \quad \psi = \sqrt{\nu x u_\infty} \zeta$$

and the governing equation becomes

$$\left(\frac{\partial \psi}{\partial y} \right) \left(\frac{\partial \tau}{\partial x} + \frac{m}{x} \tau \right) - \left(\frac{\partial \psi}{\partial x} \right) \frac{\partial \tau}{\partial y} = \alpha \frac{\partial^2 \tau}{\partial y^2}$$

Transform the various derivatives using the chain rule:

$$\frac{\partial(\quad)}{\partial x} = \frac{\partial(\quad)}{\partial \xi} \frac{\partial \xi}{\partial x} + \frac{\partial(\quad)}{\partial \eta} \frac{\partial \eta}{\partial x}$$

$$\frac{\partial(\quad)}{\partial y} = \frac{\partial(\quad)}{\partial \xi} \frac{\partial \xi}{\partial y} + \frac{\partial(\quad)}{\partial \eta} \frac{\partial \eta}{\partial y}$$

where the Blasius variables (see Eq. 9-11) are

$$\xi = x \quad \eta = \frac{y}{\sqrt{\nu x / u_\infty}}$$

Thus

$$\frac{\partial(\psi)}{\partial y} = \frac{\partial(\psi)}{\partial \xi} \frac{\partial \xi}{\partial y} + \sqrt{\nu x u_\infty} \zeta' \left(\frac{1}{\sqrt{\nu x / u_\infty}} \right) = u_\infty \zeta'$$

$$\frac{\partial(\psi)}{\partial x} = \frac{\partial(\psi)}{\partial \xi} \frac{\partial \xi}{\partial x} + \frac{\partial(\psi)}{\partial \eta} \frac{\partial \eta}{\partial x} = \frac{1}{2} \sqrt{\frac{\nu u_\infty}{x}} \zeta + \frac{1}{2} \sqrt{\frac{\nu u_\infty}{x}} \zeta' \eta = \frac{1}{2} \sqrt{\frac{\nu u_\infty}{x}} (\zeta + \zeta' \eta)$$

$$\frac{\partial(\tau)}{\partial x} = \frac{\partial(\tau)}{\partial \xi} \frac{\partial \xi}{\partial x} + \frac{\partial(\tau)}{\partial \eta} \frac{\partial \eta}{\partial x} = \frac{m}{x} \tau + \tau' \left(-\frac{1}{2} \frac{y}{\sqrt{\nu x^3 / u_\infty}} \right)$$

$$\frac{\partial(\tau)}{\partial y} = \frac{\partial(\tau)}{\partial \xi} \frac{\partial \xi}{\partial y} + \frac{\partial(\tau)}{\partial \eta} \frac{\partial \eta}{\partial y} = \tau' \left(\frac{1}{\sqrt{\nu x / u_\infty}} \right)$$

$$\frac{\partial}{\partial y} \left(\frac{\partial \tau}{\partial y} \right) = \frac{\partial}{\partial \xi} \left(\frac{\partial \tau}{\partial y} \right) \frac{\partial \xi}{\partial y} + \frac{\partial}{\partial \eta} \left(\frac{\partial \tau}{\partial y} \right) \frac{\partial \eta}{\partial y} = \tau'' \left(\frac{1}{\sqrt{\nu x / u_\infty}} \right)$$

Now, assemble all the terms and the result is

$$\tau'' + \frac{\text{Pr}}{2} \zeta \tau' = m \text{Pr} \zeta' \tau = 0$$

and the boundary conditions (it is customary to use x in place of ξ)

$$\tau(0, \eta) = 0$$

$$\tau(x, 0) = 1$$

$$\tau(x, \infty) = 0$$

To solve this set of coupled equations by traditional numerical methods such as a Runge-Kutta numerical algorithm and a “shooting technique” for the boundary-value problem ($\theta'(0)$ is unknown, just as $\zeta''(0) = 0$ would be unknown if we were solving only the momentum Blasius problem). Here is the formulation necessary for the Runge-Kutta method.

For the Blasius momentum equation

$$\begin{aligned} Y_1 &= \zeta & Y_1' &= Y_2 \\ Y_2 &= \zeta' & Y_2' &= Y_3 \\ Y_3 &= \zeta'' & Y_3' &= -\frac{1}{2}Y_1Y_3 \end{aligned}$$

along with $Y_1(0) = 0$, $Y_2(0) = 0$, and $Y_2(\infty) = 1$ specified. Note this last boundary condition has become an initial condition, which would have to be iteratively determined until $Y_2(\infty) = 1$. We will use $Y_2(0) = \zeta''(0) = 0.332$ from the Blasius momentum solution.

For the Blasius energy equation

$$\begin{aligned} Y_4 &= \tau & Y_4' &= Y_5 \\ Y_5 &= \tau' & Y_5' &= -\frac{1}{2}\text{Pr}Y_1Y_5 + m\text{Pr}Y_2Y_4 \end{aligned}$$

along with $Y_4(0) = 0$ and $Y_5(0) = \text{specified}$. Note this last boundary condition has become an initial condition, iteratively determined using the shooting method until $Y_4(\infty) = 1$.

This solution is a bit difficult because we need to estimate the infinite value for η . For the momentum solution, Table 9-1 shows $\eta_\infty > 5$, and from Eq. (10-27) we have an approximation that the ratio of the thermal boundary layer to momentum boundary layer can be estimated as $r = \Delta/\delta = 1/(1.026\text{Pr}^{1/3}) \approx 1.1$. So our first estimate is $\eta_\infty(\text{momentum}) \approx 6$ and $\eta_\infty(\text{energy}) \approx 8$. However, we really need to use much larger infinite-state values to insure the boundary value problem is correct, and nothing is lost by using a much larger number. Using a 4th-order Runge-Kutta numerical method and $\eta_\infty \approx 50$, we find the answer for $\text{Pr}=0.01$ and $m=1$ converges to $\tau'(0) = 0.48$. We formulate the Nusselt number as

$$\text{Nu}_x = \frac{hx}{k} = \frac{\dot{q}_s''x}{(T_s - T_\infty)k} = \frac{-k(T_\infty - T_s)\frac{\partial\theta}{\partial y}\big|_{y=0}}{(T_s - T_\infty)k} = \theta'(0)\sqrt{\frac{xu_\infty}{\nu}} = \theta'(0)\text{Re}_x^{1/2}$$

and obtain $\tau'(0)$ from numerical solution, and the result for $\text{Pr}=0.7$ and $m=1$ is

$$\text{Nu}_x = 0.48\text{Re}_x^{1/2}$$

A solution can be found in NACA TN3151 and TN3588 by Livingood and Donoughe.

10-6

Using the approximate solution developed in the text for a laminar boundary layer with constant free-stream velocity and a simple step in surface temperature at some arbitrary point, develop a solution for $\text{Pr} = 0.7$ and $T_s - T_\infty$ varying directly with x , using superposition theory. Compare with the exact result from Prob. 10-5.

The solution procedure is to evaluate the surface heat flux for the given surface temperature distribution and then formulate the Nusselt number. Combine Eqs. (10-31) and (10-32) to give

$$\dot{q}_s'' = \int_0^x \left\{ \frac{0.332k}{x} \text{Pr}^{1/3} \text{Re}_x^{1/2} \left[1 - \left(\frac{\xi}{x} \right)^{3/4} \right]^{-1/3} \right\} \frac{dT_s}{d\xi} d\xi + \sum_{i=1}^k h(\xi_i, x) \Delta T_{s,i}$$

For the given $(T_s - T_\infty) = Cx^m$ and $m=1$, $dT_s/d\xi = C$, and the surface heat flux becomes

$$\begin{aligned} \dot{q}_s'' &= \frac{0.332k}{x} \text{CPr}^{1/3} \text{Re}_x^{1/2} \int_0^x \left[1 - \left(\frac{\xi}{x} \right)^{3/4} \right]^{-1/3} d\xi \\ &= \frac{0.332k}{x} \text{CPr}^{1/3} \text{Re}_x^{1/2} I(\xi; x) \end{aligned}$$

Transform the integrand by letting

$$\begin{aligned} u &= 1 - \left(\frac{\xi}{x} \right)^{3/4} \\ \xi &= x(1-u)^{4/3} \quad d\xi = -\frac{4}{3}x(1-u)^{1/3} du \end{aligned}$$

and the integral becomes

$$I(\xi; x) = -\frac{4x}{3} \int_{u_1}^{u_2} u^{-1/3} (1-u)^{1/3} du = -\frac{4x}{3} \int_1^0 u^{-1/3} (1-u)^{1/3} du = \frac{4x}{3} \int_0^1 u^{-1/3} (1-u)^{1/3} du$$

If instead we use the transformation

$$\begin{aligned} u &= \left(\frac{\xi}{x} \right)^{3/4} \\ \xi &= xu^{4/3} \quad d\xi = \frac{4}{3}xu^{1/3} du \end{aligned}$$

the integral becomes

$$I(\xi; x) = \frac{4x}{3} \int_{u_1}^{u_2} u^{1/3} (1-u)^{-1/3} du = \frac{4x}{3} \int_0^1 u^{1/3} (1-u)^{-1/3} du$$

From Appendix C,

$$\int_0^1 u^{(m-1)} (1-u)^{(n-1)} du = \beta(m, n) = \frac{\Gamma(m)\Gamma(n)}{\Gamma(m+n)} = \beta(n, m)$$

Thus, the Beta function is symmetrical. With the first transformation, $m=2/3$ and $n=4/3$, and with the second transformation they are reversed, $n=2/3$ and $m=4/3$. In either case

$$I(\xi; x) = \frac{4}{3} x \frac{\Gamma\left(\frac{2}{3}\right)\Gamma\left(\frac{4}{3}\right)}{\Gamma(2)} = \frac{4}{3} x \frac{\left(\frac{1}{2/3}\right)\Gamma\left(\frac{5}{3}\right)\Gamma\left(\frac{4}{3}\right)}{\Gamma(2)} = \frac{4}{3} x \frac{(1.353)(0.893)}{(1)} = 1.611x$$

and the surface heat flux becomes

$$\dot{q}_s'' = \frac{0.332k}{x} \text{CPr}^{1/3} \text{Re}_x^{1/2} (1.611x) = 0.535Ck\text{Pr}^{1/3} \text{Re}_x^{1/2}$$

Now formulate the Nusselt number

$$\begin{aligned} \text{Nu}_x &= \frac{hx}{k} = \frac{\dot{q}_s'' x}{(T_s - T_\infty)k} = \frac{0.535Ck\text{Pr}^{1/3} \text{Re}_x^{1/2}}{(Cx)k} \\ &= 0.535\text{Pr}^{1/3} \text{Re}_x^{1/2} \end{aligned}$$

For $\text{Pr}=0.7$, $\text{Nu}_x = 0.475 \text{Re}_x^{1/2}$, which compares with the similarity solution $\text{Nu}_x = 0.48 \text{Re}_x^{1/2}$.

10-7

Consider liquid sodium at 200°C flowing normal to a 2.5-cm-diameter tube at a velocity of 0.6 m/s. Using the results of Prob. 10-3, calculate the “conduction” thickness of the thermal boundary layer at the stagnation point. Calculate the corresponding “shear” thickness of the momentum boundary layer at the stagnation point and discuss the significance of the results.

The analysis in Prob. 10-3 was for $Pr \ll 1$ and the similarity solution required $\zeta'(\eta) = u/u_\infty \approx 1$. For this approximation, the similarity solution becomes (for $m=1$) became

$$\begin{aligned} Nu_x &= \sqrt{\frac{(m+1)}{\pi}} Pr^{1/2} Re_x^{1/2} \\ &= 0.798 Pr^{1/2} Re_x^{1/2} \end{aligned}$$

which, converted from the local x -Reynolds number into a cylinder Reynolds number using the approach velocity and the cylinder diameter, where $u_\infty(x) = 2V_{app}(x/R)$, was

$$Nu_D = 1.596 Pr^{1/2} Re_D^{1/2}$$

The conduction thickness is defined for use with Eq. (10-45)

$$\Delta_4 = \frac{k}{h} = \frac{D}{Nu_D} = \frac{D}{1.596 Pr^{1/2} Re_D^{1/2}}$$

For this problem, $Re_D=30,200$ based on properties of Na at 200°C, and for $Pr=0.0074$, $\Delta_4 = 1.05E-03$ m.

For the shear thickness, combine Eq. (9-12) for the friction coefficient with Eq. (9-36) for the shear thickness, and substitute Eq. (9-25) for the Falkner-Skan wedge-flow formulation of the friction coefficient,

$$\delta_4 = \frac{\mu u_\infty}{\tau_s} = \frac{\mu}{\rho u_\infty} \frac{1}{(c_f/2)} = \frac{\nu}{u_\infty} \frac{Re_x^{1/2}}{\zeta''(0)}$$

and for the stagnation point of a cylinder, $u_\infty(x) = 2V_{app}(x/R)$

$$\frac{\delta_4}{D} = \left(\frac{1}{2\zeta''(0)} \right) Re_D^{-1/2}$$

from which $\delta_4 = 5.84E-05$ m. Thus, we find $\delta_4 \ll \Delta_4$ for $Pr \ll 1$ and this further supports our assumption that the momentum boundary layer can be approximated by the free stream velocity at that location, $\zeta' = u/u_\infty = 1$.

10-8

Let air at 540°C and 1 atm pressure flow at a velocity of 6 m/s normal to a 2.5-cm-diameter cylinder. Let the cylinder be of a thin-walled porous material so that air can be pumped inside the cylinder and out through the pores in order to cool the walls. Let the cooling air be at 40°C where it actually enters the porous material. The objective of the problem is to calculate the cylinder surface temperature in the region of the stagnation point for various cooling-air flow rates, expressed as the mass rate of cooling air per square meter of cylinder surface. The problem is to be worked first for no radiation and then assuming that the cylinder surface is a black body radiating to a large surrounding (say a large duct) at 540°C. The same cooling air could be used to cool the surface internally by convection without passing through the surface out into the main stream. Assuming that the cooling air is again available at 40°C and is ducted away from the surface at surface temperature, calculate the surface temperature as a function of cooling-air rate per square meter of cylinder surface area for this case and compare with the results above.

The first task is to perform an energy balance on a unit of surface area in the stagnation region. Let T_s be the wall, T_i be the injection or internal coolant temperature.

Case I: Blowing, no radiation effect,

$$\dot{m}_s'' c (T_s - T_i) - h (T_\infty - T_s) = 0$$

Case II: Blowing plus surface radiation for large surroundings,

$$\dot{m}_s'' c (T_s - T_i) - \sigma (T_\infty^4 - T_s^4) - h (T_\infty - T_s) = 0$$

Case III: Internal convective cooling,

$$\dot{m}_s'' c (T_s - T_i) - h (T_\infty - T_s) = 0$$

For all cases and $\dot{m}_s'' = 0$, the Nusselt number will be that for a circular cylinder, Eq. (10-22)

$$\text{Nu}_R = 0.81 \text{Re}_R^{1/2} \text{Pr}^{0.4} = 0.573 \text{Re}_D^{1/2} \text{Pr}^{0.4}$$

For Case I and Case II and $\dot{m}_s'' > 0$, the Nusselt number will come from Table 10-4 with $m=1$ for the 2-dimensional stagnation point (the stagnation region of the circular cylinder) and $u_\infty(x) = 2V_{\text{app}}(x/R) = Cx$ where $C = 4V_{\text{app}}/D$. In Table 10-4 the blowing parameter for $m=1$ converts to

$$\frac{v_s}{u_\infty} \text{Re}_x^{1/2} \left(\frac{2}{m+1} \right)^{1/2} = \frac{\dot{m}_s''}{\rho_\infty u_\infty} \text{Re}_x^{1/2} \left(\frac{2}{m+1} \right)^{1/2} = \frac{\dot{m}_s''}{\rho_\infty \sqrt{Cv}}$$

and

$$\text{Nu}_x \text{Re}_x^{-1/2} = \frac{h}{k} \sqrt{\frac{v}{C}}$$

For Case III, \dot{m}_s'' varies while h is a constant . Carry out calculations for $0 \leq \dot{m}_s'' \leq 0.13 \text{ kg}/(\text{m}^2)$.

The results have been generated with all properties of air evaluated at 800K:

\dot{m}_s'' kg/(m ² ·s)	h W/(m ² ·K)	$T_s(\text{I})$ K	$T_s(\text{II})$ K	$T_s(\text{III})$ K
0	96.5	813	813	813
0.0644	57.0	536	650	602
0.129	28.3	396	518	516

10-9

Let air at a constant velocity of 7.6 m/s, a temperature of 90°C, and 1 atm pressure flow along a smooth, flat surface. Let the plate be divided into three sections, each 10 cm in flow length. The first 10 cm section is maintained at 40°C, the second at 80°C, and the third at 40°C. Evaluate and plot the heat flux at all points along the 30 cm of plate length, and find the local heat-transfer coefficient. TEXSTAN can be used to confirm the results of this variable surface-temperature problem. Choose a starting x -location near the leading edge, say 0.1 cm, and pick fluid properties that are appropriate to air, evaluated at the free stream temperature. Use constant fluid properties and do not consider viscous dissipation. The piecewise surface temperature boundary condition is modeled easily in TEXSTAN by providing temperatures at two x locations for each segment, e.g., at $x = 0$, $x = 0.10$, $x = 0.101$, $x = 0.2$, $x = 0.201$, and $x = 0.3$ m. Because TEXSTAN linearly interpolates the surface thermal boundary condition between consecutive x locations, a total of six boundary condition locations is sufficient to describe the surface temperature variation. The initial velocity and temperature profiles (Blasius similarity profiles) can be supplied by using the $kstart=4$ choice in TEXSTAN.

The solution procedure is to evaluate the surface heat flux for the given surface temperature distribution and then formulate the Nusselt number. Combine Eqs. (10-31) and (10-32) to give

$$\dot{q}_s'' = \int_0^x h(\xi_i, x) \frac{dT_s}{d\xi} d\xi + \sum_{i=1}^k \left\{ \frac{0.332k}{x} \text{Pr}^{1/3} \text{Re}_x^{1/2} \left[1 - \left(\frac{\xi_i}{x} \right)^{3/4} \right]^{-1/3} \right\} \Delta T_{s,i}$$

For this problem, there are 3 piecewise-continuous wall temperature changes,

$$\dot{q}_s'' = \frac{0.332k}{x} \text{Pr}^{1/3} \text{Re}_x^{1/2} \sum_{i=1}^3 \left[1 - \left(\frac{\xi_i}{x} \right)^{3/4} \right]^{-1/3} \Delta T_{s,i}$$

where

$$\begin{aligned} \Delta T_{s,1} &= (T_{s,1} - T_\infty) = -50^\circ\text{C} \quad \text{and} \quad \xi_1 = 0 \\ \Delta T_{s,2} &= (T_{s,2} - T_{s,1}) = +40^\circ\text{C} \quad \text{and} \quad \xi_2 = 0.1 \text{ m} \\ \Delta T_{s,3} &= (T_{s,3} - T_{s,2}) = -40^\circ\text{C} \quad \text{and} \quad \xi_3 = 0.2 \text{ m} \end{aligned}$$

For the first segment, $0 \leq x \leq 0.1$ m

$$\begin{aligned} \dot{q}_s''(x) &= \frac{0.332k}{x} \text{Pr}^{1/3} \text{Re}_x^{1/2} \Delta T_{s,1} \\ h(x) &= \frac{\dot{q}_s''(x)}{(T_{s,1} - T_\infty)} \end{aligned}$$

For the second segment, $0.1 \text{ m} < x \leq 0.2$ m

$$\begin{aligned} \dot{q}_s''(x) &= \frac{0.332k}{x} \text{Pr}^{1/3} \text{Re}_x^{1/2} \left\{ \Delta T_{s,1} + \left[1 - \left(\frac{\xi_2}{x} \right)^{3/4} \right]^{-1/3} \Delta T_{s,2} \right\} \\ h(x) &= \frac{\dot{q}_s''(x)}{(T_{s,2} - T_\infty)} \end{aligned}$$

And for the third segment, $0.2\text{ m} < x \leq 0.3\text{ m}$

$$\dot{q}_s''(x) = \frac{0.332k}{x} \text{Pr}^{1/3} \text{Re}_x^{1/2} \left\{ \Delta T_{s,1} + \left[1 - \left(\frac{\xi_2}{x} \right)^{3/4} \right]^{-1/3} \Delta T_{s,2} + \left[1 - \left(\frac{\xi_3}{x} \right)^{3/4} \right]^{-1/3} \Delta T_{s,3} \right\}$$

$$h(x) = \frac{\dot{q}_s''(x)}{(T_{s,3} - T_\infty)}$$

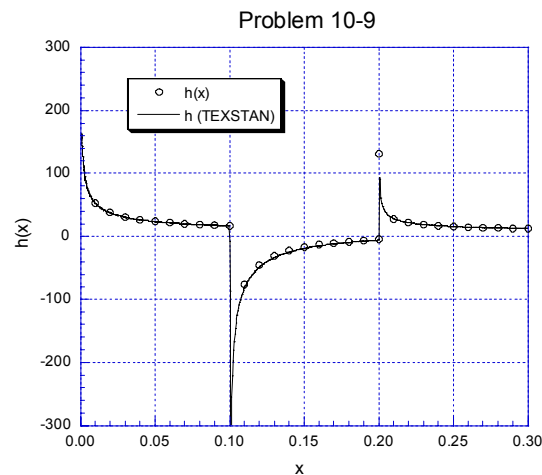
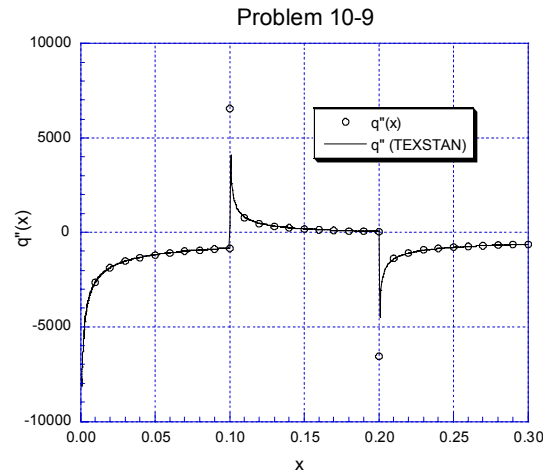
The TEXSTAN data file for this problem is *10.9.dat.txt*. The data set construction is based on the *s10.dat.txt* file for flow over a flat plate with constant free stream velocity and specified surface temperature (initial profiles: Blasius velocity and Blasius temperature). Note that *kout* has been changed to =2.

Here is an abbreviated listing of the file *fm86.txt* which contains surface heat flux and heat transfer coefficient distributions. Note the stepsize in the input data file was reduced to *deltax*=0.05 to help resolve the thermal boundary layer behavior after the step-temperature changes.

intg	x/s	htc	qflux	ts	tinf
5	1.0545108E-03	1.6303E+02	-8.1517E+03	3.1300E+02	3.6300E+02
100	2.1247649E-03	1.1485E+02	-5.7424E+03	3.1300E+02	3.6300E+02
200	4.4815527E-03	7.9004E+01	-3.9502E+03	3.1300E+02	3.6300E+02
300	7.7104196E-03	6.0194E+01	-3.0097E+03	3.1300E+02	3.6300E+02
400	1.1811678E-02	4.8614E+01	-2.4307E+03	3.1300E+02	3.6300E+02
500	1.6785027E-02	4.0771E+01	-2.0385E+03	3.1300E+02	3.6300E+02
600	2.2630397E-02	3.5107E+01	-1.7553E+03	3.1300E+02	3.6300E+02
700	2.9347767E-02	3.0825E+01	-1.5412E+03	3.1300E+02	3.6300E+02
800	3.6937127E-02	2.7474E+01	-1.3737E+03	3.1300E+02	3.6300E+02
900	4.5398475E-02	2.4780E+01	-1.2390E+03	3.1300E+02	3.6300E+02
1000	5.4731807E-02	2.2567E+01	-1.1284E+03	3.1300E+02	3.6300E+02
1100	6.4937123E-02	2.0718E+01	-1.0359E+03	3.1300E+02	3.6300E+02
1200	7.6014422E-02	1.9148E+01	-9.5741E+02	3.1300E+02	3.6300E+02
1300	8.7963703E-02	1.7800E+01	-8.8999E+02	3.1300E+02	3.6300E+02
1400	1.0079390E-01	-1.9641E+02	3.5832E+03	3.4476E+02	3.6300E+02
1500	1.1442299E-01	-6.3292E+01	6.3292E+02	3.5300E+02	3.6300E+02
1600	1.2897423E-01	-3.4873E+01	3.4873E+02	3.5300E+02	3.6300E+02
1700	1.4440159E-01	-2.2033E+01	2.2033E+02	3.5300E+02	3.6300E+02
1800	1.6070594E-01	-1.4607E+01	1.4607E+02	3.5300E+02	3.6300E+02
1900	1.7788490E-01	-9.8016E+00	9.8016E+01	3.5300E+02	3.6300E+02
2000	1.9593702E-01	-6.4844E+00	6.4844E+01	3.5300E+02	3.6300E+02
2100	2.1470582E-01	2.4559E+01	-1.2280E+03	3.1300E+02	3.6300E+02
2200	2.3447915E-01	1.8128E+01	-9.0642E+02	3.1300E+02	3.6300E+02

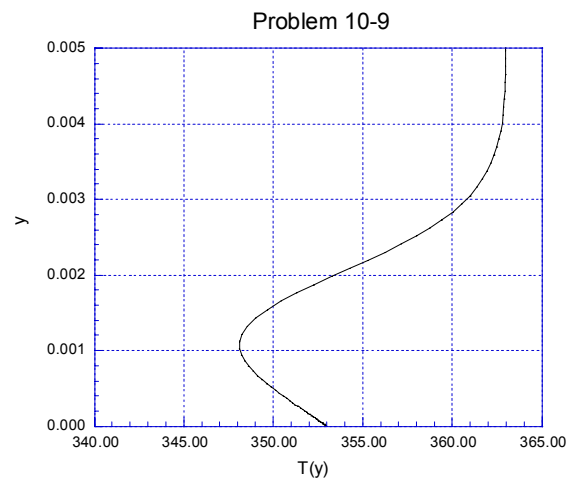
2300	2.5513199E-01	1.5378E+01	-7.6891E+02	3.1300E+02	3.6300E+02
2400	2.7666042E-01	1.3706E+01	-6.8528E+02	3.1300E+02	3.6300E+02
2500	2.9906192E-01	1.2527E+01	-6.2635E+02	3.1300E+02	3.6300E+02
2504	3.0000000E-01	1.2485E+01	-6.2427E+02	3.1300E+02	3.6300E+02

The following plots compare TEXSTAN's predictions of surface heat flux and heat transfer coefficient with the analysis



If you plot the temperature profiles in the region $0.1 \leq x \leq 0.2$ (or) $0.2 \leq x \leq 0.3$ you can see the effect of the change in surface temperature and how, in effect, there is a new thermal boundary layer that begins to grow from the step-change. To plot the profiles, you will need to add several $x(m)$ points to the file *10.9.dat.txt* and then reset the flag $k10=11$ to obtain dimensional profiles of velocity and temperature at each $x(m)$ location. You will observe the inflection in the profile near the wall, and the corresponding negative surface temperature gradient which gives a positive heat flux (Fourier's law) but $(T_s - T_\infty) < 0$,

which leads to a negative heat transfer coefficient. If the surface temperature were not changing, the thermal boundary layer near the wall will eventually grow outward and the heat flux will become negative.



10-10

Repeat Prob. 10-9 but let the surface temperature vary sinusoidally from 40°C at the leading and trailing edges to 80°C at the centerline. TEXSTAN can be used to confirm the results of this variable surface-temperature problem. For the surface temperature distribution, break up the length of the plate into 10 to 20 segments and evaluate the surface temperature at these x locations. These values then become the variable surface temperature boundary condition. Note that a larger number of points will more closely model the sine function.

The solution analysis involves evaluation of the surface heat flux for the given surface temperature distribution and then formulate the Nusselt number. Combine Eqs. (10-31) and (10-32) to give

$$\dot{q}_s'' = \int_0^x \left\{ \frac{0.332k}{x} \text{Pr}^{1/3} \text{Re}_x^{1/2} \left[1 - \left(\frac{\xi}{x} \right)^{3/4} \right]^{-1/3} \right\} \frac{dT_s}{d\xi} d\xi + \sum_{i=1}^k \left\{ \frac{0.332k}{x} \text{Pr}^{1/3} \text{Re}_x^{1/2} \left[1 - \left(\frac{\xi_i}{x} \right)^{3/4} \right]^{-1/3} \right\} \Delta T_{s,i}$$

This problem starts with a discontinuous step, where

$$\Delta T_{s,1} = (T_{s,1} - T_\infty) = (40^\circ\text{C} - 90^\circ\text{C}) = -50^\circ\text{C} \quad \text{and} \quad \xi_1 = 0$$

followed by a continuously varying surface temperature

$$(T_s - T_\infty) = (T_{s,x=0} - T_\infty) + (T_{s,x=L/2} - T_{s,x=0}) \sin(\pi x/L) = \Delta T_{s,1} + \Delta T_{\max} \sin(\pi x/L)$$

$$\frac{dT_s}{dx} = \frac{dT_s}{d\xi} = \Delta T_{\max} \frac{\pi}{L} \cos(\pi \xi/L)$$

where for this problem $\Delta T_{\max} = 40^\circ\text{C}$, and the expression for the surface heat flux becomes

$$\begin{aligned} \dot{q}_s'' &= \frac{0.332k}{x} \text{Pr}^{1/3} \text{Re}_x^{1/2} \left\{ \Delta T_{\max} \frac{\pi}{L} \int_0^x \left[1 - \left(\frac{\xi}{x} \right)^{3/4} \right]^{-1/3} \cos\left(\frac{\pi \xi}{L}\right) d\xi + \Delta T_{s,1} \right\} \\ &= \frac{0.332k}{x} \text{Pr}^{1/3} \text{Re}_x^{1/2} \left\{ \Delta T_{\max} \frac{\pi}{L} I(\xi; x) + \Delta T_{s,1} \right\} \end{aligned}$$

The integral in the heat flux can be evaluated either analytically or numerically. For the analytical approach, convert the integral using the ideas of Appendix C and a Taylor-series approximation for the cosine function.

$$I(\xi; x) = \int_0^x \left[1 - \left(\frac{\xi}{x} \right)^{3/4} \right]^{-1/3} \cos\left(\frac{\pi \xi}{L}\right) d\xi$$

Transform the step-function kernel part of the integrand by letting

$$\begin{aligned} u &= \left(\frac{\xi}{x} \right)^{3/4} \\ \xi &= xu^{4/3} \\ d\xi &= \frac{4}{3} xu^{1/3} du \end{aligned}$$

and the integral becomes

$$I(\xi; x) = \frac{4x}{3} \int_0^1 u^{1/3} [1-u]^{-1/3} \cos\left(\frac{\pi x}{L} u^{4/3}\right) du$$

From Appendix C,

$$\int_0^1 u^{(m-1)} (1-u)^{(n-1)} du = \beta(m, n) = \frac{\Gamma(m)\Gamma(n)}{\Gamma(m+n)} = \beta(n, m)$$

Note, we could have also used the transformation $u = 1 - \left(\frac{\xi}{x}\right)^{3/4}$ and we would have arrived at the same formulation because the Beta function is symmetrical. Now, for the cosine function

$$\begin{aligned} \cos(y) &= 1 - \frac{y^2}{2!} + \frac{y^4}{4!} - \frac{y^6}{6!} + \dots (-1)^k \frac{y^{2k}}{(2k)!} \\ \cos\left(\frac{\pi x}{L} u^{4/3}\right) &= 1 - \frac{\left(\frac{\pi x}{L}\right)^2 u^{8/3}}{2!} + \frac{\left(\frac{\pi x}{L}\right)^4 u^{16/3}}{4!} + \dots (-1)^k \frac{\left(\frac{\pi x}{L} u^{4/3}\right)^{2k}}{(2k)!} \\ &= \sum_{k=0}^{\infty} \frac{(-1)^k \left(\frac{\pi x}{L}\right)^{2k}}{(2k)!} u^{8k/3} \end{aligned}$$

And the integral becomes

$$I(\xi; x) = \frac{4x}{3} \left\{ \sum_{k=0}^{\infty} \frac{(-1)^k \left(\frac{\pi x}{L}\right)^{2k}}{(2k)!} \int_0^1 u^{(1+8k)/3} [1-u]^{-1/3} d\xi \right\}$$

Comparing to the form of the Beta function,

$$\begin{aligned} m &= \frac{4}{3}(1+2k) \\ n &= \frac{2}{3} \end{aligned}$$

and the integral reduces to

$$\begin{aligned} I(\xi; x) &= \frac{4x}{3} \left\{ \sum_{k=0}^{\infty} \frac{(-1)^k \left(\frac{\pi x}{L}\right)^{2k}}{(2k)!} \beta\left(\frac{4}{3}(1+2k), \frac{2}{3}\right) \right\} \\ &= \frac{4}{3} \left\{ \sum_{k=0}^{\infty} x^{(2k+1)} C_k \beta_k \right\} \end{aligned}$$

The final form of the surface heat flux becomes

$$\dot{q}_s'' = \frac{0.332k}{x} \text{Pr}^{1/3} \text{Re}_x^{1/2} \left\{ \Delta T_{\max} \frac{\pi}{L} \frac{4}{3} \left[\sum_{k=0}^{\infty} x^{(2k+1)} C_k \beta_k \right] + \Delta T_{s,1} \right\}$$

where

$$C_k = \frac{(-1)^k \left(\frac{\pi}{L}\right)^{2k}}{(2k)!} \quad \text{and} \quad \beta_k = \beta\left(\frac{4}{3}(1+2k), \frac{2}{3}\right)$$

and the heat transfer coefficient follows from its definition

$$h(x) = \frac{\dot{q}_s''(x)}{(T_{s,2} - T_\infty)}$$

Because the surface temperature distribution for this problem is a sine function,

$$(T_s - T_\infty) = \Delta T_{s,1} + \Delta T_{\max} \sin(\pi x/L)$$

examine the sine Taylor series expansion

$$\begin{aligned} \sin\left(\frac{\pi x}{L}\right) &= \left(\frac{\pi x}{L}\right) - \frac{\left(\frac{\pi x}{L}\right)^3}{3!} + \frac{\left(\frac{\pi x}{L}\right)^5}{5!} - \frac{\left(\frac{\pi x}{L}\right)^7}{7!} + \dots \\ &= \sum_{p=1}^{\infty} \frac{(-1)^{(p-1)} \left(\frac{\pi x}{L}\right)^{(2p-1)}}{(2p-1)!} \end{aligned}$$

and compare this to the power-series surface temperature distribution associated with Eq. (10-37)

$$T_s = T_\infty + A + \sum_{n=1}^{\infty} B_n x^n$$

Comparing, the coefficients are

$$\begin{aligned} A &= \Delta T_{s,1} \\ n &= 2p-1 \\ B_n &= \Delta T_{\max} \left(\frac{\pi}{L}\right)^{(2p-1)} \frac{(-1)^{(p-1)}}{(2p-1)!} \end{aligned}$$

This suggests our analysis is similar to the textbook's analysis for a surface temperature expressed as a power-series, Eq. (10-37)

$$\begin{aligned} \dot{q}_s'' &= 0.332 \frac{k}{x} \text{Pr}^{1/3} \text{Re}_x^{1/2} \left(\sum_{p=1}^{\infty} (2p-1) B_p \frac{4}{3} x^{(2p-1)} \beta_n + \Delta T_{s,1} \right) \\ \beta_n &= \frac{\Gamma\left[\frac{4}{3}(2p-1)\right] \Gamma\left(\frac{2}{3}\right)}{\Gamma\left[\frac{4}{3}(2p-1) + \frac{2}{3}\right]} \\ B_p &= \Delta T_{\max} \left(\frac{\pi}{L}\right)^{(2p-1)} \frac{(-1)^{(p-1)}}{(2p-1)!} \end{aligned}$$

The solutions compare. Note also that the textbook solution relating to Eq. (10-33) is the first term in the sine-series expansion.

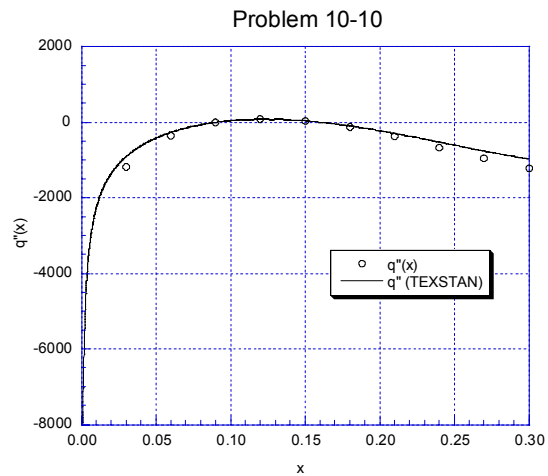
The TEXSTAN data file for this problem is *10.10.dat.txt*. The data set construction is based on the *s10.dat.txt* file for flow over a flat plate with constant free stream velocity and specified surface temperature (initial profiles: Blasius velocity and Blasius temperature). Note that *kout* has been changed to =2.

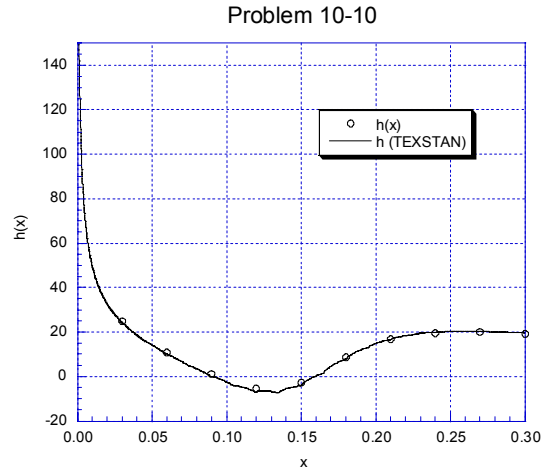
Here is an abbreviated listing of the file *fn86.txt* which contains surface heat flux and heat transfer coefficient distributions. Note the stepsize in the input data file was reduced to *deltax*=0.05 to help resolve the thermal boundary layer behavior after the step-temperature changes.

intg	x/s	htc	qflux	ts	tnf
5	1.0545108E-03	1.6292E+02	-8.0744E+03	3.1344E+02	3.6300E+02
100	2.1247659E-03	1.1371E+02	-5.5846E+03	3.1389E+02	3.6300E+02
200	4.4815757E-03	7.7113E+01	-3.7114E+03	3.1487E+02	3.6300E+02
300	7.7106651E-03	5.7588E+01	-2.6941E+03	3.1622E+02	3.6300E+02
400	1.1812232E-02	4.5243E+01	-2.0391E+03	3.1793E+02	3.6300E+02
500	1.6789076E-02	3.6588E+01	-1.5737E+03	3.1999E+02	3.6300E+02
600	2.2635270E-02	3.0002E+01	-1.2191E+03	3.2237E+02	3.6300E+02
700	2.9353246E-02	2.4606E+01	-9.3265E+02	3.2510E+02	3.6300E+02
800	3.6941989E-02	2.0128E+01	-7.0360E+02	3.2804E+02	3.6300E+02
900	4.5354936E-02	1.5966E+01	-5.0634E+02	3.3129E+02	3.6300E+02
1000	5.4680583E-02	1.2190E+01	-3.4603E+02	3.3461E+02	3.6300E+02
1100	6.4900384E-02	8.5112E+00	-2.1220E+02	3.3807E+02	3.6300E+02
1200	7.5916995E-02	4.6169E+00	-9.9127E+01	3.4153E+02	3.6300E+02
1300	8.7852042E-02	7.2654E-01	-1.3241E+01	3.4478E+02	3.6300E+02
1400	1.0056377E-01	-2.7133E+00	4.1595E+01	3.4767E+02	3.6300E+02
1500	1.1426216E-01	-5.5479E+00	7.1447E+01	3.5012E+02	3.6300E+02
1600	1.2883776E-01	-6.7064E+00	7.4401E+01	3.5191E+02	3.6300E+02
1700	1.4420596E-01	-4.8127E+00	4.9038E+01	3.5281E+02	3.6300E+02
1800	1.6053112E-01	4.2812E-01	-4.4285E+00	3.5266E+02	3.6300E+02
1900	1.7761681E-01	7.2425E+00	-8.4929E+01	3.5127E+02	3.6300E+02
2000	1.9555370E-01	1.3408E+01	-1.9416E+02	3.4852E+02	3.6300E+02
2100	2.1442505E-01	1.7668E+01	-3.3292E+02	3.4416E+02	3.6300E+02
2200	2.3420351E-01	1.9623E+01	-4.8363E+02	3.3835E+02	3.6300E+02
2300	2.5473851E-01	2.0220E+01	-6.4191E+02	3.3125E+02	3.6300E+02
2400	2.7632502E-01	2.0174E+01	-8.1242E+02	3.2273E+02	3.6300E+02
2500	2.9875782E-01	1.9571E+01	-9.6839E+02	3.1352E+02	3.6300E+02
2506	3.0000000E-01	1.9529E+01	-9.7646E+02	3.1300E+02	3.6300E+02

The following plots compare TEXSTAN's predictions of surface heat flux and heat transfer coefficient with the analysis using 10 terms in the series

x/L	x	$\dot{q}''(x)$	h
0.10000	0.030000	-933.00	24.800
0.20000	0.060000	-289.00	10.900
0.30000	0.090000	-20.400	1.1600
0.40000	0.12000	65.600	-5.5000
0.50000	0.15000	27.100	-2.7000
0.60000	0.18000	-102.00	8.5000
0.70000	0.21000	-293.00	16.600
0.80000	0.24000	-518.00	19.500
0.90000	0.27000	-748.00	19.900
1.0000	0.30000	-957.00	19.100
0.10000	0.030000	-933.00	24.800





If you plot the temperature profiles in the region where the heat flux changes sign you can see you can see how it correlates with the change in surface temperature. To plot the profiles, reset the flag $k10=11$ to obtain dimensional profiles of velocity and temperature at each $x(m)$ location. You will observe the inflection in the profile near the wall, and the corresponding negative surface temperature gradient which gives a positive heat flux (Fourier's law) but $(T_s - T_\infty) < 0$, which leads to a negative heat transfer coefficient.

10-11

The potential flow solution for the velocity along the surface of a cylinder with flow normal at a velocity V is

$$u_\infty = 2V \sin \theta$$

where θ is measured from the stagnation point. Assuming that this is a reasonable approximation for a real flow on the upstream side of the cylinder, calculate the local Nusselt number as a function of θ for $0 < \theta < \frac{1}{2}\pi$ for a fluid with $Pr = 0.7$ and prepare a plot. Compare these results with the experimental data for the average Nusselt number around a cylinder. What can you conclude about the heat-transfer behavior in the wake region on the rear surface of the cylinder? TEXSTAN can be used to confirm the results of this variable free-stream velocity problem. For the velocity distribution, break up the surface length of the cylinder over which the boundary layer flows into at least 20 segments and evaluate the velocity at these x -locations. These values then become the variable velocity boundary condition. A larger number of points will more closely model the distribution, which is especially important because this distribution is differentiated to formulate the pressure gradient, as described by Eq. (5-3). Note that TEXSTAN spline-fits these velocity boundary condition values to try to provide a smooth a velocity gradient in construction of the pressure gradient, but it is the user's responsibility to have the velocity distribution as smooth as possible. The initial velocity and temperature profiles (Falkner-Skan $m = 1$ similarity profiles, applicable to a cylinder in crossflow) can be supplied by using the $kstart=6$ choice in TEXSTAN.

The solution follows the analysis for flow over a constant-temperature body of arbitrary shape that incorporates the assumption of local flow similarity. This solution is based on the Falkner-Skan wedge-flow solutions, and it is carried out in detail in the textbook for $Pr = 0.7$. The final result is Eq. (10-48) for the conduction thickness ($Pr=0.7$),

$$\Delta_4^2 = \frac{11.68\nu \int_0^x u_\infty^{1.87} dx}{u_\infty^{2.87}}$$

where x is in the boundary layer flow direction over the cylinder, and $x=0$ is the stagnation point. For the cylinder in crossflow, $x = R\theta$, where R is the cylinder radius. Using this transformation along with the $u_\infty = 2V \sin \theta$ free stream velocity distribution, the conduction-thickness formulation based on cylinder diameter D becomes

$$\Delta_4^2 = \left(\frac{k}{h}\right)^2 = \left(\frac{D}{Nu_D}\right)^2 = \frac{11.68\nu \int_0^\theta (2V \sin \theta)^{1.87} R d\theta}{(2V \sin \theta)^{2.87}} = \frac{11.68\nu (2V)^{1.87}}{(2V \sin \theta)^{2.87}} \frac{D}{2} \int_0^\theta (\sin \theta)^{1.87} d\theta$$

or

$$Nu_D Re_D^{-1/2} = \frac{0.5852 [\sin(\theta)]^{1.435}}{\sqrt{I}}$$

and

$$I = \int_0^\theta (\sin \theta)^{1.87} d\theta$$

The integral must be numerically evaluated. However before we integrate, examine the limiting case for small θ .

$$\text{Nu}_D \text{Re}_D^{-1/2} = \frac{0.5852 \left[\frac{2x}{D} \right]^{1.435}}{\left[\int_0^x \left(\frac{2x}{D} \right)^{1.87} \frac{2}{D} dx \right]^{0.5}} = 0.5852 \sqrt{2.87} = 0.9914$$

It can be compared to the classic stagnation heat transfer solution for a cylinder in crossflow, Eq. (10-22), after converting the Nusselt and Reynolds numbers in that equation from radius to diameter, and evaluating the equation for $\text{Pr}=0.7$,

$$\frac{\text{Nu}_D}{\text{Re}_D^{1/2}} = \left[2 \frac{0.81}{\sqrt{2}} \text{Pr}^{0.4} \right] = 0.9932$$

The two solutions compare for the stagnation region.

Numerical evaluation of the integral gives the following table of results

θ	$\text{Nu}_D \text{Re}_D^{-1/2}$
0	0.9914
9	0.9876
18	0.9768
36	0.9342
54	0.8644
72	0.7692
90	0.6520

The TEXSTAN data file for this problem is *10.11.dat.txt*. The data set construction is based on the *s16.dat.txt* file for flow over a circular cylinder with variable free stream velocity [$u_{\infty}=2V\sin(x/R)$] and specified surface temperature (initial profiles: Falkner-Skan $m=1$ velocity and temperature).

There is a simplification to the TEXSTAN setup for the cylinder in crossflow. We can have TEXSTAN provide an analytic free stream velocity distribution by setting $kstart=6$. With this option TEXSTAN computes $u_{\infty}(x) = 2axx\sin(x/bxx)$, where axx and bxx are user-supplied inputs for the approach velocity and cylinder radius. Using $kstart=6$ means you do not have to input the free stream velocity distribution like the problem statement suggests. For this problem, the approach velocity is $axx=1$ m/s and cylinder radius is $bxx=1.1504$ m, and all properties were evaluated at $T=373\text{K}$. This gives a cylinder-diameter Reynolds number of 100,000.

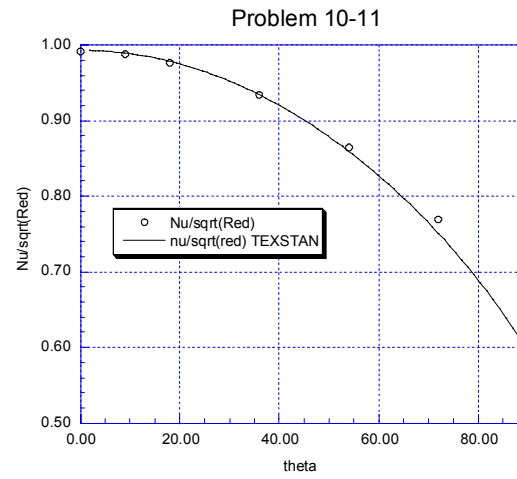
There are several output files that are useful for the cylinder. The most useful is a specially created output file called *fn83_cyl.txt* that presents data normalized by the

Here is an abbreviated listing of *fn83_cyl.txt*. In this file θ , $\text{nu}/\sqrt{\text{red}}$ is the ratio of the computed Nusselt number to the cylinder-diameter Reynolds number. Ignore the temperature-corrected column of data, because for this problem is constant property ($kfluid=1$), the ratio of surface to free stream temperature is close to unity, and the flow is not compressible.

intg	theta	nu/sqrt(red)	temp ratio corrected
------	-------	--------------	----------------------

5	.17856678E+01	.99306009E+00	.99306009E+00
100	.36672133E+01	.99210651E+00	.99210651E+00
200	.79397891E+01	.99031516E+00	.99031516E+00
300	.12282510E+02	.98645998E+00	.98645998E+00
400	.16647203E+02	.98075506E+00	.98075506E+00
500	.21043674E+02	.97321990E+00	.97321990E+00
600	.25481910E+02	.96380518E+00	.96380518E+00
700	.29972551E+02	.95242965E+00	.95242965E+00
800	.34527253E+02	.93898351E+00	.93898351E+00
900	.39159058E+02	.92332437E+00	.92332437E+00
1000	.43882859E+02	.90526908E+00	.90526908E+00
1100	.48716004E+02	.88458089E+00	.88458089E+00
1200	.53680965E+02	.86094029E+00	.86094029E+00
1300	.58804766E+02	.83391822E+00	.83391822E+00
1400	.64119621E+02	.80292822E+00	.80292822E+00
1500	.69667076E+02	.76712261E+00	.76712261E+00
1600	.75502857E+02	.72519641E+00	.72519641E+00
1700	.81710276E+02	.67490325E+00	.67490325E+00
1800	.88416550E+02	.61180075E+00	.61180075E+00
1828	.90365157E+02	.59114156E+00	.59114156E+00

From our analytical solution we see $nu/\sqrt{\text{red}}$ should be about 0.993 for small θ , and we see the TEXSTAN ratio matches this solution to within 5% out to $\theta = 30^\circ$, and to within 2% to $\theta = 15^\circ$. We also see the movement towards laminar separation around $\theta = 90^\circ$. Theoretically we would expect separation just before $\theta = 90^\circ$, and the reason we do not predict it with TEXSTAN is that the potential flow free stream velocity distribution, $u_\infty = 2V \sin \theta$, is not correct for $\theta > 45-60^\circ$. If we would have used an experimentally determined $u_\infty(x)$, or its Mach-number equivalent, we would have predicted separated flow before $\theta = 90^\circ$.



10-12

The potential flow solution for the velocity along the surface of a sphere with flow normal at a velocity V is

$$u_{\infty} = \frac{3}{2}V \sin \theta$$

Do the same problem as the preceding one for the sphere.

The solution follows the analysis for flow over a constant-temperature body of arbitrary shape that incorporates the assumption of local flow similarity. This solution is based on the Falkner-Skan wedge-flow solutions, and it is carried out in detail in the textbook for $Pr = 0.7$. The final result for the case where flow occurs over a body of revolution is the conduction thickness ($Pr=0.7$) equation just above its Stanton-number formulation, Eq. (10-52),

$$R^2 \Delta_4^2 = \frac{11.68 \nu \int_0^x u_{\infty}^{1.87} R^2 dx}{u_{\infty}^{2.87}}$$

where x is in the boundary layer flow direction over the sphere, and $x=0$ is the stagnation point. The variable R is the radius of revolution, or transverse radius of curvature of the sphere, as shown in Fig. 5-1 of the integral equation chapter. For the sphere in crossflow, $x = R_s \theta$, where R_s is the sphere radius. From geometrical considerations, $R(x) = R_s \sin(\theta)$. Using these transformations along with the $u_{\infty} = \frac{3}{2}V \sin \theta$ free stream velocity distribution, the conduction-thickness formulation becomes

$$\Delta_4^2 = \left(\frac{k}{h} \right)^2 = \left(\frac{D}{Nu_D} \right)^2 = \frac{11.68 \nu \int_0^{\theta} (1.5V \sin \theta)^{1.87} (R_s \sin \theta)^2 R_s d\theta}{(R_s \sin \theta)^2 (1.5V \sin \theta)^{2.87}}$$

or

$$\left(\frac{D}{Nu_D} \right)^2 = \frac{11.68 \nu (1.5V)^{1.87}}{(\sin \theta)^2 (1.5V \sin \theta)^{2.87}} \frac{D}{2} \int_0^{\theta} (\sin \theta)^{1.87} (\sin \theta)^2 d\theta$$

$$Nu_D Re_D^{-1/2} = \frac{0.5068 [\sin(\theta)]^{2.435}}{\sqrt{I}}$$

and

$$I = \int_0^{\theta} (\sin \theta)^{3.87} d\theta$$

The integral must be numerically evaluated. However before we integrate, examine the limiting case for small θ .

$$\text{Nu}_D \text{Re}_D^{-1/2} = \frac{0.5068 \left[\frac{2x}{D} \right]^{2.435}}{\left[\int_0^x \left(\frac{2x}{D} \right)^{3.87} \frac{2}{D} dx \right]^{0.5}} = 0.5068 \sqrt{4.87} = 1.118$$

It can be compared to the classic stagnation heat transfer solution for a cylinder in crossflow, Eq. (10-23), after converting the Nusselt and Reynolds numbers in that equation from radius to diameter, and evaluating the equation for $\text{Pr}=0.7$,

$$\frac{\text{Nu}_D}{\text{Re}_D^{1/2}} = \left[2 \frac{0.93}{\sqrt{2}} \text{Pr}^{0.4} \right] = 1.1403$$

The two solutions compare for the stagnation region.

Numerical evaluation of the integral gives the following table of results

θ	$\text{Nu}_D \text{Re}_D^{-1/2}$
0	1.1184
9	1.1073
18	1.0920
36	1.0086
54	0.9349
72	0.7692
90	0.6557

The TEXSTAN data file for this problem is *10.12.dat.txt*. The data set construction is based on the *s17.dat.txt* file for flow over a sphere with variable free stream velocity [$\text{unif}=1.5V\sin(x/R_s)$] and specified surface temperature (initial profiles: approximate similarity velocity and temperature) For this input file $k\text{geom}=2$ for flow over an axisymmetric body of revolution, and the radius of revolution is input using the $rw(m)$ variable, where $R(x) = R_s \sin(\theta)$ where $x = R_s \theta$, and R_s is the sphere radius. Here is the table, constructed using 15 values at theta angles of 0.01, 1, 2, 3, 5, 10, 18, 27, 36, 45, 54, 63, 72, 81, and 90 degrees. Note you can not choose a theta angle of 0 degrees, as this presents a radius singularity

###	x(m)	rw(m)	aux1(m)	aux2(m)	aux3(m)
	0.0020000	0.0020	0.0000	0.0000	0.0000
	0.0201000	0.02008	0.0000	0.0000	0.0000
	0.0402000	0.04015	0.0000	0.0000	0.0000
	0.0602000	0.06021	0.0000	0.0000	0.0000
	0.1004000	0.10026	0.0000	0.0000	0.0000
	0.2008000	0.19976	0.0000	0.0000	0.0000
	0.3614000	0.35549	0.0000	0.0000	0.0000

0.5421000	0.52227	0.0000	0.0000	0.0000
0.7228000	0.67619	0.0000	0.0000	0.0000
0.9035000	0.81346	0.0000	0.0000	0.0000
1.0842000	0.93069	0.0000	0.0000	0.0000
1.2649000	1.02501	0.0000	0.0000	0.0000
1.4456000	1.09410	0.0000	0.0000	0.0000
1.6263000	1.13624	0.0000	0.0000	0.0000
1.8070000	1.15040	0.0000	0.0000	0.0000

There is a simplification to the TEXSTAN setup for the sphere in crossflow. We can have TEXSTAN provide an analytic free stream velocity distribution by setting $kstart=6$. With this option TEXSTAN computes $u_{\infty}(x) = 1.5axx \sin(x/bxx)$, where axx and bxx are user-supplied inputs for the approach velocity (V) and sphere radius (R_s). Using $kstart=6$ means you do not have to input the free stream velocity distribution like problem statement 10-11 suggests. For this problem, the approach velocity is $axx=1$ m/s and sphere radius is $bxx=1.1504$ m, and all properties were evaluated at $T=373K$. This gives a sphere-diameter Reynolds number of 100,000.

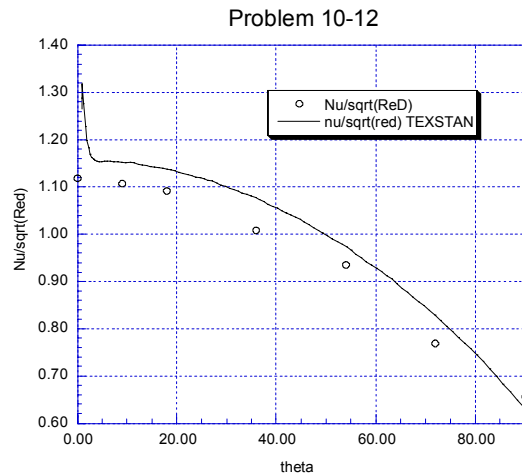
There are several output files that are useful for the cylinder. The most useful is a specially created output file called *fn83_sphere.txt* that presents data normalized by the

Here is an abbreviated listing of *fn83_sphere.txt*. In this file θ is θ , nu/\sqrt{red} is the ratio of the computed Nusselt number to the cylinder-diameter Reynolds number. Ignore the temperature-corrected column of data, because for this problem is constant property ($kfluid=1$), the ratio of surface to free stream temperature is close to unity, and the flow is not compressible.

intg	theta	nu/sqrt(red)	temp ratio corrected
5	.10053950E+01	.12655893E+01	.12655893E+01
100	.19450630E+01	.11988785E+01	.11988785E+01
200	.35902178E+01	.11559551E+01	.11559551E+01
300	.59712800E+01	.11550118E+01	.11550118E+01
400	.97477592E+01	.11514877E+01	.11514877E+01
500	.13858879E+02	.11453340E+01	.11453340E+01
600	.17988653E+02	.11380971E+01	.11380971E+01
700	.22122285E+02	.11260944E+01	.11260944E+01
800	.26334032E+02	.11147015E+01	.11147015E+01
900	.30586896E+02	.10977712E+01	.10977712E+01
1000	.34924323E+02	.10811442E+01	.10811442E+01
1100	.39318151E+02	.10590670E+01	.10590670E+01
1200	.43833358E+02	.10365953E+01	.10365953E+01
1300	.48434526E+02	.10082867E+01	.10082867E+01
1400	.53204787E+02	.97914426E+00	.97914426E+00
1500	.58107202E+02	.94272106E+00	.94272106E+00
1600	.63207863E+02	.90542010E+00	.90542010E+00

1700	.68598481E+02	.85783335E+00	.85783335E+00
1800	.74263750E+02	.80562934E+00	.80562934E+00
1900	.80385911E+02	.74423324E+00	.74423324E+00
2000	.87045547E+02	.66656614E+00	.66656614E+00
2041	.89997596E+02	.63079697E+00	.63079697E+00

From our analytical solution we see nu/\sqrt{red} should be about 1.140 for small θ , and we see the TEXSTAN ratio matches this solution to within 5% out to $\theta = 30^\circ$, and to within 2% to $\theta = 15^\circ$. Note that the initial condition profiles currently programmed into TEXSTAN for a sphere are approximate profiles, and this is the source of error for small theta. For large theta, we see the movement towards laminar separation around $\theta = 90^\circ$. Theoretically we would expect separation around $\theta = 90^\circ$, and the reason we do not predict it with TEXSTAN is that the potential flow free stream velocity distribution, $u_\infty = 1.5V \sin \theta$, is not correct for $\theta > 45-60^\circ$. If we would have used an experimentally determined $u_\infty(x)$, or its Mach-number equivalent, we would have predicted separated flow before $\theta = 90^\circ$.



This comparison shows the correct trend, but not nearly as accurate as with the cylinder in crossflow. This will be partly related to not having correct initial conditions. For the cylinder we have the Falkner-Skan $m=1$ profiles.

10-13

Let air at a constant velocity of 7.6 m/s, a temperature of -7°C , and 1 atm pressure flow along a smooth, flat surface. The plate is 15 cm long (in the flow direction). The entire surface of the plate is adiabatic except for a 2.5 cm wide strip, located between 5 and 7.5 cm from the leading edge, which is electrically heated so that the heat-transfer rate per unit of area on this strip is uniform. What must be the heat flux from this strip such that the temperature of the surface at the trailing edge of the plate is above 0°C ? Plot the temperature distribution along the entire plate surface. Discuss the significance of this problem with respect to wing deicing. (A tabulation of incomplete beta functions, necessary for this solution, is found in App. C). TEXSTAN can be used to confirm the results of this variable surface heat flux problem. Choose a starting x -location near the leading edge, say 0.1 cm, and pick fluid properties that are appropriate to air, evaluated at the free stream temperature. Use constant fluid properties and do not consider viscous dissipation. The piecewise surface heat flux boundary condition is modeled easily in TEXSTAN by providing heat flux values at two x -locations for each segment, e.g. at $x = 0$, $x = 0.05$, $x = 0.0501$, $x = 0.075$, $x = 0.0751$, and $x = 0.15$ m. Because TEXSTAN linearly interpolates the surface thermal boundary condition between consecutive x -locations, a total of 6 boundary condition locations is sufficient to describe the surface heat flux variation. The initial velocity and temperature profiles (Blasius similarity profiles) can be supplied by using the $kstart=4$ choice in TEXSTAN.

The solution procedure is to evaluate the surface temperature distribution for the given surface heat flux distribution. Equation (10-41) gives the computing equation,

$$T_s(x) - T_{\infty} = \frac{0.623}{k} \text{Pr}^{-1/3} \text{Re}_x^{-1/2} \int_0^x \left[1 - \left(\frac{\xi}{x} \right)^{3/4} \right]^{-2/3} \dot{q}_s''(\xi) d\xi$$

For this problem statement, we know $T_s(x=L)=0^{\circ}\text{C}$, and the distribution of surface heat flux is piecewise, being adiabatic everywhere except $0.05 \text{ m} \leq x \leq 0.075 \text{ m}$ and the surface heat flux is constant in that interval, so

$$\begin{aligned} T_s(x) - T_{\infty} &= \frac{0.623}{k} \text{Pr}^{-1/3} \text{Re}_x^{-1/2} \dot{q}_s'' \left\{ \int_{0.05}^{0.075} \left[1 - \left(\frac{\xi}{x} \right)^{3/4} \right]^{-2/3} d\xi \right\} \\ &= \frac{0.623}{k} \text{Pr}^{-1/3} \text{Re}_x^{-1/2} \dot{q}_s'' I(\xi; x) \end{aligned}$$

Transform the integrand by letting

$$\begin{aligned} u &= 1 - \left(\frac{\xi}{x} \right)^{3/4} \\ \xi &= x(1-u)^{4/3} \quad d\xi = -\frac{4}{3} x(1-u)^{1/3} du \end{aligned}$$

and the integral becomes

$$I(\xi; x) = -\frac{4x}{3} \int_{u_1}^{u_2} u^{-2/3} (1-u)^{1/3} du =$$

From Appendix C, we recognize this as an integral in the Beta function family with $m=1/3$ and $n=4/3$ in Table C-3.

$$\begin{aligned}\int_{u_1}^{u_2} u^{(m-1)} [1-u]^{(n-1)} du &= \int_0^{u_2} u^{(m-1)} [1-u]^{(n-1)} du - \int_0^{u_1} u^{(m-1)} [1-u]^{(n-1)} du \\ &= \beta_{u_2}(m, n) - \beta_{u_1}(m, n) \\ &= \beta_1(m, n) \left[\left(\frac{\beta_{u_2}(m, n)}{\beta_1(m, n)} \right) - \left(\frac{\beta_{u_1}(m, n)}{\beta_1(m, n)} \right) \right]\end{aligned}$$

For our problem, we want to evaluate the integral at $x=0.15\text{m}$ where $T_s(x=L)=0^\circ\text{C}$ to solve for the required heat flux to achieve this temperature. Therefore

$$u_2 = 1 - \left(\frac{0.075}{x} \right)^{3/4} = 0.405$$

$$u_1 = 1 - \left(\frac{0.05}{x} \right)^{3/4} = 0.561$$

and $m=1/3$ and $n=4/3$ for all evaluations of the Beta functions.. The integral becomes.

$$\begin{aligned}I(\xi; x) &= -\frac{4}{3}x \left\{ \beta_1 \left[\left(\frac{\beta_r}{\beta_1} \right)_{r=0.41} - \left(\frac{\beta_r}{\beta_1} \right)_{r=0.56} \right] \right\} \\ &= -\frac{4}{3}x (2.65) [0.809 - 0.881] = 0.254x\end{aligned}$$

and

$$\begin{aligned}T_s(x) - T_\infty &= \frac{0.623}{k} \text{Pr}^{-1/3} \text{Re}_x^{-1/2} \dot{q}_s'' \left\{ \int_{0.05}^{0.075} \left[1 - \left(\frac{\xi}{x} \right)^{3/4} \right]^{-2/3} d\xi \right\} \\ &= \frac{0.623}{k} \text{Pr}^{-1/3} \text{Re}_x^{-1/2} \dot{q}_s'' (0.254x)\end{aligned}$$

With the properties for air evaluated at 263 K, the required heat flux is $\dot{q}_s'' = 1829 \text{ W/m}^2$.

The TEXSTAN data file for this problem is *10.13.dat.txt*. The data set construction is based on the *s11.dat.txt* file for flow over a flat plate with constant free stream velocity and specified surface heat flux (initial profiles: Blasius velocity and Blasius temperature).

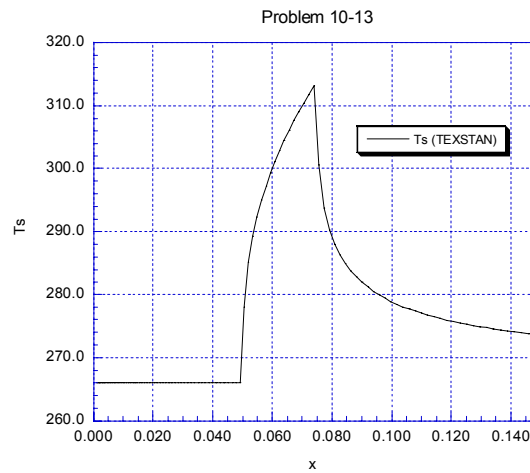
Here is an abbreviated listing of the file *fm86.txt* which contains the surface temperature distribution. Note the stepsize in the input data file was reduced to *deltax=0.05* to help resolve the thermal boundary layer behavior after the step heat flux changes.

intg	x/s	htc	qflux	ts	tinf
5	1.0511671E-03	0.0000E+00	0.0000E+00	2.6600E+02	2.6600E+02
50	1.2137448E-03	0.0000E+00	0.0000E+00	2.6600E+02	2.6600E+02
100	1.8219660E-03	0.0000E+00	0.0000E+00	2.6600E+02	2.6600E+02
150	2.5535141E-03	0.0000E+00	0.0000E+00	2.6600E+02	2.6600E+02
200	3.4086695E-03	0.0000E+00	0.0000E+00	2.6600E+02	2.6600E+02
250	4.3873001E-03	0.0000E+00	0.0000E+00	2.6600E+02	2.6600E+02

300	5.4894155E-03	0.0000E+00	0.0000E+00	2.6600E+02	2.6600E+02
350	6.7150241E-03	0.0000E+00	0.0000E+00	2.6600E+02	2.6600E+02
400	8.0641306E-03	0.0000E+00	0.0000E+00	2.6600E+02	2.6600E+02
450	9.5367375E-03	0.0000E+00	0.0000E+00	2.6600E+02	2.6600E+02
500	1.1132846E-02	0.0000E+00	0.0000E+00	2.6600E+02	2.6600E+02
550	1.2852458E-02	0.0000E+00	0.0000E+00	2.6600E+02	2.6600E+02
600	1.4695574E-02	0.0000E+00	0.0000E+00	2.6600E+02	2.6600E+02
650	1.6662194E-02	0.0000E+00	0.0000E+00	2.6600E+02	2.6600E+02
700	1.8752319E-02	0.0000E+00	0.0000E+00	2.6600E+02	2.6600E+02
750	2.0965948E-02	0.0000E+00	0.0000E+00	2.6600E+02	2.6600E+02
800	2.3303082E-02	0.0000E+00	0.0000E+00	2.6600E+02	2.6600E+02
850	2.5763722E-02	0.0000E+00	0.0000E+00	2.6600E+02	2.6600E+02
900	2.8347866E-02	0.0000E+00	0.0000E+00	2.6600E+02	2.6600E+02
950	3.1055516E-02	0.0000E+00	0.0000E+00	2.6600E+02	2.6600E+02
1000	3.3886671E-02	0.0000E+00	0.0000E+00	2.6600E+02	2.6600E+02
1050	3.6841332E-02	0.0000E+00	0.0000E+00	2.6600E+02	2.6600E+02
1100	3.9919498E-02	0.0000E+00	0.0000E+00	2.6600E+02	2.6600E+02
1150	4.3121170E-02	0.0000E+00	0.0000E+00	2.6600E+02	2.6600E+02
1200	4.6446347E-02	0.0000E+00	0.0000E+00	2.6600E+02	2.6600E+02
1250	4.9895030E-02	0.0000E+00	0.0000E+00	2.6600E+02	2.6600E+02
1300	5.3388496E-02	8.0094E+01	1.8610E+03	2.8924E+02	2.6600E+02
1350	5.7081513E-02	6.1854E+01	1.8610E+03	2.9609E+02	2.6600E+02
1400	6.0898035E-02	5.2997E+01	1.8610E+03	3.0112E+02	2.6600E+02
1450	6.4838063E-02	4.7332E+01	1.8610E+03	3.0532E+02	2.6600E+02
1500	6.8901597E-02	4.3239E+01	1.8610E+03	3.0904E+02	2.6600E+02
1550	7.3088637E-02	4.0069E+01	1.8610E+03	3.1244E+02	2.6600E+02
1600	7.7356267E-02	0.0000E+00	0.0000E+00	2.9368E+02	2.6600E+02
1650	8.1789105E-02	0.0000E+00	0.0000E+00	2.8707E+02	2.6600E+02
1700	8.6345449E-02	0.0000E+00	0.0000E+00	2.8372E+02	2.6600E+02
1750	9.1025299E-02	0.0000E+00	0.0000E+00	2.8153E+02	2.6600E+02
1800	9.5828654E-02	0.0000E+00	0.0000E+00	2.7993E+02	2.6600E+02
1850	1.0075552E-01	0.0000E+00	0.0000E+00	2.7870E+02	2.6600E+02
1900	1.0580588E-01	0.0000E+00	0.0000E+00	2.7771E+02	2.6600E+02
1950	1.1097975E-01	0.0000E+00	0.0000E+00	2.7689E+02	2.6600E+02
2000	1.1627713E-01	0.0000E+00	0.0000E+00	2.7620E+02	2.6600E+02
2050	1.2169802E-01	0.0000E+00	0.0000E+00	2.7561E+02	2.6600E+02
2100	1.2724241E-01	0.0000E+00	0.0000E+00	2.7509E+02	2.6600E+02

2150	1.3291030E-01	0.0000E+00	0.0000E+00	2.7464E+02	2.6600E+02
2200	1.3870170E-01	0.0000E+00	0.0000E+00	2.7423E+02	2.6600E+02
2250	1.4461661E-01	0.0000E+00	0.0000E+00	2.7387E+02	2.6600E+02
2295	1.5000000E-01	0.0000E+00	0.0000E+00	2.7358E+02	2.6600E+02

Based on the analytical solution for the required heat flux, we see the TEXSTAN prediction of the surface temperature at $x=0.15\text{m}$ is 273.6K , which matches the required $T_s(x=L)=0^\circ\text{C}$. Here is a plot of the TEXSTAN surface temperature distribution.



10-14

Let air at a constant velocity of 15 m/s, a temperature of 300°C, and 1 atm pressure flow along a smooth, flat surface. Let the first 15 cm of the surface be cooled by some internal means to a uniform temperature of 90°C. How does the surface temperature vary for the next 45 cm? *Hint:* Note that the first 15 cm must be treated as a surface-temperature-specified problem, while the last 45 cm must be treated as a surface-heat-flux-specified problem. Because this problem requires two different types of thermal boundary condition, TEXSTAN is not suitable for this problem.

The surface heat flux for $0 \leq x \leq 0.15\text{m}$ is the constant surface temperature solution using Eq. (10-29)

$$\dot{q}_s''(x) = h_x(T_s - T_\infty) = \frac{\text{Nu}_x k}{x}(T_s - T_\infty) = \frac{k}{x}(0.332 \text{Pr}^{1/3} \text{Re}_x^{1/2})(T_s - T_\infty)$$

and for $0.15\text{m} < x \leq 0.60\text{m}$ $\dot{q}_s''(x) = 0$. The solution procedure is to evaluate the surface temperature distribution for the variable surface heat flux distribution using Eq. (10-41), where the integral contribution for $x > 0.15\text{m}$ is zero,

$$\begin{aligned} T_s(x) - T_\infty &= \frac{0.623}{k} \text{Pr}^{-1/3} \text{Re}_x^{-1/2} \int_0^{x^{0.15}} \left[1 - \left(\frac{\xi}{x} \right)^{3/4} \right]^{-2/3} \left[\frac{k}{\xi} (0.332 \text{Pr}^{1/3} \text{Re}_\xi^{1/2})(T_{s,1} - T_\infty) \right] d\xi \\ &= 0.623 \text{Re}_x^{-1/2} \left[0.332 \left(\frac{u_\infty}{\nu} \right)^{1/2} (T_{s,1} - T_\infty) \right] \int_0^{x^{0.15}} \left[1 - \left(\frac{\xi}{x} \right)^{3/4} \right]^{-2/3} \frac{1}{\sqrt{\xi}} d\xi \end{aligned}$$

or

$$T_s(x) - T_\infty = \left[(0.623)(0.332) \left(\frac{u_\infty}{\nu} \right)^{1/2} (T_{s,1} - T_\infty) \right] \text{Re}_x^{-1/2} I(\xi; x)$$

Transform the integrand by letting

$$\begin{aligned} u &= 1 - \left(\frac{\xi}{x} \right)^{3/4} \\ \xi &= x(1-u)^{4/3} \quad d\xi = -\frac{4}{3} x(1-u)^{1/3} du \\ \xi^{-1/2} &= x^{-1/2} (1-u)^{-2/3} \end{aligned}$$

For our problem, we want to evaluate the integral for $x > 0.15\text{m}$. Therefore

$$u_2 = 1 - \left(\frac{0.15}{x} \right)^{3/4}$$

$$u_1 = 1$$

and the integral becomes

$$\begin{aligned} I(\xi; x) &= \int_1^{u_2} u^{-2/3} \left[x^{-1/2} (1-u)^{-2/3} \right] \left[-\frac{4}{3} x (1-u)^{1/3} \right] du \\ &= -\frac{4}{3} x^{1/2} \int_1^{u_2} u^{-2/3} (1-u)^{-1/3} du \\ &= +\left(\frac{4}{3} x^{1/2} \right) \left\{ \int_0^1 u^{-2/3} (1-u)^{-1/3} du - \int_0^{u_2} u^{-2/3} (1-u)^{-1/3} du \right\} \end{aligned}$$

From Appendix C, we recognize this as an integral in the Beta function family with $m=1/3$ and $n=2/3$ in Table C-3.

$$\begin{aligned} \int_{u_1}^{u_2} u^{(m-1)} [1-u]^{(n-1)} du &= \int_0^{u_2} u^{(m-1)} [1-u]^{(n-1)} du - \int_0^{u_1} u^{(m-1)} [1-u]^{(n-1)} du \\ &= \beta_{u_2}(m, n) - \beta_{u_1}(m, n) = \beta_1(m, n) \left[\left(\frac{\beta_{u_2}(m, n)}{\beta_1(m, n)} \right) - \left(\frac{\beta_{u_1}(m, n)}{\beta_1(m, n)} \right) \right] \end{aligned}$$

The integral becomes.

$$I(\xi; x) = \left(+\frac{4}{3} x^{1/2} \right) \left\{ \beta_1 - \beta_1 \left(\frac{\beta_r}{\beta_1} \right)_{r=u_2} \right\}$$

Note, the alternative for numerical integration would be

$$I(\xi; x) = +\left(\frac{4}{3} x^{1/2} \right) \left[\beta_1(m, n) - \int_0^{u_2} u^{-2/3} (1-u)^{-1/3} du \right]$$

The surface temperature formulation becomes

$$\begin{aligned} T_s(x) - T_\infty &= \left[(0.623)(0.332) \left(\frac{u_\infty}{\nu} \right)^{1/2} (T_{s,1} - T_\infty) \right] \text{Re}_x^{-1/2} \left(+\frac{4}{3} x^{1/2} \right) \left[\beta_1 - \beta_1 \left(\frac{\beta_r}{\beta_1} \right)_{r=u_2} \right] \\ &= (0.2758)(T_{s,1} - T_\infty) \left[\beta_1 - \beta_1 \left(\frac{\beta_r}{\beta_1} \right)_{r=u_2} \right] \end{aligned}$$

where $r = u_2 = 1 - \left(\frac{0.15}{x} \right)^{3/4}$ and with $m=1/3$ and $n=2/3$. A table of results for this analysis is shown in the table below.

x (m)	r	$\beta(r)/\beta(m, n)$	$\beta(r)$	$T_s(x)$ (°C)
0.16	0.047	0.293	1.063	151.42
0.2	0.194	0.486	1.762	191.92
0.25	0.318	0.576	2.090	210.87
0.3	0.405	0.638	2.314	223.88
0.4	0.521	0.701	2.543	237.16
0.5	0.595	0.742	2.692	245.78

0.6	0.646	0.769	2.791	251.53
-----	-------	-------	-------	--------

The problem statement indicates this problem is not suitable for TEXSTAN. This is not completely correct. TEXSTAN is programmed so that the thermal boundary condition is either Dirichlet (temperature) or Neumann (heat flux) for all $x(m)$ values. What can be done is to convert the boundary condition over the range $0 \leq x \leq 0.15m$ from $T_s=90^\circ\text{C}$ to its heat flux equivalent using

$$\dot{q}_s''(x) = h_x(T_s - T_\infty) = \frac{\text{Nu}_x k}{x}(T_s - T_\infty) = \frac{k}{x}(0.332 \text{Pr}^{1/3} \text{Re}_x^{1/2})(T_s - T_\infty)$$

The problem then is truly a variable heat flux problem, $\dot{q}_s''(x) = 0$ for $0.15m < x \leq 0.60m$.

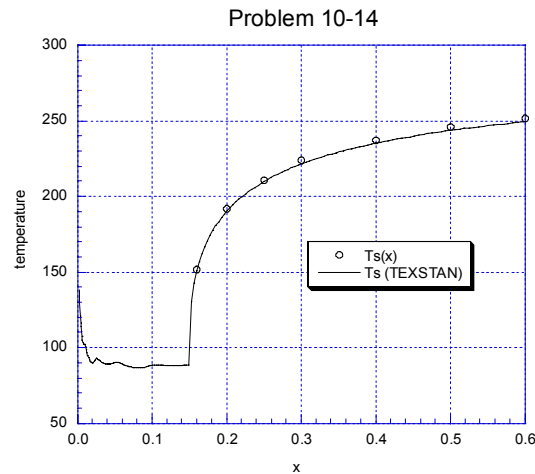
The TEXSTAN data file for this problem is *10.14.dat.txt*. The data set construction is based on the *s11.dat.txt* file for flow over a flat plate with constant free stream velocity and specified surface heat flux (initial profiles: Blasius velocity and Blasius temperature). The heat flux formula given above was used to set the heat flux boundary condition, and 8 $x(m)$ locations were used. This is a minimum number because TEXSTAN linearly interpolates between boundary condition points for heat flux, and the flux is rapidly changing with x .

Here is an abbreviated listing of the file *fm86.txt* which contains the surface temperature distribution. Note the stepsize in the input data file was reduced to *deltax*=0.05 to help resolve the thermal boundary layer behavior after the step heat flux changes.

intg	x/s	htc	qflux	ts	tnf
5	3.2248679E-03	1.6600E+02	-2.6883E+04	1.3805E+02	3.0000E+02
100	5.0621646E-03	1.1552E+02	-2.1487E+04	1.1400E+02	3.0000E+02
200	8.6609354E-03	8.5591E+01	-1.6941E+04	1.0207E+02	3.0000E+02
300	1.3203350E-02	6.9107E+01	-1.4052E+04	9.6659E+01	3.0000E+02
400	1.8720567E-02	5.7192E+01	-1.1991E+04	9.0341E+01	3.0000E+02
500	2.5208464E-02	4.6437E+01	-9.6209E+03	9.2817E+01	3.0000E+02
600	3.2653331E-02	4.1909E+01	-8.7797E+03	9.0505E+01	3.0000E+02
700	4.1061222E-02	3.7080E+01	-7.8297E+03	8.8845E+01	3.0000E+02
800	5.0393175E-02	3.2492E+01	-6.8040E+03	9.0593E+01	3.0000E+02
900	6.0723345E-02	3.0287E+01	-6.3913E+03	8.8977E+01	3.0000E+02
1000	7.2016505E-02	2.7910E+01	-5.9402E+03	8.7169E+01	3.0000E+02
1100	8.4272619E-02	2.5547E+01	-5.4506E+03	8.6649E+01	3.0000E+02
1200	9.7491744E-02	2.3219E+01	-4.9225E+03	8.7999E+01	3.0000E+02
1300	1.1170201E-01	2.1820E+01	-4.6152E+03	8.8490E+01	3.0000E+02
1400	1.2684915E-01	2.0520E+01	-4.3471E+03	8.8157E+01	3.0000E+02
1500	1.4295934E-01	1.9200E+01	-4.0620E+03	8.8434E+01	3.0000E+02
1600	1.5994744E-01	0.0000E+00	0.0000E+00	1.5071E+02	3.0000E+02
1700	1.7797949E-01	0.0000E+00	0.0000E+00	1.7430E+02	3.0000E+02
1800	1.9697111E-01	0.0000E+00	0.0000E+00	1.8815E+02	3.0000E+02
1900	2.1691975E-01	0.0000E+00	0.0000E+00	1.9814E+02	3.0000E+02

2000	2.3782359E-01	0.0000E+00	0.0000E+00	2.0597E+02	3.0000E+02
2100	2.5968880E-01	0.0000E+00	0.0000E+00	2.1239E+02	3.0000E+02
2200	2.8252108E-01	0.0000E+00	0.0000E+00	2.1780E+02	3.0000E+02
2300	3.0631980E-01	0.0000E+00	0.0000E+00	2.2246E+02	3.0000E+02
2400	3.3108446E-01	0.0000E+00	0.0000E+00	2.2654E+02	3.0000E+02
2500	3.5681461E-01	0.0000E+00	0.0000E+00	2.3016E+02	3.0000E+02
2600	3.8350986E-01	0.0000E+00	0.0000E+00	2.3338E+02	3.0000E+02
2700	4.1116988E-01	0.0000E+00	0.0000E+00	2.3629E+02	3.0000E+02
2800	4.3979433E-01	0.0000E+00	0.0000E+00	2.3893E+02	3.0000E+02
2900	4.6938289E-01	0.0000E+00	0.0000E+00	2.4134E+02	3.0000E+02
3000	4.9993528E-01	0.0000E+00	0.0000E+00	2.4355E+02	3.0000E+02
3100	5.3145120E-01	0.0000E+00	0.0000E+00	2.4559E+02	3.0000E+02
3200	5.6393038E-01	0.0000E+00	0.0000E+00	2.4747E+02	3.0000E+02
3300	5.9737253E-01	0.0000E+00	0.0000E+00	2.4922E+02	3.0000E+02
3308	6.0000000E-01	0.0000E+00	0.0000E+00	2.4935E+02	3.0000E+02

Based on the analytical solution for the required surface temperature followed by an adiabatic wall, we see the TEXSTAN prediction of the surface temperature $0 \leq x \leq 0.15\text{m}$ matches $T_s=90^\circ\text{C}$ within about 2°C over most of the interval. This could be easily improved by increasing the number of $x(\text{m})$ locations, which matches the required $T_s(x=L)=0^\circ\text{C}$. Here is a plot of the TEXSTAN surface temperature distribution compared with the values from the analysis.



10-15

Water at 10°C flows from a reservoir through the convergent nozzle shown in Fig. 10-7 into a circular tube. The mass flow rate of the water is 9 g/s. Making a plausible assumption as to the origin of the boundary layer in the nozzle and assuming that the nozzle surface is at a uniform temperature different from 10°C, calculate the heat-transfer coefficient at the throat of the nozzle. How does this compare with the coefficient far downstream in the tube if the tube surface is at a uniform temperature?

The solution to this problem follows that for problem 9-5 to some degree. The solution involves calculating the Stanton number for a given Pr using Eq. (10-54).

There are several geometric variables to be defined. The nozzle radius of curvature is $r_{noz}=0.012$ m. The nozzle transverse radius at the throat, $R_b=0.003$ m, and nozzle transverse radius at the start of the nozzle ($x_a=0$) is $R_a=0.0135$ m. From geometry, $x_b = r_{noz} \pi/2 = 0.018849$ m. Using this geometry, the function for the transverse radius of the nozzle wall becomes

$$R(x) = R_a - r_{noz} \sin(\theta) = R_a - r_{noz} \sin\left(\frac{x}{r_{noz}}\right)$$

Assuming constant density, the Stanton number equation Eq. (10-52) at the throat becomes

$$St(x = x_b) = \frac{C_1 \mu^{1/2} R_{x_b} [G_\infty(x = x_b)]^{C_2}}{\left(\int_0^{x_b} [G_\infty(x)]^{C_3} \left(R_a - r_c \sin \frac{x}{r_c} \right)^2 dx \right)^{1/2}}$$

where $G_\infty = \rho_\infty u_\infty$.

The free stream velocity just outside the boundary layer of the nozzle wall really needs to be developed from an inviscid or Euler analysis of the incompressible flow in a converging nozzle.

The first approximation for this axisymmetric nozzle is to use the model defined by problem 9-5. The free stream velocity at the nozzle wall is assumed to vary linearly along the nozzle surface from the sharp corner to the throat, $x_a \leq x \leq x_b$, and with a mass flow rate of 0.009 kg/s, the throat velocity is $u_{\infty,b} = 0.318$ m/s.

$$u_\infty(x) = \cancel{u_{\infty,a}} + \left(\frac{u_{\infty,b} - u_{\infty,a}}{x_b - x_a} \right) (x - x_a) = 16.89x \text{ m/s}$$

Note that the requirement of $u_{\infty,a} = 0$ is a requirement of the problem statement and is not really needed.

The integral can be evaluated using standard methods. The properties are for water at 20°C. From Table 10-6 for Pr=9.42, the coefficients in the solution are $C_1=0.0781$, $C_2=0.675$, and $C_3=2.35$. The results using the linear free stream velocity approximation are

$$\begin{aligned} St &= 0.001402 \\ h &= 1871 \text{ W/(m}^2 \cdot \text{K)} \end{aligned}$$

The second approximation for this axisymmetric nozzle is to assume the free stream velocity at the nozzle wall is defined by the 1-D mass flow rate equation along the nozzle surface from the sharp corner to the throat, $x_a \leq x \leq x_b$,

$$u_{\infty}(x) = \frac{\dot{m}}{\rho A_c} = \frac{\dot{m}}{\rho \pi [R(x)]^2}$$

The results using this approximation for the free stream velocity approximation are

$$\begin{aligned} \text{St} &= 0.002148 \\ h &= 2867 \text{ W}/(\text{m}^2 \cdot \text{K}) \end{aligned}$$

We see the two approximations are significantly different and are strongly dependent on the boundary layer edge velocity approximation. Because acceleration strongly suppresses the momentum and displacement thicknesses, we did not see this effect in problem 9-7. There is no acceleration term in the corresponding energy equation and the convective transport is changed by the free stream velocity distribution.

For comparison, the thermally fully-developed flow for this problem gives

$$\begin{aligned} \text{Re}_D &= 1460 \\ \text{Nu} &= 3.66 \\ \text{St} &= \frac{\text{Nu}}{\text{Re}_D \text{Pr}} = .000266 \\ h &= 355 \text{ W}/(\text{m}^2 \cdot \text{K}) \end{aligned}$$

10-16

TEXSTAN analysis of the laminar thermal boundary layer over a flat plate with constant surface temperature and zero pressure gradient: Choose a starting x -Reynolds number of about 1000 (a momentum Re of about 20) and pick fluid properties that are appropriate to fluids with a Prandtl number = 0.7, 1.0, and 5.0, evaluated at the free stream temperature. Use constant fluid properties and do not consider viscous dissipation. The geometrical dimensions of the plate are 1 m wide (a unit width) by 0.2 m long in the flow direction, corresponding to an ending Re_x of about 2×10^5 (a momentum Re of about 300). Let the velocity boundary condition at the free stream be 15 m/s and let the energy boundary conditions be a free stream temperature of 300 K and a constant surface temperature of 295 K. The initial velocity and temperature profiles appropriate to the starting x -Reynolds number (Blasius similarity profiles) can be supplied by using the $kstart=4$ choice in TEXSTAN. For each Prandtl number calculate the boundary layer flow and evaluate the concept of boundary-layer similarity by comparing nondimensional temperature profiles at several x locations to themselves for independence of x . Compare the Nusselt number results based on x -Reynolds number with Eq. (10-10). Convert the Nusselt number to Stanton number and compare the Stanton number results based on x -Reynolds number with Eq. (10-13) and based on enthalpy-thickness Reynolds number with Eq. (10-16). Calculate the Stanton number distribution using energy integral Eq. (5-24) and compare with the TEXSTAN calculations. Feel free to investigate any other attribute of the boundary-layer flow.

The data file for this problem is *10.16a.dat.txt*. The data set construction is based on the *s10.dat.txt* file for flow over a flat plate with constant free stream velocity and specified surface temperature (initial profiles: Blasius velocity and Blasius temperature). Note that *kout* has been changed to =2.

For this problem statement, the output file *fm85.txt* presents most of the nondimensional variables needed for comparison. The print variable *k5* was changed to reduce the lines of output for this example, but it would typically much lower to obtain a high resolution for plotting. Here is the output file for $Pr=0.7$

x/s	rex	rem	$cf/2$	reh	st	nu
1.0491386E-03	9.9925781E+02	2.0995E+01	1.050E-02	2.602E+01	1.327E-02	9.280E+00
2.2759022E-03	2.1676955E+03	3.0941E+01	7.130E-03	3.858E+01	9.006E-03	1.366E+01
5.3070683E-03	5.0547463E+03	4.7265E+01	4.667E-03	5.920E+01	5.890E-03	2.084E+01
9.6072666E-03	9.1504937E+03	6.3589E+01	3.469E-03	7.979E+01	4.375E-03	2.802E+01
1.5175948E-02	1.4454415E+04	7.9912E+01	2.760E-03	1.004E+02	3.480E-03	3.521E+01
2.2012902E-02	2.0966309E+04	9.6234E+01	2.292E-03	1.210E+02	2.889E-03	4.240E+01
3.0118088E-02	2.8686138E+04	1.1256E+02	1.959E-03	1.415E+02	2.469E-03	4.958E+01
3.9491493E-02	3.7613889E+04	1.2888E+02	1.711E-03	1.621E+02	2.156E-03	5.677E+01
5.0112671E-02	4.7730088E+04	1.4517E+02	1.519E-03	1.826E+02	1.914E-03	6.395E+01
6.2020205E-02	5.9071484E+04	1.6149E+02	1.366E-03	2.032E+02	1.720E-03	7.114E+01
7.5195952E-02	7.1620796E+04	1.7782E+02	1.240E-03	2.237E+02	1.562E-03	7.833E+01
8.9639910E-02	8.5378024E+04	1.9414E+02	1.136E-03	2.443E+02	1.431E-03	8.552E+01
1.0532451E-01	1.0031691E+05	2.1043E+02	1.048E-03	2.648E+02	1.320E-03	9.270E+01
1.2230275E-01	1.1648793E+05	2.2675E+02	9.726E-04	2.854E+02	1.225E-03	9.989E+01
1.4054921E-01	1.3386686E+05	2.4308E+02	9.073E-04	3.059E+02	1.143E-03	1.071E+02
1.6011250E-01	1.5250003E+05	2.5944E+02	8.501E-04	3.265E+02	1.071E-03	1.143E+02
1.8089844E-01	1.7229771E+05	2.7576E+02	7.998E-04	3.471E+02	1.007E-03	1.215E+02

The corresponding *ftn85.txt* file for Pr=1.0 (the Pr value in the file for Pr=0.7 was all that was changed)

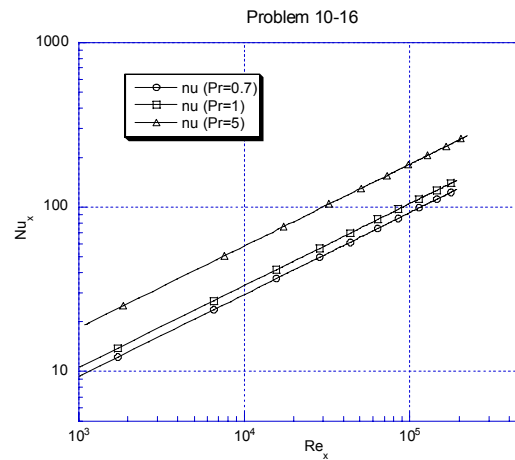
x/s	rex	rem	cf/2	reh	st	nu
1.0473838E-03	9.9758644E+02	2.0978E+01	1.052E-02	2.098E+01	1.052E-02	1.049E+01
2.2750415E-03	2.1668757E+03	3.0934E+01	7.132E-03	3.094E+01	7.131E-03	1.545E+01
5.3054060E-03	5.0531630E+03	4.7244E+01	4.669E-03	4.725E+01	4.669E-03	2.359E+01
9.6028167E-03	9.1462553E+03	6.3562E+01	3.470E-03	6.357E+01	3.470E-03	3.174E+01
1.5167316E-02	1.4446193E+04	7.9880E+01	2.761E-03	7.988E+01	2.761E-03	3.989E+01
2.1998918E-02	2.0952990E+04	9.6196E+01	2.293E-03	9.620E+01	2.293E-03	4.804E+01
3.0097678E-02	2.8666699E+04	1.1251E+02	1.960E-03	1.125E+02	1.960E-03	5.619E+01
3.9463617E-02	3.7587338E+04	1.2883E+02	1.712E-03	1.288E+02	1.712E-03	6.435E+01
5.0112622E-02	4.7730041E+04	1.4517E+02	1.519E-03	1.452E+02	1.519E-03	7.252E+01
6.2014725E-02	5.9066264E+04	1.6148E+02	1.366E-03	1.615E+02	1.366E-03	8.067E+01
7.5184021E-02	7.1609433E+04	1.7780E+02	1.240E-03	1.778E+02	1.240E-03	8.883E+01
8.9620513E-02	8.5359548E+04	1.9411E+02	1.136E-03	1.941E+02	1.136E-03	9.699E+01
1.0532226E-01	1.0031476E+05	2.1043E+02	1.048E-03	2.104E+02	1.048E-03	1.051E+02
1.2229299E-01	1.1647863E+05	2.2674E+02	9.727E-04	2.267E+02	9.727E-04	1.133E+02
1.4053092E-01	1.3384944E+05	2.4306E+02	9.074E-04	2.431E+02	9.074E-04	1.215E+02
1.5990690E-01	1.5230420E+05	2.5927E+02	8.507E-04	2.593E+02	8.507E-04	1.296E+02
1.8067109E-01	1.7208117E+05	2.7558E+02	8.003E-04	2.756E+02	8.003E-04	1.377E+02
2.0000000E-01	1.9049110E+05	2.8995E+02	7.607E-04	2.900E+02	7.607E-04	1.449E+02

Before we compute the flow for Pr=5.0, we need to change some of the input variables because Pr=5 corresponds to water at about 34°C. Using properties at about this temperature, the output file (ftn85.txt)

x/s	rex	rem	cf/2	reh	st	nu
5.4503707E-05	1.0962853E+03	2.1991E+01	1.003E-02	7.470E+00	3.496E-03	1.916E+01
1.1482879E-04	2.3096615E+03	3.1928E+01	6.910E-03	1.093E+01	2.408E-03	2.781E+01
2.6200392E-04	5.2699358E+03	4.8249E+01	4.572E-03	1.662E+01	1.593E-03	4.197E+01
4.6917584E-04	9.4369833E+03	6.4566E+01	3.416E-03	2.230E+01	1.189E-03	5.611E+01
7.3635037E-04	1.4810921E+04	8.0883E+01	2.727E-03	2.798E+01	9.488E-04	7.026E+01
1.0635293E-03	2.1391785E+04	9.7199E+01	2.269E-03	3.366E+01	7.892E-04	8.441E+01
1.4507133E-03	2.9179588E+04	1.1351E+02	1.943E-03	3.933E+01	6.756E-04	9.857E+01
1.8979026E-03	3.8174334E+04	1.2983E+02	1.699E-03	4.500E+01	5.906E-04	1.127E+02
2.4050973E-03	4.8376027E+04	1.4615E+02	1.509E-03	5.068E+01	5.246E-04	1.269E+02
2.9722974E-03	5.9784666E+04	1.6246E+02	1.358E-03	5.635E+01	4.718E-04	1.410E+02
3.5995030E-03	7.2400254E+04	1.7878E+02	1.234E-03	6.202E+01	4.287E-04	1.552E+02
4.2867142E-03	8.6222790E+04	1.9509E+02	1.131E-03	6.769E+01	3.929E-04	1.694E+02
5.0339308E-03	1.0125227E+05	2.1141E+02	1.043E-03	7.336E+01	3.625E-04	1.835E+02
5.8411530E-03	1.1748871E+05	2.2772E+02	9.685E-04	7.903E+01	3.365E-04	1.977E+02

6.7083807E-03	1.3493209E+05	2.4404E+02	9.038E-04	8.470E+01	3.140E-04	2.119E+02
7.6356140E-03	1.5358242E+05	2.6035E+02	8.471E-04	9.036E+01	2.943E-04	2.260E+02
8.6228528E-03	1.7343970E+05	2.7667E+02	7.972E-04	9.603E+01	2.770E-04	2.402E+02
9.6700972E-03	1.9450393E+05	2.9299E+02	7.528E-04	1.017E+02	2.615E-04	2.543E+02
1.0777347E-02	2.1677511E+05	3.0930E+02	7.131E-04	1.074E+02	2.477E-04	2.685E+02
1.1000000E-02	2.2125354E+05	3.1248E+02	7.058E-04	1.085E+02	2.452E-04	2.713E+02

Comparing the three data sets is best done by plotting. Also, in the $Pr=1$ output we clearly see the Reynolds analogy where $c_f/2 = St$



The data can be easily compared with the Blasius solution, Eq. (10-10) by changing the input file print variable to $kout=8$, which prints ratios of the TEXSTAN-computed friction coefficient and Nusselt number to the Blasius solution. Here is an abbreviated listing of the output file for $Pr=5$ (it will be called *out.txt* when you execute TEXSTAN using an input data set)

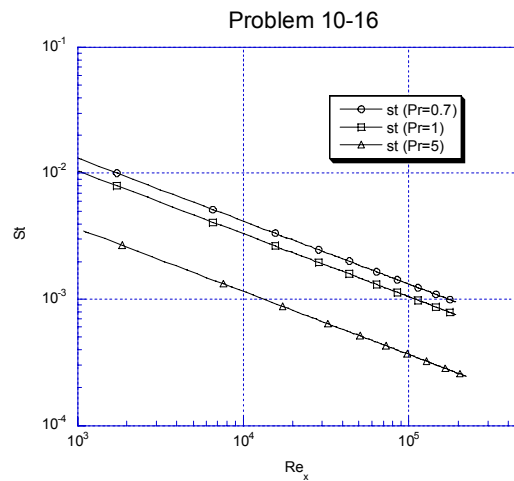
intg	rex	rem	cf2	nu	cfrat	nurat	h12	reh
5	1.096E+03	2.199E+01	1.003E-02	19.2	1.000	1.025	2.590	7.470E+00
100	2.310E+03	3.193E+01	6.910E-03	27.8	1.000	1.025	2.590	1.093E+01
200	5.270E+03	4.825E+01	4.572E-03	42.0	1.000	1.024	2.590	1.662E+01
300	9.437E+03	6.457E+01	3.416E-03	56.1	1.000	1.023	2.590	2.230E+01
400	1.481E+04	8.088E+01	2.727E-03	70.3	1.000	1.022	2.590	2.798E+01
500	2.139E+04	9.720E+01	2.269E-03	84.4	1.000	1.022	2.590	3.366E+01
600	2.918E+04	1.135E+02	1.943E-03	98.6	1.000	1.022	2.590	3.933E+01
700	3.817E+04	1.298E+02	1.699E-03	112.7	1.000	1.022	2.590	4.500E+01
800	4.838E+04	1.461E+02	1.509E-03	126.9	1.000	1.022	2.590	5.068E+01
900	5.978E+04	1.625E+02	1.358E-03	141.0	1.000	1.022	2.590	5.635E+01
1000	7.240E+04	1.788E+02	1.234E-03	155.2	1.000	1.021	2.590	6.202E+01

1100	8.622E+04	1.951E+02	1.131E-03	169.4	1.000	1.021	2.590	6.769E+01
1200	1.013E+05	2.114E+02	1.043E-03	183.5	1.000	1.021	2.590	7.336E+01
1300	1.175E+05	2.277E+02	9.685E-04	197.7	1.000	1.021	2.590	7.903E+01
1400	1.349E+05	2.440E+02	9.038E-04	211.9	1.000	1.021	2.590	8.470E+01
1500	1.536E+05	2.604E+02	8.471E-04	226.0	1.000	1.021	2.590	9.036E+01
1600	1.734E+05	2.767E+02	7.972E-04	240.2	1.000	1.021	2.590	9.603E+01
1700	1.945E+05	2.930E+02	7.528E-04	254.3	1.000	1.021	2.590	1.017E+02
1800	2.168E+05	3.093E+02	7.131E-04	268.5	1.000	1.021	2.590	1.074E+02
1820	2.213E+05	3.125E+02	7.058E-04	271.3	1.000	1.021	2.590	1.085E+02

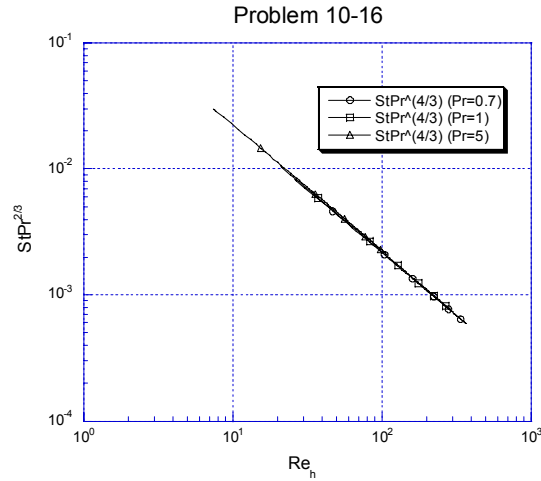
In this output we see the c_{frat} value is 1.000 for all Re_x , and the corresponding $nurat$ is within 2%. This 2% error will not be there for $Pr=0.7$ or $Pr=1$. Recall the Blasius theory is

$$Nu_x = \theta'(\eta=0) Re_x^{1/2}$$

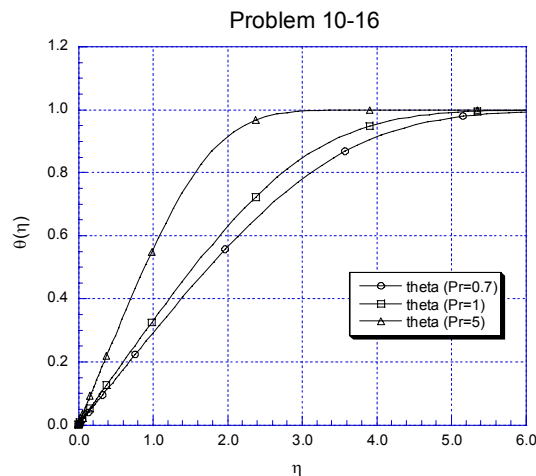
and $\theta'(\eta=0) = 0.332 Pr^{1/3}$ is merely a curve-fit for gases and light liquids ($0.7 \leq Pr \leq (10-20)$). Here is the Stanton number data for comparison with Eq. (10-13)



To confirm the correlation between Stanton number and the enthalpy-thickness Reynolds number, we can use Eq. (10-16). The plot below compares $St Pr^{4/3}$ and the slope will be 0.2204 on this ln-ln graph.



To plot the developing temperature profiles for a given Pr or to plot profiles for different Pr , choose either $k10=10$ for nondimensional profiles (Blasius variables) or $k10=11$ for dimensional variables. The profiles will be printed as a part of the file *out.txt*. You can choose where to print the profiles by adding x locations to the $x(m)$. Be sure to change the two nxb variables and add the appropriate sets of two lines of boundary condition information for each new x -location. This is explained in detail in the *s10.man* user manual. The plot shown below shows the Blasius similarity for the flat-plate laminar boundary layer with $u_\infty = c$ and the three Prandtl numbers at an arbitrary x -location. We can compare this plot with Fig. 10-2.



To confirm the energy integral equation for computing Stanton number, Eq. (5-24), use the enthalpy thickness data in *ftn84.txt*. Note that this equation requires constant surface temperature and constant free stream velocity and flow over a flat surface. The enthalpy thickness distribution is contained in the output file *ftn84.txt*. You will want to set $k5=1$ to obtain enough points for numerically approximating $d\Delta_2/dx$, and use of a higher-order first-derivative approximation is useful. In the world of experimental heat transfer, this can be a good estimation of the Stanton number.

10-17

TEXSTAN analysis of the laminar thermal boundary layer stagnation flow (the Falkner-Skan $m = 1$ case) and constant surface temperature: Refer to Prob. 9-8 for the plate geometry and the setup of the velocity boundary condition. Pick fluid properties that are appropriate to fluids with a Prandtl number = 0.7, 1.0, and 5.0, evaluated at the free stream temperature. Use constant fluid properties and do not consider viscous dissipation. The energy boundary conditions are a free stream temperature of 300 K and a constant surface temperature of 295 K. For each Prandtl number calculate the boundary layer flow and evaluate the concept of boundary-layer similarity by comparing nondimensional temperature profiles at several x locations to themselves for independence of x . Compare the Nusselt number results based on x -Reynolds number with Table 10-2. Evaluate the concepts of thermal and velocity profile similarity for $Pr = 1.0$, examine the development of the momentum and thermal boundary layers, and discuss the validity of $h = \text{const}$ for this case. Convert the Nusselt number to Stanton number calculate the Stanton number distribution using energy integral Eq. (5-24) and compare with the TEXSTAN calculations. Also, evaluate the validity of the approximate integral solution, Eq. (10-52). Feel free to investigate any other attribute of the boundary-layer flow.

The data file for this problem is *10.17.dat.txt*. The data set construction is based on the *s15.dat.txt* file for flow over a flat plate with variable free stream velocity and specified surface temperature (initial profiles: Falkner-Skan $m=1$ velocity and temperature). Note that *kout* has been changed to =2.

There needs to be a slight modification to the instructions in the problem statement regarding the calculations of $xstart$ and axx . For the given starting x -Reynolds number =200, there are not unique numbers for $xstart$ and axx , so choose $xstart$ (=0.00195 m) which uniquely determines the value of free stream velocity at that location (=1.615 m/s), and then calculate A (which is the variable axx) to match this velocity, $u_{\infty} = A \cdot xstart$ for $B=1$, $C=0$ and $m=1$.

For this problem statement, the output file *fm85.txt* presents most of the nondimensional variables needed for comparison. The print variable *k5* was changed to reduce the lines of output for this example, but it would typically much lower to obtain a high resolution for plotting. Here is the output file for $Pr=0.7$

x/s	rex	rem	$cf/2$	reh	st	nu
1.9664195E-03	2.0337307E+02	4.1689E+00	8.640E-02	1.009E+01	4.968E-02	7.072E+00
7.1044387E-03	2.6546094E+03	1.5086E+01	2.387E-02	3.647E+01	1.375E-02	2.555E+01
1.3677744E-02	9.8394315E+03	2.9020E+01	1.241E-02	7.024E+01	7.142E-03	4.919E+01
2.0229941E-02	2.1524365E+04	4.2910E+01	8.393E-03	1.039E+02	4.829E-03	7.275E+01
2.6799205E-02	3.7773298E+04	5.6836E+01	6.337E-03	1.377E+02	3.645E-03	9.638E+01
3.3367786E-02	5.8559299E+04	7.0760E+01	5.090E-03	1.714E+02	2.927E-03	1.200E+02
3.9935931E-02	8.3881988E+04	8.4683E+01	4.253E-03	2.051E+02	2.446E-03	1.436E+02
4.6502162E-02	1.1373323E+05	9.8603E+01	3.653E-03	2.389E+02	2.101E-03	1.672E+02
5.3069782E-02	1.4812750E+05	1.1253E+02	3.201E-03	2.726E+02	1.841E-03	1.909E+02
5.9637231E-02	1.8705789E+05	1.2645E+02	2.848E-03	3.064E+02	1.638E-03	2.145E+02
6.6206109E-02	2.3053518E+05	1.4037E+02	2.566E-03	3.401E+02	1.475E-03	2.381E+02
7.2773314E-02	2.7853860E+05	1.5429E+02	2.334E-03	3.738E+02	1.342E-03	2.617E+02
7.9340428E-02	3.3107788E+05	1.6821E+02	2.141E-03	4.076E+02	1.231E-03	2.853E+02
8.5907466E-02	3.8815296E+05	1.8214E+02	1.978E-03	4.413E+02	1.137E-03	3.090E+02

8.7207000E-02	3.9998507E+05	1.8489E+02	1.948E-03	4.480E+02	1.120E-03	3.136E+02
---------------	---------------	------------	-----------	-----------	-----------	-----------

The data can be easily compared with the Falkner-Skan solution, Table 10-2, by changing the input file print variable to *kout=8*, which prints ratios of the TEXSTAN-computed friction coefficient and Nusselt number to the Blasius solution. Here is an abbreviated listing of the output file for $Pr=0.7$ (it will be called *out.txt* when you execute TEXSTAN using an input data set)

intg	rex	rem	cf2	nu	cf _{frat}	nurat	h12	reh
5	2.034E+02	4.169E+00	8.640E-02	7.1	.999	.997	2.216	1.009E+01
200	2.655E+03	1.509E+01	2.387E-02	25.5	.997	.997	2.216	3.647E+01
400	9.839E+03	2.902E+01	1.241E-02	49.2	.998	.997	2.216	7.024E+01
600	2.152E+04	4.291E+01	8.393E-03	72.8	.999	.997	2.216	1.039E+02
800	3.777E+04	5.684E+01	6.337E-03	96.4	.999	.997	2.216	1.377E+02
1000	5.856E+04	7.076E+01	5.090E-03	120.0	.999	.997	2.216	1.714E+02
1200	8.388E+04	8.468E+01	4.253E-03	143.6	.999	.997	2.216	2.051E+02
1400	1.137E+05	9.860E+01	3.653E-03	167.2	.999	.997	2.216	2.389E+02
1600	1.481E+05	1.125E+02	3.201E-03	190.9	.999	.997	2.216	2.726E+02
1800	1.871E+05	1.264E+02	2.848E-03	214.5	.999	.997	2.216	3.064E+02
2000	2.305E+05	1.404E+02	2.566E-03	238.1	.999	.997	2.216	3.401E+02
2200	2.785E+05	1.543E+02	2.334E-03	261.7	.999	.997	2.216	3.738E+02
2400	3.311E+05	1.682E+02	2.141E-03	285.3	.999	.997	2.216	4.076E+02
2600	3.882E+05	1.821E+02	1.978E-03	309.0	.999	.997	2.216	4.413E+02
2640	4.000E+05	1.849E+02	1.948E-03	313.6	.999	.997	2.216	4.480E+02

We can see from the various files that there is duplication, and which to choose depends on the plotting data needs. In the benchmark output (*kout=8*) we see the *cf_{frat}* and *nurat*, which present a ratio of TEXSTAN-calculated values for c_f and Nu to Falkner-Skan $m=1$ solution values at the same x -Reynolds number, Table 9-2 for momentum and Table 10-2 for heat transfer. We can use these ratios to help determine if a data set construction is correct. At the present time only some of the “*s*” data sets in Appendix H can be used with *kout=8*.

Here is an abbreviated listing of the output file for $Pr=1.0$ (it will be called *out.txt* when you execute TEXSTAN using an input data set)

intg	rex	rem	cf2	nu	cf _{frat}	nurat	h12	reh
5	2.007E+02	4.141E+00	8.700E-02	8.1	1.000	1.003	2.213	8.154E+00
200	2.725E+03	1.528E+01	2.357E-02	29.8	.998	1.003	2.216	2.980E+01
400	9.970E+03	2.921E+01	1.233E-02	56.9	.998	1.003	2.216	5.697E+01
600	2.173E+04	4.312E+01	8.353E-03	84.1	.999	1.003	2.216	8.411E+01
800	3.805E+04	5.704E+01	6.314E-03	111.3	.999	1.003	2.216	1.113E+02
1000	5.889E+04	7.097E+01	5.076E-03	138.4	.999	1.003	2.216	1.384E+02
1200	8.429E+04	8.489E+01	4.243E-03	165.6	.999	1.003	2.216	1.656E+02
1400	1.142E+05	9.881E+01	3.645E-03	192.8	.999	1.003	2.216	1.928E+02
1600	1.487E+05	1.127E+02	3.195E-03	220.0	.999	1.003	2.216	2.200E+02

1800	1.876E+05	1.267E+02	2.844E-03	247.1	.999	1.003	2.216	2.471E+02
2000	2.312E+05	1.406E+02	2.562E-03	274.3	.999	1.003	2.216	2.743E+02
2200	2.793E+05	1.545E+02	2.331E-03	301.5	.999	1.003	2.216	3.015E+02
2400	3.319E+05	1.684E+02	2.139E-03	328.6	.999	1.003	2.216	3.286E+02
2600	3.890E+05	1.823E+02	1.976E-03	355.8	.999	1.003	2.216	3.558E+02
2637	4.000E+05	1.849E+02	1.948E-03	360.8	.999	1.003	2.216	3.608E+02

Once again we see the *cf_{rat}* and *nurat* show agreement between the theoretical Falkner-Skan solution and the TEXSTAN-computed solution. It is interesting to examine the output file *f85.txt* to compare the *cf_f/2* value with the *st* value to see the Reynolds analogy for *Pr*=1 will not hold if there is a pressure gradient.

x/s	rex	rem	cf/2	reh	st	nu
1.9664195E-03	2.0337307E+02	4.1689E+00	8.640E-02	1.009E+01	4.968E-02	7.072E+00
7.1044387E-03	2.6546094E+03	1.5086E+01	2.387E-02	3.647E+01	1.375E-02	2.555E+01
1.3677744E-02	9.8394315E+03	2.9020E+01	1.241E-02	7.024E+01	7.142E-03	4.919E+01
2.0229941E-02	2.1524365E+04	4.2910E+01	8.393E-03	1.039E+02	4.829E-03	7.275E+01
2.6799205E-02	3.7773298E+04	5.6836E+01	6.337E-03	1.377E+02	3.645E-03	9.638E+01
3.3367786E-02	5.8559299E+04	7.0760E+01	5.090E-03	1.714E+02	2.927E-03	1.200E+02
3.9935931E-02	8.3881988E+04	8.4683E+01	4.253E-03	2.051E+02	2.446E-03	1.436E+02
4.6502162E-02	1.1373323E+05	9.8603E+01	3.653E-03	2.389E+02	2.101E-03	1.672E+02
5.3069782E-02	1.4812750E+05	1.1253E+02	3.201E-03	2.726E+02	1.841E-03	1.909E+02
5.9637231E-02	1.8705789E+05	1.2645E+02	2.848E-03	3.064E+02	1.638E-03	2.145E+02
6.6206109E-02	2.3053518E+05	1.4037E+02	2.566E-03	3.401E+02	1.475E-03	2.381E+02
7.2773314E-02	2.7853860E+05	1.5429E+02	2.334E-03	3.738E+02	1.342E-03	2.617E+02
7.9340428E-02	3.3107788E+05	1.6821E+02	2.141E-03	4.076E+02	1.231E-03	2.853E+02
8.5907466E-02	3.8815296E+05	1.8214E+02	1.978E-03	4.413E+02	1.137E-03	3.090E+02
8.7207000E-02	3.9998507E+05	1.8489E+02	1.948E-03	4.480E+02	1.120E-03	3.136E+02

Here is an abbreviated listing of the output file for *Pr*=5.0 (it will be called *out.txt* when you execute TEXSTAN using an input data set). Note this accelerating flow causes a fairly strong pressure gradient, and the initial pressure needs to be large enough so the pressure does not go negative. For this data set it was increased to 4 atmospheres. The negative pressure-checking in TEXSTAN is only a preventative measure for when variable properties are used.

intg	rex	rem	cf2	nu	cfrat	nurat	h12	reh
5	2.789E+02	4.882E+00	7.377E-02	17.4	.999	1.004	2.215	3.530E+00
200	3.034E+03	1.613E+01	2.233E-02	57.4	.998	1.003	2.216	1.152E+01
400	1.055E+04	3.006E+01	1.198E-02	107.1	.998	1.003	2.216	2.146E+01
600	2.261E+04	4.398E+01	8.190E-03	156.8	.999	1.003	2.216	3.140E+01
800	3.914E+04	5.786E+01	6.226E-03	206.4	.999	1.004	2.216	4.130E+01
1000	6.024E+04	7.178E+01	5.019E-03	256.0	.999	1.004	2.216	5.124E+01
1200	8.588E+04	8.570E+01	4.204E-03	305.7	.999	1.004	2.216	6.117E+01

1400	1.160E+05	9.961E+01	3.616E-03	355.4	.999	1.004	2.216	7.110E+01
1600	1.507E+05	1.135E+02	3.173E-03	405.1	.999	1.004	2.216	8.104E+01
1800	1.900E+05	1.274E+02	2.827E-03	454.8	.999	1.004	2.216	9.097E+01
2000	2.338E+05	1.414E+02	2.548E-03	504.4	.999	1.004	2.216	1.009E+02
2200	2.821E+05	1.553E+02	2.320E-03	554.1	.999	1.004	2.216	1.108E+02
2400	3.349E+05	1.692E+02	2.129E-03	603.8	.999	1.004	2.216	1.208E+02
2600	3.923E+05	1.831E+02	1.967E-03	653.5	.999	1.004	2.216	1.307E+02
2769	4.443E+05	1.949E+02	1.849E-03	695.5	.999	1.004	2.216	1.391E+02

Once again we see the *cf_{rat}* and *nurat* show agreement between the theoretical Falkner-Skan solution and the TEXSTAN-computed solution for this higher Pr value.

To plot the developing velocity profiles, choose either *k10*=10 for nondimensional profiles (Blasius variables) or *k10*=11 for dimensional variables. The profiles will be printed as a part of the file *out.txt*. You can choose where to print the profiles by adding *x* locations to the *x(m)*. Be sure to change the two *nxbc* variables and add the appropriate sets of two lines of boundary condition information for each new *x*-location. This is explained in detail in the *s10.man* user manual.

To confirm the energy integral equation for computing Stanton number, we use the ideas in Chapter 5. Be careful, you can not use Eq. (5-24), because this equation requires a constant free stream velocity, along with a constant surface temperature and flow over a flat surface. Instead, use Eq. (5-18) to compute the surface heat flux in terms of the enthalpy thickness variation and free stream velocity variation and then formulate the Stanton number. The enthalpy thickness distribution is contained in the output file *fm84.txt*. You will want to set *k5*=1 to obtain enough points for numerically approximating $d\Delta_2/dx$, and use of a higher-order first-derivative approximation is useful. In the world of experimental heat transfer, this can be a good estimation of the Stanton number.

11-1

Using the Van Driest equation for the mixing length in the sublayer, determine u^+ as a function of y^+ for $p^+ = 0$ and $v_s^+ = 0$ by numerical integration of the momentum equation in the region where the Couette flow approximation is valid, for $A^+ = 22, 25$, and 27 , and compare with the experimental data in Fig. 11-3. (It is presumed that a programmable computer is used for this problem.)

The equation which must be numerically integrated is :

$$\frac{du^+}{dy^+} = \frac{2}{1 + \sqrt{1 + 4\kappa^2 y^{+2} D^2}}$$

where $D = 1 - e^{-y^+/A^+}$

The following table lists some values of $u^+(y^+)$ which will be obtained using various value of A^+

y^+	$A^+=22$	$A^+=25$	$A^+=27$	Eq. (11-16)
59.59	14.41	15.01	15.40	14.97
79.32	15.13	15.75	16.14	15.67
95.97	15.60	16.22	16.62	16.14

11-2

Develop a law of the wall for a transpired turbulent boundary layer (that is, $v_s^+ \neq 0$) based on the Prandtl mixing-length theory and a two-layer model of the Couette flow region near the wall. Note that you need to develop a new relation for both the viscous sublayer and the fully turbulent region, and the apparent thickness of the sublayer will be a constant to be determined from experiments. The table at the top of the next page shows two sets of experimental points for turbulent velocity profiles for $p^+ = 0$ but $v_s^+ \neq 0$. Plot these profiles on semi-logarithmic paper and superimpose the equation you have derived for the fully turbulent region, determining the apparent sublayer thickness from the best fit to the data. Note that there is a “wake” or outer region for which your analysis does not apply. Finally, plot the apparent sublayer thickness y_{crit}^+ as a function of v_s^+ and discuss the significance of the results.

$v_s^+ = 0.1773$		$v_s^+ = -0.065$	
y^+	u^+	y^+	u^+
30.6	16.84	35.6	12.33
50.3	19.37	48.7	13.02
99.6	23.41	81.7	13.59
148.9	25.72	150.8	14.24
247.6	29.99	249.6	14.80
362.6	34.11	364.8	15.34
510.6	39.36	496.5	15.87
724.3	45.13	628.2	16.20
921.5	47.29	792.8	16.31
1053.0	47.32	990.4	16.31

For

$$y^+ \leq y_{crit}^+, \quad u^+ = \frac{1}{v_s^+} \exp\left(\frac{v_s^+ y_{crit}^+}{2}\right) - \frac{1}{v_s^+}$$

For

$$y^+ > y_{crit}^+, \quad u^+ = \frac{v_s^+}{4\kappa^2} \left(\ln \frac{y^+}{y_{crit}^+}\right)^2 + \frac{1}{\kappa} \exp\left(\frac{v_s^+ y_{crit}^+}{2}\right) \ln \frac{y^+}{y_{crit}^+} + \frac{1}{v_s^+} \exp\left(\frac{v_s^+ y_{crit}^+}{2}\right) + \frac{1}{v_s^+}$$

for $v_s^+ = 0.1773$, $y_{crit}^+ \approx 4.4$ and $v_s^+ = -0.065$, $y_{crit}^+ \approx 35$

11-3

Repeat Prob. 11-2 using the Van Driest equation for the sublayer mixing length and numerical integration of the momentum equation. Determine the values of A^+ that best fit the experimental data, and plot these as a function of v_s^+ . (It is presumed that a programmable computer is used for this problem.)

The equation which must be numerically integrated is:

$$\frac{du^+}{dy^+} = \frac{2(1 + v_s^+ u^+)}{1 + \sqrt{1 + 4\kappa^2 y^{+2} D^2 (1 + v_s^+ u^+)^2}}$$

where $D = 1 - \exp(-y^+/A^+)$

For $v_s^+ = 0.1773$, $A^+ \approx 10.2$ and $v_s^+ = -0.065$, $A^+ \approx 80$

Eq. (11-26) gives close to the same result for the first case, but gives 60 for the second. This is simply the result of fairly large experimental uncertainty for the experiments with strong suction.

11-4

Consider constant-property flow along a flat plate with constant u_∞ . Let the boundary layer starting at the origin of the plate be laminar, but assume that a transition to a turbulent boundary layer takes place abruptly at some prescribed critical Reynolds number. Assuming that at the point of transition the momentum thickness of the turbulent boundary layer is the same as the laminar boundary layer (and this is a point for discussion), calculate the development of the turbulent boundary layer and the friction coefficient for the turbulent boundary layer. Plot the friction coefficient as a function of Reynolds number on log-log paper for transition Reynolds numbers (based on distance from the leading edge) of 300,000 and 1,000,000, and compare with the turbulent flow friction coefficient that would obtain were the boundary layer turbulent from the plate origin. On the basis of these results, determine a “virtual origin” of a turbulent boundary layer preceded by a laminar boundary layer; that is, the turbulent boundary layer will behave as if the boundary layer had been entirely a turbulent one starting at the virtual origin.

In the turbulent region:

$$C_f/2 = 0.0287 \left[\text{Re}_x + (37\text{Re}_t^{0.625} - \text{Re}_t) \right]^{-0.2}$$

where Re_t is the transition Reynolds number. The virtual origin of the turbulent boundary layer will be at:

$$x = \frac{\nu}{u_\infty} [\text{Re}_t - 37\text{Re}_t^{0.625}]$$

11-5

Redevelop Eq. (11-21) for the case where density and viscosity are functions of x .

Following the steps for this equation leads to

$$\delta_2 = \frac{0.036}{\rho R u_\infty^{3.29}} \left[\int_0^x \mu^{.25} \rho R^{1.25} u_\infty^{3.86} dx \right]^{0.8}$$

11-6

A nuclear rocket nozzle of circular cross section has the geometry shown in Fig. 11-18. The working fluid is helium, and the stagnation pressure and temperature are 2100 kPa and 2475 K, respectively. Assuming one-dimensional isentropic flow, constant specific heats, and a specific heat ratio of 1.67, calculate the mass flow rate and the gas pressure, temperature, and density as functions of distance along the axis. Then, assuming that a laminar boundary layer originates at the corner where the convergence starts, calculate the momentum thickness of the boundary layer and the momentum thickness Reynolds number as functions of distance along the surface. Assume that a transition to a turbulent boundary layer takes place if and when the momentum thickness Reynolds number exceeds 162. An approximate analysis may be carried out on the assumption of constant fluid properties, in which case let the properties be those obtaining at the throat. Alternatively, a better approximation can be based on the results of Prob. 11-5. In either case it may be assumed that the viscosity varies approximately linearly from $\mu = 5.9 \times 10^{-5}$ Ns/m² at 1400 K to $\mu = 8.3 \times 10^{-5}$ Ns/m² at 2500 K.

z, cm (axial)	x, cm	P, kPa	T, K	δ_2 , m	Re_{δ_2}
0	0	2089.5	2473	0	0
1	1.38	2087.4	2471	6.77E-5	70.5
2	2.75	2085.2	2468	7.84E-5	94.8
3	4.13	2079.0	2466	7.81E-5	111
4	5.50	2072.7	2463	7.29E-5	123
5	6.88	2062.2	2457	6.54E-5	134
6	8.25	2051.7	2450	5.68E-5	144
8 transition	11.0	1932.0	2401	3.87E-5	164
10	13.7	1627.5	2232	5.13E-5	369
12 throat	15.7	1022.1	1854	5.16E-5	504
14	17.5	449.40	1332	7.50E-5	745
16	19.8	189.40	943	1.56E-4	1362
18	22.1	95.970	718	2.90E-4	2200
22	26.7	36.120	485	6.59E-4	3854

The resulting mass flow rate is $\dot{m} = 5.28$ kg/s

11-7

Work Prob. 11-6 but let the fluid be air and the stagnation pressure and temperature be 2100 kPa and 1275 K, respectively. Calculate the displacement thickness of the boundary layer at the throat of the nozzle. Is any correction to the mass flow rate warranted on the basis of this latter calculation?

z, cm (axial)	x, cm	P, kPa	T, K	δ_z , m	Re_{δ_z}
0 transition	0	2100.0	1275	0	0
1.56	2.15	2090.6	1273	3.13E-5	209
2.36	3.22	2088.1	1273	5.00E-5	375
3	4.13	2085.1	1272	5.87E-5	489
4	5.5	2079.0	1271	6.26E-5	627
6	8.25	2053.1	1267	5.99E-5	906
8	11	1964.6	1251	4.60E-5	1153
10	13.7	1672.0	1195	3.77E-5	1577
12 throat	15.7	1109.4	1063	3.65E-5	2014
14	17.5	531.85	861	5.19E-5	2683
18	22.1	139.23	587	3.01E-4	10075
22	26.7	58.901	459	6.19E-4	14158
28	33.6	23.90	355	1.47E-3	22418
34	40.5	12.12	292	2.88E-3	32082

The resulting mass flow rate is $\dot{m} = 18.7$ kg/s

11-8

A gas turbine blade, as illustrated in Fig. 11-19, has the following operating conditions:

Fluid: air

Stagnation conditions: $P_s = 515.7 \text{ kPa}$, $T_s = 1139 \text{ K}$

Conditions just upstream of the blade:

$$P = 473.7 \text{ kPa}, \quad T = 1111 \text{ K}$$

$$V = 253 \text{ m/s}, \quad G = 376 \text{ kg}/(\text{s} \cdot \text{m}^2)$$

Free-stream conditions along blade surface (see Fig. 11-19):

Point	Distance from leading edge, cm	G_∞ , kg/(s · m ²)	ρ , kg/m ³	T , K
<i>a</i>	0.38	537	1.36	1072
<i>b</i>	1.40	586	1.31	1052
<i>c</i>	2.41	635	1.10	988
<i>d</i>	3.18	620	1.23	1031
<i>e</i>	4.19	576	1.31	1056
<i>f</i>	5.21	547	1.34	1068
<i>g</i>	6.22	537	1.36	1072
<i>h</i>	0.25	293	1.52	1122
<i>i</i>	1.27	317	1.51	1121
<i>j</i>	2.29	327	1.51	1118
<i>k</i>	3.30	352	1.50	1116
<i>l</i>	4.32	430	1.45	1100
<i>m</i>	5.33	537	1.36	1072

Calculate the momentum thickness and the momentum thickness Reynolds number along both surfaces of the blade. Assume that a transition to a turbulent boundary layer takes place when the momentum thickness Reynolds number exceeds 162. Describe how the forces acting on the blade could be analyzed from the given data.

This problem is a direct application of Eq.(9-42) for the laminar parts, and Eq.(11-21) for the turbulent parts. (The R cancels out in both cases.) Problems 9-4 and 11-5 should be solved first to get equation forms applicable to varying free-stream density. The laminar stagnation region near the leading edge is probably best handled by using Eq.(10-20) to evaluate the local velocity tangential to the surface, but just outside of the boundary layer. (Note that $u_\infty = 0$ at $x = 0$.) The momentum thickness at the stagnation point will be finite, not zero. Because there is a laminar boundary layer preceding the turbulent boundary layer, Eq.(11-21) should be modified by using the value of δ_2 from the laminar analysis as the lower limit on δ_2 when integrating the equation preceding (11-21).

x , cm from stagnation point	Re_{δ_2} upper surface	Re_{δ_2} lower surface
0.2	82	59
0.5	140	105
1.0	200	152
2.0	430	260
3.0	820	420
5.0	1900	450
6.0	2200	-

11-9

The following table is an actual velocity profile measured through a turbulent boundary layer on a rough surface made up of 1.27 mm balls packed in a dense, regular pattern. There is no pressure gradient

y , cm	u , m/s	y , cm	u , m/s
0.020	12.94	0.660	27.38
0.030	14.08	1.10	31.10
0.051	15.67	1.61	34.15
0.081	17.31	2.12	37.21
0.127	19.24	2.82	39.37
0.191	20.87	3.58	39.68
0.279	22.68		
0.406	24.54		

or transpiration. The fluid is air at 1 atm and 19°C; and $u_\infty = 39.7$ m/s, $\delta_2 = 0.376$ cm, $Re_{\delta_2} = 9974$, $c_f/2 = 0.00243$. The distance y is measured from the plane of the tops of the balls. The objective of this problem is to analyze these data in the framework of the rough-surface theory developed in the text. What is the apparent value of k_s ? Of Re_k ? What is the roughness regime? What is the apparent value of κ ? How does the wake compare with that of a smooth surface? Do the data support the theory? The use of the plane of the tops of the balls as the origin for y is purely arbitrary. Feel free to move the origin if this will provide a more coherent theory.

The apparent roughness is $k_s = 0.05$ cm and $Re_k = 124$. The surface is fully rough. To fit the theory the origin for y should be shifted a distance of 0.018 cm into the wall. The data then fit Eq. (11-56) very well, although of course there is a distinct "wake" region, virtually identical to that for a smooth surface. $c_f/2$ corresponds closely to Eq. (11-57).

11-10

TEXSTAN analysis of the turbulent momentum boundary layer over a flat plate with zero pressure gradient: Choose a starting x -Reynolds number of about 2×10^5 (corresponding to a momentum Reynolds number of about 700) and pick fluid properties that are appropriate to air, evaluated at a free stream temperature of 300 K. Use constant fluid properties, and note that the energy equation does not have to be solved. The geometrical dimensions of the plate are 1 m wide (a unit width) by 3.0 m long in the flow direction, corresponding to an ending Re_x of about 2.9×10^6 (a momentum Reynolds number of about 5400). Let the velocity boundary condition at the free stream be 15 m/s. The initial velocity profile appropriate to the starting x -Reynolds number (a fully turbulent boundary layer profile) can be supplied by using the $kstart=3$ choice in TEXSTAN. For a turbulence model, choose the mixing-length turbulence model with the Van Driest damping function ($ktmu=5$). Calculate the boundary layer flow and compare the friction coefficient results based on x Reynolds number and momentum thickness Reynolds number with the results in the text, Eqs. (11-20) and (11-23). Evaluate the virtual origin concept as described in Prob. 11-4, and observe whether this affects your ability to compare with Eq. (11-23). Calculate the friction coefficient distribution using momentum integral Eq. (5-11) and compare with the TEXSTAN calculations. Feel free to investigate any other attribute of the boundary-layer flow. For example, you can investigate the mixing length distribution, comparing to Fig. 11-2 and the law of the wall, comparing to Fig. 11-5.

The data file for this problem is *11.10.dat.txt*. The data set construction is based on the *200_5.dat.txt* file for flow over a flat plate with constant free stream velocity and specified surface temperature (initial profiles: fully turbulent velocity and temperature profiles). The turbulence model is the van-Driest mixing length model, along with a variable turbulent Prandtl number model for liquid metals and gases, and a constant turbulent Prandtl number for liquids. Note that the turbulent data set manual *s200.man.doc* is very helpful in understanding this data set construction.

Here is an abbreviated listing of the output file (it will be called *out.txt* when you execute TEXSTAN using an input data set)

intg	rex	rem	cf2	st	cfrat	strat	hl2	reh
5	2.020E+05	6.963E+02	2.496E-03	3.149E-03	1.026	1.043	1.469	5.877E+02
250	2.753E+05	8.744E+02	2.345E-03	2.891E-03	1.020	1.037	1.454	8.100E+02
500	3.804E+05	1.112E+03	2.181E-03	2.636E-03	1.008	1.021	1.437	1.099E+03
750	5.113E+05	1.388E+03	2.054E-03	2.450E-03	1.003	1.014	1.422	1.431E+03
1000	6.729E+05	1.711E+03	1.946E-03	2.301E-03	1.001	1.010	1.408	1.814E+03
1250	8.704E+05	2.086E+03	1.852E-03	2.175E-03	1.001	1.008	1.397	2.256E+03
1500	1.109E+06	2.518E+03	1.769E-03	2.067E-03	1.002	1.008	1.387	2.762E+03
1750	1.396E+06	3.015E+03	1.694E-03	1.972E-03	1.004	1.009	1.380	3.341E+03
2000	1.738E+06	3.581E+03	1.626E-03	1.888E-03	1.006	1.010	1.373	4.000E+03
2250	2.141E+06	4.224E+03	1.565E-03	1.813E-03	1.009	1.012	1.367	4.746E+03
2500	2.614E+06	4.951E+03	1.508E-03	1.744E-03	1.012	1.014	1.363	5.587E+03
2630	2.891E+06	5.365E+03	1.480E-03	1.711E-03	1.014	1.015	1.361	6.065E+03

In the benchmark output ($kout=8$) we see $cfrat$ and $strat$, which present ratios of TEXSTAN-calculated values for c_f to Eq. (11-20) at the same momentum-thickness Reynolds number and for St to Eq. (12-19) at the same enthalpy-thickness Reynolds number. We can use these ratios to help determine if a data set construction is correct. At the present time only some of the “s” data sets in Appendix H can be used with $kout=8$. We see the $cfrat$ and $strat$ show agreement between the turbulent correlations and the TEXSTAN-computed solution.

The output file *fn85.txt* presents most of the dimensionless variables needed for comparison, including the x Reynolds number, the momentum thickness Reynolds number, and the enthalpy thickness Reynolds number, along with the friction coefficient, Stanton number, and Nusselt number. Note that by reducing the print variable $k5$ to a small number we can obtain enough data points for high-resolution plotting. The output file *fn85.txt* presents most of the momentum boundary layer variables, including the boundary layer 99% thickness, the momentum thickness, shape factor, and enthalpy thickness. The files *fn86.txt* and *fn87.txt* contain heat transfer variables.

To plot the developing velocity profiles, set $kout=2$ and choose either $k10=10$ for nondimensional profiles (plus variables) or $k10=11$ for dimensional variables. The profiles will be printed as a part of the file *out.txt*. You can choose where to print the profiles by adding x locations to the $x(m)$. Be sure to change the two $nxbc$ variables and add the appropriate sets of two lines of boundary condition information for each new x -location. This is explained in detail in the *s10.man* user manual.

Here is an abbreviated listing from the *out.txt* file that contains profiles when $kout=2$ and $k10=10$.

intg	x	rem	cf2	h12	reh	st		
2630	3.000E+00	5.365E+03	1.480E-03	1.361E+00	6.065E+03	1.711E-03		
i	y(i)	u(i)	yp1	up1	hpl	kpl	ep1	
1	0.000E+00	0.000E+00	0.000E+00	0.000E+00	0.000E+00	0.000E+00	0.000E+00	
2	5.091E-06	1.086E-01	1.881E-01	1.881E-01	1.330E-01	0.000E+00	0.000E+00	
3	1.393E-05	2.972E-01	5.150E-01	5.150E-01	3.641E-01	0.000E+00	0.000E+00	
4	2.178E-05	4.645E-01	8.049E-01	8.049E-01	5.690E-01	0.000E+00	0.000E+00	
...								
81	5.201E-02	1.499E+01	1.922E+03	2.598E+01	2.247E+01	0.000E+00	0.000E+00	
82	5.376E-02	1.500E+01	1.987E+03	2.599E+01	2.249E+01	0.000E+00	0.000E+00	
83	5.482E-02	1.500E+01	2.026E+03	2.599E+01	2.249E+01	0.000E+00	0.000E+00	

We see profile data for momentum, $u^+(y^+)$ or ($up1$ and $yp1$), as well as data for heat transfer. $T^+(y^+)$ or (hpl and $yp1$) and for k - ϵ turbulence variables, when higher-order turbulence models are used.

This same data can be displayed in dimensional form by resetting $k10=11$. For turbulent flows, the user can also set output variables and flags to print profiles at specific locations. This is described in detail in the users manual.

To confirm the momentum integral equation for computing friction coefficient divided by two, we use the ideas in Chapter 5. The momentum thickness distribution is contained in the output file *fn84.txt*. You will want to set $k5=1$ to obtain enough points for numerically approximating $d\delta_2/dx$, and use of a higher-order first-derivative approximation is useful. In the world of experimental fluid mechanics, this can be a good estimation of the friction coefficient.

11-11

TEXSTAN analysis of the turbulent momentum boundary layer over a flat plate with zero pressure gradient: This problem is essentially a repeat of the previous problem, but choosing other turbulence models available in TEXSTAN. There exists a 1-equation model ($ktmu=11$) and four 2-equation (k - ϵ) models ($ktmu=21,22,23,24$). The initial velocity profile appropriate to the starting x -Reynolds number (a fully turbulent boundary layer profile), along with turbulence profiles for k (and ϵ) can be supplied by using the $kstart=3$ choice in TEXSTAN. Chose an initial free stream turbulence of 2%. Note that by setting the corresponding initial free stream dissipation (for the 2-equation model) equal to zero, TEXSTAN will compute an appropriate value. Calculate the boundary layer flow and compare the friction coefficient results based on x Reynolds number and momentum thickness Reynolds number with the results in the text, Eqs. (11-20) and (11-23). Calculate the friction coefficient distribution using momentum integral Eq. (5-11) and compare with the TEXSTAN calculations. Feel free to investigate any other attribute of the boundary-layer flow. For example, you can calculate the mixing length model results from the previous problem and compare in a manner similar to Fig. 11-7. Likewise you can investigate the law of the wall, comparing to Fig. 11-6.

The data files for this problem are *11.11a.dat.txt* and *11.11b.dat.txt* files. Their data set construction is based on the based on the *s200_11.dat.txt* file and *s200_22.dat.txt* files for flow over a flat plate with constant free stream velocity and specified surface temperature (initial profiles: fully turbulent velocity and temperature profiles, and for the turbulence variables, the profile construction is described in the TEXSTAN input manual). The one-equation turbulence model ($ktmu=11$) is an improved model over what is described in Chapter 11, and the two-equation model ($ktmu=22$) is based on the K-Y Chien model. These models are described in Appendix F. A variable turbulent Prandtl number model is used for liquid metals and gases, and a constant turbulent Prandtl number for liquids.

Conversion of this data set to permit other turbulence models requires only the variable $ktmu$ to be changed.

Here is an abbreviated listing of the output file (it will be called *out.txt* when you execute TEXSTAN using an input data set) for the one-equation turbulence model using a mixing length and solution to the k -equation for the velocity scale. (*11.11a.dat.txt*)

intg	rex	rem	cf2	st	cfpat	strat	h12	reh
5	2.020E+05	6.963E+02	2.467E-03	3.117E-03	1.014	1.032	1.470	5.877E+02
250	2.746E+05	8.739E+02	2.343E-03	2.885E-03	1.019	1.035	1.463	8.092E+02
500	3.779E+05	1.106E+03	2.163E-03	2.613E-03	.998	1.010	1.453	1.092E+03
750	5.053E+05	1.373E+03	2.040E-03	2.433E-03	.993	1.003	1.437	1.412E+03
1000	6.618E+05	1.684E+03	1.939E-03	2.292E-03	.994	1.002	1.422	1.781E+03
1250	8.526E+05	2.045E+03	1.852E-03	2.175E-03	.996	1.003	1.409	2.207E+03
1500	1.083E+06	2.463E+03	1.774E-03	2.073E-03	1.000	1.005	1.398	2.697E+03
1750	1.360E+06	2.944E+03	1.702E-03	1.982E-03	1.003	1.007	1.388	3.257E+03
2000	1.690E+06	3.495E+03	1.637E-03	1.900E-03	1.007	1.010	1.381	3.897E+03
2250	2.080E+06	4.121E+03	1.576E-03	1.826E-03	1.010	1.013	1.374	4.624E+03
2500	2.539E+06	4.831E+03	1.520E-03	1.758E-03	1.014	1.016	1.369	5.445E+03
2669	2.891E+06	5.361E+03	1.485E-03	1.715E-03	1.017	1.018	1.366	6.057E+03

In the benchmark output ($kout=8$) we see $cfpat$ and $strat$, which present ratios of TEXSTAN-calculated values for c_f to Eq. (11-20) at the same momentum-thickness Reynolds number and for St to Eq. (12-19) at the same enthalpy-thickness Reynolds number. We can use these ratios to help determine if a data set construction is correct. At the present time only some of the “s” data sets in Appendix H can be used with

$k_{out}=8$. We see the cf_{rat} and $strat$ show agreement between the turbulent correlations and the TEXSTAN-computed solution.

Here is an abbreviated listing of the output file (it will be called *out.txt* when you execute TEXSTAN using an input data set) for the two-equation KY Chien turbulence model using solutions to the k - and ε -equations. (*11.11b.dat.txt*).

intg	rex	rem	cf2	st	cf _{rat}	strat	hl2	reh
5	2.018E+05	6.958E+02	2.490E-03	3.142E-03	1.023	1.040	1.469	5.871E+02
250	2.666E+05	8.507E+02	2.267E-03	2.782E-03	.980	.989	1.427	7.797E+02
500	3.952E+05	1.124E+03	2.026E-03	2.423E-03	.939	.941	1.413	1.110E+03
750	5.580E+05	1.444E+03	1.911E-03	2.260E-03	.943	.944	1.397	1.490E+03
1000	7.582E+05	1.818E+03	1.831E-03	2.151E-03	.957	.959	1.380	1.930E+03
1250	1.006E+06	2.262E+03	1.763E-03	2.061E-03	.972	.975	1.363	2.451E+03
1500	1.311E+06	2.791E+03	1.699E-03	1.981E-03	.988	.992	1.348	3.069E+03
1750	1.687E+06	3.419E+03	1.640E-03	1.907E-03	1.003	1.007	1.335	3.799E+03
2000	2.149E+06	4.162E+03	1.584E-03	1.839E-03	1.018	1.022	1.323	4.663E+03
2250	2.715E+06	5.044E+03	1.532E-03	1.776E-03	1.033	1.038	1.313	5.686E+03
2319	2.891E+06	5.313E+03	1.518E-03	1.760E-03	1.037	1.042	1.311	5.998E+03

Once again we see the cf_{rat} and $strat$ show agreement between the turbulent correlations and the TEXSTAN-computed solution. Similar comparisons can be made using the other turbulence models by changing $ktmu$ in the input data set.

11-12

TEXSTAN analysis of the transitional momentum boundary layer over a flat plate with zero pressure gradient: Choose a starting x -Reynolds number of about 1000 (corresponding to a momentum Reynolds number of about 20) and pick fluid properties that are appropriate to air, evaluated at a free stream temperature of 300 K. Use constant fluid properties, and note that the energy equation does not have to be solved. The geometrical dimensions of the plate are 1 m wide (a unit width) by 3.0 m long in the flow direction, corresponding to an ending Re_x of about 2.9×10^6 (a momentum Reynolds number of about 5400). Let the velocity boundary condition at the free stream be 15 m/s. The initial velocity profile appropriate to the starting x -Reynolds number (a laminar Blasius boundary layer profile) can be supplied by using the $kstart=4$ choice in TEXSTAN. For a turbulence model, choose the mixing-length turbulence model with the Van Driest damping function ($ktmu=5$), along with the *abrupt transition model*, corresponding to $ktmtr=1$ and an appropriate momentum Reynolds number for transition, specified by the variable gxx , using the minimal value suggested by Eq. (11-1) or a larger value, say 200. Note that this value typically depends on the free stream turbulence level. Calculate the boundary layer flow and compare the friction coefficient results based on x Reynolds number and momentum thickness Reynolds number with the laminar equations (9-13) and (9-16) and the turbulent equations (11-20) and (11-23). Note that once again, you can evaluate the friction coefficient distribution using momentum integral Eq. (5-11) and compare it with the TEXSTAN calculations. Feel free to investigate any other attribute of the boundary-layer flow.

The data file for this problem is *11.12.dat.txt*. The data set construction is based on the *s800_5a.dat.txt* file for flow over a flat plate with constant free stream velocity and specified surface temperature (initial profiles: Blasius profiles for both velocity and temperature). The turbulence model is the van-Driest mixing length model, along with a variable turbulent Prandtl number model for liquid metals and gases, and a constant turbulent Prandtl number for liquids, with abrupt transition specified as a function of the momentum Reynolds number.

Here is an abbreviated listing of the output file (it will be called *out.txt* when you execute TEXSTAN using an input data set), starting the calculations with laminar flow, and then switching to the mixing-length turbulence model at the abrupt transition location.

intg	rex	rem	cf2	st	cf	strat	h12	apl
5	1.008E+03	2.108E+01	1.046E-02	1.313E-02	1.000	.974	2.590	2.50E+01
500	7.899E+03	5.905E+01	3.735E-03	4.682E-03	1.000	.984	2.590	2.50E+01
1000	2.259E+04	9.986E+01	2.209E-03	2.766E-03	1.000	.986	2.590	2.50E+01
1500	4.483E+04	1.407E+02	1.568E-03	1.963E-03	1.000	.986	2.590	2.50E+01
2000	7.462E+04	1.815E+02	1.215E-03	1.521E-03	1.000	.986	2.590	2.50E+01
Flow switched abruptly to turbulent								
/// nintg = 2228 rex = 9.0711E+04 rem = 200.1								
***** cf/cf,lam,theo > 1.100 *****								
2234	9.115E+04	2.006E+02	1.235E-03	1.565E-03	1.123	1.121	2.424	2.50E+01
2250	9.231E+04	2.024E+02	1.882E-03	2.430E-03	1.727	1.757	2.115	2.50E+01
***** cf/cf,turb,theo > 0.900 *****								
2302	9.621E+04	2.124E+02	2.951E-03	3.673E-03	.901	.997	1.830	2.50E+01
2500	1.149E+05	2.720E+02	3.192E-03	3.859E-03	1.037	1.113	1.661	2.50E+01
3000	1.937E+05	5.018E+02	2.699E-03	3.236E-03	1.022	1.084	1.534	2.50E+01
3500	3.330E+05	8.488E+02	2.332E-03	2.782E-03	1.007	1.060	1.467	2.50E+01

```

4000 5.594E+05 1.343E+03 2.068E-03 2.456E-03 1.002 1.048 1.425 2.50E+01
4500 9.069E+05 2.024E+03 1.867E-03 2.208E-03 1.002 1.042 1.399 2.50E+01
5000 1.417E+06 2.932E+03 1.706E-03 2.010E-03 1.004 1.040 1.381 2.50E+01
5500 2.142E+06 4.117E+03 1.575E-03 1.850E-03 1.009 1.041 1.368 2.50E+01
5884 2.882E+06 5.248E+03 1.488E-03 1.745E-03 1.013 1.042 1.361 2.50E+01

intg= 2229 rem = 200.1 cf/2,min = 1.102E-03 rex = 9.071E+04
intg= 2415 rem = 243.7 cf/2,max = 3.234E-03 rex = 1.061E+05

```

In the benchmark output ($k_{out}=8$) we see c_{frat} and $strat$. For the laminar part of the calculations, these ratios are TEXSTAN-calculated values for c_f to Eq. (9-16) at the same momentum-thickness Reynolds number and for St to Eq. (10-16) at the same enthalpy-thickness Reynolds number. Once transition is forced, the ratios are TEXSTAN-calculated values for c_f to Eq. (11-20) at the same momentum-thickness Reynolds number and for St to Eq. (12-19) at the same enthalpy-thickness Reynolds number. The last two lines of data show the minimum and maximum surface shear stress locations, corresponding to the start and end of transition (which will be nominally the same for this abrupt transition model).

We see the c_{frat} and $strat$ show agreement from the onset for the laminar portion of the flow. We see the forced transition at $Re_{\delta_2} = 200$ and that the friction coefficient is a minimum at that location. Note this location corresponds to $Re_x = 9.07E+04$. Once transition begins, we expect a sharp rise in c_f and it becomes a maximum at a $Re_{\delta_2} = 244$, $Re_x = 1.06E+05$. and then for larger x -Reynolds numbers, the c_f value begins to fall, as transition to fully turbulent flow is completed. Because we have used an abrupt transition model, these two locations are nominally the same, as we would expect. For more advanced transition models we would expect a larger transition range. Note how fast the turbulent boundary layer is established once the transition has occurred. We can use the output file *fin85.dat.txt* along with $k5$ set to a small value to see the detailed behavior of the $c_f/2$.

12-1

The development leading to Eq. (12-17) was not expected to be applicable to a high-Prandtl-number fluid. The objective of this problem is to develop a heat-transfer solution for the turbulent boundary layer for no pressure gradient or transpiration, applicable at $Pr = 100$. Use the Van Driest mixing-length equation and $Pr_t = 0.9$, and integrate Eq. (12-12) out to about $y^+ = 100$ numerically. (It is desirable to use a programmable computer or calculator.) Then for $y^+ > 100$ neglect the $1/Pr$ term and integrate as in the text. Compare the results with Eqs. (12-15) and (12-17).

Follow the procedure leading up to the development of Eqs (12-12) through (12-15), and the result is

$$T^+ = 278.3 + 2.195 \ln y^+$$

applicable for $Pr > 100$. Then follow the procedure described relating to E. (12-17) to obtain the heat transfer results

$$St = \frac{0.0287 Re_x^{-0.2}}{46.4 Re_x^{-0.1} + 0.9}$$

These results are very insensitive to whether the numerical part of the integration is terminated at $y^+ = 100$, or at other such values as 80, or 150. It is of further interest to investigate the value of " a " that would result if an equation of the following type is used to correlate the results:

$$St Pr^a = 0.0287 Re_x^{-0.2}$$

12-2

Consider heat transfer to a turbulent boundary layer with no pressure gradient or transpiration but with a vanishingly small-Prandtl-number fluid. Why is this problem simpler than for the turbulent boundary layer at moderate and high Prandtl numbers? What closed-form solution already in hand should be a good approximation? Why?

At vanishing small Prandtl number the thermal boundary layer becomes very much thicker than the momentum boundary layer. In that case the velocity through the entire thermal boundary layer becomes essentially constant, the eddy diffusivity is zero, and the applicable solution is Eq. (10-11).

12-3

The approximate solution in the text for the development of a thermal boundary layer under an already existing momentum boundary layer, Eq. (12-29), is not valid very close to the step in surface temperature. An alternative possibility in this region may be based on the fact that for a short distance from the step the thermal boundary layer is entirely within the almost completely laminar part of the sublayer, say out to $y^+ = 5$. A heat-transfer solution for this region can then be obtained in much the same manner as for a laminar boundary layer, but with the local turbulent boundary-layer surface shear stress used to establish the velocity profile. Develop a heat-transfer solution for this region, assuming that the shear stress is a constant throughout, and compare the results with Eq. (12-29). What is the range of validity of the result? What is the influence of the Prandtl number? This problem can be solved exactly using similarity methods or integral methods (see Chaps 9 and 10).

Follow the development on p. 253 and obtain a solution based on the energy integral equation and a cubic parabola temperature profile for ξ/x near 1.

$$St = 0.165 Re_x^{-0.4} Pr^{2/3} [1 - \xi/x]^{-1/3}$$

A virtually identical result can be obtained by solution of the energy differential equation using laminar boundary layer similarity methods.

12-4

Starting with Eq. (12-34), determine the Stanton number as a function of the Prandtl number and enthalpy thickness Reynolds number for the case of *constant heat flux* along a surface. Compare with Eq. (12-19).

The result is

$$\text{St Pr}^{0.5} = 0.0125 \text{Re}_{\Delta_2}^{-0.25} \left(\frac{\text{Pr}^{0.4} \text{Re}_{\Delta_2}}{\text{Re}_{\delta_2}} \right)^{5/36}$$

and

$$\text{St Pr}^{0.5} = 0.0142 \text{Re}_{\Delta_2}^{-0.25}$$

12-5

Using Eq. (12-29) and making any mathematical approximations that seem appropriate, determine the Stanton number as a function of the Prandtl number, *enthalpy thickness* Reynolds number, and *momentum thickness* Reynolds number. Note that Eq. (12-29) provides for the possibility of the ratio Δ_2/δ_2 varying from 0 to 1.

$$\text{St Pr}^{0.44} = 0.0287 \text{Re}_x^{-0.2} \left(\frac{\Delta_2}{\delta_2} \right)^{-1/9}$$

12-6

Consider the development of a turbulent boundary layer in a convergent axisymmetric nozzle. Let both the free-stream and surface temperatures be constant. As an approximation, treat the flow as one-dimensional, so that the mass velocity G may be calculated as the mass flow rate divided by the cross-sectional area of the duct, πR^2 . Assume that the thermal boundary layer originates at the start of the convergence of the nozzle. Then take the case where the nozzle throat diameter is one-fifth the duct diameter at the start of convergence, x is a linear function of R , and the convergence angle is 45° . Derive an expression for the Stanton number at the nozzle throat as a function of the Prandtl number and a Reynolds number based on throat diameter and throat mass velocity. How sensitive is this expression to convergence angle? Would shapes other than the straight wall of this example yield significantly different results? Compare your results with the corresponding expression for fully developed turbulent flow in a circular pipe (see Chap. 14).

At the throat:

$$St = 0.287 (\sin \theta)^{0.2} Pr^{-0.4} Re_{throat}^{-0.2}$$

where θ is the angle between the wall and the axis of symmetry. Re_{throat} is a Reynolds number based on throat diameter.

12-7

Air at a temperature of -7°C and 1 atm pressure flows along a flat surface (an idealized airfoil) at a constant velocity of 46 m/s. For the first 0.6m the surface is heated at a constant rate per unit of surface area; thereafter, the surface is adiabatic. If the total length of the plate is 1.8 m, what must be the heat flux on the heated section so that the surface temperature at the trailing edge is not below 0°C ? Plot the surface temperature along the entire plate. Discuss the significance of this problem with respect to wing de-icing. (A tabulation of incomplete beta functions, necessary for this problem, is found in App. C.) TEXSTAN can be used to confirm the results of this variable surface-heat flux problem. Choose a starting x -location near the leading edge, say 0.05 cm, and pick fluid properties that are appropriate to air, evaluated at the free stream temperature. Use constant fluid properties and do not consider viscous dissipation. The piecewise surface heat flux boundary condition is modeled easily in TEXSTAN by providing heat flux values at four x -locations, two for each segment, e.g. at $x=0$, $x=0.60$ m (over which there will be a heat flux), and at $x=0.601$ m, $x=1.8$ m (over which there will be a zero heat flux, adiabatic condition). Because TEXSTAN linearly interpolates the surface thermal boundary condition between consecutive x -locations, a total of 4 boundary condition locations is sufficient to describe the surface temperature variation. The initial velocity and temperature profiles appropriate to the starting x -location (fully turbulent boundary layer profiles) can be supplied by using the $kstart=3$ choice in TEXSTAN. For a turbulence model, choose the mixing-length turbulence model with the Van Driest damping function ($ktmu=5$) and choose the variable turbulent Prandtl number model ($ktme=3$).

$$T_s(x) = T_{\infty} + 7 \left(\frac{x}{1.8} \right)^{0.2} \frac{I(0,1)}{I(0,1/3)}; \quad 0 \leq x \leq 0.6$$

$$T_s(x) = T_{\infty} + 7 \left(\frac{x}{1.8} \right)^{0.2} \frac{I(0,0.6/x)}{I(0,1/3)}; \quad 0.6 \leq x \leq 1.8$$

where

$$I(a,b) = \int_a^b (1-\eta^{0.9})^{-8/9} d\eta$$

Transform the integral using $u = 1-\eta^{0.9}$, then,

$$I(a,b) = \frac{10}{9} \int_a^b u^{-8/9} (1-\eta)^{1/9} du$$

This integral is of the form of an incomplete Beta Function, see Appendix C. The solution can be carried out either numerically or using the Beta functions. The peak temperature at $x = 0.6$ is about 59°C and the heat flux predicted by the analysis is about 8600 W/m^2 .

The data file for this problem is *12.7.dat.txt*. The data set construction is based on the *s210_5.dat.txt* file for flow over a flat plate with constant free stream velocity and specified surface heat flux (initial profiles: fully turbulent velocity and temperature profiles). The turbulence model is the van-Driest mixing length model, along with a variable turbulent Prandtl number model for liquid metals and gases, and a constant turbulent Prandtl number for liquids.

The data set was constructed using the results of the analysis for the surface heat flux. Because we are interested in surface temperature variation, the best output file is *ftn86.txt*. Here is an abbreviated listing of

the output file. Note, to see the complete surface temperature behavior, you need to make $k5$ much lower than the value selected.

intg	x/s	htc	qflux	ts	tin
5	5.0089538E-02	1.8887E+02	8.6000E+03	3.1153E+02	2.6600E+02
150	6.0992672E-02	1.8523E+02	8.6000E+03	3.1243E+02	2.6600E+02
300	7.6973245E-02	1.7611E+02	8.6000E+03	3.1483E+02	2.6600E+02
450	9.5218541E-02	1.6821E+02	8.6000E+03	3.1713E+02	2.6600E+02
600	1.1601020E-01	1.6139E+02	8.6000E+03	3.1929E+02	2.6600E+02
750	1.3963852E-01	1.5538E+02	8.6000E+03	3.2135E+02	2.6600E+02
900	1.6639556E-01	1.4998E+02	8.6000E+03	3.2334E+02	2.6600E+02
1050	1.9658700E-01	1.4508E+02	8.6000E+03	3.2528E+02	2.6600E+02
1200	2.3053448E-01	1.4059E+02	8.6000E+03	3.2717E+02	2.6600E+02
1350	2.6857745E-01	1.3644E+02	8.6000E+03	3.2903E+02	2.6600E+02
1500	3.1107460E-01	1.3259E+02	8.6000E+03	3.3086E+02	2.6600E+02
1650	3.5840502E-01	1.2899E+02	8.6000E+03	3.3267E+02	2.6600E+02
1800	4.1096877E-01	1.2562E+02	8.6000E+03	3.3446E+02	2.6600E+02
1950	4.6918786E-01	1.2247E+02	8.6000E+03	3.3622E+02	2.6600E+02
2100	5.3350729E-01	1.1950E+02	8.6000E+03	3.3797E+02	2.6600E+02
2250	6.0446178E-01	0.0000E+00	0.0000E+00	3.0687E+02	2.6600E+02
2400	6.8244919E-01	0.0000E+00	0.0000E+00	2.8597E+02	2.6600E+02
2550	7.6802463E-01	0.0000E+00	0.0000E+00	2.8220E+02	2.6600E+02
2700	8.6174588E-01	0.0000E+00	0.0000E+00	2.7995E+02	2.6600E+02
2850	9.6428667E-01	0.0000E+00	0.0000E+00	2.7830E+02	2.6600E+02
3000	1.0764266E+00	0.0000E+00	0.0000E+00	2.7698E+02	2.6600E+02
3150	1.1989989E+00	0.0000E+00	0.0000E+00	2.7588E+02	2.6600E+02
3300	1.3328881E+00	0.0000E+00	0.0000E+00	2.7493E+02	2.6600E+02
3450	1.4790343E+00	0.0000E+00	0.0000E+00	2.7411E+02	2.6600E+02
3600	1.6384378E+00	0.0000E+00	0.0000E+00	2.7338E+02	2.6600E+02
3740	1.8000000E+00	0.0000E+00	0.0000E+00	2.7278E+02	2.6600E+02

We see from the analysis that the surface temperature has returned to 273K, and the TEXSTAN predictions match the theory. The peak temperature of 64°C is close to the theoretical value of 59°C.

12-8

Work Prob. 12-7 but divide the heater section into two 0.3 m strips, with one at the leading edge and the other 0.9 m from the leading edge. What heat flux is required such that the plate surface is nowhere less than 0°C? TEXSTAN can be used to confirm the results of this variable surface-heat flux problem. Follow the general set-up described in Prob. 12-7. The piecewise surface heat flux boundary condition will require a total of eight x -locations, two for each segment, e.g. at $x=0$, $x=0.30$ m (over which there will be a heat flux) , $x=0.301$ m, $x=0.90$ m, (over which there will be a zero heat flux, adiabatic condition), $x=0.901$ m, $x=1.20$ m (over which there will again be a heat flux) , and the pair $x=1.201$ m, $x=1.8$ m, (over which there will be a zero heat flux, adiabatic condition).

The procedure for this problem is the same as for 13-7, an application of Eq. (13-33). This time the integral must be broken into four parts, corresponding to the four surface segments. The solution for the first two is the same as for the previous problem with the integration limits suitably modified.

The same TEXSTAN data set can be used and modified as suggested by the problem statement.

12-9

In film cooling the primary effect is believed to be due to the energy put into or taken out of the boundary layer, rather than the mass of fluid injected. If this is the case, it should be possible to approximate the effect of slot injection by simulating the slot with a strip heater in which the total heat rate is set equal to the product of the injection mass flow rate and the enthalpy of the injected fluid. Using the methods of the preceding two problems, carry out an investigation of the case represented by Eq. (12-45).

$$\eta = 32.6 \text{Pr}^{0.4} \text{Re}_x^{0.2} \text{M} \left[P \left(1 - \left(\frac{\xi}{x} \right)^{9/10} \right) - P \left(1 - \left(\frac{\xi + h}{x} \right)^{9/10} \right) \right]$$

and

$$P(r) = \frac{\beta_r \left(\frac{1}{9}, \frac{10}{9} \right)}{\beta_1 \left(\frac{1}{9}, \frac{10}{9} \right)}$$

where x is measured from the leading edge and ξ is the distance to beginning of strip heater.

12-10

Air at a temperature of -7°C and 1 atm pressure flows along a flat surface (an idealized airfoil) at a Consider a film-cooling application of the type described in Prob. 12-9 (Fig. 12-25). The objective of this problem is to investigate methods of calculating heat transfer to or from the surface downstream of the injection slot (that is, the heater or heat extractor, if the above analogy is employed) when the surface temperature is maintained at some temperature different from the “adiabatic wall temperature.” Since heat transfer is zero when the surface temperature is equal to T_{aw} , it would seem reasonable to define a heat-transfer coefficient based on $T_{aw} - T_s$. Such a coefficient would be useful if it turned out that it did not differ substantially from that given by, for example, Eq. (12-18). The investigation can be carried out by simulating the injection slot as in Prob. 12-9 and then specifying a constant but substantially smaller heat flux along the remainder of the plate.

This is an extension to the previous problem. A meaningful result can be obtained if the heat flux in the region downstream from the heater is set at about 10% of the heater value, and then at 5%. The question is whether or not a heat transfer coefficient based on $(T_{aw} - T_s)$ is at least approximately independent of that temperature difference.

12-11

An aircraft oil cooler is to be constructed using the skin of the wing as the cooling surface. The wing may be idealized as a flat plate over which air at 71 kPa and -4°C flows at 61 m/s. The leading edge of the cooler may be located 0.9 m from the leading edge of the wing. The oil temperature and oil-side heat-transfer resistance are such that the surface can be at approximately 54°C , uniform over the surface. How much heat can be dissipated if the cooler surface measures 60 cm by 60 cm? Would there be any substantial advantage in changing the shape to a rectangle 1.2 m wide by 0.3 m in flow length?

For the 60 cm wide by 60 cm in the flow direction cooler, $q \approx 2500 \text{ W}$, and for the 1.2 m wide by 30 cm in the flow direction cooler, $q \approx 2700 \text{ W}$.

12-12

Consider a constant free-stream velocity flow of air over a constant-surface-temperature plate. Let the boundary layer be initially a laminar one, but let a transition to a turbulent boundary layer take place in one case at $Re_x = 300,000$ and in another at $Re_x = 10^6$. Evaluate and plot (on log-log paper) the Stanton number as a function of Re_x out to $Re_x = 3 \times 10^6$. Assume that the transition is abrupt (which is not actually very realistic). Evaluate the Stanton number for the turbulent part using the energy integral equation and an analysis similar to that used to develop Eq. (12-36), matching the enthalpy thicknesses of the laminar and turbulent boundary layers at the transition point. Also plot the Stanton number for a turbulent boundary layer originating at the leading edge of the plate. Where is the “virtual origin” of the turbulent boundary layer when there is a preceding laminar boundary layer? What is the effect of changing the transition point? How high must the Reynolds number be in order for turbulent heat-transfer coefficients to be calculated with 2 percent accuracy without considering the influence of the initial laminar portion of the boundary layer? TEXSTAN can be used to confirm the results of this problem. Choose a starting x -Reynolds number of about 1000 (corresponding to a momentum Reynolds number of about 20) and pick fluid properties that are appropriate to air, evaluated at a free stream temperature of 300 K. Use constant fluid properties, and note that the energy equation does not have to be solved. The geometrical dimensions of the plate are 1 m wide (a unit width) by 3.0 m long in the flow direction, corresponding to an ending Re_x of about 3×10^6 (a momentum Reynolds number of about 5500). Let the velocity boundary condition at the free stream be 15 m/s. The initial velocity and temperature profiles appropriate to the starting x -Reynolds number (laminar Blasius boundary layer profiles) can be supplied by using the $kstart=4$ choice in TEXSTAN. For a turbulence model, choose the mixing-length turbulence model with the Van Driest damping function ($ktmu=5$), along with the *abrupt transition model*, corresponding to $ktmtr=1$ and an appropriate momentum Reynolds number for transition, specified by the variable gxx . You will have to iterate on your gxx choice, using the ideas leading up to Eq. (11-1) to create the correct transition x -Reynolds numbers. Also, choose the variable turbulent Prandtl number model ($ktme=3$).

For $Re_x < Re_{x,t}$ we have $St = 0.471 Re_x^{-0.5}$

and for $Re_x > Re_{x,t}$ we have $St = 0.033 \left[Re_x - Re_{x,tr} + 41.7 Re_{x,tr}^{-0.625} \right]^{-0.2}$

The data file for this problem is exactly the same data set used in problem 11.12. It has been renamed *12.12.dat.txt*. The data set construction is based on the *s800_5a.dat.txt* file for flow over a flat plate with constant free stream velocity and specified surface temperature (initial profiles: Blasius profiles for both velocity and temperature). The turbulence model is the van-Driest mixing length model, along with a constant turbulent Prandtl number model for transitional flows.

Here is an abbreviated listing of the output file (it will be called *out.txt* when you execute TEXSTAN using an input data set), starting the calculations with laminar flow, and then switching to the mixing-length turbulence model at the abrupt transition location.

intg	rex	rem	cf2	st	cfrat	strat	h12	apl
5	1.008E+03	2.108E+01	1.046E-02	1.313E-02	1.000	.974	2.590	2.50E+01
500	7.899E+03	5.905E+01	3.735E-03	4.682E-03	1.000	.984	2.590	2.50E+01
1000	2.259E+04	9.986E+01	2.209E-03	2.766E-03	1.000	.986	2.590	2.50E+01
1500	4.483E+04	1.407E+02	1.568E-03	1.963E-03	1.000	.986	2.590	2.50E+01
2000	7.462E+04	1.815E+02	1.215E-03	1.521E-03	1.000	.986	2.590	2.50E+01
Flow switched abruptly to turbulent								
/// nintg = 2228 rex = 9.0711E+04 rem = 200.1								
***** cf/cf,lam,theo > 1.100 *****								

```

2234 9.115E+04 2.006E+02 1.235E-03 1.565E-03 1.123 1.121 2.424 2.50E+01
2250 9.231E+04 2.024E+02 1.882E-03 2.430E-03 1.727 1.757 2.115 2.50E+01
***** cf/cf,turb,theo > 0.900 *****
2302 9.621E+04 2.124E+02 2.951E-03 3.673E-03 .901 .997 1.830 2.50E+01
2500 1.149E+05 2.720E+02 3.192E-03 3.859E-03 1.037 1.113 1.661 2.50E+01
3000 1.937E+05 5.018E+02 2.699E-03 3.236E-03 1.022 1.084 1.534 2.50E+01
3500 3.330E+05 8.488E+02 2.332E-03 2.782E-03 1.007 1.060 1.467 2.50E+01
4000 5.594E+05 1.343E+03 2.068E-03 2.456E-03 1.002 1.048 1.425 2.50E+01
4500 9.069E+05 2.024E+03 1.867E-03 2.208E-03 1.002 1.042 1.399 2.50E+01
5000 1.417E+06 2.932E+03 1.706E-03 2.010E-03 1.004 1.040 1.381 2.50E+01
5500 2.142E+06 4.117E+03 1.575E-03 1.850E-03 1.009 1.041 1.368 2.50E+01
5884 2.882E+06 5.248E+03 1.488E-03 1.745E-03 1.013 1.042 1.361 2.50E+01

intg= 2229 rem = 200.1 cf/2,min = 1.102E-03 rex = 9.071E+04
intg= 2415 rem = 243.7 cf/2,max = 3.234E-03 rex = 1.061E+05

```

In the benchmark output ($k_{out}=8$) we see c_{frat} and $strat$. For the laminar part of the calculations, these ratios are TEXSTAN-calculated values for c_f to Eq. (9-16) at the same momentum-thickness Reynolds number and for St to Eq. (10-16) at the same enthalpy-thickness Reynolds number. Once transition is forced, the ratios are TEXSTAN-calculated values for c_f to Eq. (11-20) at the same momentum-thickness Reynolds number and for St to Eq. (12-19) at the same enthalpy-thickness Reynolds number. The last two lines of data show the minimum and maximum surface shear stress locations, corresponding to the start and end of transition (which will be nominally the same for this abrupt transition model).

We see the c_{frat} and $strat$ show agreement from the onset for the laminar portion of the flow. We see the forced transition at $Re_{\delta_2} = 200$ and that the friction coefficient is a minimum at that location. Note this location corresponds to $Re_x = 9.07E+04$. Once transition begins, we expect a sharp rise in both St and c_f , and it becomes a maximum at a $Re_{\delta_2} = 244$, $Re_x = 1.06E+05$. and then for larger x -Reynolds numbers, the c_f value begins to fall, as transition to fully turbulent flow is completed. Because we have used an abrupt transition model, these two locations are nominally the same, as we would expect. For more advanced transition models we would expect a larger transition range. Note how fast the turbulent boundary layer is established once the transition has occurred. We can use the output file *fm85.dat.txt* along with $k5$ set to a small value to see the detailed behavior of the St with x .

12-13

A 12m diameter balloon is rising vertically upward in otherwise still air at a velocity of 3 m/s. When it is at 1500m elevation, calculate the heat-transfer coefficient over the entire upper hemispherical surface, making any assumptions that seem appropriate regarding the free-stream velocity distribution and the transition from a laminar to a turbulent boundary layer.

If it is assumed that transition occurs at $Re_{\delta_2} = 300$, the following results are obtained:

θ degrees from stagnation point	h W/(m ² ·K)
0	3.44
10	3.42
20	3.37
30	3.27
40	3.15
50	2.98
60 transition	11.6
70	10.99
80	10.58
90	10.07

12-14

A round cylindrical body 1.2 m in diameter has a hemispherical cap over one end. Air flows axially along the body, with a stagnation point at the center of the end cap. The air has an upstream state of 1 atm pressure, 21°C, and 60 m/s. Under these conditions, evaluate the local heat-transfer coefficient along the cylindrical part of the surface to a point 4 m from the beginning of the cylindrical surface, assuming a constant-temperature surface. Make any assumptions that seem appropriate about an initial laminar boundary layer and about the free-stream velocity distribution around the nose. It may be assumed that the free-stream velocity along the cylindrical portion of the body is essentially constant at 60 m/s, although this is not strictly correct in the region near the nose. Then calculate the heat-transfer coefficient along the same surface by idealizing the entire system as a flat plate with constant free-stream velocity from the stagnation point. On the basis of the results, discuss the influence of the nose on the boundary layer at points along the cylindrical section and the general applicability of the constant free-stream velocity idealization.

A reasonable way to handle the nose region is to use the potential flow solution for flow over a sphere:

$$u_{\infty} = 1.5V_{app} \sin\left(\frac{x}{r_s}\right)$$

Then at the point where $u_{\infty} = V_{app}$, let the free stream velocity remain at that value over the remainder of the nose and along the cylindrical body. If it is assumed that transition to a turbulent boundary layer takes place when $Re_{\delta_2} \approx 300$, transition will occur at $x = 0.4$ m (38.2°). The following table lists the heat transfer coefficients calculated as a function of distance from the stagnation point. Also listed are the values of h which would be calculated if it were assumed that the system were a simple flat plate with constant free-stream velocity, and that the turbulent boundary layer originated at the stagnation point:

x m	h W/(m ² ·K)	$h_{\text{flat plate}}$
0	53.0	
0.1	52.8	
0.2	52.0	
0.3	50.7	
0.4	48.9	(transition)
0.438	227.0	($u_{\infty} = 60$)
0.5	185.7	
0.6	163.8	
0.7	152.1	
0.8	143.7	
0.9425	134.0	116.34
1.943	106.6	100.7
2.943	96.1	92.6
3.943	89.7	87.4
4.943	85.3	83.5

12-15

Problem 11-9 is concerned with the momentum boundary layer on a rough surface, and it involves analyzing some experimental data. The corresponding measured temperature profile is given in the following table. The surface temperature is 35.22°C, constant along the surface, and the free-stream temperature is 19.16°C. $St = 0.00233$. How do the results compare with the theory developed in the text?

y, cm	T, °C	y, cm	T, °C
0.020	29.02	0.660	24.17
0.030	28.64	1.10	22.84
0.051	28.14	1.61	21.62
0.081	27.57	2.12	20.36
0.127	26.97	2.82	19.46
0.191	26.36	3.58	19.16
0.279	25.76		
0.406	25.13		

The temperature and velocity profile origin should be shifted about 0.018 cm below the nominal origin. Then, we find $T^+ = 0.165 \ln y^+ = 0.348$. This should then be compared with Eq.(13-46) using $Re_k = 124$, $k = 0.41$, and $Pr_t = 0.9$, and the result should be quite good fit.

12-16

Consider a flat surface that is 30 cm square. Hot air at 800 K is flowing across this surface at a velocity of 50 m/s. The hot-air density is 0.435 kg/m^3 . The boundary layer on the plate is turbulent, and at the leading edge of the section of interest the momentum thickness Reynolds number is 1100. There is no thermal boundary layer in the region preceding the 30 cm section of interest; i.e., the surface on which the momentum boundary layer has developed is adiabatic and thus at 800 K. Cooling air is available at 290 K, at a rate of 0.0037 kg/s . The density of the coolant is 1.2 kg/m^3 . Investigate what can be done with three methods of cooling the 30 cm section: (1) convection from the rear surface of the plate; (2) transpiration; and (3) film cooling. In the first assume that the surface is sufficiently thin that the conduction resistance is negligible, that the effective heat-transfer coefficient on the rear surface is $25 \text{ W/(m}^2 \cdot \text{K)}$, and that the effective coolant temperature is 290 K over the whole surface. For the second case let \dot{m}'' be uniform everywhere. Although the surface temperature varies in the direction of flow for each of the cooling methods used, ignore this effect on the heat-transfer coefficient, i.e., use constant-surface-temperature theory to determine h .

Note: measure x from the leading edge

$x, \text{ m}$	$T_s, \text{ K}$	$T_s, \text{ K}$	$T_s, \text{ K}$
	convective	transpiration	film
0	800	800	-
0.04	682	586	290
0.08	674	572	533
0.12	669	564	623
0.16	666	557	664
0.20	663	552	689
0.24	600	548	706
0.28	658	544	717
0.30	657	543	726

12-17

TEXSTAN analysis of the turbulent thermal boundary layer over a flat plate with constant surface temperature and with zero pressure gradient: Choose a starting x -Reynolds number of about 2×10^5 (corresponding to a momentum Reynolds number of about 700) and pick fluid properties that are appropriate to air, evaluated at a free stream temperature of 300 K. Use constant fluid properties and do not consider viscous dissipation. The geometrical dimensions of the plate are 1 m wide (a unit width) by 3.0 m long in the flow direction, corresponding to an ending Re_x of about 2.9×10^6 (a momentum Reynolds number of about 5400). Let the velocity boundary condition at the free stream be 15 m/s and let the energy boundary conditions be a free stream temperature of 300K and a constant surface temperature of 295 K. The initial velocity and temperature profiles appropriate to the starting x -Reynolds number (fully turbulent boundary layer profiles) can be supplied by using the $kstart=3$ choice in TEXSTAN. For a turbulence model, choose the mixing-length turbulence model with the Van Driest damping function ($ktmu=5$) and choose the variable turbulent Prandtl number model ($ktme=3$) corresponding to Eq. (12-7). Calculate the boundary layer flow and compare the Stanton number results based on x Reynolds number and enthalpy thickness Reynolds number with the results in the text, Eqs. (13-18) and (13-19). Calculate the Stanton number distribution using energy integral Eq. (5-24) and compare with the TEXSTAN calculations. Feel free to investigate any other attribute of the boundary-layer flow. For example, you can investigate the thermal law of the wall, comparing to Fig. 13-9

The data file for this problem is exactly the same data set used in problem 11.10. It has been renamed *12.17.dat.txt*. The data set construction is based on the *s200_5.dat.txt* file for flow over a flat plate with constant free stream velocity and specified surface temperature (initial profiles: fully turbulent velocity and temperature profiles)The turbulence model is the van-Driest mixing length model, along with a variable turbulent Prandtl number model for liquid metals and gases, and a constant turbulent Prandtl number for liquids.

Here is an abbreviated listing of the output file (it will be called *out.txt* when you execute TEXSTAN using an input data set)

intg	rex	rem	cf2	st	cfrat	strat	hl2	reh
5	2.020E+05	6.963E+02	2.496E-03	3.149E-03	1.026	1.043	1.469	5.877E+02
250	2.753E+05	8.744E+02	2.345E-03	2.891E-03	1.020	1.037	1.454	8.100E+02
500	3.804E+05	1.112E+03	2.181E-03	2.636E-03	1.008	1.021	1.437	1.099E+03
750	5.113E+05	1.388E+03	2.054E-03	2.450E-03	1.003	1.014	1.422	1.431E+03
1000	6.729E+05	1.711E+03	1.946E-03	2.301E-03	1.001	1.010	1.408	1.814E+03
1250	8.704E+05	2.086E+03	1.852E-03	2.175E-03	1.001	1.008	1.397	2.256E+03
1500	1.109E+06	2.518E+03	1.769E-03	2.067E-03	1.002	1.008	1.387	2.762E+03
1750	1.396E+06	3.015E+03	1.694E-03	1.972E-03	1.004	1.009	1.380	3.341E+03
2000	1.738E+06	3.581E+03	1.626E-03	1.888E-03	1.006	1.010	1.373	4.000E+03
2250	2.141E+06	4.224E+03	1.565E-03	1.813E-03	1.009	1.012	1.367	4.746E+03
2500	2.614E+06	4.951E+03	1.508E-03	1.744E-03	1.012	1.014	1.363	5.587E+03
2630	2.891E+06	5.365E+03	1.480E-03	1.711E-03	1.014	1.015	1.361	6.065E+03

In the benchmark output ($kout=8$) we see $cfrat$ and $strat$, which present ratios of TEXSTAN-calculated values for c_f to Eq. (11-20) at the same momentum-thickness Reynolds number and for St to Eq. (12-19) at the same enthalpy-thickness Reynolds number. We can use these ratios to help determine if a data set construction is correct. At the present time only some of the “s” data sets in Appendix H can be used with $kout=8$. We see the $cfrat$ and $strat$ show agreement between the turbulent correlations and the TEXSTAN-computed solution.

The output file *fn85.txt* presents most of the dimensionless variables needed for comparison, including the x Reynolds number, the momentum thickness Reynolds number, and the enthalpy thickness Reynolds number, along with the friction coefficient, Stanton number, and Nusselt number. Note that by reducing the print variable $k5$ to a small number we can obtain enough data points for high-resolution plotting. The output file *fn85.txt* presents most of the momentum boundary layer variables, including the boundary layer 99% thickness, the momentum thickness, shape factor, and enthalpy thickness. The files *fn86.txt* and *fn87.txt* contain heat transfer variables, including the surface heat flux, heat transfer coefficient, and surface temperature.

To plot the developing velocity profiles, set $kout=2$ and choose either $k10=10$ for nondimensional profiles (plus variables) or $k10=11$ for dimensional variables. The profiles will be printed as a part of the file *out.txt*. You can choose where to print the profiles by adding x locations to the $x(m)$. Be sure to change the two $nxbc$ variables and add the appropriate sets of two lines of boundary condition information for each new x -location. This is explained in detail in the *s10.man* user manual.

Here is an abbreviated listing from the *out.txt* file that contains profiles when $kout=2$ and $k10=10$.

intg	x	rem	cf2	h12	reh	st		
2630	3.000E+00	5.365E+03	1.480E-03	1.361E+00	6.065E+03	1.711E-03		
i	y(i)	u(i)	yp1	up1	hpl	kpl	ep1	
1	0.000E+00	0.000E+00	0.000E+00	0.000E+00	0.000E+00	0.000E+00	0.000E+00	
2	5.091E-06	1.086E-01	1.881E-01	1.881E-01	1.330E-01	0.000E+00	0.000E+00	
3	1.393E-05	2.972E-01	5.150E-01	5.150E-01	3.641E-01	0.000E+00	0.000E+00	
4	2.178E-05	4.645E-01	8.049E-01	8.049E-01	5.690E-01	0.000E+00	0.000E+00	
...								
81	5.201E-02	1.499E+01	1.922E+03	2.598E+01	2.247E+01	0.000E+00	0.000E+00	
82	5.376E-02	1.500E+01	1.987E+03	2.599E+01	2.249E+01	0.000E+00	0.000E+00	
83	5.482E-02	1.500E+01	2.026E+03	2.599E+01	2.249E+01	0.000E+00	0.000E+00	

We see profile data for momentum, $u^+(y^+)$ or ($up1$ and $yp1$), as well as data for heat transfer. $T^+(y^+)$ or (hpl and $yp1$) and for k - ϵ turbulence variables, when higher-order turbulence models are used.

This same data can be displayed in dimensional form by resetting $k10=11$. For turbulent flows, the user can also set output variables and flags to print profiles at specific locations. This is described in detail in the users manual.

To confirm the energy integral equation for computing Stanton number, we use the ideas in Chapter 5. The enthalpy thickness distribution is contained in the output file *fn84.txt*. You will want to set $k5=1$ to obtain enough points for numerically approximating $d\Delta_2/dx$, and use of a higher-order first-derivative approximation is useful. In the world of experimental heat transfer, this can be a good estimation of the Stanton number.

12-18

TEXSTAN analysis of the turbulent thermal boundary layer over a flat plate with constant surface temperature and with zero pressure gradient: This is an extension to problem 12-17 to investigate the effect of Prandtl number on heat transfer. Examine fluids ranging from gases to light liquids and compare to Fig. 13-13. Compare Eqs. (13-17) through (13-21) with the TEXSTAN results.

This problem setup is based on the TEXSTAN setup for problem 12-17. The only important idea is to make sure the pipe length is long enough for thermally fully developed flow when $Pr > 1$. Note: use variable turbulent Prandtl number for $Pr \leq 1$ and constant turbulent Prandtl number for $Pr > 1$.

12-19

TEXSTAN analysis of the turbulent thermal boundary layer over a flat plate with constant surface temperature and with zero pressure gradient: This problem is essentially a repeat of problem (12-17), but choosing higher-order turbulence models available in TEXSTAN. There exists a 1-equation model ($ktmu=11$) and four 2-equation (k - ϵ) models ($ktmu=21,22,23,24$). The initial velocity and temperature profiles appropriate to the starting x -Reynolds number (fully turbulent boundary layer profiles), along with turbulence profiles for k (and ϵ) can be supplied by using the $kstart=3$ choice in TEXSTAN. Chose an initial free stream turbulence of 2%. Note that by setting the corresponding initial free stream dissipation (for the 2-equation model) equal to zero, TEXSTAN will compute an appropriate value. For the 1- and 2-equation turbulence models it is best to choose a constant turbulent Prandtl number model ($ktme=2$), along with a choice for the turbulent Prandtl number, 0.9 is suggested, by setting $fx=0.9$. Calculate the boundary layer flow and compare the Stanton number results based on x Reynolds number and enthalpy thickness Reynolds number with the results in the text, Eqs. (13-18) and (13-19). Calculate the Stanton number distribution using energy integral Eq. (5-24) and compare with the TEXSTAN calculations. Feel free to investigate any other attribute of the boundary-layer flow. For example, you can investigate the thermal law of the wall, comparing to Fig. 13-9.

The data files for this problem are *12.19a.dat.txt* and *12.19b.dat.txt* files. Their data set construction is based on the based on the *s200_11.dat.txt* file and *s200_22.dat.txt* files for flow over a flat plate with constant free stream velocity and specified surface temperature (initial profiles: fully turbulent velocity and temperature profiles, and for the turbulence variables, the profile construction is described in the TEXSTAN input manual). The one-equation turbulence model ($ktmu=11$) is an improved model over what is described in Chapter 11, and the two-equation model ($ktmu=22$) is based on the K-Y Chien model. These models are described in Appendix F. A variable turbulent Prandtl number model is used for liquid metals and gases, and a constant turbulent Prandtl number for liquids.

Conversion of this data set to permit other turbulence models requires only the variable $ktmu$ to be changed.

Here is an abbreviated listing of the output file (it will be called *out.txt* when you execute TEXSTAN using an input data set) for the one-equation turbulence model using a mixing length and solution to the k -equation for the velocity scale. (*12.19a.dat.txt*)

intg	rex	rem	cf2	st	cfrat	strat	h12	reh
5	2.020E+05	6.963E+02	2.467E-03	3.117E-03	1.014	1.032	1.470	5.877E+02
250	2.746E+05	8.739E+02	2.343E-03	2.885E-03	1.019	1.035	1.463	8.092E+02
500	3.779E+05	1.106E+03	2.163E-03	2.613E-03	.998	1.010	1.453	1.092E+03
750	5.053E+05	1.373E+03	2.040E-03	2.433E-03	.993	1.003	1.437	1.412E+03
1000	6.618E+05	1.684E+03	1.939E-03	2.292E-03	.994	1.002	1.422	1.781E+03
1250	8.526E+05	2.045E+03	1.852E-03	2.175E-03	.996	1.003	1.409	2.207E+03
1500	1.083E+06	2.463E+03	1.774E-03	2.073E-03	1.000	1.005	1.398	2.697E+03
1750	1.360E+06	2.944E+03	1.702E-03	1.982E-03	1.003	1.007	1.388	3.257E+03
2000	1.690E+06	3.495E+03	1.637E-03	1.900E-03	1.007	1.010	1.381	3.897E+03
2250	2.080E+06	4.121E+03	1.576E-03	1.826E-03	1.010	1.013	1.374	4.624E+03
2500	2.539E+06	4.831E+03	1.520E-03	1.758E-03	1.014	1.016	1.369	5.445E+03
2669	2.891E+06	5.361E+03	1.485E-03	1.715E-03	1.017	1.018	1.366	6.057E+03

In the benchmark output ($kout=8$) we see $cfrat$ and $strat$, which present ratios of TEXSTAN-calculated values for c_f to Eq. (11-20) at the same momentum-thickness Reynolds number and for St to Eq. (12-19) at

the same enthalpy-thickness Reynolds number. We can use these ratios to help determine if a data set construction is correct. We see the *cf_{rat}* and *strat* show agreement between the turbulent correlations and the TEXSTAN-computed solution.

Here is an abbreviated listing of the output file (it will be called *out.txt* when you execute TEXSTAN using an input data set) for the two-equation KY Chien turbulence model using solutions to the *k*- and ϵ -equations. (*12.19b.dat.txt*).

intg	rex	rem	cf2	st	cf _{rat}	strat	hl2	reh
5	2.018E+05	6.958E+02	2.490E-03	3.142E-03	1.023	1.040	1.469	5.871E+02
250	2.666E+05	8.507E+02	2.267E-03	2.782E-03	.980	.989	1.427	7.797E+02
500	3.952E+05	1.124E+03	2.026E-03	2.423E-03	.939	.941	1.413	1.110E+03
750	5.580E+05	1.444E+03	1.911E-03	2.260E-03	.943	.944	1.397	1.490E+03
1000	7.582E+05	1.818E+03	1.831E-03	2.151E-03	.957	.959	1.380	1.930E+03
1250	1.006E+06	2.262E+03	1.763E-03	2.061E-03	.972	.975	1.363	2.451E+03
1500	1.311E+06	2.791E+03	1.699E-03	1.981E-03	.988	.992	1.348	3.069E+03
1750	1.687E+06	3.419E+03	1.640E-03	1.907E-03	1.003	1.007	1.335	3.799E+03
2000	2.149E+06	4.162E+03	1.584E-03	1.839E-03	1.018	1.022	1.323	4.663E+03
2250	2.715E+06	5.044E+03	1.532E-03	1.776E-03	1.033	1.038	1.313	5.686E+03
2319	2.891E+06	5.313E+03	1.518E-03	1.760E-03	1.037	1.042	1.311	5.998E+03

Once again we see the *cf_{rat}* and *strat* show agreement between the turbulent correlations and the TEXSTAN-computed solution. Similar comparisons can be made using the other turbulence models by changing *ktmu* in the input data set.

13-1

Develop an equation for the friction coefficient for fully developed turbulent flow between parallel planes, assuming that Eq. (13-7) is a reasonable approximation for the velocity profile.

The solution follows that on p 286 for Eq. (13-11). Assume $V/u_c = 0.875$ and the friction coefficient becomes

$$c_f/2 = 0.041 \text{Re}_{D_h}^{-0.25}$$

where the Re_{D_h} is the hydraulic diameter Reynolds number based on the channel height, h ,

$$\text{Re}_{D_h} = \frac{2hV}{\nu}$$

13-2

Employing numerical integration to determine the ratio of mean velocity to centerline velocity, and Eq. (13-6) for the velocity profile, evaluate the friction coefficient for fully developed turbulent flow in a circular tube for two different Reynolds numbers: 30,000 and 150,000. Compare results with other relations for the friction coefficient given in the text. (It is presumed that a programmable computer is used for this problem.)

A numerical calculation using Eq. (13-6), but using the Van Driest mixing-length for $y^+ < 100$, $A^+ = 26$, and $\kappa = 0.40$, yields the following:

$$\text{Re} = 29,100 \qquad c_f = 0.00302$$

$$\text{Re} = 102,307 \qquad c_f = 0.00220$$

13-3

Develop a solution for the friction coefficient and velocity profile in the entry region of a flat duct, assuming that the velocity is uniform over the flow cross section at the entrance, that the boundary layer that develops on the two surfaces is turbulent from its very beginning, and that Eq. (13-7) is an adequate approximation for the velocity profile both in the entry region and in the fully developed region. Employ the momentum integral equation, and assume that the velocity profile in the entry region can be divided into two parts: a uniform-velocity core region and a boundary layer that ultimately engulfs the entire core. Note that the uniform velocity in the core region accelerates because of the displacement of the boundary layer, and that part of the pressure drop in the entry region is due to this acceleration. Determine the length of the entry region.

A solution can be obtained based on a slight modification of Eq.(11-21) to account for the difference between Eqs. (11-17) and (13-7). If the integral is evaluated numerically the following is a sample of the results for

$$\text{Re}_{D_h} = \frac{2hV}{\nu} = 25,000$$

where the Re is the hydraulic diameter Reynolds number based on the channel height, h ,

$$c_f/2 = 0.041\text{Re}^{-0.25}$$

$x/2h$	$c_f/2$	V/u_c
1	.00409	.976
2	.00370	.959
3	.00352	.944
4	.00342	.931
5	.00337	.919
6	.00333	.908
7	.00331	.898
8	.00329	.888
9	.00329	.879
(entry length) 9.4	.00329	.875

and the total pressure drop is

$$\frac{\Delta P}{(\rho V^2)} = 0.155$$

13-4

Develop Eq. (13-17) by the indicated procedures.

The velocity profile is Eq. (11-56). This is substituted into Eq. (7-6). After integration is carried out to obtain a relation between the mean and center-line velocities, Eq. (13-17) is obtained from Eq. (11-56) when it is applied at the centerline.

13-5

Employing Eq. (13-6), numerical integration, and a programmable computer, determine the ratio of mean velocity to centerline velocity for fully developed flow in a circular tube for a number of different Reynolds numbers, and compare with Eq. (12-10), which was developed assuming a $\frac{1}{7}$ - power profile. Determine whether it is valid to neglect the contribution of the sublayer in these calculations.

Using Eq. (13-6) but employing the Van Driest mixing-length $y^+ < 100$, $A^+ = 26$, and $\kappa = 0.40$, yields the following:

Re	V/u_c
10,103	0.789
29,100	0.814
102,307	0.837
311,152	0.853
1,013,370	0.866

13-6

The viscous sublayer behaves as if it were almost completely laminar out to a value of y^+ of about 5.0. With this idea in mind, calculate the ratio of such a sublayer thickness to pipe diameter for fully developed turbulent flow in a smooth-walled pipe. Using these results, discuss the significance of the data in Fig. 13-2.

At $y_\ell^+ = 5$

$$\left(\frac{y}{D}\right)_\ell \frac{DV\sqrt{c_f/2}}{\nu} = 5$$

or

$$\left(\frac{y}{D}\right)_\ell = \frac{5}{\sqrt{c_f/2}} \frac{1}{\text{Re}}$$

Now, $c_f/2 = 0.023\text{Re}^{-0.2}$

so

$$\left(\frac{y}{D}\right)_\ell = 33\text{Re}^{-0.8}$$

It will be found that the line on Fig. 13-2 labeled "limit of fully rough region" is a similar function of (k_s/D) , but with a larger coefficient.

13-7

Two water tanks, open to the atmosphere, are connected by a pair of parallel pipes each having an inside diameter of 2.5 cm. The pipes are 20 m long. One is a “smooth” tube, but the other is a galvanized iron pipe. What must be the elevation difference for the two tanks in order for the total flow rate for the two pipes to be 1.00 kg/s? (Neglect entrance and exit pressure-drop effects.)

The necessary elevation difference is 1.21 m. The rough tube flow rate will be 0.45 kg/s, and the smooth tube rate 0.55 kg/s.

13-8

TEXSTAN analysis of the turbulent momentum entry flow in a circular tube: Investigate the entry length region through the hydrodynamically fully-developed region of flow in a circular tube with diameter Reynolds numbers of 30,000 and 150,000. Pick fluid properties that are appropriate to air, evaluated at a temperature of 300 K. Use constant fluid properties, and note that the energy equation does not have to be solved. Let the pipe diameter be 3.5 cm and the pipe length be 12.0 m. Let the velocity profile at the inlet to the tube be flat, which can be supplied by using the $kstart=1$ choice in TEXSTAN. For a turbulence model, choose the hybrid turbulence model comprised of a constant eddy viscosity in the outer part of the flow ($\varepsilon_m/\nu=aRe^b$ with $a = 0.005$ and $b = 0.9$) and a mixing-length turbulence model with the Van Driest damping function ($\kappa=0.40$ and $A^+=26$) in the near-wall region ($ktmu=7$). This hybrid model tends to more closely fit Fig. (13-1), and thus better predict the fully-developed friction coefficient for a given Reynolds number. Compare the friction coefficient with the set of Eqs. (13-11) through (13-14). Feel free to investigate any other attribute of the boundary-layer flow. For example, you can examine a velocity profile at the hydrodynamically fully developed state to evaluate the *law of the wall* and the ratio of mean velocity to centerline velocity, and compare with Eqs. (13-6) and (13-10) respectively.

The data file for this problem is *13.8.dat.txt*. The data set construction is based on the *s410_7.dat.txt* file for combined entry length flow in a pipe with a specified surface temperature (initial profiles: flat velocity and flat temperature). The turbulence model is a composite model that uses the van-Driest mixing length model in the near-wall region and a constant eddy viscosity in the outer region. Note that the turbulent data set manual *s400.man* is very helpful in understanding this data set construction.

Execution of the input data set generates several output files. Here is an abbreviated listing of the output file (it will be called *out.txt* when you execute TEXSTAN using *13.8.dat.txt*). Only the momentum results will be discussed. The Reynolds number is 30,000.

intg	x/dh	cf2	nu	cfrat	nurat	tm/ts	ts	qflux
5	2.500E-02	2.037E-02	546.4	6.904	7.747	.949	2.950E+02	3.049E+03
400	2.000E+00	3.783E-03	89.5	1.282	1.269	.951	2.950E+02	4.789E+02
800	4.000E+00	3.460E-03	81.2	1.173	1.152	.953	2.950E+02	4.211E+02
1200	6.106E+00	3.326E-03	77.7	1.127	1.102	.954	2.950E+02	3.904E+02
1600	9.108E+00	3.222E-03	74.9	1.092	1.062	.956	2.950E+02	3.601E+02
2000	1.358E+01	3.139E-03	72.5	1.064	1.028	.959	2.950E+02	3.276E+02
2400	2.026E+01	3.081E-03	70.8	1.044	1.003	.962	2.950E+02	2.923E+02
2800	3.022E+01	3.049E-03	69.9	1.034	.990	.967	2.950E+02	2.529E+02
3200	4.508E+01	3.038E-03	69.5	1.030	.986	.973	2.950E+02	2.072E+02
3600	6.721E+01	3.036E-03	69.5	1.029	.985	.980	2.950E+02	1.549E+02
3998	1.000E+02	3.035E-03	69.5	1.029	.985	.987	2.950E+02	1.008E+02

Here is a same abbreviated output for the Re=150,000 data set.

intg	x/dh	cf2	nu	cfrat	nurat	tm/ts	ts	qflux
5	2.500E-02	6.503E-03	822.5	3.151	3.332	.949	2.950E+02	4.598E+03
400	2.000E+00	2.626E-03	319.1	1.272	1.293	.951	2.950E+02	1.734E+03
800	4.000E+00	2.405E-03	290.7	1.165	1.178	.952	2.950E+02	1.544E+03
1200	6.106E+00	2.308E-03	278.2	1.118	1.127	.953	2.950E+02	1.444E+03
1600	9.108E+00	2.239E-03	269.1	1.085	1.090	.954	2.950E+02	1.354E+03

2000	1.358E+01	2.182E-03	261.2	1.057	1.058	.956	2.950E+02	1.257E+03
2400	2.026E+01	2.140E-03	255.1	1.037	1.033	.959	2.950E+02	1.151E+03
2800	3.022E+01	2.113E-03	251.3	1.024	1.018	.963	2.950E+02	1.031E+03
3200	4.508E+01	2.101E-03	249.7	1.018	1.012	.968	2.950E+02	8.903E+02
3600	6.721E+01	2.098E-03	249.3	1.017	1.010	.974	2.950E+02	7.218E+02
3998	1.000E+02	2.098E-03	249.3	1.016	1.010	.981	2.950E+02	5.303E+02

In these benchmark outputs ($kout=8$) we see cf_{rat} and $strat$, which present ratios of TEXSTAN-calculated values for c_f to the Kármán-Nikuradse Eq. (13-14) at the same Reynolds number and for Nu to the Gnielinski Eq. (14-8). We can use these ratios to help determine if a data set construction is correct. At the present time only some of the “s” data sets in Appendix H can be used with $kout=8$. We see the cf_{rat} and $strat$ show agreement between the turbulent correlations and the TEXSTAN-computed solution. From the output we can also see the hydrodynamic developing region is complete to within 5% by x/D_h of about 12-15 for both Reynolds numbers. The output file *fm85.txt* presents most of the momentum flow variables, including the surface shear stress and pressure drop. The files *fm82.txt* and *fm84.txt* contain heat transfer variables for the E-surface (the pipe wall).

To plot the developing velocity profiles, set $kout=4$ and choose either $k10=10$ for nondimensional profiles (plus variables) or $k10=11$ for dimensional variables. The profiles will be printed as a part of the file *out.txt*. You can choose where to print the profiles by adding x locations to the $x(m)$. Be sure to change the two $nxbc$ variables and add the appropriate sets of two lines of boundary condition information for each new x -location. This is explained in detail in the *s400.man.doc* user manual.

Here is an abbreviated listing from the *out.txt* file for $Re=30,000$ that contains profiles when $kout=4$ and $k10=10$.

intg	x/dh	cfapp	cf2(I)	cf2(E)	nu(I)	nu(E)		
3998	1.000E+02	6.416E-03	0.000E+00	3.035E-03	0.000E+00	6.948E+01		
i	y(i)	u(i)	ypl	upl	hpl	kpl	epl	
1	0.000E+00	8.292E+00	8.264E+02	2.249E+01	2.112E+01	0.000E+00	0.000E+00	
2	1.154E-03	8.292E+00	7.992E+02	2.249E+01	2.112E+01	0.000E+00	0.000E+00	
3	2.393E-03	8.282E+00	7.699E+02	2.246E+01	2.108E+01	0.000E+00	0.000E+00	
4	3.834E-03	8.263E+00	7.359E+02	2.241E+01	2.101E+01	0.000E+00	0.000E+00	
.....								
81	3.499E-02	9.428E-02	2.557E-01	2.557E-01	1.808E-01	0.000E+00	0.000E+00	
82	3.500E-02	4.024E-02	1.091E-01	1.091E-01	7.715E-02	0.000E+00	0.000E+00	
83	3.500E-02	0.000E+00	0.000E+00	0.000E+00	0.000E+00	0.000E+00	0.000E+00	

We see profile data for momentum, $u^+(y^+)$ or (upl and ypl), as well as data for heat transfer. $T^+(y^+)$ or (hpl and ypl) and for $k-\varepsilon$ turbulence variables, when higher-order turbulence models are used.

This same data can be displayed in dimensional form by resetting $k10=11$. For turbulent flows, the user can also set output variables and flags to print profiles at specific locations. This is described in detail in the users manual.

13-9

TEXSTAN analysis of the turbulent momentum entry flow between parallel plates: Investigate the entry length region through the hydrodynamically fully-developed region of flow in between parallel plates with hydraulic diameter Reynolds numbers of 30,000 and 150,000. Pick fluid properties that are appropriate to air, evaluated at a temperature of 300 K. Use constant fluid properties, and note that the energy equation does not have to be solved. Let the plate spacing be 7.0 cm and the plate length be 7.0 m. Let the velocity entry profile at the inlet to the plates be flat, which can be supplied by using the *kstart*=1 choice in TEXSTAN. For a turbulence model, choose the hybrid turbulence model comprised of a constant eddy viscosity in the outer part of the flow ($\varepsilon_m/\nu = a\text{Re}^b$ with $a = 0.0022$ and $b = 0.9$) and a mixing-length turbulence model with the Van Driest damping function ($\kappa=0.40$ and $A^+=26$) in the near-wall region (*ktmu*=7). This hybrid model follows the circular pipe idea described in Prob. 13-8, and thus better predict the fully-developed friction coefficient for a given Reynolds number. Compare the friction coefficient with the set of Eqs. (13-11) through (13-14), being careful to use the hydraulic diameter, Eq. (13-16). Feel free to investigate any other attribute of the boundary-layer flow. For example you can compare the profile shape with that described as a part of Prob. 13-1.

The data file for this problem is *13.9.dat.txt*. The data set construction is based on the *s510_7.dat.txt* file for combined entry length flow between parallel planes with a specified surface temperature (initial profiles: flat velocity and flat temperature). The turbulence model is a composite model that uses the van-Driest mixing length model in the near-wall region and a constant eddy viscosity in the outer region.

Here is an abbreviated listing of the output file (it will be called *out.txt* when you execute TEXSTAN using *13.9.dat.txt*). Only the momentum results will be discussed. The hydraulic diameter Reynolds number is 30,000.

intg	x/dh	cf2	nu	cfrat	nurat	tm/ts	ts	qflux
5	1.250E-02	2.175E-02	581.5	7.373	8.245	.949	2.950E+02	1.624E+03
500	1.250E+00	4.173E-03	99.5	1.415	1.411	.951	2.950E+02	2.696E+02
1000	2.500E+00	3.764E-03	89.1	1.276	1.263	.952	2.950E+02	2.362E+02
1500	3.750E+00	3.562E-03	83.7	1.208	1.187	.953	2.950E+02	2.173E+02
2000	5.000E+00	3.432E-03	80.1	1.163	1.136	.954	2.950E+02	2.041E+02
2500	6.420E+00	3.331E-03	77.3	1.129	1.096	.955	2.950E+02	1.929E+02
3000	8.243E+00	3.243E-03	74.9	1.099	1.062	.956	2.950E+02	1.820E+02
3500	1.058E+01	3.170E-03	72.9	1.075	1.034	.957	2.950E+02	1.715E+02
4000	1.359E+01	3.115E-03	71.4	1.056	1.013	.959	2.950E+02	1.613E+02
4500	1.745E+01	3.078E-03	70.5	1.043	.999	.961	2.950E+02	1.511E+02
5000	2.240E+01	3.056E-03	70.0	1.036	.992	.964	2.950E+02	1.405E+02
5500	2.876E+01	3.046E-03	69.8	1.033	.989	.966	2.950E+02	1.289E+02
6000	3.693E+01	3.043E-03	69.7	1.032	.988	.970	2.950E+02	1.156E+02
6500	4.741E+01	3.042E-03	69.7	1.031	.988	.974	2.950E+02	1.007E+02
7000	6.085E+01	3.042E-03	69.7	1.031	.988	.978	2.950E+02	8.442E+01
7500	7.813E+01	3.042E-03	69.7	1.031	.988	.982	2.950E+02	6.728E+01
7994	1.000E+02	3.042E-03	69.7	1.031	.988	.987	2.950E+02	5.048E+01

Here is a same abbreviated output for the $\text{Re}_{D_h} = 150,000$ data set.

intg	x/dh	cf2	nu	cfrat	nurat	tm/ts	ts	qflux
5	1.250E-02	7.902E-03	1012.7	3.828	4.102	.949	2.950E+02	2.832E+03
500	1.250E+00	2.851E-03	348.0	1.381	1.410	.950	2.950E+02	9.539E+02
1000	2.500E+00	2.592E-03	315.1	1.256	1.276	.951	2.950E+02	8.505E+02
1500	3.750E+00	2.468E-03	299.1	1.196	1.211	.952	2.950E+02	7.956E+02
2000	5.000E+00	2.386E-03	288.1	1.156	1.167	.952	2.950E+02	7.558E+02
2500	6.420E+00	2.319E-03	279.0	1.124	1.130	.953	2.950E+02	7.211E+02
3000	8.243E+00	2.258E-03	270.7	1.094	1.097	.954	2.950E+02	6.865E+02
3500	1.058E+01	2.205E-03	263.4	1.068	1.067	.955	2.950E+02	6.524E+02
4000	1.359E+01	2.161E-03	257.4	1.047	1.043	.956	2.950E+02	6.190E+02
4500	1.745E+01	2.128E-03	253.0	1.031	1.025	.958	2.950E+02	5.862E+02
5000	2.240E+01	2.105E-03	250.1	1.020	1.013	.960	2.950E+02	5.530E+02
5500	2.876E+01	2.092E-03	248.6	1.014	1.007	.962	2.950E+02	5.178E+02
6000	3.693E+01	2.086E-03	248.0	1.011	1.005	.965	2.950E+02	4.785E+02
6500	4.741E+01	2.084E-03	247.8	1.010	1.004	.968	2.950E+02	4.335E+02
7000	6.085E+01	2.084E-03	247.8	1.010	1.004	.972	2.950E+02	3.823E+02
7500	7.813E+01	2.084E-03	247.8	1.010	1.004	.976	2.950E+02	3.253E+02
7994	1.000E+02	2.084E-03	247.8	1.010	1.004	.981	2.950E+02	2.652E+02

In these benchmark outputs ($kout=8$) we see $cfrat$ and $strat$, which present ratios of TEXSTAN-calculated values for c_f to the Kármán-Nikuradse Eq. (13-14) at the same Reynolds number and for Nu to the Gnielinski Eq. (14-8). We can use these ratios to help determine if a data set construction is correct. At the present time only some of the “s” data sets in Appendix H can be used with $kout=8$. We see the $cfrat$ and $strat$ show agreement between the turbulent correlations and the TEXSTAN-computed solution. This helps confirm that for turbulent internal flows, the hydraulic diameter Reynolds number is successful in correlating data in noncircular cross sections, as discussed on p. 287. From the output we can also see the hydrodynamic developing region is complete to within 5% by x/D_h of about 12-15 for both Reynolds numbers. The output file *fin85.txt* presents most of the momentum flow variables, including the surface shear stress and pressure drop. The files *fin82.txt* and *fin84.txt* contain heat transfer variables for the E-surface (the pipe wall).

To plot the developing velocity profiles, set $kout=4$ and choose $k10=11$ for $k10=11$ for dimensional variables (the $k10=10$ does not work for this geometry). The profiles will be printed as a part of the file *out.txt*. You can choose where to print the profiles by adding x locations to the $x(m)$. Be sure to change the two $nxbc$ variables and add the appropriate sets of two lines of boundary condition information for each new x -location. This is explained in detail in the *s400.man* user manual. You can then convert the profiles to dimensionless plus variables.

14-1

Consider fully developed turbulent flow between parallel planes. Let the Reynolds number (based on hydraulic diameter) be 50,000 and let the Prandtl number of the fluid be 3. The heat flux on one plate, *into* the fluid, is constant everywhere. The heat flux on the other plate is *out* of the fluid, is also constant everywhere, and is the same in magnitude as the heat flux on the first plate. The problem is to calculate and plot the temperature distribution across the fluid from plate to plate. Use any equations for velocity distribution and or eddy diffusivity that you feel are reasonable. For simplicity, it is sufficiently precise to assume that the eddy diffusivity is constant across the center region of the duct at the value given at $r = 0$ by Eq. (13-5), and that Eq. (13-4) is valid over the remainder of the flow area, excepting the sublayer, which can be treated as in the development leading to Eq. (11-16). Explain the shape of the temperature profile by referring to the basic mechanisms involved. How would this profile change with Prandtl number? What would the profile be if the flow were laminar?

Let h = plate spacing. Then $h^+ = h\sqrt{\tau_s/\rho}/\nu = hV\sqrt{c_f/2}/2$. Use a three-layer model with a laminar sublayer extending to $y^+ = 13.2$. Under the assumptions ε_m/ν becomes constant at $y^+ = 0.394h^+$. Then the temperature profile in the three regions is:

$$\begin{aligned} \text{Sublayer} \quad T^+ &= \text{Pr } y^+ \\ \text{Log profile region -} \quad T^+ &= T_{y^+=13.2}^+ + \int_{13.2}^{y^+} \left(\frac{1}{\frac{h^+}{2} - (y^+)^2} \right) dy^+ \end{aligned}$$

where b^+ is determined from the results of Prob. 13-1,

$$c_f/2 = 0.041 \text{Re}^{-0.25}$$

where the Re is the hydraulic diameter Reynolds number based on the channel height, h . For this problem,

$$\begin{aligned} c_f/2 &= 0.041 \text{Re}_{D_h}^{-0.25} = 0.00274 \\ b^+ &= 1309 \end{aligned}$$

The centerline is at $y^+ = b^+/2 = 665$, and the value of T^+ at the centerline is 54.16.

14-2

Consider fully developed turbulent flow in a circular tube with heat transfer to or from the fluid at a constant rate per unit of tube length. Let there also be internal heat generation (perhaps from nuclear reaction) at a rate S , W/m^3 , which is everywhere constant. If the Reynolds number is 50,000 and the Prandtl number is 4, evaluate the Nusselt number as a function of the pertinent parameters. The heat-transfer coefficient in the Nusselt number should be defined in the usual manner on the basis of the heat flux *at the surface*, the surface temperature, and the mixed mean fluid temperature. Use a two-layer model to handle the sublayer [see Chap. 11 and the development leading to Eq. (11-16)] and evaluate the eddy diffusivity as described for Prob. 14-1.

$$T^+ = \int_0^{y^+} \left\{ \left[\frac{1}{\left(1 - \frac{y^+}{r_s^+}\right) \left(\frac{\varepsilon_H}{\nu} + \frac{1}{\text{Pr}}\right)} \right] \left[\frac{4}{\text{Re}} \int_0^{y^+} \left(u^+ + \frac{S r_s}{2 \dot{q}_s''} \left\{ u^+ - \frac{\text{Re}}{2 r_s^+} \right\} \right) \left(1 - \frac{y^+}{r_s^+} \right) dy^+ - 1 \right] \right\} dy^+$$

where \dot{q}_s'' is positive into the fluid and

$$r_s^+ = r_s \sqrt{\tau_s / \rho} / \nu = r_s V \sqrt{c_f / 2} / 2$$

If a 2 - layer model is used, for $0 < y^+ < 13.2$ (laminar sublayer), $u^+ = y^+$, and

$$T^+ = \text{Pr} \left[y^+ - \frac{2y^+}{3\text{Re}} + \frac{S r_s}{2 \dot{q}_s''} \left(\frac{(y^+)^2}{r_s^+} - \frac{2(y^+)^3}{3\text{Re}} \right) \right]$$

For $13.2 < y^+ < r_s^+$ a closed form solution is obtainable if we assume $u^+ = 8.6(y^+)^{1/7}$. Numerical integration using mixing-length theory, Eq. (11-25), $\varepsilon_M / \nu = (0.4 r_s^+ / 6)$ in the central region, and Eq.(12-7) for Pr_t , leads to the following results:

Pr	Re	$\frac{S r_s}{2 \dot{q}_s''}$	Nu
4	50000	0	255.1
4	50000	-1	259.3
4	50000	+1	251.1

14-3

Consider turbulent flow between parallel planes with Reynolds number equal to 100,000. For a fluid with $Pr = 10$, and then for a fluid with $Pr = 0.01$, evaluate the Nusselt number for fully developed constant heat rate for only one side heated and then for both sides equally heated, using the solutions given in the text. Discuss the differences between the cases of one side heated and both sides heated, in terms of the heat-transfer mechanisms and the temperature profiles. How is the Nusselt number related to the “shape” of the temperature profile?

For one side heated:

$$Pr = 10 \quad Nu = 680$$

$$Pr = 0.01 \quad Nu = 6.70$$

For both sides heated:

$$Pr = 10 \quad Nu = 712$$

$$Pr = 0.01 \quad Nu = 11.96$$

At $Pr = 10$ the heat transfer resistance is concentrated very near the walls, while at $Pr = 0.01$ it is distributed over the entire flow cross-section.

14-4

Consider fully developed flow in a circular tube with constant heat rate per unit of tube length. Let the mean flow velocity be 8 m/s. Evaluate the heat-transfer coefficient h for the following cases, and discuss the reasons for the differences: (a) air, 90°C, 1 atm pressure, 2.5 cm diameter tube; (b) same with 0.6 cm diameter tube; (c) hydrogen gas, 90°C, 1 atm pressure, 2.5 cm diameter tube; (d) liquid oxygen, -200°C, 2.5 cm diameter tube; (e) liquid water, 38°C, 2.5 cm diameter tube; (f) liquid sodium, 200°C, 2.5 cm diameter tube; (g) aircraft engine oil, 90°C, 2.5 cm diameter tube; (h) air, 90°C, 1000 kPa pressure, 2.5 cm diameter tube.

- (a) 33.2 W/(m² K)
- (b) 44.2 (if laminar, then 22.2)
- (c) 35.5 (laminar)
- (d) 15,732
- (e) 29,605
- (f) 54,188
- (g) 13,74
- (h) 13,74

14-5

Consider a 1.20 cm inside-diameter, 1.8 m long tube wound by an electric resistance heating element. Let the function of the tube be to heat an organic fuel from 10 to 65°C. Let the mass-flow rate of the fuel be 0.126 kg /s, and let the following average properties be treated as constant:

$$\text{Pr} = 10, \quad \rho = 753 \text{ kg/m}^3, \quad c = 2.10 \text{ kJ/(kg} \cdot \text{K)}, \quad k = 0.137 \text{ W/(m} \cdot \text{K)}$$

Calculate and plot both tube surface temperature and fluid mean temperature as functions of tube length. TEXSTAN can be used to confirm this analysis. Use constant fluid properties and do not consider viscous dissipation. Let the velocity and thermal entry profiles at the inlet to the tube be flat, which can be supplied by using the *kstart=1* choice in TEXSTAN. Let the energy boundary condition be a constant surface heat flux equal to the value from the analysis. For a turbulence model, choose the model described in Prob. 14-13.

For this problem, with the given properties, $\text{Re}_D = (4\dot{m})/(\pi\mu D) = 20,490$. The $c_f/2$ from the Kármán-Nikuradse Eq. (13-14) for this problem is 0.00324 and for Nu from the corresponding Gnielinski Eq. (14-8) is 174. Note that $L/D_h = 150$ for this problem, so the hydrodynamic and thermal entry region should be towards the entry region for the pipe. From a First-Law energy balance, the total heat transfer to the fluid is 14.553 kW, corresponding to a constant surface heat flux of 214.461 kW/m². From the Nu definition, $h = 1986 \text{ W/m}^2 \cdot \text{K}$, and based on this value, the surface temperature at the exit should be 173°C.

$x/L, \text{ m}$	$T_m, ^\circ\text{C}$	$T_s, ^\circ\text{C}$	TEXSTAN
0	10	118	
25	19.2	127	119
50	28.3	136	130
100	46.7	155	148
150	65	173	166

The data file for this problem is *14.5.dat.txt*. The data set construction is based on the *s420_7.dat.txt* file for combined entry length flow in a pipe with a specified surface heat flux (initial profiles: flat velocity and flat temperature). The turbulence model is a composite model that uses the van-Driest mixing length model in the near-wall region and a constant eddy viscosity in the outer region, along with a variable turbulent Prandtl number model for liquid metals and gases, and a constant turbulent Prandtl number for liquids. The turbulent data set manual *s400.man.doc* is very helpful in understanding this data set construction.

Execution of the input data set generates several output files. Here is an abbreviated listing of the output file (it will be called *out.txt* when you execute TEXSTAN using *14.5.dat.txt*).

intg	x/dh	cf2	nu	cfrat	nurat	tm/ts	ts	qflux
5	2.500E-02	1.631E+00	-279.5	502.818	-1.608	1.311	2.158E+02	2.145E+05
400	2.000E+00	4.187E-03	223.7	1.291	1.287	.772	3.677E+02	2.145E+05
800	4.000E+00	3.826E-03	206.8	1.180	1.190	.758	3.753E+02	2.145E+05
1200	6.106E+00	3.677E-03	200.0	1.134	1.150	.752	3.792E+02	2.145E+05
1600	9.108E+00	3.561E-03	194.9	1.098	1.121	.748	3.827E+02	2.145E+05

2000	1.358E+01	3.468E-03	190.8	1.069	1.098	.745	3.864E+02	2.145E+05
2400	2.026E+01	3.405E-03	188.0	1.050	1.082	.744	3.903E+02	2.145E+05
2800	3.022E+01	3.372E-03	186.5	1.040	1.073	.745	3.948E+02	2.145E+05
3200	4.508E+01	3.361E-03	185.9	1.036	1.069	.748	4.006E+02	2.145E+05
3600	6.721E+01	3.359E-03	185.8	1.036	1.069	.753	4.088E+02	2.145E+05
4000	1.002E+02	3.359E-03	185.8	1.036	1.069	.760	4.209E+02	2.145E+05
4400	1.402E+02	3.359E-03	185.8	1.036	1.069	.768	4.355E+02	2.145E+05
4498	1.500E+02	3.359E-03	185.8	1.036	1.069	.770	4.391E+02	2.145E+05

In these benchmark outputs ($kout=8$) we see c_{frat} and $nurat$, which present ratios of TEXSTAN-calculated values for c_f to the Kármán-Nikuradse Eq. (13-14) at the same Reynolds number and for Nu to the Gnielinski Eq. (14-8). We can use these ratios to help determine if a data set construction is correct. At the present time only some of the “s” data sets in Appendix H can be used with $kout=8$. We see the c_{frat} and $nurat$ show agreement between the turbulent correlations and the TEXSTAN-computed solution. From the output we can also see both the hydrodynamic and thermal developing regions are complete to within 5% by x/D_h of about 9-14. The output file *fn85.txt* presents most of the momentum flow variables, including the surface shear stress and pressure drop. The files *fn82.txt* and *fn84.txt* contain heat transfer variables for the E-surface (the pipe wall). Comparing TEXSTAN with the analysis, we see the thermally fully flow gives a friction coefficient that is 3.6% higher than the Kármán-Nikuradse correlation and a Nusselt number that is 6.9% higher than the Gnielinski correlation and the corresponding surface temperatures. This answer is somewhat affected by the choice of turbulence model.

14-6

Liquid potassium flows in a 2.5 cm diameter tube at a mean velocity of 2.4 m/s and a mean temperature of 550°C. Suppose the tube is heated at a constant rate per unit of length but the heat flux varies around the periphery of the tube in a sinusoidal manner, with the maximum heat flux twice the minimum heat flux. If the maximum surface temperature is 700°C, evaluate the axial mean temperature gradient, °C/m, and prepare a plot of temperature around the periphery of the tube.

ϕ	T_s °C
0	700
$\pi/2$	633
π	566
$3\pi/2$	633
2π	700

14-7

Consider the flow of first air ($Pr = 0.7$) and then mercury ($Pr = 0.01$) at a Reynolds number of 100,000 in a 2 cm diameter circular tube with constant heat rate per unit of length. At a distance of 1.2 m from the tube entrance the heating stops, and the tube is insulated from then on. Using relative units of temperature, calculate and plot the decay of surface temperature as it approaches the mean fluid temperature in the insulated region. Discuss the difference in behavior of the two fluids in terms of the basic mechanisms involved. TEXSTAN can be used to confirm this analysis. Use constant fluid properties and do not consider viscous dissipation. Let the velocity and thermal entry profiles at the inlet to the tube be flat, which can be supplied by using the $kstart=1$ choice in TEXSTAN. Let the energy boundary condition be a constant surface heat flux (you can arbitrarily choose 250 W/m^2). For a turbulence model, choose the model described in Prob. 14-13. The piecewise surface heat flux boundary condition is modeled easily in TEXSTAN by providing heat flux values at four x -locations, two for each segment, e.g. at $x=0, x=1.2 \text{ m}$ (over which there will be a heat flux), and at $x=1.201 \text{ m}, x=2.4 \text{ m}$ (arbitrary final tube length, over which there will be a zero heat flux, adiabatic condition). Because TEXSTAN linearly interpolates the surface thermal boundary condition between consecutive x -locations, a total of 4 boundary condition locations is sufficient to describe the surface heat flux variation.

The analytical results have not been calculated because there are not enough eigenvalues in Table 14-7, but in principal they could using the ideas relating of Prob. 8-10 with the coefficients in the series changed. The problem has been solved using TEXSTAN. Change this problem to a TEXSTAN problem statement and use surface heat flux of $10,000 \text{ W/m}^2$ for air and $100,000 \text{ W/m}^2$ for mercury.

The data file for this problem is *14.7.dat.txt*. The data set construction is based on the *s420_7.dat.txt* file for combined entry length flow in a pipe with a specified surface heat flux (initial profiles: flat velocity and flat temperature). The turbulence model is a composite model that uses the van-Driest mixing length model in the near-wall region and a constant eddy viscosity in the outer region, along with a variable turbulent Prandtl number model for liquid metals and gases, and a constant turbulent Prandtl number for liquids.

Here is an abbreviated listing of the *14.7.frm84.txt* output file using $k5=200$ print spacing to show the mean and surface temperature variations.

intg	x/dh	htc	qflux	tm	ts
5	2.4999990E-02	1.2462E+03	1.0000E+04	3.0001E+02	3.0804E+02
200	9.9999970E-01	3.6470E+02	1.0000E+04	3.0043E+02	3.2785E+02
400	2.0000000E+00	3.1961E+02	1.0000E+04	3.0087E+02	3.3215E+02
...					
2600	2.1505046E+01	2.4644E+02	1.0000E+04	3.0931E+02	3.4989E+02
2800	2.5524091E+01	2.4459E+02	1.0000E+04	3.1105E+02	3.5194E+02
3000	3.0257357E+01	2.4320E+02	1.0000E+04	3.1310E+02	3.5422E+02
3200	3.5831759E+01	2.4222E+02	1.0000E+04	3.1552E+02	3.5680E+02
3400	4.2396784E+01	2.4159E+02	1.0000E+04	3.1836E+02	3.5975E+02
3600	5.0128433E+01	2.4122E+02	1.0000E+04	3.2171E+02	3.6317E+02
3800	5.9234066E+01	2.4104E+02	1.0000E+04	3.2565E+02	3.6714E+02
=====					
4000	6.9199981E+01	0.0000E+00	0.0000E+00	3.2599E+02	3.2841E+02
4200	7.9200000E+01	0.0000E+00	0.0000E+00	3.2599E+02	3.2680E+02
4400	8.9200000E+01	0.0000E+00	0.0000E+00	3.2599E+02	3.2628E+02

4600	9.9200000E+01	0.0000E+00	0.0000E+00	3.2599E+02	3.2609E+02
4800	1.0920004E+02	0.0000E+00	0.0000E+00	3.2599E+02	3.2602E+02
5000	1.1920004E+02	0.0000E+00	0.0000E+00	3.2599E+02	3.2600E+02
5200	1.2920003E+02	0.0000E+00	0.0000E+00	3.2599E+02	3.2599E+02
5400	1.3920000E+02	0.0000E+00	0.0000E+00	3.2599E+02	3.2599E+02
5600	1.4920000E+02	0.0000E+00	0.0000E+00	3.2599E+02	3.2599E+02
5616	1.4999996E+02	0.0000E+00	0.0000E+00	3.2599E+02	3.2599E+02

We see that at the step change in surface heat flux, there is a rapid drop in surface temperature, especially compared to what we would see in laminar flow. The step occurs at $L/D_h = 60$ and by 10 to 15 hydraulic diameters the surface temperature has dropped to near the mean temperature. This is comparable to what we see in the entry region where the Nusselt number becomes thermally fully developed in this same interval for $Pr=0.7$ (see the output below). Note to resolve the temperature distribution, you would want to significantly reduce the $k5$ print variable.

Here is an abbreviated listing of the output file (it will be called *out.txt* when you execute TEXSTAN using *14.7.dat.txt*) and $Pr=0.7$ and $Re=100,000$.

intg	x/dh	cf2	nu	cfrat	nurat	tm/ts	ts	qflux
5	2.500E-02	7.767E-03	944.5	3.459	5.297	.974	3.080E+02	1.000E+04
400	2.000E+00	2.858E-03	242.2	1.273	1.358	.906	3.322E+02	1.000E+04
800	4.000E+00	2.617E-03	217.5	1.165	1.220	.896	3.366E+02	1.000E+04
1200	6.086E+00	2.513E-03	206.8	1.119	1.160	.892	3.393E+02	1.000E+04
1600	8.871E+00	2.442E-03	199.2	1.088	1.117	.889	3.419E+02	1.000E+04
2000	1.273E+01	2.384E-03	193.2	1.062	1.083	.886	3.447E+02	1.000E+04
2400	1.809E+01	2.341E-03	188.5	1.042	1.057	.885	3.480E+02	1.000E+04
2800	2.552E+01	2.311E-03	185.4	1.029	1.040	.884	3.519E+02	1.000E+04
3200	3.583E+01	2.295E-03	183.6	1.022	1.030	.884	3.568E+02	1.000E+04
3600	5.013E+01	2.289E-03	182.8	1.019	1.025	.886	3.632E+02	1.000E+04
4000	6.920E+01	2.287E-03	.0	1.019	.000	.993	3.284E+02	0.000E+00
4400	8.920E+01	2.287E-03	.0	1.019	.000	.999	3.263E+02	0.000E+00
4800	1.092E+02	2.287E-03	.0	1.019	.000	1.000	3.260E+02	0.000E+00
5200	1.292E+02	2.287E-03	.0	1.019	.000	1.000	3.260E+02	0.000E+00
5600	1.492E+02	2.287E-03	.0	1.019	.000	1.000	3.260E+02	0.000E+00
5616	1.500E+02	2.287E-03	.0	1.018	.000	1.000	3.260E+02	0.000E+00

From this output we confirm the combined entry length is 10-15 hydraulic diameters for $Pr=0.7$. The approximate trend of this data for the heating region can be compared with Fig. 14-7.

For mercury, we take the properties at about 200K to match the $Pr=0.01$. Because this is a constant property solution, it really does not matter greatly. Here is an abbreviated listing of the *14.7.fm84.txt* output file using $k5=200$ print spacing to show the mean and surface temperature variations.

intg	x/dh	htc	qflux	tm	ts
5	2.4999990E-02	1.1248E+05	1.0000E+05	3.0001E+02	3.0090E+02

200	1.0000000E+00	1.9572E+04	1.0000E+05	3.0058E+02	3.0569E+02
400	1.9999992E+00	1.4814E+04	1.0000E+05	3.0116E+02	3.0791E+02
600	3.0000000E+00	1.2791E+04	1.0000E+05	3.0175E+02	3.0957E+02
...					
2800	2.5524091E+01	7.9311E+03	1.0000E+05	3.1487E+02	3.2747E+02
3000	3.0257372E+01	7.8325E+03	1.0000E+05	3.1762E+02	3.3039E+02
3200	3.5831759E+01	7.7655E+03	1.0000E+05	3.2087E+02	3.3375E+02
3400	4.2396761E+01	7.7239E+03	1.0000E+05	3.2469E+02	3.3764E+02
3600	5.0128433E+01	7.7006E+03	1.0000E+05	3.2920E+02	3.4218E+02
3800	5.9234088E+01	7.6891E+03	1.0000E+05	3.3450E+02	3.4750E+02
=====					
4000	6.9199974E+01	0.0000E+00	0.0000E+00	3.3494E+02	3.3711E+02
4200	7.9199977E+01	0.0000E+00	0.0000E+00	3.3494E+02	3.3563E+02
4400	8.9200000E+01	0.0000E+00	0.0000E+00	3.3494E+02	3.3517E+02
4600	9.9200000E+01	0.0000E+00	0.0000E+00	3.3494E+02	3.3502E+02
4800	1.0920000E+02	0.0000E+00	0.0000E+00	3.3494E+02	3.3497E+02
5000	1.1920005E+02	0.0000E+00	0.0000E+00	3.3494E+02	3.3495E+02
5200	1.2920004E+02	0.0000E+00	0.0000E+00	3.3494E+02	3.3495E+02
5400	1.3920003E+02	0.0000E+00	0.0000E+00	3.3494E+02	3.3495E+02
5600	1.4920000E+02	0.0000E+00	0.0000E+00	3.3494E+02	3.3494E+02
5616	1.4999994E+02	0.0000E+00	0.0000E+00	3.3494E+02	3.3494E+02

Once again we see that at the step change in surface heat flux, there is a rapid drop in surface temperature, especially compared to what we would see in laminar flow. However, for $Pr \ll 1$, we see the change occur even faster. The step occurs at $L/D_h = 60$ and by 5 to 10 hydraulic diameters the surface temperature has dropped to near the mean temperature. This is comparable to what we see in the entry region where the Nusselt number becomes thermally fully developed in this same interval for $Pr=0.01$ (see the output below). Note to resolve the temperature distribution, you would want to significantly reduce the $k5$ print variable.

Here is an abbreviated listing of the output file (it will be called *out.txt* when you execute TEXSTAN using *14.7.dat.txt*) and $Pr=0.01$ and $Re=100,000$.

intg	x/dh	cf2	nu	cfrat	nurat	tm/ts	ts	qflux
5	2.500E-02	7.767E-03	163.8	3.459	15.749	.997	3.009E+02	1.000E+05
400	2.000E+00	2.858E-03	21.6	1.273	2.074	.978	3.079E+02	1.000E+05
800	4.000E+00	2.617E-03	16.9	1.165	1.629	.972	3.109E+02	1.000E+05
1200	6.086E+00	2.514E-03	15.0	1.120	1.447	.969	3.132E+02	1.000E+05
1600	8.871E+00	2.442E-03	13.7	1.088	1.321	.966	3.158E+02	1.000E+05
2000	1.273E+01	2.385E-03	12.7	1.062	1.224	.964	3.189E+02	1.000E+05
2400	1.809E+01	2.341E-03	12.0	1.042	1.155	.962	3.227E+02	1.000E+05
2800	2.552E+01	2.311E-03	11.5	1.029	1.110	.961	3.275E+02	1.000E+05

3200	3.583E+01	2.295E-03	11.3	1.022	1.087	.961	3.337E+02	1.000E+05
3600	5.013E+01	2.289E-03	11.2	1.019	1.078	.962	3.422E+02	1.000E+05
=====								
4000	6.920E+01	2.287E-03	.0	1.019	.000	.994	3.371E+02	0.000E+00
4400	8.920E+01	2.287E-03	.0	1.018	.000	.999	3.352E+02	0.000E+00
4800	1.092E+02	2.287E-03	.0	1.018	.000	1.000	3.350E+02	0.000E+00
5200	1.292E+02	2.287E-03	.0	1.019	.000	1.000	3.349E+02	0.000E+00
5600	1.492E+02	2.287E-03	.0	1.019	.000	1.000	3.349E+02	0.000E+00
5616	1.500E+02	2.287E-03	.0	1.018	.000	1.000	3.349E+02	0.000E+00

Note in this output the thermal boundary layer leads the momentum boundary layer development as would be expected for $Pr \ll 1$, but because this is turbulent flow, the development differences are minimized. The approximate trend of this data for the heating region can be compared with Fig. 14-7.

14-8

Let air at 21°C and 1 atm pressure flow at a Reynolds number of 50,000 in a 2.5 cm diameter circular tube. The tube wall is insulated for the first 75 cm, but for the next 125 cm the tube surface temperature is constant at 40°C. Then it abruptly increases to 50°C and remains constant for another 125 cm. Plot the local heat-transfer coefficient h as a function of an axial distance. Does the abrupt increase in surface temperature to 50°C cause a significant change in the average heat-transfer coefficient over the entire 325 cm of heated length? In simple heat-exchanger theory a mean heat-transfer coefficient with respect to tube length is generally employed. In this case how much does the mean differ from the asymptotic value of h ? TEXSTAN can be used to confirm this analysis. Use constant fluid properties and do not consider viscous dissipation. Let the velocity and thermal entry profiles at the inlet to the tube be flat, which can be supplied by using the $kstart=1$ choice in TEXSTAN. Let the energy boundary condition be a surface temperature for this problem. For a turbulence model, choose the model described in Prob. 14-13. The piecewise surface temperature boundary condition is modeled easily in TEXSTAN by providing surface temperature values at six x -locations. For the first interval from $x=0$ to $x=0.75$ m, set the surface temperature equal to the inlet temperature, effectively creating a zero heat flux boundary condition; over the interval $x=1.7501$ m to $x=2.0$ m set the surface temperature to be 40°C, and for the third interval $x=2.001$ m to $x=3.25$ m set the surface temperature to be 50°C.

The analytical results have not been calculated because there are not enough eigenvalues in Table 14-7. The problem has been solved using TEXSTAN. [Change this problem to a TEXSTAN problem statement](#)

The data file for this problem is *14.8.dat.txt*. The data set construction is based on the *s410_7.dat.txt* file for combined entry length flow in a pipe with a specified surface temperature (initial profiles: flat velocity and flat temperature). The turbulence model is a composite model that uses the van-Driest mixing length model in the near-wall region and a constant eddy viscosity in the outer region, along with a variable turbulent Prandtl number model for liquid metals and gases, and a constant turbulent Prandtl number for liquids.

Note that the first section of the pipe is adiabatic, and the rest of the pipe is a variable wall temperature problem. TEXSTAN is not set up to handle a combination of Dirichlet and Neumann boundary conditions, but for this problem, we can specify the surface temperature equal to the entry temperature over the first 75 cm, and this will become an adiabatic condition (no heat transfer) for the first section.

Execution of the input data set generates several output files. Here is an abbreviated listing of the output file (it will be called *out.txt* when you execute TEXSTAN using *14.8.dat.txt*) for $Pr=0.7$ and $Re=50,000$

intg	x/dh	cf2	nu	cfrat	nurat	tm/ts	ts	qflux
5	2.500E-02	1.180E-02	.0	4.511	.000	1.000	2.100E+01	0.000E+00
100	5.000E-01	4.282E-03	.0	1.637	.000	1.000	2.100E+01	0.000E+00
200	1.000E+00	3.737E-03	.0	1.429	.000	1.000	2.100E+01	0.000E+00
300	1.500E+00	3.488E-03	.0	1.334	.000	1.000	2.100E+01	0.000E+00
400	2.000E+00	3.337E-03	.0	1.276	.000	1.000	2.100E+01	0.000E+00
...								
1800	1.393E+01	2.769E-03	.0	1.059	.000	1.000	2.100E+01	0.000E+00
1900	1.624E+01	2.747E-03	.0	1.050	.000	1.000	2.100E+01	0.000E+00
2000	1.900E+01	2.728E-03	.0	1.043	.000	1.000	2.100E+01	0.000E+00
2100	2.231E+01	2.711E-03	.0	1.037	.000	1.000	2.100E+01	0.000E+00
2200	2.626E+01	2.699E-03	.0	1.032	.000	1.000	2.100E+01	0.000E+00
=====								

2300	3.094E+01	2.690E-03	137.8	1.028	1.325	.534	4.000E+01	2.713E+03
2400	3.594E+01	2.684E-03	113.1	1.026	1.087	.565	4.000E+01	2.079E+03
2500	4.094E+01	2.681E-03	108.2	1.025	1.040	.591	4.000E+01	1.867E+03
2600	4.594E+01	2.679E-03	105.9	1.024	1.018	.615	4.000E+01	1.719E+03
2700	5.094E+01	2.678E-03	104.7	1.024	1.006	.638	4.000E+01	1.600E+03
2800	5.594E+01	2.677E-03	104.0	1.024	1.000	.659	4.000E+01	1.498E+03
2900	6.094E+01	2.677E-03	103.6	1.023	.996	.678	4.000E+01	1.407E+03
3000	6.594E+01	2.677E-03	103.4	1.023	.994	.697	4.000E+01	1.324E+03
3100	7.094E+01	2.676E-03	103.3	1.023	.993	.714	4.000E+01	1.246E+03
3200	7.594E+01	2.676E-03	103.2	1.023	.993	.731	4.000E+01	1.174E+03
=====								
3300	8.094E+01	2.676E-03	120.1	1.023	1.154	.600	5.000E+01	2.532E+03
3400	8.594E+01	2.676E-03	108.0	1.023	1.038	.625	5.000E+01	2.136E+03
3500	9.094E+01	2.676E-03	105.6	1.023	1.015	.647	5.000E+01	1.966E+03
3600	9.594E+01	2.676E-03	104.5	1.023	1.004	.668	5.000E+01	1.832E+03
3700	1.009E+02	2.676E-03	103.9	1.023	.999	.687	5.000E+01	1.716E+03
3800	1.059E+02	2.676E-03	103.6	1.023	.996	.705	5.000E+01	1.613E+03
3900	1.109E+02	2.676E-03	103.4	1.023	.994	.722	5.000E+01	1.517E+03
4000	1.159E+02	2.676E-03	103.3	1.023	.993	.738	5.000E+01	1.429E+03
4100	1.209E+02	2.676E-03	103.2	1.023	.993	.753	5.000E+01	1.347E+03
4200	1.259E+02	2.676E-03	103.2	1.023	.992	.767	5.000E+01	1.269E+03
4281	1.300E+02	2.676E-03	103.2	1.023	.992	.778	5.000E+01	1.210E+03

In these benchmark outputs ($k_{out}=8$) we see c_{frat} and $nurat$, which present ratios of TEXSTAN-calculated values for c_f to the Kármán-Nikuradse Eq. (13-14) at the same Reynolds number and for Nu to the Gnielinski Eq. (14-8). We see the c_{frat} and $nurat$ show agreement between the turbulent correlations and the TEXSTAN-computed solution. We see the three distinct heating regions. For the first region, by $x/D_h = 26$, the friction coefficient is close to being hydrodynamically fully developed. For the second and third sections where the heating is occurring, we see the Nu takes about $10 x/D_h$ for most of the thermal boundary layer change to reduce. For this problem each heating section is about $50 x/D_h$ so the approximation of a constant Nu is not too bad.

14-9

Starting with the constant-surface-temperature, thermal-entry-length solutions for a circular tube, calculate and compare the Nusselt numbers for constant surface temperature and for a linearly varying surface temperature, for very long tubes for a Reynolds number of 50,000 and a Prandtl number of 0.01. Repeat for a Prandtl number of 0.7 and discuss the reasons for the differences noted.

The analytical results have not been calculated because there are not enough eigenvalues in Table 14-7. The problem has been solved using TEXSTAN. Change this problem to a TEXSTAN problem statement

This solution is similar to problem 14-8, but the flow for this problem is supposed to be hydrodynamically fully-developed. However, TEXSTAN is not set up for this set of initial conditions (as is it is for laminar pipe flow). The intent of this problem is to demonstrate the linear surface temperature variation is a constant heat flux problem, so we would be comparing Nusselt numbers for these two cases. We will use the geometric setup for this problem. a 2.5 cm diameter tube, and we will let the pipe length be 100 hydraulic diameters. We will let the fluid enter the pipe at $T_e=20^\circ\text{C}$. For the constant surface temperature we will let $T_s=40^\circ\text{C}$.

The data file for this problem is *14.9.dat.txt*. The data set construction is based on the *s410_7.dat.txt* file for combined entry length flow in a pipe with a specified surface temperature (initial profiles: flat velocity and flat temperature). The turbulence model is a composite model that uses the van-Driest mixing length model in the near-wall region and a constant eddy viscosity in the outer region, along with a variable turbulent Prandtl number model for liquid metals and gases, and a constant turbulent Prandtl number for liquids.

Execution of the input data set generates several output files. Here is an abbreviated listing of the output file (it will be called *out.txt* when you execute TEXSTAN using *14.9.dat.txt*) for $\text{Pr}=0.7$ and $\text{Re}=50,000$ and a constant surface temperature boundary condition.

intg	x/dh	cf2	nu	cfrat	nurat	tm/ts	ts	qflux
5	2.500E-02	1.180E-02	511.8	4.511	4.920	.501	4.000E+01	1.078E+04
500	2.500E+00	3.233E-03	128.1	1.236	1.232	.523	4.000E+01	2.580E+03
1000	5.000E+00	2.987E-03	117.6	1.142	1.130	.539	4.000E+01	2.287E+03
1500	8.242E+00	2.867E-03	112.2	1.096	1.079	.558	4.000E+01	2.092E+03
2000	1.358E+01	2.773E-03	107.8	1.060	1.036	.587	4.000E+01	1.879E+03
2500	2.239E+01	2.711E-03	104.8	1.037	1.007	.629	4.000E+01	1.642E+03
3000	3.691E+01	2.683E-03	103.5	1.026	.995	.688	4.000E+01	1.365E+03
3500	5.980E+01	2.677E-03	103.2	1.023	.992	.762	4.000E+01	1.039E+03
4000	8.480E+01	2.676E-03	103.2	1.023	.992	.822	4.000E+01	7.735E+02
4304	1.000E+02	2.676E-03	103.2	1.023	.992	.852	4.000E+01	6.467E+02

In these benchmark outputs ($k_{out}=8$) we see *cfrat* and *nurat*, which present ratios of TEXSTAN-calculated values for c_f to the Kármán-Nikuradse Eq. (13-14) at the same Reynolds number and for Nu to the Gnielinski Eq. (14-8). We see the *cfrat* and *nurat* show agreement between the turbulent correlations and the TEXSTAN-computed solution, and that the entry lengths for both momentum and energy are about equal.

Now we change the thermal boundary condition to a linear temperature variation. We can either simulate heating by requiring the surface temperature to increase in the flow direction, or we can simulate cooling by requiring the surface temperature to decrease in the flow direction. We will continue with the same geometry. Here is the output for $\text{Pr}=0.7$ and $\text{Re}=50,000$ and the linear wall temperature variation.

intg	x/dh	cf2	nu	cfrat	nurat	tm/ts	ts	qflux
5	2.500E-02	1.180E-02	511.8	4.511	4.921	.501	4.001E+01	1.078E+04
500	2.500E+00	3.233E-03	128.8	1.236	1.238	.517	4.050E+01	2.660E+03
1000	5.000E+00	2.987E-03	118.5	1.142	1.139	.527	4.100E+01	2.425E+03
1500	8.242E+00	2.867E-03	113.4	1.096	1.090	.539	4.165E+01	2.299E+03
2000	1.358E+01	2.773E-03	109.3	1.060	1.051	.556	4.272E+01	2.190E+03
2500	2.239E+01	2.711E-03	106.7	1.037	1.026	.580	4.448E+01	2.106E+03
3000	3.691E+01	2.683E-03	105.6	1.026	1.016	.613	4.738E+01	2.046E+03
3500	5.980E+01	2.677E-03	105.5	1.023	1.014	.655	5.196E+01	1.995E+03
4000	8.480E+01	2.676E-03	105.5	1.023	1.014	.691	5.696E+01	1.957E+03
4500	1.098E+02	2.676E-03	105.5	1.023	1.015	.721	6.196E+01	1.929E+03
5000	1.348E+02	2.676E-03	105.6	1.023	1.015	.744	6.696E+01	1.908E+03
5500	1.598E+02	2.676E-03	105.6	1.023	1.015	.764	7.195E+01	1.892E+03
6000	1.848E+02	2.676E-03	105.6	1.023	1.015	.781	7.695E+01	1.881E+03
6304	2.000E+02	2.676E-03	105.6	1.023	1.015	.790	7.999E+01	1.875E+03

Comparing this linear surface temperature heating case to the constant surface temperature case shows the approximation of the heat flux boundary condition beyond the developing region, and comparison of this Nusselt number with the one for a constant wall temperature shows $105.6/103.2 = 1.023$, which compares with Fig. 14-5 for $Pr=0.7$ and $Re=50,000$, and it shows that for gases (and light liquids) the difference in heat transfer coefficient for the two boundary conditions is about a 2% effect.

We now repeat this exercise for $Pr=0.01$ and the same Re . Execution of the input data set generates several output files. Here is an abbreviated listing of the output file (it will be called *out.txt* when you execute TEXSTAN using *14.9.dat.txt*) for $Pr=0.01$ and $Re=50,000$ and a constant surface temperature boundary condition.

intg	x/dh	cf2	nu	cfrat	nurat	tm/ts	ts	qflux
5	2.500E-02	1.180E-02	89.8	4.511	12.967	.514	4.000E+01	9.591E+05
500	2.500E+00	3.233E-03	9.9	1.236	1.425	.643	4.000E+01	7.742E+04
1000	5.000E+00	2.987E-03	8.2	1.142	1.187	.701	4.000E+01	5.402E+04
1500	8.242E+00	2.867E-03	7.4	1.096	1.071	.756	4.000E+01	3.984E+04
2000	1.358E+01	2.773E-03	6.9	1.060	.999	.820	4.000E+01	2.742E+04
2500	2.239E+01	2.711E-03	6.7	1.037	.971	.888	4.000E+01	1.652E+04
3000	3.691E+01	2.683E-03	6.7	1.026	.964	.949	4.000E+01	7.543E+03
3500	5.980E+01	2.677E-03	6.7	1.024	.963	.985	4.000E+01	2.224E+03
4000	8.480E+01	2.676E-03	6.7	1.023	.963	.996	4.000E+01	5.873E+02
4500	1.098E+02	2.676E-03	6.7	1.023	.963	.999	4.000E+01	1.550E+02
5000	1.348E+02	2.676E-03	6.7	1.023	.963	1.000	4.000E+01	4.094E+01
5500	1.598E+02	2.676E-03	6.7	1.023	.963	1.000	4.000E+01	1.081E+01
6000	1.848E+02	2.676E-03	6.7	1.023	.963	1.000	4.000E+01	2.854E+00

6304	2.000E+02	2.676E-03	6.7	1.023	.963	1.000	4.000E+01	1.270E+00
------	-----------	-----------	-----	-------	------	-------	-----------	-----------

We now change the thermal boundary condition to a linear temperature variation. Here is the output for $Pr=0.7$ and $Re=50,000$ and the linear wall temperature variation.

intg	x/dh	cf2	nu	cfrat	nurat	tm/ts	ts	qflux
5	2.500E-02	1.180E-02	89.8	4.511	12.969	.514	4.001E+01	9.595E+05
500	2.500E+00	3.233E-03	10.1	1.236	1.454	.637	4.050E+01	8.127E+04
1000	5.000E+00	2.987E-03	8.5	1.142	1.232	.690	4.100E+01	5.950E+04
1500	8.242E+00	2.867E-03	7.8	1.096	1.132	.739	4.165E+01	4.681E+04
2000	1.358E+01	2.773E-03	7.5	1.060	1.084	.795	4.272E+01	3.612E+04
2500	2.239E+01	2.711E-03	7.5	1.037	1.090	.853	4.448E+01	2.708E+04
3000	3.691E+01	2.683E-03	7.9	1.026	1.135	.903	4.738E+01	1.980E+04
3500	5.980E+01	2.677E-03	8.3	1.024	1.192	.934	5.196E+01	1.552E+04
4000	8.480E+01	2.676E-03	8.4	1.023	1.219	.946	5.696E+01	1.420E+04
4500	1.098E+02	2.676E-03	8.5	1.023	1.227	.952	6.196E+01	1.386E+04
5000	1.348E+02	2.676E-03	8.5	1.023	1.229	.956	6.696E+01	1.376E+04
5500	1.598E+02	2.676E-03	8.5	1.023	1.230	.959	7.195E+01	1.374E+04
6000	1.848E+02	2.676E-03	8.5	1.023	1.230	.962	7.695E+01	1.373E+04
6304	2.000E+02	2.676E-03	8.5	1.023	1.230	.963	7.999E+01	1.373E+04

Comparing this linear surface temperature heating case to the constant surface temperature case shows the approximation of the heat flux boundary condition beyond the developing region, and comparison of this Nusselt number with the one for a constant wall temperature shows $8.5/6.7 = 1.27$, which compares with Fig. 14-5 for $Pr=0.01$ and $Re=50,000$. For both of these linear surface temperature data sets, if we would have had a hydrodynamically fully-developed velocity profile to make this a thermal entry problem, we would see a constant surface heat flux from the entry onward, rather than after the hydrodynamic entry region was completed.

14-10

The following are the proposed specifications for the cooling tubes in a pressurized-water nuclear power reactor:

Tube configuration	Concentric circular-tube annulus, with heating from the inner tube (containing the uranium fuel), and the outer tube surface having no heat flux
Tube dimensions	Inner-tube diameter, 2.5 cm Outer-tube diameter, 5.0 cm Tube length, 5 m
Water temperature	Inlet, 275°C
Water mean velocity	1 m/s
Axial heat-flux distribution	$\dot{q}'' / \dot{q}''_{\max} = \frac{1}{3}[1 + 2 \sin(\pi x / L)]$

Assume that the water properties may be treated as constant at 287°C. Calculate and plot heat flux, mean water temperature, and inner and outer tube surface temperatures as functions of x . Assume that the conductance h is independent of x and that the value for fully developed constant heat rate is a reasonable approximation. (Can you justify these assumptions?) How high must the water pressure be to avoid boiling? Or is it possible to avoid boiling with the se specifications? What do you think would be the effect of local boiling at the highest-temperature parts of the system?

For this problem, the Nusselt numbers of Table 14-4 apply,

x , m	\dot{q}''_s , W/m ²	T_m , °C	T_i , °C	T_s , °C
0	80452	275	286	274
0.5	130174	276	293	274
1.0	175029	279	301	277
1.5	210626	281	309	278
2.0	233481	284	315	281
2.5	241356	288	319	285
3.0	233481	291	321	288
3.5	210626	294	321	291
4.0	175028	296	319	293
4.5	130173	299	316	298
5.0	80452	300	311	299

14-11

Helium flows in a thin-walled circular tube of 2.5 cm inside diameter. Down the center of the tube is inserted a 5 mm diameter circular electric heater. The Reynolds number of the flow, based on the hydraulic diameter of the resulting passage, is 30,000. Heat is generated and transferred through the heater surface at a rate of 30 kW/m². The outer surface of the outer tube is bare, exposed to an atmospheric environment at 21°C. Heat is transferred from the outer surface to the surroundings by both free convection and radiation. For the free convection, assume a heat-transfer coefficient h of 10 W/(m² · K). For the radiation, let the surface emissivity be 0.8. At a particular point along the tube the mixed mean fluid temperature is 200°C. Assuming that the gas is transparent to thermal radiation and that the radiation emissivity of the two inner surfaces is 0.8, calculate the surface temperature of the heater and the temperature of the outer tube. Determine the fractions of the original heat generated in the core tube that are ultimately transferred to the helium and to the surroundings. Is radiation a major factor? It may be assumed that the tube is sufficiently long that fully developed conditions are closely approached.

The entry-length functions necessary to solve this problems precisely, taking into consideration axial variation of surface heat flux, are not available. If it is solved the same way as Prob. 14-10, the following results are obtained:

$x, \text{ m}$	$\dot{q}_s'', \text{ W/m}^2$	$T_m, ^\circ\text{C}$	$T_i, ^\circ\text{C}$	$T_s, ^\circ\text{C}$
0	23285	330	332	332
0.5	37676	331	335	334
1.0	50658	334	339	337
1.5	60961	336	342	340
2.0	67576	339	346	344
2.5	69855	343	350	347
3.0	67576	346	353	350
4.0	50658	351	357	355
4.5	37676	354	357	356
5.0	23285	355	357	357

The effects of axial heat flux variation can be estimated by analyzing flow in an "equivalent" circular tube, which might be defined as having the same flow area and velocity.

14-12

Develop an equation for the friction coefficient for fully developed turbulent flow between parallel planes, assuming that Eq. (13-7) is a reasonable approximation for the velocity profile.

The solution in this problem is based on the data in Table 14-3,

$$\text{Nu}_{\text{ii}} = 79.8 \quad \theta_i^* = 0.338$$

$$\text{Nu}_{\text{oo}} = 64.3 \quad \theta_o^* = 0.055$$

together with Eqs. (8-28) and (8-29). However, since neither surface temperature is initially known, the heat transfer rate from the outer tube to the helium cannot be immediately calculated. Thus an iterative procedure is required. To start, assume that all the heat is transferred to the helium from the inner surface. This leads to an inner surface temperature of 235.5 °C and an outer surface temperature of 197.6 °C. A first estimate of the radiation exchange, and the outer surface convection, can now be made using these temperatures, and this leads to a second estimate of the heat fluxes and surface temperatures.

14-13

TEXSTAN analysis of the turbulent thermal entry flow in a circular tube with constant surface heat flux: Investigate the entry length region through the thermally fully-developed region of flow in a circular tube with diameter Reynolds numbers of 50,000 and 100,000 and fluids corresponding to $Pr = 0.01, 0.7$, and 10. Evaluate the properties at a fluid entry temperature of 280 K, use constant fluid properties, and do not consider viscous dissipation. Let the pipe diameter be 3.5 cm and the pipe length be 12.0 m. Let the velocity and thermal entry profiles at the inlet to the tube be flat, which can be supplied by using the $kstart=1$ choice in TEXSTAN. Let the energy boundary condition be a constant surface heat flux of 250 W/m^2 . For a turbulence model, choose the hybrid turbulence model comprised of a constant eddy viscosity in the outer part of the flow ($\epsilon_m/\nu = aRe^b$ with $a = 0.005$ and $b = 0.9$) and a mixing-length turbulence model with the Van Driest damping function ($\kappa=0.40$ and $A^+=26$) in the near-wall region ($ktmu=7$). This hybrid model tends to more closely fit Fig. (13-1), and thus better predict the fully-developed friction coefficient and Nusselt number for a given Reynolds number. Choose the constant turbulent Prandtl number model ($ktme=2$) along with a choice for the turbulent Prandtl number, 0.9 is suggested, by setting $fx=0.9$. Compare the thermally fully-developed Nusselt numbers for $Pr=0.7$ with the results from set of Eqs. (14-5) through (14-9). For $Pr=0.01$, compare with Eq. (14-10), and for $Pr=100$, compare with Eq. (14-8). Feel free to investigate any other attribute of the tube flow. For example, at $Pr=0.7$ you can examine a temperature profile at the thermally fully developed state to evaluate the *thermal law of the wall* and compare with Eq. (14-4). Compare your results for how Nusselt number varies in the thermal entry region, as appropriate, with Figs. 14-6, 14-7, and 14.8.

Problem modifications for 14-13 (this problem is similar to the first half of problem 14-7)

properties: Do not evaluate the properties at the entrance temperature. For convenience in obtaining properties from Appendix A, for $Pr=0.01$ use Hg at 200°C , but set $Pr=0.01$; for $Pr=0.7$ use air at 300K but set $Pr=0.7$, and for $Pr=10$, use water at 10°C , but set $Pr=10$. Because the calculations are constant property without viscous dissipation, only the values of Re and Pr for the problem set are important.

surface heat flux: for each Pr select a surface heat flux value that provides a reasonable temperature change in the fluid. Again, the actual value does not matter because this is a constant property solution without viscous dissipation.

turbulence model: use a variable turbulent Prandtl number model for Hg and air, but you must use the constant Pr_t model for water

pipe length. The solution needs to be carried out only to $L/D_h = 150$, giving a pipe length of 5.25 m. This insures complete hydrodynamic and thermal flow development for the $Pr=10$ fluid. Using the ideas for turbulent internal flows choose a set of x location s that include $(x/D_h) = 0, 5, 50, 100$ and vary the integration stepsize: for $0 \leq (x/D_h) \leq 5$ the stepsize (aux1 value) should be 0.01 (an integration stepsize of 1% of the pipe radius), for the interval $5 \leq (x/D_h) \leq 50$ the stepsize is increased from 0.01 to 0.1 (an integration stepsize of 10% of the pipe radius), and for the interval $50 \leq (x/D_h) \leq 100$ it will further increase to 0.20, and then remain constant beyond this value if the pipe length is longer.

The data file for this problem is *14.13.dat.txt*. The data set construction is based on the *s420_7.dat.txt* file for combined entry length flow in a pipe with a specified surface heat flux (initial profiles: flat velocity and flat temperature) and composite turbulence model, using the van-Driest mixing length turbulence model in the near-wall region and a constant eddy viscosity in the outer region, along with a variable turbulent Prandtl number model for liquid metals and gases, and a constant turbulent Prandtl number for liquids.

Execution of the input data set generates several output files. Here is an abbreviated listing of the output file (it will be called *out.txt* when you execute TEXSTAN using *14.13.dat.txt*). The surface heat flux value was $\dot{q}_s'' = 1000 \text{ W/m}^2$ for the air to obtain a reasonable temperature rise in the air.

re,dh = 1.0000E+05 prm = .700								
=====								
intg	x/dh	cf2	nu	cfrat	nurat	tm/ts	ts	qflux
5	2.500E-02	7.767E-03	944.5	3.459	5.297	.995	2.814E+02	1.000E+03
400	2.000E+00	2.858E-03	242.2	1.273	1.358	.981	2.856E+02	1.000E+03
800	4.000E+00	2.617E-03	217.5	1.165	1.220	.979	2.863E+02	1.000E+03
1200	6.106E+00	2.513E-03	206.7	1.119	1.159	.978	2.868E+02	1.000E+03
1600	9.108E+00	2.438E-03	198.8	1.086	1.115	.977	2.873E+02	1.000E+03
2000	1.358E+01	2.375E-03	192.2	1.058	1.078	.976	2.879E+02	1.000E+03
2400	2.026E+01	2.330E-03	187.3	1.038	1.051	.976	2.885E+02	1.000E+03
2800	3.022E+01	2.302E-03	184.3	1.025	1.034	.975	2.894E+02	1.000E+03
3200	4.508E+01	2.290E-03	183.0	1.020	1.026	.975	2.906E+02	1.000E+03
3600	6.721E+01	2.287E-03	182.6	1.019	1.024	.975	2.923E+02	1.000E+03
4000	1.002E+02	2.287E-03	182.6	1.018	1.024	.976	2.947E+02	1.000E+03
4400	1.402E+02	2.287E-03	182.6	1.019	1.024	.976	2.977E+02	1.000E+03
4498	1.500E+02	2.287E-03	182.6	1.019	1.024	.976	2.985E+02	1.000E+03

In the $Pr=0.7$ output we see $cfrat$ and $nurat$, which present ratios of TEXSTAN-calculated values for c_f to the Kármán-Nikuradse Eq. (13-14) at the same Reynolds number and for Nu to the Gnielinski Eq. (14-8). We see the $cfrat$ and $nurat$ show agreement between the turbulent correlations and the TEXSTAN-computed solution, and that the entry lengths for both momentum and energy are about the same at $x/D_h \approx 15 - 20$. In this output, if we take the ratio of $nurat$ at $x/dh=20.26$ to its value at $x/dh=150$ we get 1.026, which compares favorably with Figure 14-7 for $Re=100,000$ and $Pr=0.7$ (we can do the same for $x/dh=9.108$ and we get 1.089, which again compares favorably).

The problem statement asks you to compare the TEXSTAN results to several choices for the Nusselt number.

Equation (14-5) for the Nusselt number comes from using the law-of-the wall theories of Eq. (13-4) and Eq. (14-4), valid for gases and light liquids, $Pr \leq 10$ (note: its Re range comes from your choice of $c_f/2$)

$$Nu = \frac{Re Pr c_f/2}{0.88 + 13.39(Pr^{2/3} - 0.78)\sqrt{c_f/2}}$$

Because this equation requires the friction coefficient, there becomes several choices:

(a) Eq. (13-11) the friction coefficient developed from the power-law model; for $10^4 \leq Re \leq 5 \times 10^4$

$$c_f/2 = 0.039 Re^{-0.25}$$

(b) Eq. (13-12), the friction coefficient developed from the law-of-the wall theories of Eq. (13-4); called the “classical” Kármán-Nikuradse equation,

$$\frac{1}{\sqrt{c_f/2}} = 2.46 \ln(Re \sqrt{c_f/2}) + 0.30$$

(c) Eq. (13-13), the reduced form of the “classical” Kármán-Nikuradse equation, for $3 \times 10^4 \leq Re \leq 10^6$

$$c_f/2 = 0.023 \text{Re}^{-0.2}$$

(d) Eq. (13-14), the Petukhov form of the “classical” Kármán–Nikuradse equation, for $10^4 \leq \text{Re} \leq 5 \times 10^6$

$$c_f/2 = (2.236 \ln \text{Re} - 4.639)^{-2}$$

When Eq. (14-4) is combined with Eq. (13-13) we have Eq. (14-6), which makes it valid for $3 \times 10^4 \leq \text{Re} \leq 10^6$ and for gases and light liquids, $\text{Pr} \leq 10$

$$\text{Nu} = \frac{0.023 \text{Re}^{0.8} \text{Pr}}{0.88 + 2.03(\text{Pr}^{2/3} - 0.78) \text{Re}^{-0.1}}$$

When this equation is restricted to gases only, we have Eq. (14-7), which becomes valid for $3 \times 10^4 \leq \text{Re} \leq 10^6$ and $\text{Pr} \leq 1$

$$\text{Nu} = 0.022 \text{Pr}^{0.5} \text{Re}^{0.8}$$

A much less restrictive Nusselt number formulation is the Gnielinski correlation, tested for the ranges $2300 \leq \text{Re} \leq 5 \times 10^6$ and $0.5 \leq \text{Pr} \leq 2000$

$$\text{Nu} = \frac{(\text{Re} - 1000) \text{Pr} c_f/2}{1.0 + 12.7 \sqrt{c_f/2} (\text{Pr}^{2/3} - 1.0)}$$

which compares favorably with Eq. (14-5)

The last two equations for Nusselt number is the Sleicher and Rouse correlation, Eq. (14-9), and the classic undergraduate-text-quoted (and often misinterpreted) Dittus-Boelter correlations.

Now, compute the same data set, changing the properties to mercury, and use a surface heat flux value of $\dot{q}_s'' = 20,000 \text{ W/m}^2$ to obtain a reasonable temperature rise in the mercury.

re,dh = 1.0000E+05 prm = .010								
=====								
intg	x/dh	cf2	nu	cfrat	nurat	tm/ts	ts	qflux
5	2.500E-02	7.767E-03	163.8	3.459	15.749	.999	2.803E+02	2.000E+04
400	2.000E+00	2.858E-03	21.6	1.273	2.074	.992	2.828E+02	2.000E+04
800	4.000E+00	2.617E-03	16.9	1.165	1.629	.989	2.838E+02	2.000E+04
1200	6.106E+00	2.513E-03	15.0	1.119	1.446	.988	2.846E+02	2.000E+04
1600	9.108E+00	2.438E-03	13.7	1.086	1.313	.987	2.856E+02	2.000E+04
2000	1.358E+01	2.375E-03	12.6	1.058	1.209	.986	2.868E+02	2.000E+04
2400	2.026E+01	2.330E-03	11.8	1.038	1.138	.985	2.884E+02	2.000E+04
2800	3.022E+01	2.302E-03	11.4	1.025	1.097	.985	2.906E+02	2.000E+04
3200	4.508E+01	2.290E-03	11.2	1.020	1.080	.985	2.937E+02	2.000E+04
3600	6.721E+01	2.287E-03	11.2	1.019	1.076	.985	2.983E+02	2.000E+04
4000	1.002E+02	2.287E-03	11.2	1.019	1.076	.985	3.050E+02	2.000E+04

4400	1.402E+02	2.287E-03	11.2	1.019	1.076	.985	3.131E+02	2.000E+04
4498	1.500E+02	2.287E-03	11.2	1.019	1.076	.986	3.151E+02	2.000E+04

In the $Pr=0.01$ output we see *cfrat* and *nurat*, which present ratios of TEXSTAN-calculated values for c_f to the Kármán-Nikuradse Eq. (13-14) at the same Reynolds number and for Nu to the Sleicher and Rouse Eq. (14-10) for constant surface heat flux. We see the *cfrat* shows agreement between the turbulent correlation and the TEXSTAN-computed solution and *nurat* shows reasonable agreement. The entry length for momentum remains $x/D_h \approx 15-20$ because the Re has not changed, and thermal entry length is somewhat longer than the momentum entry length. This is in contrast to what we would expect for laminar flows where the thermal entry length would be much shorter than the momentum length. In this output, if we take the ratio of *nurat* at $x/dh=20.26$ to its value at $x/dh=150$ we get 1.058, which somewhat lower than in Figure 14-7 for $Re=100,000$ and $Pr=0.01$ (we can do the same for $x/dh=9.108$ and we get 1.220, which is a more favorable comparison).

Now, compute the same data set, changing the properties to water, and use a surface heat flux value of $\dot{q}_s'' = 100,000 \text{ W/m}^2$ to obtain a reasonable temperature rise in the water.

re,dh = 1.0000E+05 prm = 10.000								
=====								
intg	x/dh	cf2	nu	cfrat	nurat	tm/ts	ts	qflux
5	2.500E-02	7.767E-03	2422.1	3.459	3.480	.991	2.826E+02	1.000E+05
400	2.000E+00	2.858E-03	847.2	1.273	1.217	.974	2.876E+02	1.000E+05
800	4.000E+00	2.617E-03	794.9	1.165	1.142	.972	2.881E+02	1.000E+05
1200	6.106E+00	2.513E-03	771.5	1.119	1.108	.971	2.884E+02	1.000E+05
1600	9.108E+00	2.438E-03	754.3	1.086	1.084	.971	2.887E+02	1.000E+05
2000	1.358E+01	2.375E-03	739.9	1.058	1.063	.970	2.890E+02	1.000E+05
2400	2.026E+01	2.330E-03	729.0	1.038	1.047	.970	2.893E+02	1.000E+05
2800	3.022E+01	2.302E-03	722.2	1.025	1.038	.970	2.896E+02	1.000E+05
3200	4.508E+01	2.290E-03	719.2	1.020	1.033	.969	2.900E+02	1.000E+05
3600	6.721E+01	2.287E-03	718.4	1.019	1.032	.969	2.906E+02	1.000E+05
4000	1.002E+02	2.287E-03	718.3	1.019	1.032	.970	2.914E+02	1.000E+05
4400	1.402E+02	2.287E-03	718.3	1.019	1.032	.970	2.924E+02	1.000E+05
4498	1.500E+02	2.287E-03	718.3	1.018	1.032	.970	2.927E+02	1.000E+05

In the $Pr=10$ output we see *cfrat* and *nurat*, which present ratios of TEXSTAN-calculated values for c_f to the Kármán-Nikuradse Eq. (13-14) at the same Reynolds number and for Nu to the Gnielinski Eq. (14-8). We see the *cfrat* and *nurat* show agreement between the turbulent correlations and the TEXSTAN-computed solution. The entry length for momentum remains $x/D_h \approx 15-20$ because the Re has not changed, and thermal entry length matches the momentum entry length. This is in contrast to what we would expect for laminar flows where the thermal entry length would be much longer than the momentum length. In this output, if we take the ratio of *nurat* at $x/dh=20.26$ to its value at $x/dh=150$ we get 1.015, which matches Figure 14-7 for $Re=100,000$ and $Pr=10$ (we can do the same for $x/dh=9.108$ and we get 1.05, which is a slightly larger than in the figure).

For $Re=50,000$ the data sets are easily changed by only changing the *reyn* value.

To plot the developing velocity profiles, set *kout*=4 and choose either *k10*=10 for nondimensional profiles (plus variables) or *k10*=11 for dimensional variables. The profiles will be printed as a part of the file

out.txt. You can choose where to print the profiles by adding x locations to the $x(m)$. Be sure to change the two $nxbc$ variables and add the appropriate sets of two lines of boundary condition information for each new x -location. This is explained in detail in the *s400.man.doc* user manual.

14-14

TEXTAN analysis of the turbulent thermal entry flow in a circular tube with constant surface temperature: Investigate the entry length region through the thermally fully-developed region of flow in a circular tube with diameter Reynolds numbers of 50,000 and 100,000 and fluids corresponding to $Pr = 0.01$ and 0.7 . Let the energy boundary condition be a constant surface temperature of 295 K. Follow the set-up instructions of Prob. 14-13. Compare the thermally fully-developed Nusselt number results with Eq. (14-12) for $Pr=0.7$ and Eq. (14-13) for $Pr=0.01$, and compare with Fig. 14-5. It is suggested you use TEXTAN to compute the corresponding Nusselt number with a constant heat flux boundary condition to create the Nusselt number ratio in making the comparison in Fig. 14-5.

Problem modifications for 14-14 (identical to problem 14-13 with the thermal boundary condition changed to a constant surface temperature)

properties: Do not evaluate the properties at the entrance temperature. For convenience in obtaining properties from Appendix A, for $Pr=0.01$ use Hg at 200°C, but set $Pr=0.01$; for $Pr=0.7$ use air at 300K but set $Pr=0.7$, and for $Pr=10$, use water at 10°C, but set $Pr=10$. Because the calculations are constant property without viscous dissipation, only the values of Re and Pr for the problem set are important.

turbulence model: use a variable turbulent Prandtl number model for Hg and air, but you must use the constant Pr_t model for water

pipe length. The solution needs to be carried out only to $L/D_h = 150$, giving a pipe length of 5.25 m. This insures complete hydrodynamic and thermal flow development for the $Pr=10$ fluid. Using the ideas for turbulent internal flows choose a set of x location s that include $(x/D_h) = 0, 5, 50, 100$ and vary the integration stepsize: for $0 \leq (x/D_h) \leq 5$ the stepsize (aux1 value) should be 0.01 (an integration stepsize of 1% of the pipe radius), for the interval $5 \leq (x/D_h) \leq 50$ the stepsize is increased from 0.01 to 0.1 (an integration stepsize of 10% of the pipe radius), and for the interval $50 \leq (x/D_h) \leq 100$ it will further increase to 0.20, and then remain constant beyond this value if the pipe length is longer.

The data file for this problem is *14.14.dat.txt*. The data set construction is based on the *s410_7.dat.txt* file for combined entry length flow in a pipe with a specified surface temperature(initial profiles: flat velocity and flat temperature) and composite turbulence model, using the van-Driest mixing length turbulence model in the near-wall region and a constant eddy viscosity in the outer region, along with a variable turbulent Prandtl number model for liquid metals and gases, and a constant turbulent Prandtl number for liquids.

Execution of the input data set generates several output files. Here is an abbreviated listing of the output file (it will be called *out.txt* when you execute TEXTAN using *14.14.dat.txt*).

re,dh = 1.0000E+05 prm = .700								
=====								
intg	x/dh	cf2	nu	cfrat	nurat	tm/ts	ts	qflux
5	2.500E-02	7.767E-03	659.0	3.459	3.696	.949	2.950E+02	7.499E+03
400	2.000E+00	2.858E-03	229.3	1.273	1.286	.951	2.950E+02	2.529E+03
800	4.000E+00	2.617E-03	208.7	1.165	1.171	.952	2.950E+02	2.246E+03
1200	6.106E+00	2.513E-03	199.8	1.119	1.121	.953	2.950E+02	2.098E+03
1600	9.108E+00	2.438E-03	193.1	1.086	1.083	.955	2.950E+02	1.960E+03
2000	1.358E+01	2.375E-03	187.3	1.058	1.050	.957	2.950E+02	1.811E+03

2400	2.026E+01	2.330E-03	182.9	1.038	1.026	.960	2.950E+02	1.648E+03
2800	3.022E+01	2.302E-03	180.3	1.025	1.011	.964	2.950E+02	1.465E+03
3200	4.508E+01	2.290E-03	179.2	1.020	1.005	.969	2.950E+02	1.251E+03
3600	6.721E+01	2.287E-03	179.0	1.019	1.004	.975	2.950E+02	9.958E+02
4000	1.002E+02	2.287E-03	178.9	1.018	1.004	.982	2.950E+02	7.107E+02
4400	1.402E+02	2.287E-03	178.9	1.019	1.004	.988	2.950E+02	4.722E+02
4498	1.500E+02	2.287E-03	178.9	1.019	1.004	.989	2.950E+02	4.272E+02

In the $Pr=0.7$ output we see *cfrat* and *nurat*, which present ratios of TEXSTAN-calculated values for c_f to the Kármán-Nikuradse Eq. (13-14) at the same Reynolds number and for Nu to the Gnielinski Eq. (14-8). We note that the Gnielinski equation was developed for a constant surface heat flux boundary condition. We see the *cfrat* and *nurat* show agreement between the turbulent correlations and the TEXSTAN-computed solution.

The entry lengths for both momentum and energy are about the same at $x/D_h \approx 15 - 20$. In this output, if we take the ratio of *nurat* at $x/dh=20.26$ to its value at $x/dh=150$ we get 1.022 (we can do the same for $x/dh=9.108$ and we get 1.079). If we compare these results with problem 14-13 for the same Re and Pr the constant heat flux results were 1.026, and 1.089, showing a very slight shift in thermal development length, but no where near what would be found for laminar flow.

The problem statement asks for a comparison of the Nu_∞ value with Eq. (14-12) for gases (presumably the Re range for this equation is similar to Eq. 14-7, $3 \times 10^4 \leq Re \leq 10^6$). These two equations are

$$Nu = 0.022 Pr^{0.5} Re^{0.8} \quad \dot{q}_s'' = \text{constant} \quad \text{Eq. (14-7)}$$

$$Nu = 0.021 Pr^{0.5} Re^{0.8} \quad T_s = \text{constant} \quad \text{Eq. (14-12)}$$

The file *out.txt* uses the Gnielinski Eq. (14-8) for *nurat*, but if we replace it with Eq. (14-12) we find *nurat* = 1.018, or the TEXSTAN-generated Nu is 1.8% higher than Eq. (14-12), whereas it is only 0.4% higher using Eq. (14-12).

Now compare the TEXSTAN-calculated $Nu_\infty = 182.6$ for a constant surface heat flux (problem 14-13) and $Re=100,000$ and $Pr=0.7$ to the TEXSTAN-calculated $Nu_\infty = 178.9$ for a constant surface temperature (for this problem, 14-14) and the same Re and Pr . This ratio is 1.021.

Now take the ratio of Eq. (14-7) with Eq. (14.12) at the same Re and Pr , $0.022/0.021=1.048$, which is significantly higher than the TEXSTAN-calculated ratio of 1.021. The 1.048 ratio may be attributed to either roundoff or uncertainty errors in the two-digit coefficients of these equations.

It is interesting to evaluate Eq. (14-13) and Eq. (14.12) at $Re=100,000$ and $Pr=0.7$, and we get $Nu_\infty = 178$ and we get $Nu_\infty = 175.7$, and this ratio is 1.013, which is similar to the TEXSTAN-calculated ratio.

With any of these ratios, the number is quite small compared to the laminar-predicted ratio $4.36/3.66=1.19$ (Table 8-2) for pipe flow. The turbulent surface heat flux to surface temperature ratio of 1.02 helps confirm why we rarely need to consider thermal boundary conditions for turbulent flow of gases.

Now, compute the same data set, changing the properties to mercury.

re,dh = 1.0000E+05 prm = .010								
=====								
intg	x/dh	cf2	nu	cfrat	nurat	tm/ts	ts	qflux
5	2.500E-02	7.767E-03	104.2	3.459	12.076	.950	2.950E+02	6.013E+05

400	2.000E+00	2.858E-03	15.1	1.273	1.750	.959	2.950E+02	7.214E+04
800	4.000E+00	2.617E-03	12.3	1.165	1.429	.963	2.950E+02	5.290E+04
1200	6.106E+00	2.513E-03	11.3	1.119	1.308	.966	2.950E+02	4.386E+04
1600	9.108E+00	2.438E-03	10.4	1.086	1.208	.971	2.950E+02	3.557E+04
2000	1.358E+01	2.375E-03	9.7	1.058	1.126	.975	2.950E+02	2.769E+04
2400	2.026E+01	2.330E-03	9.3	1.038	1.075	.981	2.950E+02	2.055E+04
2800	3.022E+01	2.302E-03	9.1	1.025	1.054	.987	2.950E+02	1.398E+04
3200	4.508E+01	2.290E-03	9.0	1.020	1.048	.992	2.950E+02	8.118E+03
3600	6.721E+01	2.287E-03	9.0	1.019	1.047	.997	2.950E+02	3.647E+03
4000	1.002E+02	2.287E-03	9.0	1.019	1.047	.999	2.950E+02	1.110E+03
4400	1.402E+02	2.287E-03	9.0	1.019	1.047	1.000	2.950E+02	2.622E+02
4498	1.500E+02	2.287E-03	9.0	1.019	1.047	1.000	2.950E+02	1.842E+02

In the $Pr=0.01$ output we see *cfrat* and *nurat*, which present ratios of TEXSTAN-calculated values for c_f to the Kármán-Nikuradse Eq. (13-14) at the same Reynolds number and for Nu to the Sleicher and Rouse Eq. (14-13) for constant surface temperature. We see the *cfrat* shows agreement with the turbulent correlation, but the and *nurat* is about 5% high.

I am not so sure about the limit of validity of Eq. (14-13). If we repeat this experiment with $Pr=0.001$ and both $Re=100,000$ and $=50,000$, the *nurat* is about 1. This suggests a problem with the correlation Eq. (14-13).

If we compare the TEXSTAN-predicted $Nu_\infty=9.0$ for the constant surface temperature and $Re=100,000$ and $Pr=0.01$ with the TEXSTAN-predicted $Nu_\infty=11.2$ for the constant surface heat flux (problem 14-13), we find the ratio is 1.24. We can compare this to the laminar ratio for a pipe, $4.36/3.66=1.19$ (Table 8-2), and we see a similar effect strong effect of thermal boundary condition for turbulent flow of low Pr fluids. The molecular transport contribution to the total thermal diffusivity is very important for liquid metal flows, and they have somewhat of a laminar-like behavior. Recall also that the Peclet number, $Pe=Re \cdot Pr$ must be >100 for the assumption of neglecting axial conduction to hold. This is ok for our test cases.

Now, compute the same data set, changing the properties to water.

re,dh = 1.0000E+05 prm = 10.000								
=====								
intg	x/dh	cf2	nu	cfrat	nurat	tm/ts	ts	qflux
5	2.500E-02	7.767E-03	1661.3	3.459	2.387	.949	2.950E+02	3.909E+05
400	2.000E+00	2.858E-03	837.3	1.273	1.203	.950	2.950E+02	1.955E+05
800	4.000E+00	2.617E-03	788.7	1.165	1.133	.950	2.950E+02	1.830E+05
1200	6.106E+00	2.513E-03	767.1	1.119	1.102	.950	2.950E+02	1.768E+05
1600	9.108E+00	2.438E-03	750.9	1.086	1.079	.951	2.950E+02	1.715E+05
2000	1.358E+01	2.375E-03	737.2	1.058	1.059	.951	2.950E+02	1.662E+05
2400	2.026E+01	2.330E-03	726.9	1.038	1.044	.952	2.950E+02	1.607E+05
2800	3.022E+01	2.302E-03	720.5	1.025	1.035	.954	2.950E+02	1.548E+05
3200	4.508E+01	2.290E-03	717.7	1.020	1.031	.956	2.950E+02	1.477E+05
3600	6.721E+01	2.287E-03	717.0	1.019	1.030	.958	2.950E+02	1.385E+05

4000	1.002E+02	2.287E-03	717.0	1.019	1.030	.962	2.950E+02	1.260E+05
4400	1.402E+02	2.287E-03	716.9	1.019	1.030	.966	2.950E+02	1.123E+05
4498	1.500E+02	2.287E-03	716.9	1.018	1.030	.967	2.950E+02	1.092E+05

In the $Pr=10$ output we see *cfrat* and *nurat*, which present ratios of TEXSTAN-calculated values for c_f to the Kármán-Nikuradse Eq. (13-14) at the same Reynolds number and for Nu to the Gnielinski Eq. (14-8). We see the *cfrat* and *nurat* show agreement between the turbulent correlations and the TEXSTAN-computed solution, and that the entry lengths for both momentum and energy are about the same at $x/D_h \approx 15 - 20$.

For $Re=50,000$ the data sets are easily changed by only changing the *reyn* value.

To plot the developing velocity profiles, set *kout*=4 and choose either *k10*=10 for nondimensional profiles (plus variables) or *k10*=11 for dimensional variables. The profiles will be printed as a part of the file *out.txt*. You can choose where to print the profiles by adding x locations to the *x(m)*. Be sure to change the two *nxbc* variables and add the appropriate sets of two lines of boundary condition information for each new x -location. This is explained in detail in the *s400.man.doc* user manual.

14-15

TEXSTAN analysis of the turbulent thermal entry flow in a circular tube with constant surface heat flux: This problem is essentially a repeat of problem (14-13), but choosing higher-order turbulence models available in TEXSTAN. For this problem there exists four 2-equation (k - ε) models ($ktmu=21,22,23,24$). The initial velocity and temperature profiles remain the flat profiles along with flat entry turbulence profiles for k and ε , all supplied by using the $kstart=1$ choice in TEXSTAN. Chose an entry turbulence of 10%. Note that by setting the corresponding entry dissipation equal to zero, TEXSTAN will compute an appropriate value. For the 2-equation turbulence models it is best to choose a constant turbulent Prandtl number model ($ktme=2$), along with a choice for the turbulent Prandtl number, 0.9 is suggested, by setting $fx=0.9$.

Problem modifications for 14-15 (identical to the modifications for problem 14-13)

properties: Do not evaluate the properties at the entrance temperature. For convenience in obtaining properties from Appendix A, for $Pr=0.01$ use Hg at 200°C, but set $Pr=0.01$; for $Pr=0.7$ use air at 300K but set $Pr=0.7$, and for $Pr=10$, use water at 10°C, but set $Pr=10$. Because the calculations are constant property without viscous dissipation, only the values of Re and Pr for the problem set are important.

surface heat flux: for each Pr select a surface heat flux value that provides a reasonable temperature change in the fluid. Again, the actual value does not matter because this is a constant property solution without viscous dissipation.

turbulence model: use a variable turbulent Prandtl number model for Hg and air, but you must use the constant Pr_t model for water

pipe length. The solution needs to be carried out only to $L/D_h = 150$, giving a pipe length of 5.25 m. This insures complete hydrodynamic and thermal flow development for the $Pr=10$ fluid. Using the ideas for turbulent internal flows choose a set of x location s that include $(x/D_h) = 0, 5, 50, 100$ and vary the integration stepsize: for $0 \leq (x/D_h) \leq 5$ the stepsize (aux1 value) should be 0.01 (an integration stepsize of 1% of the pipe radius), for the interval $5 \leq (x/D_h) \leq 50$ the stepsize is increased from 0.01 to 0.1 (an integration stepsize of 10% of the pipe radius), and for the interval $50 \leq (x/D_h) \leq 100$ it will further increase to 0.20, and then remain constant beyond this value if the pipe length is longer.

The data file for this problem is *14.15.dat.txt* for the $ktmu=22$ turbulence model of K-Y Chien. The data set construction is based on the *s420_22.dat.txt* file for combined entry length flow in a pipe with a specified surface heat flux (initial profiles: fully turbulent velocity and temperature profiles, and for the turbulence variables, the profile construction is described in the TEXSTAN input manual). The four choices for turbulence models are described in Appendix F. A variable turbulent Prandtl number model is used for liquid metals and gases, and a constant turbulent Prandtl number for liquids.

Conversion of this data set to permit other turbulence models requires only the variable $ktmu$ to be changed.

Execution of the input data set generates several output files. Here is an abbreviated listing of the output file (it will be called *out.txt* when you execute TEXSTAN using *14.13.dat.txt*). The surface heat flux value is $\dot{q}_s'' = 1000 \text{ W/m}^2$ for air to obtain a reasonable temperature rise in the air.

re,dh = 1.0000E+05 prm = .700								
=====								
intg	x/dh	cf2	nu	cfrat	nurat	tm/ts	ts	qflux
5	2.500E-02	2.489E-02	2381.3	11.087	13.354	.998	2.806E+02	1.000E+03
400	2.000E+00	2.558E-03	224.5	1.139	1.259	.980	2.860E+02	1.000E+03
800	4.000E+00	2.341E-03	197.3	1.042	1.106	.977	2.870E+02	1.000E+03

1200	6.106E+00	2.253E-03	186.1	1.003	1.043	.975	2.875E+02	1.000E+03
1600	9.108E+00	2.200E-03	178.6	.980	1.002	.974	2.880E+02	1.000E+03
2000	1.358E+01	2.179E-03	174.4	.971	.978	.974	2.886E+02	1.000E+03
2400	2.026E+01	2.194E-03	174.0	.977	.976	.974	2.891E+02	1.000E+03
2800	3.022E+01	2.236E-03	177.2	.996	.994	.974	2.897E+02	1.000E+03
3200	4.508E+01	2.250E-03	179.1	1.002	1.004	.975	2.907E+02	1.000E+03
3600	6.721E+01	2.243E-03	178.4	.999	1.001	.975	2.924E+02	1.000E+03
4000	1.002E+02	2.243E-03	178.5	.999	1.001	.975	2.949E+02	1.000E+03
4400	1.402E+02	2.243E-03	178.5	.999	1.001	.975	2.979E+02	1.000E+03
4498	1.500E+02	2.243E-03	178.5	.999	1.001	.975	2.986E+02	1.000E+03

In the $Pr=0.7$ output we see *cfrat* and *nurat*, which present ratios of TEXSTAN-calculated values for c_f to the Kármán-Nikuradse Eq. (13-14) at the same Reynolds number and for Nu to the Gnielinski Eq. (14-8). We see the *cfrat* and *nurat* show agreement between the turbulent correlations and the TEXSTAN-computed solution, and that the entry lengths for both momentum and energy are about the same at $x/D_h \approx 15 - 20$. We can compare this solution with problem 14-13 where the thermally fully developed values were $c_f/2 = 2.287E-03$ and $Nu=182.6$, showing a favorable comparison between the mixing length model and the KYC two-equation model for this Re and Pr .

The entry length behavior will be expected to be different between using a mixing-length model and using a two-equation model. Experimental data shows that the behavior of both the friction and heat transfer in the entry region (and the centerline velocity - or momentum) is to undershoot its asymptotic value and then converge to their thermally fully-developed values. This physical behavior is captured by the two-equation models, and we can see some evidence of this around x/D_h 10-15, and the entry region appears to be somewhat longer. However, within experimental (and numerical uncertainty) we typically design using x/D_h about 10-15 for gases.

Now, compute the same data set, changing the properties to mercury, and use a surface heat flux value of $\dot{q}_s'' = 20,000 \text{ W/m}^2$ to obtain a reasonable temperature rise in the mercury.

re,dh = 1.0000E+05 prm = .010								
=====								
intg	x/dh	cf2	nu	cfrat	nurat	tm/ts	ts	qflux
5	2.500E-02	2.489E-02	166.3	11.087	15.990	.999	2.803E+02	2.000E+04
400	2.000E+00	2.558E-03	21.7	1.139	2.089	.992	2.828E+02	2.000E+04
800	4.000E+00	2.341E-03	16.4	1.042	1.582	.989	2.839E+02	2.000E+04
1200	6.106E+00	2.253E-03	14.1	1.003	1.358	.987	2.849E+02	2.000E+04
1600	9.108E+00	2.200E-03	12.5	.980	1.202	.986	2.859E+02	2.000E+04
2000	1.358E+01	2.179E-03	11.4	.971	1.098	.984	2.872E+02	2.000E+04
2400	2.026E+01	2.194E-03	10.9	.977	1.050	.984	2.888E+02	2.000E+04
2800	3.022E+01	2.236E-03	11.0	.996	1.062	.984	2.908E+02	2.000E+04
3200	4.508E+01	2.250E-03	11.3	1.002	1.087	.985	2.937E+02	2.000E+04
3600	6.721E+01	2.243E-03	11.3	.999	1.082	.985	2.982E+02	2.000E+04
4000	1.002E+02	2.243E-03	11.3	.999	1.082	.985	3.050E+02	2.000E+04

4400	1.402E+02	2.243E-03	11.3	.999	1.082	.986	3.131E+02	2.000E+04
4498	1.500E+02	2.243E-03	11.3	.999	1.082	.986	3.151E+02	2.000E+04

In the $Pr=0.01$ output we see *cfrat* and *nurat*, which present ratios of TEXSTAN-calculated values for c_f to the Kármán-Nikuradse Eq. (13-14) at the same Reynolds number and for Nu to the Sleicher and Rouse Eq. (14-10) for constant surface heat flux. We see the *cfrat* shows agreement between the turbulent correlation and the TEXSTAN-computed solution and *nurat* seems high compared to the correlation. We can compare this solution with problem 14-13 where the thermally fully developed values were $c_f/2 = 2.287E-03$ and $Nu=11.2$, showing a favorable comparison between the mixing length model and the KYC two-equation model for this Re and Pr .

Now, compute the same data set, changing the properties to water, and use a surface heat flux value of $\dot{q}_s'' = 100,000 \text{ W/m}^2$ to obtain a reasonable temperature rise in the water. For this data set, the

re,dh = 1.0000E+05 prm = 10.000								
=====								
intg	x/dh	cf2	nu	cfrat	nurat	tm/ts	ts	qflux
5	2.500E-02	2.489E-02	9166.5	11.087	13.170	.998	2.807E+02	1.000E+05
400	2.000E+00	2.558E-03	818.6	1.139	1.176	.973	2.878E+02	1.000E+05
800	4.000E+00	2.341E-03	769.1	1.042	1.105	.971	2.884E+02	1.000E+05
1200	6.106E+00	2.253E-03	749.1	1.003	1.076	.971	2.887E+02	1.000E+05
1600	9.108E+00	2.200E-03	736.2	.980	1.058	.970	2.889E+02	1.000E+05
2000	1.358E+01	2.179E-03	730.1	.971	1.049	.970	2.891E+02	1.000E+05
2400	2.026E+01	2.194E-03	732.2	.977	1.052	.970	2.892E+02	1.000E+05
2800	3.022E+01	2.236E-03	741.3	.996	1.065	.970	2.894E+02	1.000E+05
3200	4.508E+01	2.250E-03	744.5	1.002	1.070	.970	2.897E+02	1.000E+05
3600	6.721E+01	2.243E-03	742.8	.999	1.067	.970	2.903E+02	1.000E+05
4000	1.002E+02	2.243E-03	743.0	.999	1.067	.971	2.911E+02	1.000E+05
4400	1.402E+02	2.243E-03	743.0	.999	1.067	.971	2.921E+02	1.000E+05
4498	1.500E+02	2.243E-03	743.0	.999	1.067	.971	2.924E+02	1.000E+05

In the $Pr=10$ output we see *cfrat* and *nurat*, which present ratios of TEXSTAN-calculated values for c_f to the Kármán-Nikuradse Eq. (13-14) at the same Reynolds number and for Nu to the Gnielinski Eq. (14-8). We see the *cfrat* shows agreement between the turbulent correlation and the TEXSTAN-computed solution and *nurat* seems low compared to the correlation. We can compare this solution with problem 14-13 where the thermally fully developed values were $c_f/2 = 2.287E-03$ and $Nu=718.3$, showing a favorable comparison between the mixing length model and the KYC two-equation model at this Re and Pr .

For $Re=50,000$ the data sets are easily changed by only changing the *reyn* value.

To plot the developing velocity profiles, set *kout*=4 and choose either *k10*=10 for nondimensional profiles (plus variables) or *k10*=11 for dimensional variables. The profiles will be printed as a part of the file *out.txt*. You can choose where to print the profiles by adding *x* locations to the *x(m)*. Be sure to change the two *nxbc* variables and add the appropriate sets of two lines of boundary condition information for each new *x*-location. This is explained in detail in the *s400.man.doc* user manual.

14-16

TEXSTAN analysis of the turbulent thermal entry flow between parallel plates with constant surface heat flux: Investigate the entry length region through the thermally fully-developed region of flow between parallel plates with hydraulic diameter Reynolds numbers of 30,000 and 100,000 and fluids corresponding to $Pr = 0.01$, 0.7 , and 10 . Evaluate the properties at a fluid entry temperature of 280 K , use constant fluid properties, and do not consider viscous dissipation. Let the plate spacing be 7.0 cm and the plate length be 7.0 m . Let the velocity and thermal entry profiles at the inlet to the plates be flat, which can be supplied by using the $kstart=1$ choice in TEXSTAN. Let the energy boundary condition be a constant surface heat flux of 250 W/m^2 . For a turbulence model, choose the hybrid turbulence model comprised of a constant eddy viscosity in the outer part of the flow ($\epsilon_m/\nu = aRe^b$ with $a = 0.0022$ and $b = 0.9$) and a mixing-length turbulence model with the Van Driest damping function ($\kappa=0.40$ and $A^+=26$) in the near-wall region ($ktmu=7$). This hybrid model follows the circular pipe idea described in Prob. 14-13, and thus better predict the fully-developed friction coefficient and Nusselt number for a given Reynolds number. Choose the constant turbulent Prandtl number model ($ktme=2$) along with a choice for the turbulent Prandtl number, 0.9 is suggested, by setting $fx=0.9$. Compare the thermally fully-developed Nusselt numbers for $Pr=0.7$ with the results from set of Eqs. (14-5) through (14-9). For $Pr=0.01$, compare with Eq. (14-10), and for $Pr=100$, compare with Eq. (14-8). Be careful to use the hydraulic diameter, Eq. (14-18). Feel free to investigate any other attribute of the tube flow.

Problem modifications for 14-16 (they are similar to the modifications for problem 14-13)

properties: Do not evaluate the properties at the entrance temperature. For convenience in obtaining properties from Appendix A, for $Pr=0.01$ use Hg at 200°C , but set $Pr=0.01$; for $Pr=0.7$ use air at 300 K but set $Pr=0.7$, and for $Pr=10$, use water at 10°C , but set $Pr=10$. Because the calculations are constant property without viscous dissipation, only the values of Re and Pr for the problem set are important.

surface heat flux: for each Pr select a surface heat flux value that provides a reasonable temperature change in the fluid. Again, the actual value does not matter because this is a constant property solution without viscous dissipation.

turbulence model: use a variable turbulent Prandtl number model for Hg and air, but you must use the constant Pr_t model for water

channel length. The solution needs to be carried out only to $L/D_h = 150$, giving a channel length of 21 m . This insures complete hydrodynamic and thermal flow development for the $Pr=10$ fluid. Using the ideas for turbulent internal flows choose a set of x locations that include $(x/D_h) = 0, 5, 50, 100$ and vary the integration stepsize: for $0 \leq (x/D_h) \leq 5$ the stepsize (aux1 value) should be 0.01 (an integration stepsize of 1% of the channel half-height), for the interval $5 \leq (x/D_h) \leq 50$ the stepsize is increased from 0.01 to 0.1 (an integration stepsize of 10% of the channel half-height), and for the interval $50 \leq (x/D_h) \leq 100$ it will further increase to 0.20 , and then remain constant beyond this value if the channel length is longer.

The data file for this problem is *14.16.dat.txt*. The data set construction is based on the *s520_7.dat.txt* file for combined entry length flow between parallel planes with a specified surface heat flux (initial profiles: flat velocity and flat temperature). The turbulence model is a composite model that uses the van-Driest mixing length model in the near-wall region and a constant eddy viscosity in the outer region, along with a variable turbulent Prandtl number model for liquid metals and gases, and a constant turbulent Prandtl number for liquids.

Execution of the input data set generates several output files. Here is an abbreviated listing of the output file (it will be called *out.txt* when you execute TEXSTAN using *14.16.dat.txt*). The surface heat flux value was $\dot{q}_s'' = 500\text{ W/m}^2$ for the air to obtain a reasonable temperature rise in the air.

re,dh = 1.0000E+05 prm = .700								
=====								
intg	x/dh	cf2	nu	cfrat	nurat	tm/ts	ts	qflux
5	1.250E-02	9.439E-03	1301.8	4.204	7.301	.993	2.820E+02	5.000E+02
800	2.000E+00	2.907E-03	246.0	1.295	1.380	.963	2.910E+02	5.000E+02
1600	4.000E+00	2.666E-03	221.6	1.187	1.242	.959	2.925E+02	5.000E+02
2400	6.107E+00	2.536E-03	208.7	1.129	1.171	.957	2.935E+02	5.000E+02
3200	9.109E+00	2.431E-03	198.3	1.083	1.112	.955	2.946E+02	5.000E+02
4000	1.359E+01	2.350E-03	190.1	1.047	1.066	.953	2.959E+02	5.000E+02
4800	2.027E+01	2.300E-03	184.7	1.025	1.036	.952	2.973E+02	5.000E+02
5600	3.023E+01	2.279E-03	182.2	1.015	1.022	.952	2.990E+02	5.000E+02
6400	4.510E+01	2.274E-03	181.5	1.013	1.018	.952	3.013E+02	5.000E+02
7200	6.725E+01	2.273E-03	181.4	1.013	1.017	.952	3.046E+02	5.000E+02
8000	1.003E+02	2.273E-03	181.4	1.012	1.017	.953	3.096E+02	5.000E+02
8800	1.403E+02	2.273E-03	181.4	1.012	1.017	.954	3.156E+02	5.000E+02
8994	1.500E+02	2.273E-03	181.4	1.012	1.017	.954	3.171E+02	5.000E+02

In the $Pr=0.7$ output we see $cfrat$ and $nurat$, which present ratios of TEXSTAN-calculated values for c_f to the Kármán-Nikuradse Eq. (13-14) at the same hydraulic diameter Reynolds number and for Nu to the Gnielinski Eq. (14-8). We see the $cfrat$ and $nurat$ show agreement between the circular pipe turbulent correlations and the TEXSTAN-computed solution, replacing the pipe-diameter Re with the hydraulic-diameter Re . We can also compare directly with Table 14-5 and use Eq. (8-28) or (8-29) because this is symmetrical heating from both walls. From the table, at $Re=100,000$ and $Pr=0.7$, $Nu_{ii}=155$ and $\theta^*=0.170$, giving $Nu_i (=Nu_o)=186.7$.

We see that the entry lengths for both momentum and energy are about the same at $x/D_h \approx 15 - 20$.

Now, compute the same data set, changing the properties to mercury, and use a surface heat flux value of $\dot{q}_s'' = 5,000 \text{ W/m}^2$ to obtain a reasonable temperature rise in the mercury. We also have to change to $k_{out}=4$ because we do not have analytical Nu values to compare with the TEXSTAN-calculated values. Here is an abbreviated listing of the output file (it will be called *out.txt* when you execute TEXSTAN using *14.16.dat.txt*).

Reynolds number= 1.0000E+05 Prandtl number= .010						
=====						
intg	x/dh	cfapp	cf2(I)	cf2(E)	nu(I)	nu(E)
5	1.250E-02	1.019E-01	0.000E+00	9.439E-03	0.000E+00	2.313E+02
800	2.000E+00	9.663E-03	0.000E+00	2.907E-03	0.000E+00	2.288E+01
1600	4.000E+00	7.997E-03	0.000E+00	2.666E-03	0.000E+00	1.831E+01
2400	6.107E+00	7.241E-03	0.000E+00	2.536E-03	0.000E+00	1.629E+01
3200	9.109E+00	6.640E-03	0.000E+00	2.431E-03	0.000E+00	1.495E+01
4000	1.359E+01	6.118E-03	0.000E+00	2.350E-03	0.000E+00	1.415E+01
4800	2.027E+01	5.677E-03	0.000E+00	2.300E-03	0.000E+00	1.378E+01

5600	3.023E+01	5.327E-03	0.000E+00	2.279E-03	0.000E+00	1.366E+01
6400	4.510E+01	5.075E-03	0.000E+00	2.274E-03	0.000E+00	1.365E+01
7200	6.725E+01	4.902E-03	0.000E+00	2.273E-03	0.000E+00	1.364E+01
8000	1.003E+02	4.785E-03	0.000E+00	2.273E-03	0.000E+00	1.364E+01
8800	1.403E+02	4.717E-03	0.000E+00	2.273E-03	0.000E+00	1.364E+01
8994	1.500E+02	4.706E-03	0.000E+00	2.273E-03	0.000E+00	1.364E+01

Because we are using $k_{geom}=5$, which computes the parallel-planes channel which assumes symmetrical thermal boundary conditions, we will have no output for the I-surface. The $c_f/2$ result must be the same for all Pr because the Re is the same and we are not using variable properties. The Nu value is in the magnitude range that we would expect for the turbulent flow of a low Pr fluid. To see the surface and mean temperatures examine the output file *fm84.txt*. We can also compare directly with Table 14-5 and use Eq. (8-28) or (8-29) because this is symmetrical heating from both walls. From the table, at $Re=100,000$ and $Pr=0.01$, $Nu_{ii}=6.70$ and $\theta^*=0.440$, giving $Nu_i (=Nu_o)=12.0$, showing an agreement with TEXSTAN of 14%.

Now, compute the same data set, changing the properties to water, and use a surface heat flux value of $\dot{q}_s'' = 50,000 \text{ W/m}^2$ to obtain a reasonable temperature rise in the water. For this data set, we can switch back to $k_{out}=8$.

re,dh = 1.0000E+05 prm = 10.000								
=====								
intg	x/dh	cf2	nu	cfrat	nurat	tm/ts	ts	qflux
5	1.250E-02	9.439E-03	3307.5	4.204	4.752	.986	2.839E+02	5.000E+04
800	2.000E+00	2.907E-03	856.0	1.295	1.230	.950	2.950E+02	5.000E+04
1600	4.000E+00	2.666E-03	804.5	1.187	1.156	.946	2.960E+02	5.000E+04
2400	6.107E+00	2.536E-03	776.7	1.129	1.116	.945	2.967E+02	5.000E+04
3200	9.109E+00	2.431E-03	753.5	1.083	1.083	.943	2.974E+02	5.000E+04
4000	1.359E+01	2.350E-03	735.1	1.047	1.056	.942	2.980E+02	5.000E+04
4800	2.027E+01	2.300E-03	723.1	1.025	1.039	.941	2.987E+02	5.000E+04
5600	3.023E+01	2.279E-03	717.5	1.015	1.031	.941	2.993E+02	5.000E+04
6400	4.510E+01	2.274E-03	715.9	1.013	1.029	.941	3.001E+02	5.000E+04
7200	6.725E+01	2.273E-03	715.6	1.013	1.028	.941	3.012E+02	5.000E+04
8000	1.003E+02	2.273E-03	715.6	1.012	1.028	.941	3.029E+02	5.000E+04
8800	1.403E+02	2.273E-03	715.6	1.012	1.028	.942	3.050E+02	5.000E+04
8994	1.500E+02	2.273E-03	715.6	1.012	1.028	.942	3.055E+02	5.000E+04

In the $Pr=10$ output we see *cfrat* and *nurat*, which present ratios of TEXSTAN-calculated values for c_f to the Kármán-Nikuradse Eq. (13-14) at the same Reynolds number and for Nu to the Gnielinski Eq. (14-8). We see the *cfrat* and *nurat* show agreement between the turbulent correlations and the TEXSTAN-computed solution. We can also compare directly with Table 14-5 and use Eq. (8-28) or (8-29) because this is symmetrical heating from both walls. From the table, at $Re=100,000$ and $Pr=10$, $Nu_{ii}=680$ and $\theta^*=0.045$, giving $Nu_i (=Nu_o)=712$, showing a good agreement with TEXSTAN.

The entry length for momentum remains $x/D_h \approx 15-20$ because the Re has not changed, and thermal entry length matches the momentum entry length. This is in contrast to what we would expect for laminar

flows where the thermal entry length would be much longer than the momentum length. In this output, if we take the ratio of *nurat* at $x/dh=20.27$ to its value at $x/dh=150$ we get 1.011, which matches the circular pipe result in Figure 14-7 for $Re=100,000$ and $Pr=10$.

For $Re=30,000$ the data sets are easily changed by only changing the *reyn* value.

To plot the developing velocity profiles, set *kout*=4 and choose *k10*=11 for dimensional variables. The profiles will be printed as a part of the file *out.txt*. You can choose where to print the profiles by adding *x* locations to the *x(m)*. Be sure to change the two *nxbc* variables and add the appropriate sets of two lines of boundary condition information for each new *x*-location. This is explained in detail in the *s400.man.doc* user manual.

14-17

TEXSTAN analysis of the turbulent thermally fully developed flow between parallel plates with asymmetrical surface heat flux: Investigate the thermally fully-developed Nusselt numbers of flow between parallel plates with hydraulic diameter Reynolds numbers of 30,000 and 100,000 and fluids corresponding to $Pr = 0.01, 0.7$, and 10 . Evaluate the properties at a fluid entry temperature of 280 K , use constant fluid properties, and do not consider viscous dissipation. Let the plate spacing be 7.0 cm and the plate length be 7.0 m . Start the flow at $x=0$, as if it were entry flow. Let the velocity and thermal entry profiles at the inlet to the plates be flat, which can be supplied by using the $kstart=1$ choice in TEXSTAN. Let the energy boundary condition be a constant surface heat flux of 250 W/m^2 on one surface and a zero heat flux on the other surface. Note that in TEXSTAN this geometry will be $kgeom=6$ (it will be $kgeom=5$, corresponding to symmetric thermal boundary conditions for Prob. 14-16). Compare the thermally fully-developed Nusselt numbers with the results shown in Table 14-5.

Problem modifications for 14-17 (almost identical to problem 14-16 with the heat flux boundary condition changed and $kgeom=6$ because of the asymmetrical boundary conditions). Note the $rw(m)$ definition changes from channel half-height for $kgeom=5$ to channel height for $kgeom=6$.

properties: Do not evaluate the properties at the entrance temperature. For convenience in obtaining properties from Appendix A, for $Pr=0.01$ use Hg at 200°C , but set $Pr=0.01$; for $Pr=0.7$ use air at 300 K but set $Pr=0.7$, and for $Pr=10$, use water at 10°C , but set $Pr=10$. Because the calculations are constant property without viscous dissipation, only the values of Re and Pr for the problem set are important.

surface heat flux: for each Pr select a surface heat flux value that provides a reasonable temperature change in the fluid. Again, the actual value does not matter because this is a constant property solution without viscous dissipation.

turbulence model: DO NOT USE mixing length at this time. Use only two-equation models. Use a variable turbulent Prandtl number model for Hg and air, but you must use the constant Pr_t model for water.

channel length. The solution needs to be carried out only to $L/D_h = 150$, giving a channel length of 21 m . This insures complete hydrodynamic and thermal flow development for the $Pr=10$ fluid. Using the ideas for turbulent internal flows choose a set of x locations that include $(x/D_h) = 0, 5, 50, 100$ and vary the integration stepsize: for $0 \leq (x/D_h) \leq 5$ the stepsize (aux1 value) should be 0.01 (an integration stepsize of 1% of the channel half-height), for the interval $5 \leq (x/D_h) \leq 50$ the stepsize is increased from 0.01 to 0.1 (an integration stepsize of 10% of the channel half-height), and for the interval $50 \leq (x/D_h) \leq 100$ it will further increase to 0.20 , and then remain constant beyond this value if the channel length is longer.

The data file for this problem is *14.17.dat.txt* for the $ktmu=22$ turbulence model of K-Y Chien. The data set construction is based on the *s526_22.dat.txt* file for flow over a flat plate with constant free stream velocity and specified surface heat flux (initial profiles: fully turbulent velocity and temperature profiles, and for the turbulence variables, the profile construction is described in the TEXSTAN input manual). The four choices for turbulence models are described in Appendix F. A variable turbulent Prandtl number model is used for liquid metals and gases, and a constant turbulent Prandtl number for liquids.

The data files for this problem is *14.17.dat.txt*. The data set construction is based on the *s526_22.dat.txt* file for combined entry length flow between parallel planes with a specified surface heat flux (initial profiles: flat velocity and flat temperature). The turbulence model is a composite model that uses the van-Driest mixing length model in the near-wall region and a constant eddy viscosity in the outer region, along with a variable turbulent Prandtl number model for liquid metals and gases, and a constant turbulent Prandtl number for liquids.

Execution of the input data set generates several output files. Here is an abbreviated listing of the output file for $kout=4$ (it will be called *out.txt* when you execute TEXSTAN using *14.17.dat.txt*). The surface heat flux value was $\dot{q}_s'' = 500\text{ W/m}^2$ for the air to obtain a reasonable temperature rise in the air.

Reynolds number= 1.0000E+05 Prandtl number= .700						
=====						
intg	x/dh	cfapp	cf2(I)	cf2(E)	nu(I)	nu(E)
5	1.250E-02	3.160E-01	8.598E-03	8.598E-03	1.261E+03	0.000E+00
800	2.000E+00	1.036E-02	2.497E-03	2.497E-03	2.118E+02	0.000E+00
1600	4.000E+00	8.039E-03	2.329E-03	2.329E-03	1.891E+02	0.000E+00
2400	6.107E+00	7.061E-03	2.266E-03	2.266E-03	1.792E+02	0.000E+00
3200	9.109E+00	6.340E-03	2.240E-03	2.240E-03	1.724E+02	0.000E+00
4000	1.359E+01	5.768E-03	2.253E-03	2.253E-03	1.682E+02	0.000E+00
4800	2.027E+01	5.342E-03	2.300E-03	2.300E-03	1.663E+02	0.000E+00
5600	3.023E+01	5.092E-03	2.314E-03	2.314E-03	1.631E+02	0.000E+00
6400	4.510E+01	4.939E-03	2.309E-03	2.309E-03	1.598E+02	0.000E+00
7200	6.725E+01	4.834E-03	2.309E-03	2.309E-03	1.582E+02	0.000E+00
8000	1.003E+02	4.763E-03	2.309E-03	2.309E-03	1.576E+02	0.000E+00
8800	1.403E+02	4.722E-03	2.309E-03	2.309E-03	1.575E+02	0.000E+00
8994	1.500E+02	4.715E-03	2.309E-03	2.309E-03	1.575E+02	0.000E+00

We can compare the friction solution with the mixing-length solution in problem 14-16 for the hydrodynamically fully developed value where $c_f/2 = 2.273E-03$, showing a favorable comparison between the mixing length model and the KYC two-equation model for this Re and Pr. For the Nusselt number we compare with Table 14-5 for Re=100,000 and Pr=0.7 and this asymmetrical heating (constant heat flux on the I-surface and zero heat flux on the E-surface), where Nu=155. We see complete agreement between the two-equation result and the table.

Now, compute the same data set, changing the properties to mercury, and use a surface heat flux value of $\dot{q}_s'' = 10,000 \text{ W/m}^2$ to obtain a reasonable temperature rise in the mercury. We also have to change to $k_{out}=4$ because we do not have analytical Nu values to compare with the TEXSTAN-calculated values. Here is an abbreviated listing of the output file (it will be called *out.txt* when you execute TEXSTAN using *14.16.dat.txt*).

Reynolds number= 1.0000E+05 Prandtl number= .010						
=====						
intg	x/dh	cfapp	cf2(I)	cf2(E)	nu(I)	nu(E)
5	1.250E-02	3.160E-01	8.598E-03	8.598E-03	1.991E+02	0.000E+00
800	2.000E+00	1.036E-02	2.497E-03	2.497E-03	2.049E+01	0.000E+00
1600	4.000E+00	8.039E-03	2.329E-03	2.329E-03	1.530E+01	0.000E+00
2400	6.107E+00	7.061E-03	2.267E-03	2.267E-03	1.302E+01	0.000E+00
3200	9.109E+00	6.340E-03	2.240E-03	2.240E-03	1.139E+01	0.000E+00
4000	1.359E+01	5.768E-03	2.253E-03	2.253E-03	1.023E+01	0.000E+00
4800	2.027E+01	5.342E-03	2.300E-03	2.300E-03	9.511E+00	0.000E+00
5600	3.023E+01	5.092E-03	2.314E-03	2.314E-03	9.047E+00	0.000E+00
6400	4.510E+01	4.939E-03	2.309E-03	2.309E-03	8.729E+00	0.000E+00

7200	6.725E+01	4.834E-03	2.309E-03	2.309E-03	8.603E+00	0.000E+00
8000	1.003E+02	4.763E-03	2.309E-03	2.309E-03	8.573E+00	0.000E+00
8800	1.403E+02	4.722E-03	2.309E-03	2.309E-03	8.570E+00	0.000E+00
8994	1.500E+02	4.715E-03	2.309E-03	2.309E-03	8.570E+00	0.000E+00

The friction solution will be the same because the Reynolds number has not changed and the flow is constant properties. For the Nusselt number we compare with Table 14-5 for $Re=100,000$ and $Pr=0.01$ and this asymmetrical heating (constant heat flux on the I-surface and zero heat flux on the E-surface), where $Nu=6.70$. We see the TEXSTAN result is 28% high.

Now, compute the same data set, changing the properties to water, and use a surface heat flux value of $\dot{q}_s'' = 100,000 \text{ W/m}^2$ to obtain a reasonable temperature rise in the water.

Reynolds number= 1.0000E+05 Prandtl number= 10.000						
=====						
intg	x/dh	cfapp	cf2(I)	cf2(E)	nu(I)	nu(E)
5	1.250E-02	3.160E-01	8.598E-03	8.598E-03	3.509E+03	0.000E+00
800	2.000E+00	1.036E-02	2.497E-03	2.497E-03	7.901E+02	0.000E+00
1600	4.000E+00	8.039E-03	2.329E-03	2.329E-03	7.550E+02	0.000E+00
2400	6.107E+00	7.061E-03	2.267E-03	2.267E-03	7.397E+02	0.000E+00
3200	9.109E+00	6.340E-03	2.240E-03	2.240E-03	7.304E+02	0.000E+00
4000	1.359E+01	5.768E-03	2.252E-03	2.252E-03	7.277E+02	0.000E+00
4800	2.027E+01	5.342E-03	2.300E-03	2.300E-03	7.307E+02	0.000E+00
5600	3.023E+01	5.092E-03	2.314E-03	2.314E-03	7.264E+02	0.000E+00
6400	4.510E+01	4.939E-03	2.309E-03	2.309E-03	7.205E+02	0.000E+00
7200	6.725E+01	4.834E-03	2.309E-03	2.309E-03	7.177E+02	0.000E+00
8000	1.003E+02	4.763E-03	2.309E-03	2.309E-03	7.166E+02	0.000E+00
8800	1.403E+02	4.722E-03	2.309E-03	2.309E-03	7.164E+02	0.000E+00
8994	1.500E+02	4.715E-03	2.309E-03	2.309E-03	7.164E+02	0.000E+00

The friction solution will be the same because the Reynolds number has not changed and the flow is constant properties. For the Nusselt number we compare with Table 14-5 for $Re=100,000$ and $Pr=10$ and this asymmetrical heating (constant heat flux on the I-surface and zero heat flux on the E-surface), where $Nu=680$. We see the TEXSTAN result is 5% high..

For $Re=30,000$ the data sets are easily changed by only changing the *reyn* value.

15-1

Consider fully developed laminar flow between symmetrically heated parallel plates with constant heat rate per unit of duct length. The plate spacing is 1 cm, the fluid is an aircraft engine oil, and the heat flux is 1.4 kW/m^2 . The mass velocity G is $600 \text{ kg/(s} \cdot \text{m}^2)$. At a particular point in question the surface temperature is 110°C . Assuming that the viscosity is the only temperature-dependent property of significance, carry out the necessary calculations (numerical integration is necessary) to evaluate the friction coefficient and the heat-transfer conductance. Compare the results with the recommended procedures given in the text.

$$h = 56 \text{ W/(m}^2\text{K)}$$

$$c_f = 0.027$$

Referring to Eqs. (15-3) and (15-4), $n = -0.34$ and $m = 0.48$.

15-2

For air as a working substance and using the actual tabulated properties, compare the recommended temperature ratio and reference property schemes for evaluating heat-transfer coefficients and friction coefficients for a laminar boundary layer with constant free-stream velocity for both heating and cooling

For this problem select some suitable values for pressure, free-stream temperature, free-stream velocity, and distance x along the surface. Then T_s and h should be evaluated for several values of surface temperature, both above and below free-stream temperature, using Eqs (9-13) and (10-13), first by evaluating all properties at free-stream temperature and then using the exponents from Table 15-1, and second by evaluating all properties according to Eq. (15-15). The result should be quite comparable although not necessarily identical.

You can also easily investigate the temperature-ratio part of this problem with TEXSTAN using a problem description similar to problem 10-16 to analyze the laminar thermal boundary layer over a flat plate with constant surface temperature and zero pressure gradient: Choose a starting x -Reynolds number of about 500 to 1000 (a momentum Re of about 10 to 20). The initial velocity and temperature profiles appropriate to this starting x -Reynolds number (Blasius similarity profiles) can be supplied by using the $kstart=4$ choice in TEXSTAN. The geometrical dimensions of the plate are 1 m wide (a unit width) by 0.2 m long in the flow direction, corresponding to an ending Re_x of about 1 to 2×10^5 (a momentum Re of about 150-200). Note these are approximate values due to our variable property effects.

Let the velocity boundary condition at the free stream be 15 m/s and assume the free stream stagnation pressure is one atmosphere. Note that TEXSTAN interprets the input pressure variable, po , as stagnation pressure. To evaluate the density, we will need the free stream static pressure, which can be computed using

$$\frac{P_{static}}{P_{stag}} = \left(1 + \frac{\gamma - 1}{2} M^2 \right)^{\frac{\gamma}{\gamma - 1}}$$

For the energy boundary condition choose the wall temperature to be 295 K and investigate two free stream values, $(T_s/T_\infty) = 0.7$ and $(T_s/T_\infty) = 1.4$. This provides the two free stream temperature values, $T_\infty = 421.4\text{K}$ (the surface cooling case, $T_s < T_\infty$) and $T_\infty = 210.7\text{K}$ (the surface heating case, $T_s > T_\infty$).

For the variable properties, we have several choices, as described in Appendix F. Choose the variable fluid property routine $kfluid=2$ because it realistically varies all of the thermophysical properties and matches the property table for air in Appendix A fairly close. We could choose the variable fluid property routine $kfluid=14$ for air because this is also used in the various analytical results of this chapter and the high-speed chapter 16. The $kfluid=14$ model assumes the Sutherland law for dynamic viscosity, and it uses a constant specific heat and constant Prandtl number.

Note that we could not be sure if this is heating or cooling if the Mach number were large, because of near-wall viscous heating effects. However, for a free stream velocity of 15 m/s and this level of free stream temperature, we will expect the Mach number to be near zero. We can compute the Mach number using Eq. (16-32), assuming the ratio of specific heats for air is $\gamma=1.4$,

$$M = (u_\infty / \sqrt{\gamma R T_\infty}) = (15) / \sqrt{(1.4)(8314/28.97)(295/0.7)} = 0.036$$

Note that for the larger temperature ratio the mach number will be smaller. This confirms our assumption that viscous dissipation effects are not important. Therefore we keep input viscous work variable $jsor(1)=1$.

TEXSTAN requires stagnation temperature for the input variable, $tstag$. Based on the $kfluid=14$ model, we can use the compressible gas flow calculation,

$$\frac{T_{stag}}{T_{static}} = \left(1 + \frac{\gamma - 1}{2} M^2 \right) = 1.0003$$

So for this problem we can use the free stream static temperature, T_∞ , as the stagnation temperature for both cases, and because of the low Mach number we can use 1 atm for P_∞ .

There are four data files for this problem file *15.2a.dat.txt* is for the variable-property flow of air at a temperature ratio of 0.7, and *15.2b.dat.txt* is the same data set with *kfluid*=1 to permit comparison of a variable property calculation to a constant property calculation. For *15.2b.dat.txt* the properties of air were 400 K (about the same free stream temperature as the variable-property calculation). File *15.2c.dat.txt* is for the variable-property flow of air at a temperature ratio of 1.4, and *15.2d.dat.txt* is the same data set with *kfluid*=1 to permit comparison of a variable property calculation to a constant property calculation. For *15.2d.dat.txt* the properties of air were 200 K (about the same free stream temperature as the variable-property calculation).

For *15.2a.dat.txt* here is an abbreviated listing of the output file (it will be called *out.txt* when you execute TEXSTAN using an input data set) for *kout*=8, $(T_s/T_\infty) = 0.7$

intg	rex	rem	cf2	nu	cfrat	nurat	hl2	reh
5	5.547E+02	1.571E+01	1.517E-02	7.6	1.076	1.090	1.716	1.913E+01
200	3.451E+03	3.990E+01	5.795E-03	17.6	1.025	1.014	1.724	4.964E+01
400	1.054E+04	6.981E+01	3.312E-03	30.6	1.024	1.011	1.723	8.715E+01
600	2.149E+04	9.971E+01	2.319E-03	43.7	1.024	1.010	1.722	1.246E+02
800	3.631E+04	1.296E+02	1.784E-03	56.8	1.024	1.010	1.722	1.621E+02
1000	5.500E+04	1.595E+02	1.449E-03	69.9	1.024	1.010	1.722	1.995E+02
1200	7.755E+04	1.894E+02	1.221E-03	83.0	1.024	1.010	1.722	2.370E+02
1400	1.040E+05	2.193E+02	1.054E-03	96.1	1.024	1.010	1.722	2.744E+02
1412	1.056E+05	2.210E+02	1.046E-03	96.8	1.024	1.010	1.722	2.765E+02

In the benchmark output (*kout*=8) we see *cfrat* and *nurat*, which present ratios of TEXSTAN-calculated values for c_f to Eq. (9-13) and for Nu to Eq. (10-13), both at the same *x*-Reynolds number. From Table 15-1, for cooling and constant free stream velocity, $m=-0.05$ and $n=0$ to be used with

$$\frac{c_f}{c_{fCP}} = \left(\frac{T_s}{T_\infty} \right)^m = (0.7)^{-0.05} = 1.018$$

$$\frac{Nu}{Nu_{CP}} = \left(\frac{T_s}{T_\infty} \right)^n = (0.7)^{0.0} = 1.00$$

Comparison of the output with these models show about what we would expect.

A better validation is to run the same data set with constant properties, *15.2b.dat.txt* (properties at 400K)

intg	rex	rem	cf2	nu	cfrat	nurat	hl2	reh
5	6.067E+02	1.636E+01	1.348E-02	7.2	1.000	.995	2.590	2.023E+01
200	4.110E+03	4.263E+01	5.174E-03	18.8	.999	.993	2.590	5.330E+01
400	1.282E+04	7.528E+01	2.930E-03	33.2	.999	.992	2.590	9.436E+01
600	2.637E+04	1.079E+02	2.044E-03	47.6	1.000	.992	2.590	1.354E+02

800	4.475E+04	1.406E+02	1.569E-03	62.0	1.000	.992	2.590	1.764E+02
1000	6.796E+04	1.732E+02	1.273E-03	76.4	1.000	.992	2.590	2.174E+02
1200	9.600E+04	2.059E+02	1.071E-03	90.8	1.000	.992	2.590	2.584E+02
1322	1.154E+05	2.257E+02	9.772E-04	99.6	1.000	.992	2.590	2.833E+02

If we now take the ratio of the *cfrat* for variable properties to constant properties at the same *Rex*, we find the ratio to be 1.024, in line with the model. For the heat transfer we find the ratio to be 1.018, which is within 2% of the property-ratio model.

To examine $(T_s/T_\infty) = 1.4$, we use *15.2c.dat.txt*. Here is an abbreviated listing of the output file (it will be called *out.txt* for *kout=8*,

intg	rex	rem	cf2	nu	cfrat	nurat	h12	reh
5	1.891E+03	2.874E+01	7.213E-03	12.7	.945	.977	3.743	3.455E+01
400	2.092E+04	9.448E+01	2.251E-03	43.3	.981	.999	3.724	1.165E+02
800	6.586E+04	1.675E+02	1.270E-03	76.8	.982	.998	3.726	2.072E+02
1200	1.359E+05	2.405E+02	8.842E-04	110.3	.982	.998	3.727	2.978E+02
1600	2.310E+05	3.136E+02	6.783E-04	143.8	.982	.998	3.727	3.884E+02
2000	3.512E+05	3.866E+02	5.501E-04	177.4	.982	.998	3.727	4.789E+02
2029	3.609E+05	3.919E+02	5.427E-04	179.8	.982	.998	3.727	4.855E+02

In the benchmark output (*kout=8*) we see *cfrat* and *nurat*, which present ratios of TEXSTAN-calculated values for c_f to Eq. (9-13) and for *Nu* to Eq. (10-13), both at the same *x*-Reynolds number. From Table 15-1, for heating and constant free stream velocity, $m=-0.10$ and $n=-0.01$ to be used with

$$\frac{c_f}{c_{fCP}} = \left(\frac{T_s}{T_\infty} \right)^m = (1.4)^{-0.10} = 0.967$$

$$\frac{Nu}{Nu_{CP}} = \left(\frac{T_s}{T_\infty} \right)^n = (1.4)^{-0.01} = 0.997$$

Comparison of the output with these models show about what we would expect for the friction, but the heat transfer seems to be more affected than the model predicts.

A better validation is to run the same data set with constant properties, *15.2d.dat.txt* (properties at 200K)

intg	rex	rem	cf2	nu	cfrat	nurat	h12	reh
5	2.079E+03	3.028E+01	7.283E-03	13.9	1.000	.996	2.590	3.538E+01
400	1.801E+04	8.919E+01	2.473E-03	40.7	1.000	.995	2.590	1.051E+02
800	5.404E+04	1.545E+02	1.428E-03	70.5	1.000	.994	2.590	1.823E+02
1200	1.094E+05	2.197E+02	1.004E-03	100.3	1.000	.994	2.590	2.594E+02
1600	1.841E+05	2.850E+02	7.738E-04	130.1	1.000	.994	2.590	3.365E+02
2000	2.781E+05	3.503E+02	6.296E-04	159.9	1.000	.994	2.590	4.137E+02
2400	3.914E+05	4.156E+02	5.307E-04	189.7	1.000	.994	2.590	4.908E+02
2419	3.972E+05	4.187E+02	5.268E-04	191.1	1.000	.994	2.590	4.944E+02

If we now take the ratio of the c_{frat} for variable properties to constant properties at the same Re_x , we find the ratio to be 0.98, in line with the model. For the heat transfer we find the ratio to be 1.00, which is much closer to the model. By taking these numerical-predicted ratios, we remove the calculation bias.

15-3

Repeat Prob. 15-2 but for a turbulent boundary layer with constant free-stream velocity.

This problem is the same as problem 15-2 except that the equations under investigation are (11-23) and (12-18), and the temperature ratio exponents suggested are -0.4 for $(T_s/T_\infty) < 1$ and 0.0 for $(T_s/T_\infty) > 1$. For this problem the comparison of methods may not be so favorable but there exists virtually no experimental data upon which to base a judgment.

Change to the problem statement: use Eq. (11-20) which permits comparison at the same momentum-thickness Reynolds number, and use Eq. (12-19) which permits comparison at the same enthalpy thickness Reynolds number.

You can also easily investigate the temperature-ratio part of this problem with TEXSTAN using a problem description similar to problem 12-17 to analyze the turbulent thermal boundary layer over a flat plate with constant surface temperature and zero pressure gradient: Choose a starting x -Reynolds number of about $1-2 \times 10^5$ (a momentum Re of about 500-700). The initial turbulent velocity and temperature profiles appropriate to this starting x -Reynolds number can be supplied by using the $kstart=3$ choice in TEXSTAN. The geometrical dimensions of the plate are 1 m wide (a unit width) by 3 m long in the flow direction, corresponding to an ending Rex of about 3×10^6 (a momentum Re of about 3000-4000). Note these are approximate values due to our variable property effects.

Let the velocity boundary condition at the free stream be 15 m/s and assume the free stream stagnation pressure is one atmosphere. Note that TEXSTAN interprets the input pressure variable, po , as stagnation pressure. To evaluate the density, we will need the free stream static pressure, which can be computed using

$$\frac{P_{static}}{P_{stag}} = \left(1 + \frac{\gamma - 1}{2} M^2 \right)^{\frac{\gamma}{\gamma - 1}}$$

For the energy boundary condition choose the wall temperature to be 295 K and investigate two free stream values, $(T_s/T_\infty) = 0.7$ and $(T_s/T_\infty) = 1.4$. This provides the two free stream temperature values, $T_\infty = 421.4\text{K}$ (the surface cooling case, $T_s < T_\infty$) and $T_\infty = 210.7\text{K}$ (the surface heating case, $T_s > T_\infty$).

For the variable properties, we have several choices, as described in Appendix F. Choose the variable fluid property routine $kfluid=2$ because it realistically varies all of the thermophysical properties and matches the property table for air in Appendix A fairly close. We could choose the variable fluid property routine $kfluid=14$ for air because this is also used in the various analytical results of this chapter and the high-speed chapter 16. The $kfluid=14$ model assumes the Sutherland law for dynamic viscosity, and it uses a constant specific heat and constant Prandtl number.

Note that we could not be sure if this is heating or cooling if the Mach number were large, because of near-wall viscous heating effects. However, for a free stream velocity of 15 m/s and this level of free stream temperature, we will expect the Mach number to be near zero. We can compute the Mach number using Eq. (16-32), assuming the ratio of specific heats for air is $\gamma=1.4$,

$$M = (u_\infty / \sqrt{\gamma R T_\infty}) = (15) / \sqrt{(1.4)(8314/28.97)(295/0.7)} = 0.036$$

Note that for the larger temperature ratio the mach number will be smaller. This confirms our assumption that viscous dissipation effects are not important. Therefore we keep input viscous work variable $jsor(1)=1$.

TEXSTAN requires stagnation temperature for the input variable, $tstag$. Based on the $kfluid=14$ model, we can use the compressible gas flow calculation,

$$\frac{T_{stag}}{T_{static}} = \left(1 + \frac{\gamma - 1}{2} M^2 \right) = 1.0003$$

So for this problem we can use the free stream static temperature, T_∞ , as the stagnation temperature for both cases, and because of the low Mach number we can use 1 atm for P_∞ .

There are four data files for this problem file *15.3a.dat.txt* is for the variable-property flow of air at a temperature ratio of 0.7, and *15.3b.dat.txt* is the same data set with *kfluid*=1 to permit comparison of a variable property calculation to a constant property calculation. For *15.3b.dat.txt* the properties of air were 400 K (about the same free stream temperature as the variable-property calculation). File *15.3c.dat.txt* is for the variable-property flow of air at a temperature ratio of 1.4, and *15.3d.dat.txt* is the same data set with *kfluid*=1 to permit comparison of a variable property calculation to a constant property calculation. For *15.2d.dat.txt* the properties of air were 200 K (about the same free stream temperature as the variable-property calculation).

For *15.3a.dat.txt* here is an abbreviated listing of the output file (it will be called *out.txt* when you execute TEXSTAN using an input data set) for *kout*=8, (T_s/T_∞) = 0.7

intg	rex	rem	cf2	st	cfrat	strat	hl2	reh
5	1.110E+05	4.757E+02	2.322E-03	2.903E-03	.867	.875	1.160	4.107E+02
250	1.568E+05	5.957E+02	2.569E-03	3.149E-03	1.015	1.025	1.086	5.593E+02
500	2.234E+05	7.615E+02	2.421E-03	2.908E-03	1.017	1.022	1.041	7.602E+02
750	3.073E+05	9.591E+02	2.294E-03	2.721E-03	1.021	1.023	1.007	9.956E+02
1000	4.117E+05	1.193E+03	2.183E-03	2.566E-03	1.026	1.025	.982	1.271E+03
1250	5.403E+05	1.467E+03	2.084E-03	2.434E-03	1.032	1.029	.962	1.592E+03
1500	6.971E+05	1.786E+03	1.995E-03	2.319E-03	1.037	1.033	.947	1.964E+03
1750	8.866E+05	2.156E+03	1.914E-03	2.218E-03	1.043	1.038	.935	2.393E+03
2000	1.114E+06	2.583E+03	1.840E-03	2.127E-03	1.050	1.043	.926	2.886E+03
2250	1.384E+06	3.071E+03	1.773E-03	2.045E-03	1.056	1.049	.918	3.449E+03
2415	1.589E+06	3.430E+03	1.731E-03	1.995E-03	1.060	1.052	.914	3.862E+03

In the benchmark output (*kout*=8) we see *cfrat* and *strat*, which present ratios of TEXSTAN-calculated values for c_f to Eq. 11-20) at the same momentum thickness Reynolds number and for *St* to Eq. (12-18), both at the same enthalpy thickness Reynolds number. From p. 341, for cooling and constant free stream velocity, $m=-0.22$ and $n=-0.14$ to be used with

$$\frac{c_f}{c_{fCP}} = \left(\frac{T_s}{T_\infty} \right)^m = (0.7)^{-0.22} = 1.082$$

$$\frac{St}{St_{CP}} = \left(\frac{T_s}{T_\infty} \right)^n = (0.7)^{-0.14} = 1.051$$

Comparison of the output with these models show about what we would expect.

A better validation is to run the same data set with constant properties, *15.3b.dat.txt* (properties at 400K)

intg	rex	rem	cf2	st	cfrat	strat	hl2	reh
5	1.214E+05	4.716E+02	2.764E-03	3.499E-03	1.030	1.051	1.529	4.019E+02
250	1.710E+05	6.048E+02	2.582E-03	3.189E-03	1.024	1.045	1.500	5.687E+02

500	2.444E+05	7.864E+02	2.386E-03	2.884E-03	1.011	1.026	1.473	7.904E+02
750	3.380E+05	1.002E+03	2.232E-03	2.662E-03	1.005	1.016	1.450	1.049E+03
1000	4.559E+05	1.258E+03	2.103E-03	2.486E-03	1.002	1.011	1.430	1.352E+03
1250	6.026E+05	1.557E+03	1.992E-03	2.339E-03	1.001	1.008	1.415	1.705E+03
1500	7.828E+05	1.907E+03	1.894E-03	2.213E-03	1.001	1.007	1.402	2.115E+03
1750	1.002E+06	2.312E+03	1.806E-03	2.104E-03	1.002	1.006	1.392	2.588E+03
2000	1.266E+06	2.779E+03	1.728E-03	2.007E-03	1.004	1.007	1.383	3.130E+03
2250	1.581E+06	3.312E+03	1.657E-03	1.921E-03	1.006	1.008	1.376	3.749E+03
2359	1.737E+06	3.568E+03	1.628E-03	1.886E-03	1.007	1.009	1.373	4.045E+03

If we now take the ratio of the c_{frat} for variable properties to constant properties at the same Re_{δ_2} , we find the ratio to be 1.052, within about 3% the model and with the right trend. For the heat transfer we find the ratio to be 1.042, which is within 1% of the property-ratio model.

To examine $(T_s/T_\infty) = 1.4$, we use *15.3c.dat.txt*. Here is an abbreviated listing of the output file (it will be called *out.txt* for $kout=8$,

intg	rex	rem	cf2	st	cfrat	strat	hl2	reh
5	1.084E+05	3.983E+02	3.405E-03	4.354E-03	1.217	1.285	2.036	3.421E+02
250	1.549E+05	5.296E+02	2.660E-03	3.279E-03	1.021	1.067	2.082	5.056E+02
500	2.258E+05	7.083E+02	2.402E-03	2.898E-03	.991	1.031	2.073	7.219E+02
750	3.190E+05	9.225E+02	2.210E-03	2.634E-03	.975	1.010	2.057	9.770E+02
1000	4.389E+05	1.178E+03	2.056E-03	2.430E-03	.964	.997	2.041	1.278E+03
1250	5.904E+05	1.479E+03	1.927E-03	2.265E-03	.956	.988	2.026	1.631E+03
1500	7.794E+05	1.832E+03	1.817E-03	2.127E-03	.951	.981	2.013	2.042E+03
1750	1.012E+06	2.243E+03	1.721E-03	2.009E-03	.947	.976	2.002	2.519E+03
2000	1.294E+06	2.717E+03	1.636E-03	1.905E-03	.945	.973	1.992	3.068E+03
2129	1.461E+06	2.987E+03	1.596E-03	1.857E-03	.944	.972	1.988	3.381E+03

In the benchmark output ($kout=8$) we see c_{frat} and $strat$, which present ratios of TEXSTAN-calculated values for c_f to Eq. 11-20) at the same momentum thickness Reynolds number and for St to Eq. (12-18), both at the same enthalpy thickness Reynolds number. From p. 341, for heating and constant free stream velocity, $m=-0.33$ and $n=-0.30$ to be used with

$$\frac{c_f}{c_{fCP}} = \left(\frac{T_s}{T_\infty} \right)^m = (1.4)^{-0.33} = 0.895$$

$$\frac{St}{St_{CP}} = \left(\frac{T_s}{T_\infty} \right)^n = (1.4)^{-0.30} = 0.904$$

Comparison of the output with these models show about a 5-10% discrepancy.

A better validation is to run the same data set with constant properties, *15.2d.dat.txt* (properties at 200K)

intg	rex	rem	cf2	st	cfrat	strat	hl2	reh
------	-----	-----	-----	----	-------	-------	-----	-----

5	1.194E+05	4.657E+02	2.773E-03	3.295E-03	1.031	1.038	1.531	4.032E+02
250	1.684E+05	5.977E+02	2.590E-03	3.025E-03	1.025	1.034	1.502	5.588E+02
500	2.409E+05	7.777E+02	2.393E-03	2.753E-03	1.011	1.019	1.474	7.673E+02
750	3.335E+05	9.918E+02	2.238E-03	2.551E-03	1.005	1.012	1.451	1.012E+03
1000	4.502E+05	1.245E+03	2.109E-03	2.388E-03	1.002	1.009	1.431	1.300E+03
1250	5.955E+05	1.543E+03	1.997E-03	2.252E-03	1.001	1.007	1.415	1.637E+03
1500	7.741E+05	1.891E+03	1.898E-03	2.134E-03	1.001	1.007	1.403	2.028E+03
1750	9.914E+05	2.293E+03	1.810E-03	2.031E-03	1.002	1.008	1.392	2.480E+03
2000	1.253E+06	2.756E+03	1.731E-03	1.940E-03	1.004	1.010	1.383	3.000E+03
2250	1.566E+06	3.286E+03	1.660E-03	1.859E-03	1.006	1.012	1.376	3.593E+03
2281	1.609E+06	3.357E+03	1.652E-03	1.849E-03	1.006	1.013	1.375	3.673E+03

If we now take the ratio of the c_{frat} for variable properties to constant properties at the same momentum thickness Re we find the ratio to be 0.94, or 4% higher than the model. For the heat transfer we find the ratio to be 0.96, or 6% higher than the model. By taking these numerical-predicted ratios, we remove the calculation bias, but there is still discrepancy. Furthermore, there will be a strong Reynolds number dependence.

16-1

Consider an aircraft flying at Mach 3 at an altitude of 17,500 m. Suppose the aircraft has a hemispherical nose with a radius of 30 cm. If it is desired to maintain the nose at 80°C, what heat flux must be removed at the stagnation point by internal cooling? As a fair approximation, assume that the air passes through a normal detached shock wave and then decelerates isentropically to zero at the stagnation point; then the flow near the stagnation point is approximated by low-velocity flow about a sphere.

$$\dot{q}_s'' = 31 \text{ kW/m}^2$$

16-2

In Prob. 16-1 it is desired to cool a particular rectangular section of the aircraft body to 65°C. The section is to be 60 cm wide by 90 cm long (in the flow direction) and is located 3 m from the nose. Estimate the total heat-transfer rate necessary to maintain the desired surface temperature. As an approximation, the boundary layer may be treated as if the free-stream velocity were constant along a flat surface for the preceding 3 m. It may also be assumed that the preceding 3 m of surface is adiabatic. To obtain the state of the air just outside the boundary layer, it is customary to assume that the air accelerates from behind the normal shock wave at the nose, isentropically to the free-stream static pressure. In this case the local Mach number then becomes 2.27, and the ratio of local absolute static temperature to free-stream stagnation temperature is 0.49. The local static pressure is the same as the free-stream, that is, the pressure at 17,500 m altitude.

$$\dot{q}_s'' = 11 \text{ kW/m}^2$$

16-3

Consider a laminar constant-property boundary layer on a flat plate with constant free-stream velocity. Evaluate the recovery factor for a fluid with $Pr = 100$, using Eq. (16-20). The correct answer is 7.63. Why is it difficult to obtain accuracy in solving this problem numerically?

Numerical integration is required. At the large values of h considerable error is introduced unless care is taken and a fairly sophisticated integration scheme is employed.

16-4

Listed below, as functions of *axial* distance, are the radius, mass velocity, temperature, and pressure inside a supersonic nozzle. The fluid is air. It is desired to maintain the nozzle surface uniformly at 200°C. Calculate the necessary heat flux along the nozzle surface. Assume that a turbulent boundary layer originates at the start of the nozzle.

Axial distance cm	Radius cm	Mass velocity kg/(s · m ²)	Pressure kPa	<i>T</i> K
0	9.70	0	2068	893
1.94	8.59	98	2068	893
6.07	6.15	366	2068	891
8.14	4.95	561	2048	890
10.20	3.81	879	2013	886
12.26	2.62	1733	1841	856
13.50	2.13	2734	1262	806
14.33	2.06	2710	931	669
15.15	2.29	1855	331	518
16.39	2.84	1318	172	446
18.45	3.76	928	96.5	380
20.51	4.57	698	62.1	334
22.58	5.28	586	48.3	308
24.64	5.92	464	34.5	287
26.72	6.48	391	27.6	265
28.75	6.99	352	20.7	250
30.81	7.44	322	17.3	237
34.95	8.20	249	13.8	219

The results:

<i>x</i> , axial distance cm	\dot{q}_s'' kW/m ²
1.94	119
6.07	141
8.14	774
10.2	889
12.26	1282

13.5	1872
14.33	1246
15.15	802
16.39	637
18.45	434
20.51	302
22.58	217
24.64	185
26.72	128
28.75	164
30.81	159
34.95	77

The following is a set of experimental data points obtained for the nozzle under study. Experimental uncertainty is about ± 15 percent.

z (axial distance) cm	h W/(m ² K)
6.71	1143
12.27	3169
12.97	4470
13.51	3820
14.54	3492
14.74	2707
15.24	2375
15.65	2069
18.16	1241
20.72	901
23.39	808
28.34	478
31.02	384
33.49	333

16-5

In Prob. 16-4 the nozzle is to be constructed of 0.5 cm thick stainless-steel walls. The entire nozzle is to be surrounded by a bath of water, maintained at 27°C by constant changing. The heat-transfer coefficient on the water side of the nozzle walls is estimated to be 1100 W/(m² · K) uniformly. Calculate the temperature along the inner surface of the nozzle wall and the local heat flux. Assume that heat conduction in the nozzle wall is significant in the radial direction only.

The following results have been obtained assuming an initial laminar boundary layer with transition at a momentum thickness Reynolds number of 300. Note that at the throat it makes little difference whether an initial laminar boundary layer is assumed, or not.) The assumed wall conductivity is 17.3 W/(m·K).

z (axial distance) cm	h W/(m ² K)	T_s K
0	-	-
1.94	284	455
6.07	337	475
8.14	1848	713
10.2	2126	729
12.26	3162	761
13.5	4278	812
14.33	3821	713
15.15	2401	687
16.39	1704	684
18.45	1188	636
20.51	877	585
22.58	689	545
24.64	569	520
26.72	466	
28.75	414	508
30.81	368	505
34.95	272	425

16-6

Repeat Prob. 16-4 but assume that the nozzle is constructed with a uniformly porous wall so that transpiration cooling may be used. Air is available as a coolant at 30°C. Determine the transpiration air rate, as a function of position along the surface, to maintain the surface of 200°C.

z (axial distance) cm	h W/(m ² K)	\dot{m}'' kg/(s m ²)
0	-	-
1.94	234	0.535
6.07	526	1.198
8.14	688	1.568
10.2	935	2.128
12.26	1573	3.484
13.5	2195	5.272
14.33	2147	3.975
15.15	1377	2.775
16.39	950	2.216
18.45	678	1.583
20.51	515	1.157
22.58	440	0.914
24.64	345	0.747
26.72	298	0.556
28.75	246	0.655
30.81	218	0.631
34.95	182	0.353

Total transpiration flow rate = 0.13 kg/s.

16-7

A particular rocket ascends vertically with a velocity that increases approximately linearly with altitude, reaching 3000 m/s at 60,000 m. Consider a point on the cylindrical shell of the rocket 5 m from the nose. Calculate and plot, as functions of altitude, the adiabatic wall temperature, the local convection conductance, and the internal heat flux necessary to prevent the skin temperature from exceeding 50°C (see Prob. 16-2 for remarks about the state of the air just outside the boundary layer in such a situation).

Altitude	Re_x	T_{aw}	h	\dot{q}_s''
m		K	W/(m ² K)	kW/m ²
0	0	288	0	0
1000	10e06	283	66.6	-2.68
4500	53e06	287	164	-5.92
10000	63e06	336	172	2.22
20000	12.9e06	678	65.0	23.09
30000	2.0e06	1245	20.4	18.82
40000	0.6e06	2006	10.4	17.5
transition to laminar				
50000	97900	2867	1.41	3.59
60000	17800	3729	0.71	2.42

16-8

Consider again Prob. 16-7, but let the skin be of 3 mm thick stainless steel, insulated on the inner side. Treating the skin as a single element of capacitance, calculate the skin temperature as a function of altitude. [The specific heat of stainless steel is 0.46 kJ/(kg·K).]

To fit the specifications of the problem an initial velocity must be assumed. Using $V = 10$ m/s as the velocity at zero altitude, and a density of 7849 kg/m^3 for the metal skin, the following results are obtained:

Altitude m	Flight time, s	T_s K
0	0	288
1000	35.8	288
4500	63.1	288
10000	78.6	293
20000	92.3	323
30000	100.3	354
40000	106.1	367
50000	110.5	373
60000	114.1	374

16-9

Consider the gas turbine blade on which Prob. 11-8 is based (see Fig. 11-19). It is desired to maintain the blade surface uniformly at 650°C by internal cooling. Calculate the necessary heat flux around the periphery of the blade.

location cm	\dot{q}_s'' kW/m ² upper surface	\dot{q}_s'' kW/m ² lower surface
stagnation point	1016	1016
0.2	431	295
0.5	250	255
1.0	193	125
transition		
2.0	352	250
3.0	420	241
5.0	346	204
6.0	306	-

16-10

In Prob. 16-9 the turbine blade is 15 cm long, and for present purposes it may be assumed that blade dimensions and operating conditions are the same along the entire blade length. It appears feasible to allocate up to 0.03 kg/s of air at 200°C to cool the blade. Assuming a hollow blade of mild-steel construction, a minimum wall thickness of 0.75 mm, and any kind of internal inserts as desired (a solid core leaving a narrow passage just inside the outer wall could be used, for example), make a study of the feasibility of internally cooling this blade. Assume that the cooling air can be introduced at the blade root and discharged through the tip. Treat the blade as a simple heat exchanger.

There is no "correct" answer for this problem. The results of Prob. 16-9 are to be used for a design study, but the types of internal flow passages that could be used are quite varied. The problem is to get a high enough heat transfer coefficient on the inside surface so as to pull the surface temperature down. Internal fins are a possible answer.

16-11

The gas turbine blade of Prob. 11-8 is to be cooled to a uniform surface temperature of 650°C by transpiration of air through a porous surface. If the cooling air is available at 200°C, calculate the necessary cooling-air mass-transfer rate per unit of surface area as a function of position along the blade surface. Discuss the probable surface temperature distribution if it is only mechanically feasible to provide a transpiration rate that is uniform along the surface.

location cm	\dot{m}'' kg/(s m ²)
stagnation point	2.1
0.2	1.66
0.5	1.56
1.0	1.67
2.0	1.88
3.0	1.75
5.0	1.54
6.0	1.48

16-12

Consider the rocket nozzle described in Prob. 11-6 (Fig. 11-18). Calculate the heat flux along the nozzle surface necessary to maintain the surface at 1100°C. If the convergent part of the nozzle is exposed to black-body radiation at 2200°C (the reactor core) and the nozzle surface itself is a black body, will thermal radiation contribute significantly to the heat flux through the nozzle walls?

z (axial distance) cm	h W/(m ² K)	\dot{q}_s'' W/m ²	Re _{Δ₂}
0	∞	∞	0
1	1604	1.77e06	105
2	1263	1.39e06	161
3	1156	1.27e06	216
4	1134	1.25e06	274
5	1161	1.27e06	341
6	1232	1.35e06	420
8	1500	1.63e06	654
transition			
10	7233	7.78e06	1187
12 (throat)	7742	8.03e06	1938
14	5849	5.70e06	2777
16	3767	3.56e06	3752
18	2509	2.31e06	4858
22	1372	1.23e06	6712

16-13

Suppose the nozzle of Prob. 16-12 is constructed of 6 mm thick molybdenum. Copper cooling tubes are then to be wrapped around the nozzle and bonded to the surface. Room-temperature water is available as a coolant. Make a study of the feasibility of water cooling in this manner, after first choosing a tubing size, flow arrangement, and reasonable water velocity

The results of this problem depend almost completely on the ingenuity of the student in devising a suitable cooling system. It will be found to be extremely difficult to hold the surface uniformly at 100°C, but the objective of the problem is to see what can be done. Local boiling may have to be accepted. Although surface temperature will probably not be constant, it will be sufficiently accurate to use values of h from Prob. 16-12.

16-14

The helium rocket nozzle of Probs. 11-6 and 16-12 is to be cooled to a uniform surface temperature of 800°C by transpiration of additional helium that is available at 38°C. Calculate the necessary local transpiration rates if this turns out to be a feasible scheme. What is the total necessary coolant rate? How does this compare with the total hot-helium rate passing through the nozzle?

x (along surface) m	h W/m ² K	\dot{m}'' kg/(s m ²)	B
0.0138	1458	0.380	1.35
0.0275	1412	0.368	1.35
0.0413	1480	0.386	1.35
0.055	1612	0.420	1.35
0.0688	1805	0.470	1.35
0.0825	2075	0.540	1.35
0.110	2970	0.771	1.35
0.137	4196	1.07	1.33
0.157	4620	1.15	1.29
0.175	3582	0.849	1.23
0.198	2352	0.545	1.20
0.221	1591	0.461	1.18
0.267	886	0.197	1.15

Up to this point the total coolant required is 0.037 kg/s, less than one percent of the thru-flow, which is 5.28 kg/s. A turbulent boundary layer has been assumed from $x = 0$.

16-15

Consider again Prob. 13-11, but let the aircraft speed be 300 m/s. At what airspeed does direct cooling become impossible?

For the 60 cm by 60 cm cooler, $\dot{q} \approx 3600 \text{ W}$. For the 1.2 by 30 cm cooler, $\dot{q} \approx 3900 \text{ W}$. No cooling is possible when V reaches 360 m/s (800 MPH).

17-1

Investigate Eq. (17-29) for very large values of Pr. Compare your result to Eq. (17-33). What is your conclusion? What result do you obtain by using Eq. (17-42) instead of Eq. (17-29)?

Equation (17-29) is given by

$$\text{Nu}_x = \frac{3}{4} \left[\frac{2 \text{Pr}}{5(1 + 2 \text{Pr}^{1/2} + 2 \text{Pr})} \right]^{1/4} (\text{Gr}_x \text{Pr})^{1/4}$$

For very large values of the Prandtl number ($\text{Pr} \rightarrow \infty$), this equation results in

$$\text{Pr} \rightarrow \infty: \text{Nu}_x = \frac{3}{4} \left[\frac{1}{5} \right]^{1/4} (\text{Gr}_x \text{Pr})^{1/4} = 0.5016 (\text{Gr}_x \text{Pr})^{1/4}$$

From Eq. (17-33) we have

$$\text{Pr} \rightarrow \infty: \text{Nu}_x = 0.503 (\text{Gr}_x \text{Pr})^{1/4}$$

The relative difference between these two equations is about 0.3%. From Eq. (17-42) one obtains for very large Prandtl numbers

$$\text{Pr} \rightarrow \infty: \text{Nu}_x = 0.508 (\text{Gr}_x \text{Pr})^{1/4}$$

Comparing this result to Eq. (17-33) one sees that both equations differ by about 1%.

17-2

Investigate Eq. (17-29) for very small values of Pr. Compare your result to Eq. (17-32). What is your conclusion? What result do you obtain by using Eq. (17-42) instead of Eq. (17-29)?

For very small values of the Prandtl number the terms containing the Prandtl number explicitly in the denominator of Eq. (17-29) can be neglected compared to one. This results for Eq. (17-29) in:

$$\text{Pr} \rightarrow 0: \text{Nu}_x = \frac{3}{4} \left[\frac{2 \text{Pr}}{5} \right]^{1/4} (\text{Gr}_x \text{Pr})^{1/4} = \frac{3}{4} \left[\frac{2}{5} \right]^{1/4} (\text{Gr}_x \text{Pr}^2)^{1/4} = 0.5965 (\text{Gr}_x \text{Pr}^2)^{1/4}$$

Comparing this expression with Eq. (17-32) one sees that there is only a 0.6% difference between both Equations.

From Eq. (17-42) one obtains for very small values of the Prandtl number

$$\text{Pr} \rightarrow 0: \text{Nu}_x = 0.514 (\text{Gr}_x \text{Pr}^2)^{1/4}$$

This expression shows a relative difference of about 14% compared to Eq. (17-32).

17-3

Show that the volumetric coefficient of thermal expansion $\beta = -1/\rho(\partial\rho/\partial T)_p$ is equal to $1/T$ for an ideal gas.

The definition of the volumetric coefficient of thermal expansion is given by

$$\beta = -\frac{1}{\rho} \left(\frac{\partial \rho}{\partial T} \right)_p$$

The law for an ideal gas is given by $\rho = p/(RT)$, where R is the specific gas constant. Performing the partial derivative $(\partial\rho/\partial T)_p$ one obtains

$$\left(\frac{\partial \rho}{\partial T} \right)_p = -\frac{p}{RT^2}$$

From this, we obtain for the volumetric coefficient of thermal expansion

$$\beta = -\frac{1}{\rho} \left(\frac{\partial \rho}{\partial T} \right)_p = \frac{p}{RT^2} \frac{RT}{p} = \frac{1}{T}$$

17-4

Consider a flat plate surrounded by a fluid at rest (at rest outside the boundary layer) and oriented vertically to a gravity field of strength g . If the plate is heated to a temperature above that of the fluid, the fluid immediately adjacent to the plate will be heated, its density will decrease below that of the surrounding fluid, the resulting buoyancy force will put the fluid in motion, and a free-convection boundary layer will form. If the thermal expansion coefficient for the fluid is defined as

$$\beta = -\frac{1}{\rho} \left(\frac{\partial \rho}{\partial T} \right)_p$$

develop the applicable momentum integral equation of the boundary layer under conditions where the density variation through the boundary layer is small relative to the free-fluid density.

The development parallels that on pages 41-43, except that $u_\infty = 0$ and a body force acts in the x - direction. In addition there is no mass transfer through the wall and the radius of curvature R tends to infinity in the here considered case. One obtains from Eq. (5-2):

$$-\tau_s = \frac{d}{dx} \left(\int_0^Y \rho u^2 dy \right) + \int_0^Y \frac{dP}{dx} dy + \int_0^Y \rho g dy$$

Carrying out the integration for the second integral results in

$$-\tau_s = \frac{d}{dx} \left(\int_0^Y \rho u^2 dy \right) + \frac{dP}{dx} Y + \int_0^Y \rho g dy$$

Now, from hydrostatics $dP/dx = -\rho_\infty g$, and according to Eq. (17-5) $\rho_\infty - \rho = \rho\beta(T - T_\infty)$. Thus, one obtains

$$\begin{aligned} -\tau_s &= \frac{d}{dx} \left(\int_0^Y \rho u^2 dy \right) - \rho_\infty g Y + \int_0^Y \rho g dy = \frac{d}{dx} \left(\int_0^Y \rho u^2 dy \right) + \int_0^Y (\rho - \rho_\infty) g dy \\ &= \frac{d}{dx} \left(\int_0^Y \rho u^2 dy \right) - \beta g \int_0^Y \rho (T - T_\infty) dy \end{aligned}$$

17-5

For laminar flow over a constant-heat-flux surface develop two expressions for the mean Nusselt number. In the first case base the heat-transfer coefficient on the temperature difference between the average surface temperature and the ambient; in the second case let the temperature difference be the surface minus the ambient at $\frac{1}{2}L$. Compare the two mean Nusselt numbers with those for a constant-wall-temperature surface, Eq. (17-34), at Prandtl numbers of 0.1, 0.72, 1.0, and 100.0, and discuss.

If $T_s - T_\infty$ varies as $x^{1/5}$, a constant-heat-flux boundary condition $\dot{q}_s = \text{constant}$ is obtained (see page 379). Now let us define a mean temperature difference between surface and free-stream for the first case by

$$\overline{(T_s - T_\infty)} = \frac{1}{L} \int_0^L (T_s - T_\infty) dx = \frac{1}{L} \int_0^L C_1 x^{1/5} dx = \frac{5}{6} C_1 L^{1/5} = \frac{5}{6} (T_s - T_\infty)_{x=L} = \frac{5}{6} \Delta T_L = \overline{\Delta T_L}$$

From the definition $\text{Nu}_x = C Gr_x^{1/4}$ at $x = L$ we obtain

$$\frac{\dot{q}_s L}{\Delta T_L k} = C \left(\frac{g \beta}{\nu^2} \Delta T_L L^3 \right)^{1/4}$$

Substituting $\Delta T_L = 6/5 \overline{\Delta T_L}$ from the definition of the mean temperature for the first case, one obtains

$$\begin{aligned} \frac{\dot{q}_s L}{6/5 \overline{\Delta T_L} k} &= C \left(\frac{g \beta}{\nu^2} \frac{6}{5} \overline{\Delta T_L} L^3 \right)^{1/4} \\ \overline{\text{Nu}}_L &= \left(\frac{6}{5} \right)^{5/4} C Gr_L^{1/4} = 1.256 C Gr_L^{1/4} \end{aligned}$$

For the second case $(T_s - T_\infty)_{L/2} = (1/2)^{1/5} (T_s - T_\infty)_L$ (recall that $T_s - T_\infty$ varies as $x^{1/5}$). Substituting this expression into the definition of the Nusselt number results in

$$\overline{\text{Nu}}_L = (2^{1/5})^{5/4} C Gr_L^{1/4} = 1.181 C Gr_L^{1/4}$$

Use Table 17-2 for C and compare with Table 17-1, modified by Eq. (17-34). One obtains:

Pr	0.1	0.72	1.0	10	100
$\overline{\text{Nu}}_L Gr_L^{-1/4} \ (\dot{q} = \text{const.})$	0.237	0.51	0.574	1.17	2.185
$\overline{\text{Nu}}_L Gr_L^{-1/4} \ (\dot{q} = \text{const.})$	0.223	0.479	0.540	1.10	2.055
$\overline{\text{Nu}}_L Gr_L^{-1/4} \ (T_s = \text{const.})$	0.219	0.476	0.535	1.10	2.067

Table 17-2 shows nicely that the Nusselt numbers based on the mean temperature of case 2 are very close to the mean Nusselt numbers for constant wall temperature.

17-6

Develop an analytic solution for the laminar temperature profile and Nusselt number for the case of large wall suction. Start with Eq. (17-36). The final expression will contain n , $F(0)$, and Pr as parameters. Compare this asymptotic expression for Nusselt number with the results in Table 17-3.

For the case of very large wall suction ($v \gg u$), we can assume that $F = \text{constant} = F(0)$. This means also that $F' = 0$. With these assumptions we obtain from Eq. (17-36)

$$\theta'' + Pr [(n+3)F\theta'] = 0$$

This equation has to be solved together with the boundary conditions

$$\theta(0) = 1$$

$$\theta(\infty) = 0$$

Because the unknown function θ does not appear explicitly in the above differential equation, this equation can be solved easily by setting $Z = \theta'$. This results in

$$Z' + Pr [(n+3)F(0)]Z = 0$$

$$\frac{dZ}{Z} = -Pr [(n+3)F(0)]d\eta, \quad Z = D \exp(-Pr [(n+3)F(0)]\eta)$$

From this equation, we finally obtain the solution for the temperature field

$$\theta = \exp(-Pr (n+3)F(0) \eta)$$

The Nusselt number can be obtained from this equation as described in Chap. 17 (after Eq. 17-38)

$$Nu_x = \frac{-\theta'(0)}{\sqrt{2}} Gr_x^{1/4} = (n+3) Pr \frac{F(0)}{\sqrt{2}} Gr_x^{1/4}$$

Comparison with Table 17-3, $T_s = \text{constant}$ ($n = 0$, $Pr = 0.73$) results in:

$F(0)$	Suction		
	+ 1.0	+ 0.8	+ 0.4
$Nu_x Gr_x^{-1/4}$	1.55	1.27	0.758
(Table 17-3)			
$Nu_x Gr_x^{-1/4}$	1.549	1.239	0.619
(large suction)			

It can be seen that the here obtained solution for large suction is in good agreement with the data reported in Table 17-3 for $F(0) \geq 0.8$.

17-7

A flat ribbon heat strip is oriented vertically on an insulating substrate. Let the ribbon be 1 m wide by 3 m long. Its energy dissipation is 0.5 W/cm^2 to air at 25°C . What are the average heat-transfer coefficient and surface temperature of the ribbon? Where will transition to turbulent flow occur? Would you be justified in neglecting the laminar contribution to the heat transfer?

Modify the problem statement: Let the ribbon be 1 m wide and 3 m high. Its energy dissipation is 0.5 W/cm^2 to air at 25°C .

The solution must be iterated, because T_s is unknown. First guess for $(T_s - T_\infty)$ would be based on $h \approx 8 \text{ W/(m}^2\text{K)}$ (order of magnitude for free convection). After 3 – 4 iterations one finds

$$Gr_L^* = \frac{g\beta}{kv^2} \dot{q}_s'' L^4 \approx 3 \cdot 10^{13}$$

Thus the ribbon is mostly in turbulent flow. Find $\overline{\text{Nu}} = \text{Nu}_L \approx 380$, $h = 6.2 \text{ W/(m}^2\text{K)}$, $T_s = 820^\circ\text{C}$.

17-8

Using the approximate integral solution method for turbulent free convection over a vertical and constant-temperature surface, develop an equation for δ/x . Compare and discuss how the boundary-layer thickness varies with x for laminar and turbulent free and forced convection.

This problem is developed in some detail in Ref. 16 and in the text (pp. 383-386). Substitute the profiles and expressions for u and δ into the integral equations (17-39, 17-40) to obtain two algebraic equations, each of which contains x to the exponential powers m and n . The algebraic equations must be valid for all x ; hence equate the exponents. Find $m = 1/2$ and $n = 7/10$. Substitute these back into the algebraic equations and solve for C_u and C_δ :

$$C_u = 0.0689 \nu C_\delta^{-5} \text{Pr}^{-8/3}$$

$$C_\delta = 0.00338 \frac{\nu^2}{g \beta (T_s - T_\infty)} (1 + 0.494 \text{Pr}^{2/3}) \text{Pr}^{-16/3}$$

Introduce the Grashof number definition, which results in:

$$\frac{\delta}{x} = 0.0565 Gr_x^{-1/10} [1 + 0.494 \text{Pr}^{2/3}]^{1/10} \text{Pr}^{-8/15}$$

17-9

Consider the free-convection cooling of a thick, square plate of copper with one surface exposed to air and the other surfaces insulated. Let the air temperature be 25°C and the copper temperature be 45°C. The copper is 10 cm on a side. Compare the average heat-transfer coefficients for three exposed face orientations: vertical, inclined 45° to the vertical, and horizontal.

For this problem $Gr_L = 2.3 \cdot 10^6$. For horizontal upward facing surfaces, Eq. (17-50) gives $Nu = 19.4$. For inclined surfaces, the +45° orientation is out of the recommended range for using $g \cos \gamma$, but for this low Gr_L , it is probably OK. Find $\overline{Nu} = 17.1$ from a correlation based on the entries on Table 17-1 for $Pr = 0.72$ with the mean value of the Nusselt number according to Eq. (17-34). For a vertical surface, $\overline{Nu} = 18.6$. Note all values within 12%.

17-10

Consider the wire on a constant-temperature hot-wire anemometer sensor. The wire diameter is 0.00038 cm and its length is 580 diameters. Let the wire temperature be 260°C and the air temperature be 25°C. Compare the heat-transfer coefficients for the wire placed in the horizontal and vertical positions. Note that the effects of the wire support prongs are neglected.

For the horizontal case, $Gr_D = 4.1 \cdot 10^{-7}$. Using Eq. (17-51) (laminar) and Eq. (17-52) for correction, find $Nu = 0.37$. For the vertical orientation, Eq. (17-53) is not satisfied. Thus Eq. (17-29), for the local values, must be corrected by Eq. (17-52). Find $\overline{Nu} = 2.3$. Note that Eq. (17-29) must be multiplied by 4/3 before using Eq. (17-52).

18-1

Consider a binary mixture gas mass-transfer system in which the considered phase is a mixture of gases 1 and 2. Let gas 2 be injected into the mixture at the interface; that is, gas 2 is the only transferred substance. Show that if there is no phase change from the L state to the S state then $\dot{q}_s'' = \dot{q}_L''$, regardless of the mass-transfer aspects of the problem (start with Eq. (18-27)).

For solving this problem, we will need the following equations:

$$\dot{m}'' = \frac{\sum_j \left[\gamma_j \left(\partial m_j / \partial y \right) \right]_s i_{j,s} + \left[\Gamma c \left(\partial T / \partial y \right) \right]_s}{i_s - i_T} = \frac{\sum_j \left[\gamma_j \left(\partial m_j / \partial y \right) \right]_s i_{j,s} + \dot{q}_s''}{i_s - i_T}$$

$$\dot{m}'' i_L - \dot{q}_L'' - \dot{m}'' i_T = 0$$

$$i_T = i_L - \frac{\dot{q}_L''}{\dot{m}''}$$

For the binary mixture of gases one obtains:

$$\sum_j \left[\gamma_j \left(\partial m_j / \partial y \right) \right]_s i_{j,s} = \left[\gamma_1 \left(\partial m_1 / \partial y \right) \right]_s i_{1,s} + \left[\gamma_2 \left(\partial m_2 / \partial y \right) \right]_s i_{2,s}$$

$$m_1 + m_2 = 1$$

$$\frac{\partial m_1}{\partial y} + \frac{\partial m_2}{\partial y} = 0$$

$$i_s = (m_1 i_1)_s + (m_2 i_2)_s$$

$$\gamma_1 = \gamma_2$$

Gas 2 is the only transferred substance in this problem. This means that

$$m_{2,T} = 1, \quad m_{1,T} = 0, \quad i_L = i_{2,s}$$

$$\dot{m}'' = \frac{\left[\gamma_j \frac{\partial m_j}{\partial y} \right]_s}{m_{j,s} - m_{j,T}} = \frac{\left[\gamma_1 \frac{\partial m_1}{\partial y} \right]_s}{m_{1,s}}$$

Inserting Eq. (18-25) and the above expressions into Eq. (18-27) results in

$$\dot{m}'' = \frac{\left(\gamma_1 \frac{\partial m_1}{\partial y} \right) i_{1,s} + \left(\gamma_2 \frac{\partial m_2}{\partial y} \right) i_{2,s} + \dot{q}_s''}{i_s - i_{2,s} + \dot{q}_L'' / \dot{m}''} = \frac{\left(\gamma_1 \frac{\partial m_1}{\partial y} \right) (i_{1,s} - i_{2,s}) + \dot{q}_s''}{i_s - i_{2,s} + \dot{q}_L'' / \dot{m}''}$$

Replacing \dot{m}'' on the left hand side of the equation results in

$$\frac{\left(\gamma_1 \frac{\partial m_1}{\partial y}\right)_s}{m_1} = \frac{\left(\gamma_1 \frac{\partial m_1}{\partial y}\right)_s (i_{1,s} - i_{2,s}) + \dot{q}_s''}{i_s - i_{2,s} + \dot{q}_L'' / \dot{m}''} = \frac{\left(\gamma_1 \frac{\partial m_1}{\partial y}\right)_s (i_{1,s} - i_{2,s}) + \dot{q}_s''}{(m_1 i_1)_s + (m_2 i_2)_s - i_{2,s} + \dot{q}_L'' / \dot{m}''}$$

Rearranging gives

$$\frac{\left(\gamma_1 \frac{\partial m_1}{\partial y}\right)_s}{m_1} [(m_1 i_1)_s + (m_2 i_2)_s - i_{2,s}] + \dot{q}_L'' = \left(\gamma_1 \frac{\partial m_1}{\partial y}\right)_s (i_{1,s} - i_{2,s}) + \dot{q}_s''$$

From this equation one finds the result that $\dot{q}_s'' = \dot{q}_L''$.

18-2

Consider the same problem as in Prob. 18-1. In addition to no phase change at the interface, let the Lewis number be everywhere 1. At the outer edge of the boundary layer let the mixture be exclusively component 1. Show that under these conditions,

$$\dot{q}_L'' = \dot{q}_s'' = g(i_{1,\infty} - i_{1,s})$$

If the specific heat of component 1 may be considered as constant, what is the implied relationship between St and g/G_∞ ?

If the Lewis number is equal to one, the enthalpy is a conserved property of the second kind and we can write

$$\dot{m}'' = g \frac{i_\infty - i_s}{i_s - i_T} = g \frac{i_\infty - i_s}{i_s - i_L + \dot{q}_L'' / \dot{m}''}$$

Furthermore, for $Le = 1$, the mass concentration m_2 is also a conserved property and one can write

$$\dot{m}'' = g \frac{m_{2,\infty} - m_{2,s}}{m_{2,s} - m_{2,T}} = g \frac{-m_{2,s}}{m_{2,s} - 1}$$

In Problem 18-1 it has already been shown that $\dot{q}_s'' = \dot{q}_L''$. Now we want to show that $\dot{q}_L'' = \dot{q}_s'' = g(i_{1,\infty} - i_{1,s})$. For this, we start with the first equation from above. Rearranging, results in

$$\dot{q}_L'' = g(i_{1,\infty} - i_s) - \dot{m}''(i_s - i_{2,s})$$

Now we introduce the enthalpy expressions from Problem 8-1. This results in

$$\begin{aligned}\dot{q}_L'' &= g(i_{1,\infty} - i_{2,s} - m_{1,s}(i_{1,s} - i_{2,s})) - \dot{m}''m_{1,s}(i_{1,s} - i_{2,s}) \\ \dot{q}_L'' &= g(i_{1,\infty} - i_{2,s}) - m_{1,s}(i_{1,s} - i_{2,s})(g + \dot{m}'')\end{aligned}$$

Now, from the second equation above we get

$$\dot{m}'' = g \frac{-m_{2,s}}{m_{2,s} - 1}; \quad 1 - m_{1,s} = \frac{\dot{m}''}{\dot{m}'' + g}; \quad -m_{1,s} = \frac{-g}{\dot{m}'' + g}$$

Introducing this expression into the equation for \dot{q}_L'' results in

$$\dot{q}_L'' = g(i_{1,\infty} - i_{2,s}) + \frac{g}{g + \dot{m}''}(i_{1,s} - i_{2,s})(g + \dot{m}'') = g(i_{1,\infty} - i_{1,s}) = \dot{q}_s''$$

If the specific heat, c_1 , is constant, then it follows that

$$\dot{q}_s'' = gc_1(T_\infty - T_s)$$

from which we obtain

$$St = \frac{g}{G_\infty}$$

18-3

Show that for the case $\dot{m}''=0$ the heat flux at the interface is proportional to the enthalpy differences between the s and ∞ states, for any case for which enthalpy is a conserved property.

If the enthalpy i is a conserved quantity it follows

$$\dot{m}'' = g \frac{i_{\infty} - i_s}{i_s - i_T} = g \frac{i_{\infty} - i_s}{i_s - i_L + \dot{q}_L'' / \dot{m}''}$$

Which can be rewritten according to

$$\dot{m}''(i_s - i_L) + \dot{q}_L'' = g(i_{\infty} - i_s)$$

For the case $\dot{m}'' = 0$ it follows

$$\dot{q}_L'' = g(i_{\infty} - i_s)$$

Furthermore, from Problem 18-1 it is known that for the case under consideration $\dot{q}_L'' = \dot{q}_s''$ and we obtain

$$\dot{q}_s'' = g(i_{\infty} - i_s)$$

18-4

Demonstrate, with the aid of a suitable model, that in a turbulent flow, under the assumption of the Reynolds analogy, the “turbulent” Lewis number is equal to one.

Refer to pages 231-232 in the text. Let there be a concentration gradient for some component “j”. Then the rate of that component in the direction of the gradient would be:

$$G_{diff,j} = C \sqrt{v'^2} \rho \overline{\delta m_j}$$

The procedure then follows in complete analogy with that for turbulent heat transfer. Let ε_{diff} be the eddy diffusivity for mass diffusion. Then,

$$\overline{\delta m_j} \approx \ell \frac{d\overline{m_j}}{dy}; \quad \frac{G_{y,diff,j}}{\rho} = \varepsilon_{diff} \frac{d\overline{m_j}}{dy}; \quad \varepsilon_{diff} = \varepsilon_M$$

Hence, it follows

$$Sc_t = \frac{\varepsilon_M}{\varepsilon_{diff}} = 1$$

Because the turbulent Prandtl number is equal to one, it follows, that also the turbulent Lewis number is equal to one.

18-5

Starting with the energy equation of the boundary layer in the form of Eq. (4-26), show that for the case of a fluid with $Pr = 1$ the stagnation enthalpy is a conserved property of the second kind.

See the development in Chapter 16 starting on page 346. This leads to Eq. (16-5) for a laminar boundary layer, or Eq. (16-7) for a turbulent boundary layer. Let $Pr = 1$ or $Pr_{\text{eff}} = 1$. In either case, the resulting equation is the same as Eq. (18-15). Therefore, the stagnation enthalpy is a conserved property of the second kind.

18-6

Prove the theorem for the conserved property of the second kind, given after Eq. (18-18), by introducing a linear combination of two conserved properties of the second kind ($\mathcal{P}_I, \mathcal{P}_{II}$) into Eq. (18-15).

The theorem after Eq. (18-18) states: *If, in any steady flow, there are two conserved properties of the second kind, \mathcal{P}_I and \mathcal{P}_{II} , and at each point $\Phi_I = \Phi_{II}$, then a linear combination of \mathcal{P}_I and \mathcal{P}_{II} is a conserved property of the second kind.*

We want to prove this theorem by introducing a linear combination of two conserved properties of the second kind into Eq. (18-15)

$$G_x \frac{\partial \mathcal{P}}{\partial x} + G_y \frac{\partial \mathcal{P}}{\partial y} - \frac{\partial}{\partial y} \left(\Phi \frac{\partial \mathcal{P}}{\partial y} \right) = 0$$

Assume that \mathcal{P}_I and \mathcal{P}_{II} satisfy Eq. (18-15). Introducing now a linear combination of these quantities

$$\mathcal{P} = \mathcal{P}_I + a \mathcal{P}_{II}$$

into Eq. (18-5) results in ($\Phi_I = \Phi_{II} = \Phi$)

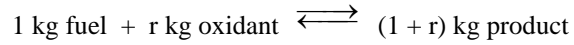
$$G_x \frac{\partial \mathcal{P}_I}{\partial x} + G_y \frac{\partial \mathcal{P}_I}{\partial y} - \frac{\partial}{\partial y} \left(\Phi \frac{\partial \mathcal{P}_I}{\partial y} \right) + a \left\{ G_x \frac{\partial \mathcal{P}_{II}}{\partial x} + G_y \frac{\partial \mathcal{P}_{II}}{\partial y} - \frac{\partial}{\partial y} \left(\Phi \frac{\partial \mathcal{P}_{II}}{\partial y} \right) \right\} = 0$$

Because we assumed above that \mathcal{P}_I and \mathcal{P}_{II} satisfy Eq. (18-15) separately, it can be seen that also \mathcal{P} must be a conserved property of the second kind.

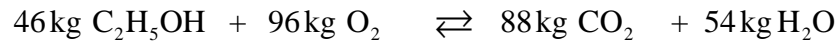
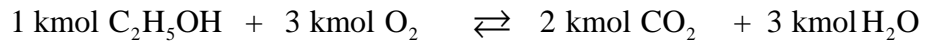
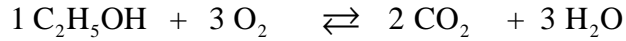
18-7

Consider a chemical reaction of $\text{C}_2\text{H}_5\text{OH}$ with O_2 . It is assumed that the fuel combines with the oxidant and forms a product consisting of CO_2 and H_2O . Write down the reaction equation in kmol and in kg of the reactants. What value has the stoichiometric ratio r ?

The general reaction equation is



For the special case considered here, it follows:



$$\text{and } r = 96/46 = 48/23 = 2.087$$

19-1

Consider a laminar Couette flow with mass transfer through the s surface. Let the transferred substance be CO_2 alone (this means that $m_T = 1$), and let the considered phase be a binary mixture of CO_2 and air, all at 1.013 bar pressure and 16°C . Let the thickness of the layer be such that the concentration of CO_2 at the ∞ state is always effectively zero. Using actual properties that vary with concentration, evaluate g/g^* as a function of B . Compare with the results given in Fig. 19-3.

The reader is referred to the text, pp. 418 – 420. The problem is sketched in Fig. 19-2. However, for Problem 19-1 the properties vary with concentration. We can start by using the Eqs. (19-14, 19-15).

$$\dot{m}'' = (\rho v)_s = \text{constant}$$

$$\dot{m}'' m_1 - \gamma_1 \frac{dm_1}{dy} - \dot{m}'' = 0$$

Eq. (19-14) simply states the fact that the net mass transfer rate is constant. The only transferred substance, 1 is CO_2 . Therefore, Eq. (19-5) might also be written as

$$\dot{m}'' m_{\text{CO}_2} - \gamma_{\text{CO}_2} \frac{dm_{\text{CO}_2}}{dy} - \dot{m}'' = 0$$

Rearranging gives

$$\dot{m}'' dy = \frac{\gamma_{\text{CO}_2}}{(m_{\text{CO}_2} - 1)} dm_{\text{CO}_2}$$

In this equation, \dot{m}'' can be replaced by using Eq. (18-33). In addition, the left hand side of the above equation can be integrated between the surface and the thickness of the layer ($y = \delta$), where the concentration of CO_2 is zero. One obtains:

$$g B \delta = \int_{m_{\text{CO}_2,s}}^0 \frac{\gamma_{\text{CO}_2}}{(m_{\text{CO}_2} - 1)} dm_{\text{CO}_2}, \quad B = \frac{m_{\text{CO}_2,s} - m_{\text{CO}_2,\infty}}{1 - m_{\text{CO}_2,s}} = \frac{m_{\text{CO}_2,s}}{1 - m_{\text{CO}_2,s}}$$

The mass transfer conductance g^* for the case of negligible mass transferred from the interface to the flow is given by Eq. (19-20). Hence, we obtain the following equation, which must be solved:

$$\frac{g}{g^*} = \frac{1}{B (\gamma_{\text{CO}_2})_{m_{\text{CO}_2} \rightarrow \infty}} \int_0^{m_{\text{CO}_2,s}} \frac{\gamma_{\text{CO}_2}}{(1 - m_{\text{CO}_2})} dm_{\text{CO}_2}$$

Using data from Table A-19, and integrating numerically:

$m_{\text{CO}_2,s}$	B	g / g^*
0	0.00	1.0
0.2	0.25	0.925
0.5	1.00	0.769
0.8	4.00	0.488

19-2

Consider again Prob. 19-1, but let $m_T \ll 1$ so that γ can be treated as constant. Let the remainder of the transferred substance be air. Compare the results of both problems. Can you suggest an empirical correlation of the variable-property results with the constant property results?

$$\frac{g}{g^*} = \frac{1}{B (\gamma_{CO_2})_{m_{CO_2} \rightarrow \infty}} \int_0^{m_{CO_2,s}} \frac{\gamma_{CO_2}}{(1 - m_{CO_2})} dm_{CO_2}$$

If γ_{CO_2} can be treated as constant, the above given equation can easily be integrated and one obtains

$$\frac{g}{g^*} = \frac{\gamma_{CO_2}}{B (\gamma_{CO_2})_{m_{CO_2} \rightarrow \infty}} \int_0^{m_{CO_2,s}} \frac{dm_{CO_2}}{(1 - m_{CO_2})} = \frac{1}{B} \ln(1 - m_{CO_2,s}) = \frac{1}{B} \ln(1 + B)$$

This is (of course) the same result, we obtained in Eq. (19-21).

The following modification of this result fits the results of Problem 19-1 reasonably well:

$$\frac{g}{g^*} \left(\frac{\mathfrak{M}_\infty}{\mathfrak{M}_s} \right)^a = \frac{\ln(1 + B)}{B}$$

where \mathfrak{M} is the molecular weight and the exponent $a = 0.6$.

19-3

Consider mass transfer from a fuel droplet, which can be approximated as a sphere. Let there be no effects of transverse flow; that is, the mass flows out symmetrically in all directions. Solve the \mathcal{P} equation under the assumption of constant fluid properties to obtain an expression for g . What is the result for g/g^* ?

The \mathcal{P} -Equation in three-dimensional space is given by Eq. (18-18)

$$G \cdot \nabla \mathcal{P} - \nabla \cdot \Phi \nabla \mathcal{P} = 0$$

Referring to Appendix D of the text, in spherical coordinates we have

$$G_r \frac{\partial \mathcal{P}}{\partial r} + \frac{G_\theta}{r} \frac{\partial \mathcal{P}}{\partial \theta} + \frac{G_\phi}{r \sin \theta} \frac{\partial \mathcal{P}}{\partial \phi} + \frac{-\Phi}{r^2} \frac{\partial}{\partial r} \left(r^2 \frac{\partial \mathcal{P}}{\partial r} \right) - \frac{\Phi}{r^2 \sin \theta} \frac{\partial}{\partial \theta} \left(\sin \theta \frac{\partial \mathcal{P}}{\partial \theta} \right) - \frac{\Phi}{r^2 \sin^2 \theta} \frac{\partial}{\partial \phi} \left(\frac{\partial \mathcal{P}}{\partial \phi} \right) = 0$$

With symmetrical flow, this equation reduces to

$$G_r \frac{\partial \mathcal{P}}{\partial r} - \frac{\Phi}{r^2} \frac{\partial}{\partial r} \left(r^2 \frac{\partial \mathcal{P}}{\partial r} \right) = 0$$

where Φ is constant and only variations of \mathcal{P} in the radial direction are considered. This means also, that we might replace the partial differentials by total differentials. Hence,

$$G_r \frac{d\mathcal{P}}{dr} - \frac{\Phi}{r^2} \frac{d}{dr} \left(r^2 \frac{d\mathcal{P}}{dr} \right) = 0$$

At the surface of the sphere we have

$$G_{r_s} = \dot{m}'' , \quad \dot{m} = \dot{m}'' (4\pi r_s^2)$$

By continuity at a radius r , we can write

$$\dot{m} = G_r (4\pi r^2), \quad (4\pi r_s^2) \dot{m}'' = G_r (4\pi r^2), \quad G_r = \dot{m}'' \frac{r_s^2}{r^2}$$

Inserting this expression for G_r into the differential equation for \mathcal{P} results in the following equation

$$\dot{m}'' \frac{r_s^2}{r^2} \frac{d\mathcal{P}}{dr} - \frac{\Phi}{r^2} \frac{d}{dr} \left(r^2 \frac{d\mathcal{P}}{dr} \right) = 0$$

This equation has to be solved with the following boundary conditions

$$\begin{aligned} r = r_s : \quad \mathcal{P} &= \mathcal{P}_s, \quad \dot{m}'' (\mathcal{P}_s - \mathcal{P}_T) = \left(\Phi \frac{d\mathcal{P}}{dr} \right)_s \\ r = r_\infty : \quad \mathcal{P} &= \mathcal{P}_\infty \end{aligned}$$

The above ordinary differential equation can be integrated easily. One obtains

$$\frac{\dot{m}'' r_s^2}{\Phi} \left(\frac{1}{r_s} - \frac{1}{r_\infty} \right) = \ln \left(\frac{\mathcal{P}_\infty - \mathcal{P}_T}{\mathcal{P}_s - \mathcal{P}_T} \right)$$

Now $B = (\mathcal{P}_\infty - \mathcal{P}_s) / (\mathcal{P}_s - \mathcal{P}_T)$ and we can write

$$\frac{\dot{m}'' r_s}{\Phi} \left(1 - \frac{r_s}{r_\infty} \right) = \ln(B + 1)$$

Finally, we consider that $r_\infty \gg r_s$ and that $\dot{m}'' = gB$ and obtain

$$g = \frac{\Phi \ln(B + 1)}{r_s B}$$

From this equation g^* can be obtained easily by looking for the limit where $B \rightarrow 0$. This results in

$$g^* = \frac{\Phi}{r_s}$$

Hence,

$$\frac{g}{g^*} = \frac{\ln(B + 1)}{B}$$

19-4

Let the transferred substance of Prob. 19-3 be benzene and the surrounding fluid be air. Using the concentration of the benzene as the conserved property, calculate g/g^* as a function of B using the actual variable properties, assuming that the system is isothermal. Let the temperature be 150°C (Note that the Schmidt number for the dilute mixture is relatively independent of temperature and pressure, that D_j is relatively independent of composition, and that γ_j is relatively independent of pressure. On this basis, γ_j can be estimated as a function of composition). Compare the results with those of Prob. 19-3.

$m_{C_6H_6,s}$	B	g / g^*
0	0.00	1.0
0.2	0.25	0.959
0.5	1.00	0.7850
0.8	4.00	0.607

Again, these results correlate well with the constant property results using the following equation:

$$\frac{g}{g^*} \left(\frac{\mathfrak{M}_\infty}{\mathfrak{M}_s} \right)^a = \frac{\ln(B+1)}{B}$$

19-5

Prepare a plot of g/g^* as a function of B for a laminar constant-property boundary layer at an axisymmetric stagnation point, and at a two-dimensional stagnation point, for $Sc = 0.5$. Compare with the similar results on the flat plate, $m = 0$.

Axisymmetric Stagnation Point:

We will first develop an expression for g^* by analogy with the heat transfer solution. In Chap. 10 a correlation has been given for the heat transfer at a three-dimensional axisymmetric stagnation point:

$$Nu_x = 0.76 Re_x^{1/2} Pr^{0.4}$$

With the knowledge of Chap. 19 (pp. 414-416), we can obtain an equation for the Sherwood number and therefore for g^*

$$Sh_x = \frac{g^* x}{\Phi} = 0.76 Re_x^{1/2} Sc^{0.4}$$

If the Lewis number is assumed to be one, one gets

$$\frac{g^* x}{\Phi Re_x^{1/2}} = 0.76 \cdot 0.7^{0.4} = 0.66$$

Now, after finding g^* , we need to relate this value to the value of the mass transfer conductance with blowing. Howe J.T. and Mersman W.A. (Ref. 5 in Chap. 10) solved the laminar boundary layer equations for transpiration at the stagnation regions of blunt bodies. The applicable portion of their work is summarized in Table 10-5 of the text. Following the text on pp. 420-422, the following table can be constructed out of Table 10-5

$\frac{v_s}{u_\infty} \sqrt{Re_x}$	$\frac{gx/\Phi}{\sqrt{Re_x}}$	B
0	0.664	0.0
0.567	0.419	0.950
1.154	0.227	3.560

For g^* we obtained above the relationship $g^* x / (\Phi Re_x^{1/2}) = 0.66$, whereas the values in the above table show a value of 0.664 for this case. Because both values deviate by only 0.6%, we take the value from the above table. With this, we can obtain g/g^* . One obtains

B	g/g^*
0	$0.664/0.664 = 1$
0.950	0.663
3.560	0.342

Two – dimensional Stagnation Point:

We following here the same procedure as outlined in the previous paragraph. An equation for g^* can be obtained from Eq. (10-18). For Lewis equal to one, one finds

$$\frac{g^* x}{\Phi \text{Re}_x^{1/2}} = 0.495$$

Using Table 10-4, one obtains

$\frac{v_s}{u_\infty} \sqrt{\text{Re}_x}$	$\frac{gx/\Phi}{\sqrt{\text{Re}_x}}$	B
0	0.496	0.0
0.5	0.293	1.195
1.0	0.146	4.9700

and finally for g/g^*

B	g/g^*
1.0	$0.496/0.496 = 1$
1.195	0.592
4.970	0.294

The higher the value of g/g^* the better the mass transfer. The above tables show that large values of blowing lead to large values of B and therefore to small mass transfer rates, because the boundary layer tends to be blown away from the surface. The highest value of g/g^* is obtained for the two-dimensional stagnation point. The axisymmetric case yields slightly lower results. The flat plate (Chap. 19) gives considerably lower values.

19-6

It is required to estimate the average mass-transfer rate per unit area of benzene evaporating from the outer surface of a circular cylinder across which air is flowing at 6 m/s. The driving force B has been evaluated to be 0.9. It is found that if a cylinder of the same diameter is placed in the same air stream, the heat-transfer coefficient is $h = 85 \text{ W/(m}^2\cdot\text{K)}$. Estimate the mass-transfer rate explaining in detail the reasons for any assumptions that you build into the analysis. Evaluate the concentrations of benzene in the s state, assuming no chemical reaction.

Following the same procedure as in Problem 19-5, we might first obtain the mass transfer conductance for $B \rightarrow 0$, g^* , from the heat transfer correlations. This results in

$$\frac{St_m}{St_h} = \left(\frac{Sc}{Pr}\right)^{-0.6}, \quad g^* = \frac{h}{c_p} \left(\frac{Sc}{Pr}\right)^{-0.6}$$

The ratio g/g^* might now be obtained from Fig. 19-3, which gives a value of $g/g^* = 0.6$. Alternatively, this ratio could also be obtained from Eq. (19-21)

$$\frac{g}{g^*} = \frac{\ln(B+1)}{B}$$

resulting in $g/g^* = 0.713$. If we use the value given by Eq. (19-21), one obtains

$$g = 0.6 \frac{h}{c_p} \left(\frac{Sc}{Pr}\right)^{-0.6} = 0.713 \frac{85 \text{ W/(mK)}}{1004 \text{ J/(kgK)}} \left(\frac{1.71}{0.7}\right)^{-0.6} = 0.0353 \text{ kg/(sm}^2\text{)}$$

This gives an average rate of mass transferred per unit area of

$$\dot{m}'' = gB = 0.0318 \text{ kg/(sm}^2\text{)}$$

The mass transfer driving force is given for the present problem by the equation

$$B = \frac{m_{C_6H_6,\infty} - m_{C_6H_6,s}}{m_{C_6H_6,s} - m_{C_6H_6,T}}$$

Because the benzene is the only quantity which is transferred, $m_{C_6H_6,T} = 1$. Furthermore, we can assume that $m_{C_6H_6,\infty} \approx 0$. With this, we obtain finally

$$B = \frac{-m_{C_6H_6,s}}{m_{C_6H_6,s} - 1}, \quad m_{C_6H_6,s} = \frac{B}{1+B} = 0.47$$

20-1

Consider the burning of a droplet of ethyl alcohol (or a wet wick) in an atmosphere of pure oxygen. How does the burning rate compare with the same droplet in atmospheric air, assuming that the logarithmic equation for g/g^* is applicable, other things being equal?

The solution of this problem will follow closely the example for the “burning of a volatile fuel in air” in the text (pp. 442-444). Making the same assumptions as in the text, we obtain for the enthalpy

$$i = m_{O_2} \frac{H_0}{r} + c(T - T_0)$$

with the quantities (see page 443)

$H_0 = 28,145 \text{ kJ} / (\text{kg fuel vapor})$, heat of combustion of fuel

$i_{fg,0} = 854 \text{ kJ} / (\text{kg fuel})$, latent heat of vaporization of fuel

$c = 1.005 \text{ kJ} / (\text{kg} \cdot \text{K})$ (same as air)

For convenience, let us set the s state as the datum for enthalpy, so that $T_0 = T_s$. Then

$$i_s = 0 \text{ kJ/kg}$$

$$i_\infty = m_{O_2,\infty} \frac{H_0}{r} + c(T_\infty - T_s) \approx m_{O_2,\infty} \frac{H_0}{r}$$

$$i_T = i_L \quad (\text{since } \dot{q}_L'' = 0 \text{ by the conditions of this problem})$$

$$= -i_{fg,0} = -854 \text{ kJ/kg}$$

where the term $c(T_\infty - T_s)$ has been neglected compared to $m_{O_2,\infty} H_0 / r$ in the equation for the enthalpy.

This results now in the following values for the driving force B :

Burning in pure oxygen:

$$i_\infty = m_{O_2,\infty} \frac{H_0}{r} = 1 \cdot \frac{28,145 \text{ kJ}}{2.09 \text{ kg}} = 14,072.5 \frac{\text{kJ}}{\text{kg}}$$

$$B_{O_2} = \frac{i_\infty - i_s}{i_s - i_T} = \frac{14,072.5}{854} = 16.5$$

Burning in air:

$$i_\infty = m_{O_2,\infty} \frac{H_0}{r} = 0.232 \cdot \frac{28,145 \text{ kJ}}{2.09 \text{ kg}} = 3124.2 \frac{\text{kJ}}{\text{kg}}$$

$$B_{air} = \frac{i_\infty - i_s}{i_s - i_T} = \frac{3124.2}{854} = 3.66$$

The burning rate is given by $\dot{m}'' = g B$, where the logarithmic equation for g/g^* is assumed to be applicable. Hence $\dot{m}'' = g^* \ln(1 + B)$. Since g^* is equal for burning in air or in pure oxygen, one obtains

$$\frac{\dot{m}_{O_2}''}{\dot{m}_{air}''} = \frac{\ln(1 + B_{O_2})}{\ln(1 + B_{air})} = 1.86$$

20-2

Suppose you dip the wick of a wet-bulb thermometer in ethyl ether and expose it to atmospheric air at 20 °C. What equilibrium temperature will the thermometer record under the unit-Lewis-number assumption?

$$T_s = -29^{\circ}\text{C} \text{ (based on data from } \textit{Handbook of Chemistry and Physics})$$

20-3

Dry air at 315 °C flows along a flat wet surface (water) at 9 m/s. The pressure is 1.013 bar. If the surface is insulated (except for exposure to the air) and radiation is neglected, what equilibrium temperature will the surface assume? If the boundary layer is turbulent what is the mass-transfer rate per unit area at a point 1.5 m from the virtual origin of the boundary layer?

We assume that the Lewis number is one. Then m_{H_2O} and i are both conserved properties of the second kind. Thus,

$$\dot{m}'' = g B$$

$$B = \frac{m_{H_2O,\infty} - m_{H_2O,s}}{m_{H_2O,s} - m_{H_2O,T}}$$

$$B = \frac{i_\infty - i_s}{i_s - i_T}$$

For the air – vapor mixture, we can assume thermodynamic equilibrium at the interface. Hence,

$$m_{H_2O} = \frac{P_{H_2O}}{1.61P - 0.61P_{H_2O}}$$

where P_{H_2O} is the vapor pressure of H_2O at $T_{sat} = T_s = T_L$. The enthalpies can be predicted as shown in Chap. 20 (page 433), where $i_{air,0} = 0$ is fixed at 0°C for simplicity. This gives for a air-water-vapor mixture

$$i = \sum_j m_j i_j = m_{air} i_{air} + m_{H_2O} i_{H_2O} = (1 - m_{H_2O}) i_{air} + m_{H_2O} i_{H_2O}$$

Combining Eq. (20-13) with the enthalpy models for air and water yields

$$i = (1.005 + 0.875 m_{H_2O}) T (^\circ C) + 2503 m_{H_2O}, \text{ kJ/kg mixture}$$

Note that for the pure liquid phase, the water enthalpy is given by

$$i_{liquid} = c_{liquid} T (^\circ C)$$

where $c_{liquid} = 4.2 \text{ kJ/(kg} \cdot \text{K)}$.

Now the driving force can be evaluated (recall that from the problem specifications it follows that $m_{H_2O,\infty} = 0$, $m_{H_2O,T} = 0$). Hence,

$$B = \frac{m_{H_2O,\infty} - m_{H_2O,s}}{m_{H_2O,s} - m_{H_2O,T}} = \frac{0 - m_{H_2O,s}}{m_{H_2O,s} - 1} = \frac{m_{H_2O,s}}{1 - m_{H_2O,s}}$$

As stated above, the driving force B can also been evaluated from the enthalpy differences. Here we note, that

$$i_T = i_L - \frac{\dot{q}_L''}{\dot{m}''} = i_L, \text{ insulated body}$$

and $T_T = T_L$. Because of the thermal equilibrium $T_L = T_s$. Thus,

$$B = \frac{i_\infty - i_s}{i_s - i_T}$$

$$\begin{aligned} i_\infty &= (1.005 + 0.875 m_{H_2O}) T(^{\circ}C) + 2503 m_{H_2O} \\ &= 1.005 \frac{\text{kJ}}{\text{kg K}} 315 = 316.6 \frac{\text{kJ}}{\text{kg}} \end{aligned}$$

$$i_s = (1.005 + 0.875 m_{H_2O,s}) T_s(^{\circ}C) + 2503 m_{H_2O,s}$$

$$i_T = c_{liquid} T_s(^{\circ}C)$$

After inserting the above given expressions for the enthalpies into the definition of the driving force B , both expressions for B can be equated. Now from Appendix A (see also Fig. 20-1) we obtain

$$m_{H_2O,s} = m_{H_2O,s}(T_s, P)$$

and one obtains after iteration: $T_s = 54^{\circ}C$, $B = 0.111$.

The mass transfer rate is given by $\dot{m}'' = 0.111 \text{ g}$. Therefore, we have to obtain an expression for g . Assuming that the logarithmic relation for g/g^* , given by Eq. (19-21), can be used, we need to obtain an expression for g^* (mass transfer without blowing).

The Reynolds number is

$$\text{Re}_x = \frac{\rho V x}{\mu} = \frac{0.60114 \cdot 9 \cdot 1.5}{29.9 \cdot 10^{-6}} = 2.72 \cdot 10^5$$

which shows that the flow is turbulent. For turbulent flow over a flat plate we derived an equation for heat transfer in Chap. 12 (Eq. (12-18))

$$\text{St} = \frac{g^*}{G_\infty} = 0.0287 \text{Pr}^{-0.4} \text{Re}_x^{-0.2}$$

Because $\text{Le} = 1$, $\text{Pr} = \text{Sc}$ and we obtain for g finally

$$\begin{aligned} g &= 0.0287 \rho_\infty V_\infty \text{Sc}^{-0.4} \text{Re}_x^{-0.2} \frac{\ln(1+B)}{B} \\ g &= 0.0287 \cdot 0.60114 \cdot 9 \cdot 0.6^{-0.4} \cdot (2.72 \cdot 10^5)^{-0.2} \frac{\ln(1.111)}{0.111} \\ g &= 0.01479 \text{ kg/(s m}^2\text{)} \end{aligned}$$

This results in a mass transfer rate $\dot{m}'' = 0.111 \cdot 0.01479 = 0.0016 \text{ kg/(s m}^2\text{)}$

20-4

Consider flow of air normal to a cylinder as described in Prob. 19-4. Let the air be at 20 °C, 1.013 bar pressure, and 60 percent relative humidity. Inside the cylinder there is water at 90 °C. The surface is porous so that the water can be forced out at a rate sufficient to keep the outer surface moist. What is the average surface temperature and the average mass-transfer rate per unit of surface area?

$$T_s = 15.2\text{ °C}$$

$$\dot{m}'' = 0.00019\text{ kg/(s m}^2\text{)}$$

(It is difficult to evaluate B and \dot{m}'' precisely for this problem).

20-5

A thin plate of solid salt (NaCl), 0.15 m by 0.15 m, is to be dragged through seawater (edgewise) at 20 °C at a velocity of 5 m/s. Seawater has a salt concentration of about 3 percent by weight. Saturated NaCl-H₂O at 20 °C has a concentration of 0.036 kg NaCl/0.1 kg H₂O. Estimate the total rate at which salt goes into solution.

$$\dot{m} = 0.047 \text{ kg/s (total from both sides)}$$

Boundary layer assumed turbulent over entire surface.

$$\text{Re}_x = 750,000$$

$$B = 0.32, \quad g = 3.24$$

20-6

Consider an axisymmetric stagnation point on a missile traveling through the atmosphere at 5500 m/s where the static air temperature is near zero degrees absolute. It is desired to maintain the surface at 1200 °C by transpiration of hydrogen through the wall. The hydrogen is available from a reservoir at 38 °C. If the "heat of combustion" of hydrogen is approximately 116,000 kJ/kg at 1200 °C and the mean specific heats of hydrogen and air are, respectively, 15 kJ/(kg·K) and 1.1 kJ/(kg·K), evaluate the driving force B from the energy equation under the unit-Lewis-number assumption for the conditions of (1) reaction of H_2 with O_2 , and (2) no reaction.

Suggestion: Use the surface temperature as the temperature datum for enthalpy. Note that the free-stream enthalpy must include the very large contribution of the stagnation enthalpy.

With reaction, $B = 0.98$, $m_{H_2,s} = 0.48$

With no reaction, $B = 0.79$, $m_{H_2,s} = 0.44$

For the first case a "simple" chemical reaction is assumed, together with the assumption that $Le = 1$. It is assumed that the "flame" is detached, so that $m_{O_2,s} = 0$. There will be inert substances at the surface (N_2 and combustion products), since H_2 is only 0.48. Note also that $m_{O_2,\infty} = 0.232$ (atmospheric air). In the second case B is computed from the energy equation alone, but the combustion case requires both the energy and the simple chemical reaction mass diffusion equation. In both cases, $i_\infty = 13,805,000 \text{ J/kg}$.

20-7

In Prob. 16-9 the cooling of a gas turbine blade is considered. Considering only the stagnation point at the leading edge of the blade, evaluate the surface temperature and the necessary water rate per square foot of stagnation area to cool by water injection through a porous surface. Assume that the water is available at 38 °C and that the mass concentration of water vapor in the products of combustion is 0.01.

From Prob. 16-9, $h = 4700 \text{ W}/(\text{m}^2 \text{ K})$. Then $g^* = h/c = 4.05 \text{ kg}/(\text{sm}^2)$, $T_s = 124.5^\circ\text{C}$, $B = 0.3$, $g^* = 3.54 \text{ kg}/(\text{sm}^2)$, $\dot{m}'' = 1.06 \text{ kg}/(\text{sm}^2)$. Note that Eq. (20-10) must be used to determine $m_{H_2O,s}$ because the local pressure is the stagnation pressure, 51600 Pa. Table A-20 only goes to 100°C, so vapor pressure data must be obtained from other sources.

20-8

Continue Prob. 20-7 to include the entire blade surface, using what you feel to be the best available approximations for various parts of the surface.

Because of the extensive calculations involved, it is suggested that this problem be solved on a computer. Pressure must first be determined along the blade surface using the tabulated values, Prob. 11-8, then at each point m_{H_2O} as a function of T must be calculated from vapor pressure data, after which local values of T_s and B can be computed as in Prob. 20-7. Values of g^* can be determined from values of h calculated for Prob. 16-9.

20-9

A rocket nozzle is to be constructed with dimensions as shown in Fig. 11-18. The following table gives the composition of the exhaust products:

Compound	m_j , kg/(kg mixture)
CO ₂	0.278
CO	0.279
H ₂ O	0.209
H ₂	0.022
N ₂	0.212

The stagnation pressure is 3400 kPa and the stagnation temperature is 3000 °C. The nozzle is to be constructed of graphite. The objective of the problem is to estimate the rate of erosion (ablation) of the graphite at the throat, and particularly to estimate the time elapsed for a 10 percent increase in throat diameter.

Molecular weight of mixture:	$\mathfrak{M} = 21.5 \text{ kg/kmol}$
Specific heat of mixture:	$c_p = 1546 \text{ J/(kg K)}$
Ratio of specific heats:	$\gamma = 1.33$
Mass velocity at throat:	$G = 2030 \text{ kg/(sm}^2\text{)}$
Viscosity of mixture at throat:	$\mu = 7.67 \cdot 10^{-5} \text{ Pa s}$
Pressure and temperature at throat:	$P = 1836000 \text{ Pa}, \quad T = 2807 \text{ K}$

20-10

Consider an axisymmetric blunt-nosed vehicle entering the Earth's atmosphere. At 60,000 m altitude the velocity is 6100 m/s. The radius of curvature of the nose is 1.8 m. Calculate the convective heat flux to the vehicle at the stagnation point. (Note that this calculation neglects radiation from the very high-temperature dissociated gases behind the shock wave). If the surface is insulated, calculate the equilibrium surface temperature assuming that the surface radiates as a black body to the surroundings. Suppose the surface is a graphite heat shield; calculate the rate of ablation of the graphite in millimeters per minute.

$$\dot{q}_s'' = 657 \text{ kW/m}^2, \quad T_s = 1850 \text{ K}$$

For graphite density (2200 kg/m^3), the rate of ablation is 0.015 cm/min.

20-11

Let a piece of ice uniformly at 0 °C be immersed in water at 27 °C. Evaluate the rate at which melting occurs in terms of the conductance g . How would you evaluate g ?

In the present problem, we have a single species (H_2O). Because of this, there is no mass diffusion, only energy transfer by natural convection or/and conduction. This means that the enthalpy is a conserved property of the second kind and that we can write

$$\dot{m}'' = g B$$

where the driving force B is given by

$$B = \frac{i_\infty - i_s}{i_s - i_T}$$

Choosing the datum point for the enthalpy at 0°C, we obtain for the liquid and the ice at 0°C

$$\begin{aligned} i_{liquid} &= 0 \\ i_{solid} &= -i_{fg,0} = -333.3 \text{ kJ/kg} \end{aligned}$$

Note that the value $i_{fg,0}$ is called the latent heat of fusion. With this, the enthalpy values can be calculated. One obtains:

$$\begin{aligned} i_\infty &= c_{liquid} T_\infty = 4.2 \text{ kJ/(kg K)} \cdot 27^\circ\text{C} = 113.4 \text{ kJ/kg} \\ i_s &= 0 \\ i_L &= -333.3 \text{ kJ/kg} \end{aligned}$$

Hence

$$B = \frac{i_\infty - i_s}{i_s - i_T} = \frac{113.4 - 0}{0 + 333.3} = 0.34$$

In order to find the rate of melting, we can consider a spherical control volume with diameter D . The mass within this sphere is $m = \rho_L \pi D^3 / 6$. Because the sphere will loose solid ice, there will be an outflow over the surface of the sphere $\dot{m}'' \pi D^2$. Following the conservation law of mass, we must have

$$\frac{dm}{dt} + \dot{m}'' \pi D^2 = 0$$

Inserting the expression for the mass gives

$$\frac{d(\rho_L \pi D^3 / 6)}{dt} + \dot{m}'' \pi D^2 = 0, \quad \frac{dD}{dt} + \frac{2\dot{m}''}{\rho_L} = 0$$

Replacing the mass transfer rate by Eq. (18-33) gives finally

$$\frac{dD}{dt} = -\frac{2 g B}{\rho_L}$$

This ordinary differential equation has to be integrated with the boundary conditions

$$t = 0: D = D_1$$

$$t = t_M: D = 0$$

Now we need an expression for the mass transfer conductance g . Assuming that the logarithmic expression for g/g^* (Eq. 19-21) can be used, we need to search for an expression for g^* . For the pure conduction of a sphere in an infinite stagnant medium, one can set (Rohsenow and Choi)

$$Nu = \frac{hD}{k} = 2, \quad Nu = \frac{g^*D}{\Gamma}, \quad \Gamma = \frac{k}{c}$$

where the fluid properties have to be taken at $0.5(T_s + T_\infty)$. Inserting this expression and Eq. (19-21) into the differential equation for D results in

$$\frac{dD}{dt} = -\frac{4B}{\rho_L} \frac{\ln(1+B)}{B} \frac{\Gamma}{D} = -\frac{1}{D} \frac{4\Gamma}{\rho_L} \ln(1+B)$$

This equation can be integrated between the given boundaries. Hence

$$\int_{D_1}^0 \frac{dD}{D} = -\frac{4\Gamma}{\rho_L} \ln(1+B) \int_0^{t_M} dt$$

From this equation one obtains an expression for the time, after which the sphere is molten:

$$t_M = \frac{\rho_L D_1^2}{8\Gamma \ln(1+B)}$$

20-12

Consider a 1.2 m square wet towel hanging from a clothes line. Let sunlight fall on one side at an angle of 45° . The normal solar flux is 946 W/m^2 , and the absorptivity and emissivity of the towel are 1. The surrounding air is at 21°C , with a relative humidity of 65 percent. At the equilibrium temperature of the system it is determined that an equivalent system with no mass transfer would have a free-convection coefficient of $8.5 \text{ W/(m}^2\text{K)}$. What is the drying rate during the period when the towel is sufficiently wet that the surface can be idealized as a liquid surface? (Note that, in addition to the high-frequency solar flux, the 21°C surroundings radiate to *both* sides of the towel, and the towel radiates to the surroundings. Assume that the towel is at a uniform temperature throughout its thickness).

$$\dot{m} = 2.74 \cdot 10^{-4} \text{ kg/s}$$

$$T_s = T_L = 26^\circ\text{C}$$

$$B = 0.0113$$

$$m_{H_2O,s} = 0.00125$$

20-13

In a diesel engine the fuel is injected as small droplets, and, after an initial ignition delay, during which time part of the fuel vaporizes and then burns rather abruptly, the remainder of the fuel burns as fast as the fuel vaporizes from each individual droplet. The objective of this problem is to estimate the time required for complete consumption of a spherical droplet 5 μm in diameter. During this period, let it be assumed that the combustion chamber pressure is 6200 kPa and the air temperature is 800 °C. The fuel may be idealized as $\text{C}_{12}\text{H}_{26}$, with "heat of combustion" of 44,000 kJ/kg and latent heat of vaporization 358 kJ/kg. It may be assumed that these values are relatively independent of temperature. The boiling point of the fuel is approximately 427°C at this pressure.

The mass of a spherical droplet of radius r_s is simply

$$m = \frac{4}{3} \rho \pi r_s^3$$

If \dot{m}'' is the mass flux of evaporation from the surface, then the rate of change of mass of the droplet is given by

$$\frac{dm}{dt} = -\dot{m}'' A_s = -\dot{m}'' 4\pi r_s^2$$

Combining the two equations above, we have

$$\rho \frac{dr_s}{dt} = -\dot{m}''$$

From Prob. 19-3 we found

$$\dot{m}'' = \Phi \frac{\ln(B+1)}{r_s}$$

Then

$$\rho \frac{dr_s}{dt} = -\Phi \frac{\ln(B+1)}{r_s}$$

By using the method of separation of variables, this ordinary differential equation can be solved easily. This equation has to be integrated in accordance with the boundary conditions

$$\begin{aligned} t = 0: & \quad r_s = R_0 \\ t = \tau: & \quad r_s = 0 \end{aligned}$$

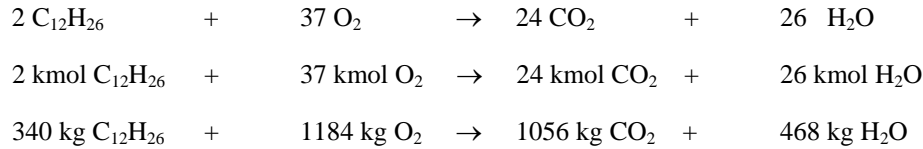
This results in

$$\rho \int_{R_0}^0 r_s dr_s = -\Phi \ln(B+1) \int_0^\tau dt, \quad \tau = \frac{\rho R_0^2}{2\Phi \ln(B+1)}$$

We now need to evaluate Φ and B . As suggested in the statement of the problem, the combustion process is controlled by the rate of evaporation. With this condition, there can be no oxygen at the s -state and no fuel at the ∞ -state.

Assuming that we have a simple chemical reaction and equal specific heats, then the conserved property is enthalpy with $\Phi = \Gamma$.

The following determination of the driving force B will follow that of the text. For burning of a volatile fuel in air, a chemical balance yields



From these equations we find $r = 1184/340 = 3.48$. The other various constants are:

$$m_{O_2,\infty} = 0.232, \quad T_\infty = 800^\circ\text{C}, \quad H_0 = 44,000 \text{ kJ/kg}, \quad i_{fg,0} = 358 \text{ kJ/kg}, \quad c = 1.16 \text{ kJ/(kg K)}$$

It will be assumed that $T_s = T_L = 427^\circ\text{C}$.

From Eq. (F-17) we have

$$i = m_o \frac{H_0}{r} + \int_{T_0}^T c d\tilde{T} \approx m_o \frac{H_0}{r} + c(T - T_0)$$

Now, we will use the s -state for the datum for enthalpy. With the assumption of instantaneous reaction, then

$$m_{O_2,s} = 0$$

and

$$i_s = 0$$

$$i_\infty = \frac{0.232 \cdot 44,000}{3.48} + 1.16(800 - 427) = 3366 \text{ kJ/kg}$$

$$i_T = i_L = -i_{fg,0} = -358 \text{ kJ/kg}$$

From these quantities we obtain for the driving force B

$$B = \frac{i_\infty - i_s}{i_s - i_T} = \frac{3366 - 0}{0 - 358} = 9.4$$

Now, $\Gamma = k/c = 0.0732/1160 = 6.3 \cdot 10^{-5} \text{ kg/(ms)}$. The density of the fuel is about 881 kg/m^3 . With this we get

$$\tau = \frac{\rho R_0^2}{2\Phi \ln(B+1)} = \frac{881 \cdot (2.5 \cdot 10^{-6})^2}{2 \cdot 6.3 \cdot 10^{-5} \ln(10.4)} = 1.86 \cdot 10^{-5} \text{ s}$$

20-14

Calculate the evaporation (sublimation) rate from a snow bank if the ambient air temperature is -23°C , solar energy is falling on the bank at a rate per unit area of 600 W/m^2 , the underside of the bank is effectively insulated, and the heat-transfer coefficient for free convection from an equivalent surface with no mass transfer is $6\text{ W/(m}^2\text{K)}$. The absorptivity *and* emissivity of snow may be assumed to be 1. The absolute humidity of the air is $0.0003\text{ kg H}_2\text{O/kg dry air}$.

The equations on page 433 may be used for enthalpy. It is only necessary to reduce the T-state enthalpy by 333 kJ/kg , the latent heat of fusion. Assuming that the bulk of the snow is at -23°C ,

$$i_T = 4.2(-23) - 333 = -430\text{ kJ/kg}$$

$$T_s = T_L = 5^{\circ}\text{C}$$

The snow is evidently melting before evaporating...

$$m_{\text{H}_2\text{O},s} = 0.0051, \quad B = 0.0048, \quad \dot{m}'' = 2.88 \cdot 10^{-5}\text{ kg/(sm}^2\text{)}$$

If the specific heat of the snow is about 0.1, the snow is evaporating at a rate of 1mm/hr.

20-15

At a particular region in a steam condenser the fluid is a mixture of 80 percent steam (by mass) and 20 percent air. The total pressure is 6.75 kPa, and the temperature is that of saturated steam at that pressure. What is the necessary condition at the surface of the tubes for condensation to take place? In simple condensation the resistance to heat transfer is usually considered to be entirely that of the liquid film that forms on the surface. How does the present problem differ? Suppose the liquid film has an average thickness of 0.1 mm; investigate the effect of the air on the overall resistance to heat transfer between the tube metal surfaces and the free-stream mixture.

The mixture temperature is 38 °C. With 20% air present (the air ejector is provided to hold this percentage low), condensation at this point in the condenser can only occur if $B < 0$. This requires that $T_s = T_L < 35.6^\circ\text{C}$. The cooling water and the tube surface must then be less than 35.6 °C. One can then write

$$\dot{q}_L'' = \frac{T_s - T_{wall}}{R}$$

A 0.1 mm liquid film would give $R = 1.63 \text{ E-}04$. If there were no air in the system this would be essentially the only resistance. With the Lewis number $Le = 1$ assumption, the effective additional resistance can now be investigated by assuming various values of T_{wall} and evaluating \dot{m}'' . Then compare with the condensation would be were $T_s = 38^\circ\text{C}$, $R = 1.63\text{e-}04$, and $\dot{m}'' = \dot{q}'' / L$, where $L = 2409 \text{ kJ/kg}$, the latent heat of vaporization.

20-16

A wet surface is to be dried by blowing dry air at 32 °C over it, while at the same time electrically heating it from the rear with a fixed heat flux of 25,000 W/m². Investigate the variation of the drying rate per unit area \dot{m}'' as the conductance g is varied (presumably by varying the air velocity).

g kg/(s·m ²)	\dot{m}'' kg/(s·m ²)	B	T_s
0.0188	0.01040	0.5520	80
0.0362	0.01010	0.2790	70
0.1109	0.00963	0.0868	50
0.1978	0.00971	0.0490	40
0.2720	0.00998	0.0367	35
0.5900	0.01190	0.0202	25
2.6700	0.02860	0.0107	15

20-17

In Prob. 20-16 the heat is to be supplied from the rear by condensing steam. Let the steam be available at 110 °C, and let it be assumed that the *overall conductance* for heat transfer from the steam to the L surface (including the condensing resistance, the wall resistance, and the resistance of the material being dried) is 280 W/(m²·K). Investigate the influence of the mass-transfer conductance g on the drying rate.

g kg/(s·m ²)	\dot{m}'' kg/(s·m ²)	B	T_s
0.0063	0.00349	0.5520	80
0.0162	0.00452	0.2790	70
0.0745	0.00647	0.0868	50
0.1550	0.00761	0.0490	40
0.2290	0.00837	0.0367	35
0.5620	0.01140	0.0202	25
2.8400	0.03040	0.0107	15

20-18

Consider a laundry convective clothes dryer for which there is available dry air at 20 °C and 1.013 bar pressure. There is also available superheated steam at 1.013 bar pressure and 260 °C. Considering only the "constant-drying-rate" period during which the cloth surface is totally wet, investigate whether it is possible to increase the drying rate by mixing some of the steam with the air. That is, how does drying rate vary with steam-air ratio?

$\dot{m}_{steam} / \dot{m}_{air}$	T_s	B	\dot{m}''
0	6.0	0.00578	0.00577 g*
0.01	17.8	0.00275	0.00275 g*
0.02	25.9	0.00142	0.00142 g*

These results suggest that mixing steam at this temperature with the dry air will reduce drying rate despite higher system temperatures.

20-19

In a part of a solar-operated seawater desalting plant, air saturated with water vapor at 1.013 bar and 55 °C passes into a condenser where the fresh water is recovered. The condenser is built up of a bank of circular tubes with cooling seawater flowing inside the tubes and the saturated air flowing normally. The heat-transfer coefficient on the inside of the tubes is estimated to be 1400 W/(m²K). The tube wall is 0.75 mm thick and has a thermal conductivity of 100 W/(mK). On the outside of the tubes, it is estimated that if there were no mass transfer, the average heat-transfer coefficient would be 70 W/(m²K). If the cooling-water temperature in the first row of tubes (the tubes over which the 55 °C saturated air is flowing) is 46 °C, calculate the rate of condensation per unit of surface area and the rate of heat transfer to the coolant. Neglect the resistance of the condensate film on the tubes. (Would it be significant if the film thickness was, say, 0.1mm?)

$$\dot{m}'' = -0.00193 \text{ kg}/(\text{sm}^2)$$

$$\dot{q}_L'' = 4.85 \text{ kW}/\text{m}^2$$

$$T_s = 49.5^\circ\text{C}, \quad B = -0.0274$$

A condensate film of 0.01 mm would increase resistance by 22 percent.

20-20

Air, saturated with water vapor, at 1.013 bar and 77°C, flows downward along a flat, smooth plate at a velocity of 3 m/s. The plate is 30 cm high (flow direction) and 1.8 m wide. It is cooled by circulating water on its back side. The cooling water is circulates so that its average temperature is effectively 18 °C over the entire back surfaces. The heat-transfer coefficient between the coolant and the back surface is estimated to be 1100 W/(m²K). The wall is 1.3 mm thick and has a thermal conductivity of 26 W/(mK). Estimate the total rate of condensation of water and the total heat-transfer rate to the coolant, assuming that the condensate on the plate surface runs off fast enough that its heat-transfer resistance may be neglected. Is B a constant along the surface? What are the necessary conditions for B to be a constant? Describe how you would propose to analyze the problem, taking into consideration the liquid condensate film on the plate surface.

$$\dot{m}'' = -4.17 \text{ kg}/(\text{sm}^2) \quad (\text{condensation rate})$$

$$\dot{q}_L'' = 11.58 \text{ kW}/\text{m}^2$$

$$B = -0.29$$

$$g^* = 0.0122$$

$$T_s = T_L = 29.1^\circ\text{C}$$

$$\text{Re}_x = 43626 \quad (\text{laminar boundary layer})$$

20-21

Air at 1100 °C and 1013 kPa pressure flows along a flat surface at a uniform velocity of 30 m/s. Investigate the problem of cooling this surface by transpiration cooling. At a point 1 m from the leading edge of the surface, consider the use of first air, then helium, as coolants, both of which are assumed to be available at 20 °C. Prepare a plot of surface temperature as a function of coolant mass-flow rate per unit of surface area. Also calculate the surface temperature as a function of coolant mass-flow rate if the coolant were used merely to absorb heat rather than to pass into the boundary layer, assuming that the coolant leaves the system at surface temperature.

This problem can be approached at least in two ways. In the first the Lewis number $Le = 1$ approximation can be used and constant properties assumed. In the second the variable properties shown on Fig. 20-9 can be used. In the first, Eq. (12-18) together with Eq. (19-21) can be used for g . The differences provide a good way to assess the accuracy of the more approximate procedure.

$$Re_x = 1,509,393 \quad (\text{turbulent}) \quad g^* = 0.148$$

Air injection:

T_s	\dot{m}'' kg/(s·m ²) constant properties	\dot{m}'' kg/(s·m ²) variable properties	B
800	0.0526	0.0549	0.426
600	0.0992	0.106	0.954
400	0.164	0.180	2.039

Helium injection:

T_s	\dot{m}'' kg/(s·m ²) constant properties	\dot{m}'' kg/(s·m ²) variable properties	B
800	0.0121	0.130	0.085
600	0.0259	0.0283	0.191
400	0.0507	0.0477	0.408